Anti-inflammatory effects of intravenous immunoglobulin (IVIg): what are the mechanisms of action?

Inauguraldissertation

zur
Erlangung der Würde eines Doktors der Philosophie
vorgelegt der
Philosophisch-Naturwissenschaftlichen Fakultät
der Universität Basel

von

Laetitia Sordé
Aus Frankreich

Basel, 2016

Genehmigt von der Philosophisch-Naturwissenschaftlichen Fakultät

auf Antrag von

Faculty representative: Prof. E. Palmer
Dissertation supervisor: Dr. A. Karle
Co-examiner: Prof. G. De Libero

Basel, den 22.03.2016

Prof. Dr. Jörg Schibler

Table of contents

Abbreviations

AHR: airway hyperresponsiveness
AIA: antigen-induced arthritis
AICD: activation-induced cell death
APCs: Antigen-presenting cells
APRIL: a proliferation-inducing ligand
ASC: antibody-secreting cells
Asn297: asparagine 297
ATI: Autoimmunity, Transplantation and Inflammation
aTreg: adaptive regulatory T cells
BAFF: B cell-activating factor
BCR: B-cell receptor
BLAST: Basic Local Alignment Search Tool
BSA: Bovine Serum Albumin
CD: cluster of differentiation
CFA: Complete Freund Adjuvant
CFSE: carboxyfluorescein succinimidyl ester
CIDP: Chronic Inflammatory Demyelinating Polyneuropathy
CNS: central nervous system
COX-2: cyclooxygenase 2
cTEC: cortical thymic epithelial cells
CVID: common variable immunodeficiencies
DCs: dendritic cells
ddH$_2$O: distilled deionized water
DMSO: Dimethylsulfoxid
DPBS: Dulbecco's Phosphate-Buffered Saline
dsDNA: double-stranded
EAE: experimental autoimmune encephalomyelitis
EAMG: Experimental autoimmune myasthenia gravis
EBA: epidermolysis bullosa acquisita pemphigus
EGFR: epidermal growth factor receptor
ELISA: enzyme-linked immunosorbent assay
ELISPOT: Enzyme-Linked ImmunoSpot assay
ESI: electron-spray ionisation
Fab: fragment antigen-binding
Fc: fragment crystallizable region
FCS: Fetal Calf serum
FcγRs: Fcγ receptors
FDA: Food and Drug Administration
FDCs: Follicular Dendritic Cells
FoxP3: forkhead box P3
GC: Germinal Center
GM-CSF: granulocyte-macrophage colony-stimulating factor
H: antibody heavy chain
h: hour

HIV: Human immunodeficiency virus
HLA: Human Leukocyte Antigen
HPLC: high performance liquid chromatography
HRP: Horseradish peroxidase
HSE: herpes simplex encephalitis
i.d: intra-dermal
i.v: intravenous
IBP: Integrated Biologics Profiling Unit
IdeS: immunoglobulin-degrading enzyme from *Streptococcus pyogenes*
IFN: interferon
Ig: Immunoglobulin
IL: interleukin
IPI: International Protein Index
ISC: Ig-secreting cells
ISC: immunoglobulin-secreting cells
ITAMS: Immunoreceptor tyrosine-based activation motif
ITP: Immune thrombocytopenia
IVIg: Intravenous Immunoglobulin
KD: Kawasaki disease
KO: knock-out
L: antibody light chain
LC: liquid chromatography
LPS: lipopolysaccharide
mAb: monoclonal antibody
MAPPs: MHC-II associated peptide proteomics
MBL: mannose-binding lectin
mBSA: methylated BSA
MFI: micro-flow imaging
MHC: Major Histocompatibility Complex
min: minute
MNN: Multifocal Motor Neuropathy
MPLA-SM: Monophosphoryl Lipid A from *Salmonella minnesota* R595
mRNA: messenger RNA
MS: mass spectrometry
mTEC: cortical thymic epithelial cells
NCBI: National Center for Biotechnology Information
NHS: N-hydroxysuccinimide
NIST: National Institute of Standards and Technology
NK: Natural killers
NLRs: NOD-like receptors
NOD: nucleotide-binding oligomerization domain
NP: 4-Hydroxy-3-nitrophenylacetic
nTreg: naturally-occuring regulatory T cells
O.D: optical density
OCT: Optimum Cutting Temperature
ODN: oligodeoxynucleotide
OVA: Ovalbumin
PAMPs: pathogens-associated molecular patterns

PBMCs : peripheral mononuclear blood cells
PCA: Physico-chemical Analytics
PFA: Paraformaldehyde
PGE2: cyclo-oxygenase dependent prostaglandin E2
PGE2: prostaglandin E2
PHA: phytohemagglutinin
PNA: Peanut agglutinin
PRRs: pattern recognition receptors
qRT-PCR: quantitative real time polymerase chain reaction
RA: rheumatoid arthritis
Ref: Reference
RT: room temperature
s.c: subcutaneous
sIgG: sialylated IgG
SIGLEC-9: sialic acid-binding Ig-like lectin 9
SIGNR1: specific intercellular adhesion molecule 3-grabbing non integrin-related 1
SLE: systemic lupus erythematosus
SNA: *Sambucus nigra* agglutinin
TCR: T cell receptor
TD NBEs: Technical Development New Biologic Entities
TD: Thymus-dependent antigen
Th: T-helper cell
TI: Thymus-independent antigen
TLRs: Toll-like receptors
TMB:3,3',5,5'-tetramethylbenzidine
Treg: regulatory T cells
Tregitope: regulatory T cells epitope
TT: tetanus toxoid
US: United States (of America)
VEGF-A: Vascular endothelial growth factor A

Abstract

Intravenous immunoglobulin (IVIg) is a pool of plasma polyclonal IgG derived from thousands of healthy donors. Initially employed as a replacement therapy in patients suffering from immunodeficiency, in the 80's, IVIg was shown to surprisingly ameliorate immune thrombocytopenia by some immunosuppressive properties. Since then, the use of IVIg has rocketed in the treatment of a wide range of autoimmune and severe inflammatory diseases. It is commonly administered in the clinic at very high doses (1 to 4 g/kg) in order to achieve anti-inflammatory effects. However, its mechanisms of action remain poorly understood. This PhD project aimed at investigating whether IVIg has a direct impact on immune cell populations *in vivo* in mice, characterizing the antibody response upon IVIg treatment and exploring how these different effects could explain the immunomodulatory properties of IVIg.

By using an OVA-immunization mouse model, we demonstrated that IVIg was able to significantly reduce the OVA-specific antibody response in a dose-dependent manner, as observed in the clinic. Intriguingly, IVIg injection led to B- and T-cell expansion in the corresponding draining lymph nodes, as translated by their considerable increase in weight. IVIg augmented the number of CD69+ activated T cells but didn't promote Tregs activation. Notably, it induced a marked stimulation of B cells as shown by the up-regulation of the co-stimulatory molecules CD86 and CD83, as well as the early activation marker CD69. More strikingly, IVIg administration in mice resulted in the formation of large and numerous germinal centers in lymphoid organs. Analysis of the bone marrow revealed that less mature B cells were re-circulating, suggesting that they get trapped in the lymph nodes. In addition, the number of total IgG immunoglobulin-secreting cells was greatly enhanced upon IVIg treatment, whereas the ratio of OVA-IgG antibodies secreting cells was diminished. All these effects were dependent on the presence of adjuvant and could not be reproduced by the administration of a human monoclonal antibody at the same high dose. These data collectively point to the direction that IVIg triggers immune activation, although the resulting outcome is the inhibition of the OVA-antibody response. This was confirmed by further data showing that IVIg raised an IVIg specific antibody response in mice, mainly targeted towards its variable regions. This suggests that IVIg directly activates B cells after binding to the BCR most probably via an anti-idiotypic interaction. Very interestingly, mouse immunization with NP-Ficoll revealed that IVIg was not able to

significantly downregulate antibodies against a thymus-independent antigen, implying a competition at the T cell level.

Research over the past decades has emphasized the role of IVIg in promoting anti-inflammatory effects, e.g. activation of Tregs, induction of inhibitory FcγRIIB expression, saturation of FcRn, or modulation of co-stimulatory molecules expression on DCs. In contrast, our data indicate an immediate and massive immune reaction against IVIg *in vivo*. We propose that the many different variable sequences present in IVIg introduce a multitude of new foreign epitopes re-directing the immune system. Antigenic competition of IVIg with the response against OVA may occur at different stages in the immune reaction. Driven by the high diversity of T- and B cell epitopes, competition may occur during i) scanning of peptides by T cells on dendritic cells ii) priming of B cells by cognate T helper cells at the B/T cell border iii) priming of B cells by cognate T follicular helper cells within the germinal center.

Therefore, we suggest that rather than acting as an active anti-inflammatory component, IVIg interferes with establishing an efficient immune response against a specific antigen via a huge diversity of epitopes re-directing the immune system towards a massive immune response against IVIg.

Introduction

1. Immune cells interplay

1.1. Innate Immunity

The innate immunity provides immediate protection against pathogens. The innate immune system uses receptors that are encoded in germline and are thus specifically inherited in the genome. Due to their limited number, these receptors recognize features that are common to many pathogens. Innate immunity is thus characterized by its broad specificity and the absence of immunological memory. The immediate innate defenses comprise epithelial barriers, secreted antimicrobial proteins and the complement system. Epithelial cells from the skin, gut, lungs, eyes, nose and oral cavities prevent entry of pathogens by forming tight junctions. Movement of cilia found in lungs and gut provide another mechanical barrier. Epithelial surfaces are also associated with a normal microbiota composed of non-pathogenic commensal bacteria, competing with pathogens for nutrients and surface attachment. Moreover epithelial cells produce chemical microbicide substances. For example, lysozymes contained in tears and saliva degrade peptidoglycan from Gram-positive bacteria. α-defensins are short positively-charged peptides contained in the intestinal tract attracted by the negatively charged LPS (lipopolysaccharide) from bacteria, which lead to pores formation and thus bacteria membrane disruption. Acid pH and digestive enzymes from the stomach create a non-friendly environment for the pathogens. Complement can also be activated early in case of infection. The complement system consists of numerous soluble proteins present in blood. Upon detection of a pathogen these inactive proteins become locally activated and trigger a series of powerful inflammatory events. The complement cascade can be initiated upon direct binding of complement proteins on the pathogen surface or by recognition of sugar patterns on the surface of pathogens by a free lectin receptor. All complement pathways result in the same three consequences, meaning either direct elimination of the pathogen by formation of a membrane-attack complex creating pores in the membrane, opsonization of pathogens, or recruitment of phagocytes to the site of infection by release of anaphylatoxins.

If a pathogen crosses the epithelial barrier, in addition to the free complement receptors in serum it will also be neutralized by macrophages and dendritic cells (DCs) that reside in tissues and constitutively express phagocytic receptors. They recognize microbial components that have a repetitive structure, the pathogens-associated molecular patterns (PAMPs), as well as host molecules such as nuclear or cytosolic proteins named DAMPs (danger- associated molecular patterns) (Gallucci and Matzinger, 2001). PAMPs and DAMPs are recognized via pattern recognition receptors (PRRs). PRRs include C-type lectin family, scavenger receptors and complement receptors. They bind a wide range of pathogens and enable their phagocytosis. Different sets of PAMPs can specifically activate different Toll-like receptors (TLRs) that are located on cell surface or intracellular membranes, as well as cytosol receptors, the NOD-like receptors (NLRs). Interaction with pathogens results in the activation of the NFκB pathway in macrophages and DCs, to release pro-inflammatory cytokines and chemokines. This is the acute-phase response, which consists of the recruitment of more effector cells to sites of infection to destroy the pathogens. Subsequent dilation of local blood vessels allows extravasation of leukocytes and plasma proteins to the infection site and local blood clotting occurs to avoid spread of the infection. This accounts for pain, redness, fever and swelling. Neutrophils make up the first wave of cells that cross the blood vessel wall to enter the inflamed tissue. They are followed by monocytes, which differentiate either into tissue macrophages or DCs, depending on the cytokine environment. At the late stage of the inflammation eosinophils and lymphocytes will also join the infected site. Viruses induce the release of specific cytokines that activate the killer functions of NK cells (Natural Killers) which therefore act as an early innate defense against intracellular infections. The released pro-inflammatory cytokines have another important role, they induce the expression of co-stimulatory molecules on macrophages and DCs thus enabling them to act as antigen-presenting cells (APCs) to T lymphocytes and thereby initiate an adaptive immune response.

1.2. Adaptive immunity

1.2.1. Priming of T cells

If innate immunity accounts for the early detection and destruction of pathogens, it also produces molecules that activate and shape an appropriate adaptive immune response. In contrast to the innate response whose specificity is fixed in the genome, cells from the adaptive response can develop an enormous repertoire that consists of several billions of different antigen receptors (up to 10^{13}). Knowing that the human genome possesses a limiting capacity of about 30 000 genes, the broad repertoire of immunoglobulin and T cell receptors (TCR) is generated by cell rearrangements from gene segments (somatic recombination) which confer them a very tuned specificity allowing fine distinctions between closely related molecules. Unlike innate immunity, adaptive immunity provides long term immunological memory to protect against reinfection.

An adaptive response is mainly driven by two types of lymphocytes: B cells, which develop in the bone marrow, and T cells, which develop in the thymus. T and B-cell responses are initiated in peripheral lymphoid organs by activated APCs, as depicted in Figure 1. APCs comprise three cell types: DCs, macrophages, monocytes and B cells. While DCs and macrophages actively take up antigens non-specifically from a broad range of pathogens and self-molecules by phagocytosis and macropinocytosis, B cells bind soluble molecules specifically through their surface immunoglobulin and internalize them by endocytosis. Once bound, microorganisms are engulfed in APCs and the internalized proteins are degraded to peptides that are then displayed as peptide: MHC complexes on the APC's surface. At the same time, recognition of PAMPs and/or DAMPs by APCs via PRRs, leads to cell activation. This results in the up-regulation of co-stimulatory molecules CD80 and CD86 on surface of APCs as well as increases expression of MHC receptor. APC activation also further triggers antigen processing and directs APCs to migrate to peripheral lymphoid organs (spleen and lymph nodes).
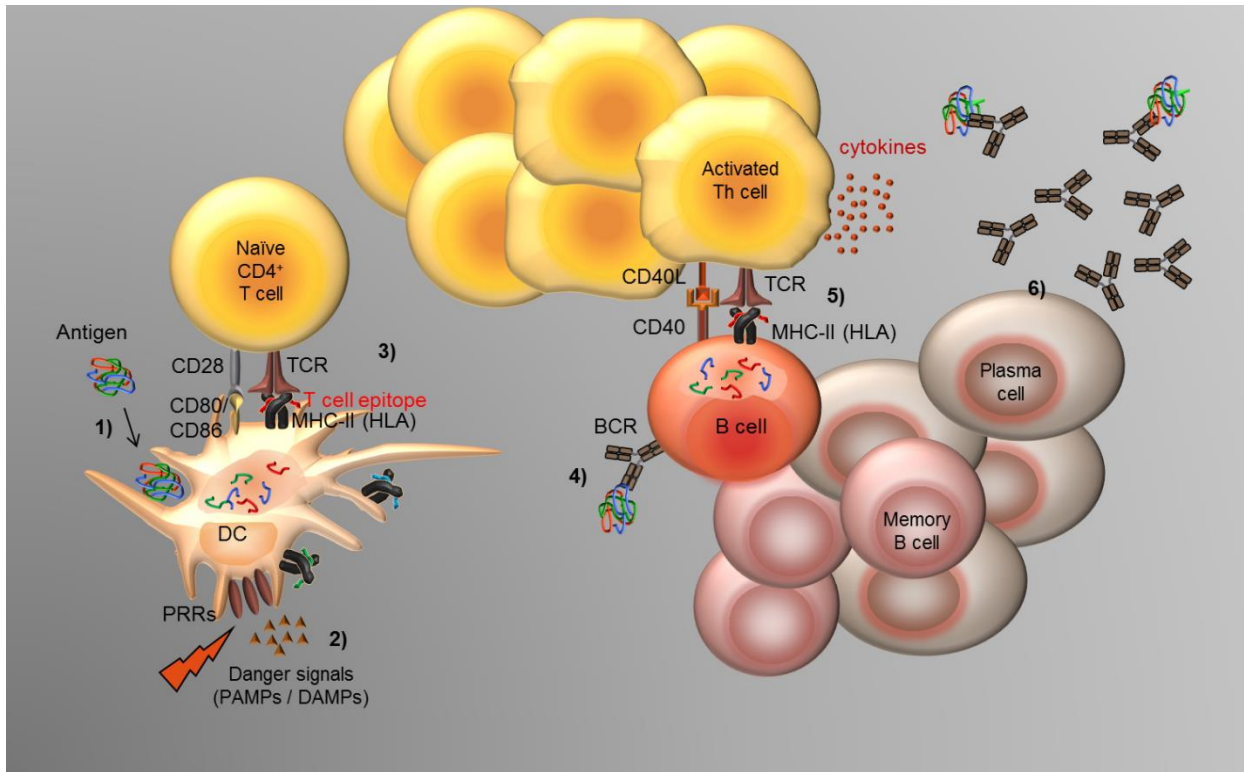
Figure 1: Immune cells interplay during the adaptive immune response. 1) A dendritic cell (DC) takes up antigens unspecifically by macropinocytosis and processes them to peptides inside into acidified endosomes. 2) The pattern-recognition receptors (PRRs) sense the presence of a pathogen via the detection of pathogens-associated molecular patterns (PAMPs) or danger-associated molecular patterns (DAMPs). 3) For extracellular antigens, this results in the presentation of antigen-derived peptides on the MHCClass II molecules on the surface of the DC, together with the expression of co-stimulatory molecules such as CD80 or CD86. A CD4+ T cell clone recognizes both its specific peptide (T cell epitope) and the MHC-II molecule via its T-cell receptor (TCR). Interaction of the TCR with the MHC:peptide omplexe and the CD28 with CD86/CD80 leads to T cell activation and clonal expansion. 4) Antigen uptake in B cells occurs via recognition by its specific B cells receptor (BCR) followed by endocytosis and peptides processing 5) T helper cell (Th)recognize its cognate B cell and activate it thanks to CD40 ligand (CD40L) / CD40 interaction. 6) Activated B cellsproliferate, undergo affinity maturation and finally differentiate into either antibody-secreting plasma cells or memory B cells. Cytokines released by activated T cells play an important role in the antibody class orientation. Adapted from A. Karle.

We can distinguish MHC class I and class II molecules whose function is to deliver peptides to the cell surface to activate the cognate T cells. MHC molecules are also commonly named HLA (Human Leukocyte Antigen). MHC class I molecules are expressed by all cells in the body except red blood cells, whereas MHC class II molecules expression is limited to macrophages, B cells, DCs, thymic cortical epithelial cells and to a very low extend in human to T cells. MHC-I is formed of a heterodimer of α-chain and β-microglobulin and MHC-II is a heterodimer of α-chain and β-chain (see Figure 2).
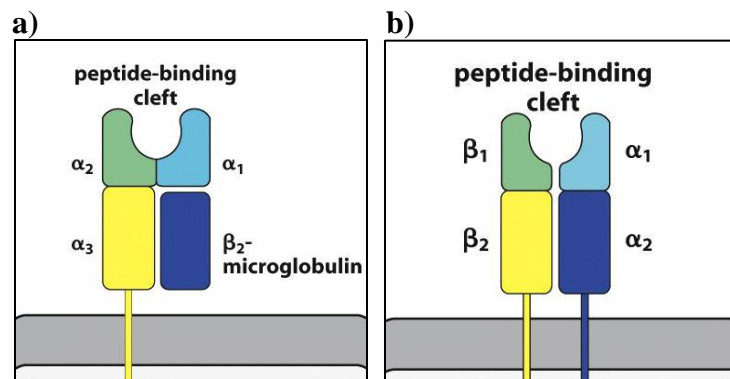
Figure 2: Structure of the MHC class I molecule (a) and the MHC class II molecule (b). Immunobiology, 7ed.(© Garland Science 2008).

Pathogen-derived proteins in the cytosol of APCs are degraded by the proteasome and peptides are loaded on the MHC Class I, while MHC Class II binds peptides generated in acidified endocytic vesicles from extracellular or intravesicular pathogens. Therefore MHC Class I exposes peptides derived from the intracellular compartment, and in contrast MHC Class II exposes peptides derived from proteins that have been taken-up from outside of the cell. MHC genes are highly polymorphic. Most of the allelic variation occurs specifically at the peptide-binding groove and is thus restricted to α1 and α2 of MHC Class I and to β1 of MHC Class II, thus extending the range of antigens that can be recognized. Expression of each allele is co-dominant. Polymorphism combined to polygeny ensures a broad MHC diversity and the outcome is an increased repertoire of peptides being able to be presented, therefore limiting the possibilities for a pathogen to fully escape MHC presentation.

The TCR differs from BCR in the way that it does not bind antigen directly, but only recognize fragments of protein antigens presented on MHC molecules. The TCR is a heterodimer

that resembles a membrane-bound Fab fragment, composed of two transmembrane glycoprotein chains, α and β, each consisting of an extracellular constant and a variable region. This antigen-recognition part is associated with a complex of four invariant signaling chains (two ε, one δ, one γ) forming the CD3, and with two invariant ζ chains. All of the intracellular domains of these invariant chains contain ITAMs (immunoreceptor tyrosine-based activation motif) responsible of the signaling function of the TCR (Pitcher and van Oers, 2003) as shown on Figure 3.
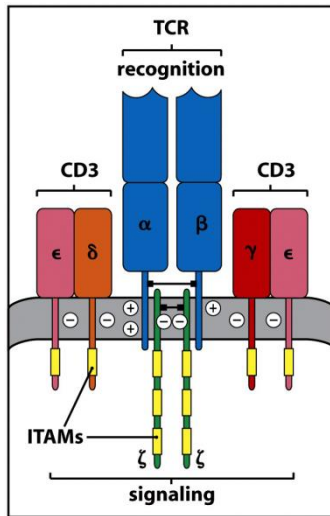
Figure 3: The T-cell receptor complex (TCR). The TCR α:β heterodimer recognizes and binds its peptide:MHC ligand, but cannot signal to the cell that antigen has bound. In the functional receptor complex, α:β heterodimers are associated with a complex of four other signaling chains (two ε, one δ, one γ) collectively called CD3, and with two invariant ζ chains. All of the chains contain a similar motif called ITAM (yellow segments) required for signaling. Immunobiology, 7ed.(© Garland Science 2008).

Importantly, the TCR recognizes both the peptide and the MHC molecule, as demonstrated by (Dunlop et al., 1977), who showed that virus specific T cells could not kill MHC mismatched infected cells, or MHC matched uninfected cells or cells infected with unrelated viruses. T-cell co-receptors CD4 or CD8 bind to the non-variable region of MHC and direct T cells to the correct respective MHC, namely MHC-II for CD4 helper T cells and MHC-I for CD8 cytotoxic T cells.

APCs take-up antigens from site of infection and upon activation by pathogens they will leave the periphery to enter secondary lymphoid organs via the lymph, where they mature. Free antigens also travel to lymphoid organs where they can be taken up and presented by APCs. Naïve T cells continuously re-circulate through peripheral lymphoid tissues, entering from arterial blood. There they scan mature APCs for their cognate peptide. If no interaction occurs, T cells leave via the lymph and return later into the blood. Priming of naive T cells by APCs requires three distinct signals: i) activation by TCR interaction with the MHC: peptide complex ii) survival and clonal expansion by T-cell CD28 receptor interaction with CD80/CD86 co-

stimulatory molecules iii) differentiation into various effector cells depending on the cytokines produced by the APCs. Priming of naïve CD8 T cells generates cytotoxic T cells that will directly kill pathogen-infected cells (production of perforin, granzymes and granulysin). Variation in signal 3 causes naïve CD4 T cells to develop into distinct effector cells: T_H1, T_H2, T_H17 or T regulatory cells (Tregs). T_H1 are specialized to activate macrophages that have ingested pathogens to become highly microbicidal. T_H2 (and to some extend T_H1) provide help in B cells activation for the induction of the humoral immune response. T_H17 promote acute inflammation by helping to recruit neutrophils to sites of infection. Tregs exert inhibitory actions through mechanisms that are not well understood.

1.2.2.   The humoral immune response

The humoral immune response is mediated by antibodies that are secreted by plasma cells. Antibodies contribute to host protection by i) neutralization of pathogens and thus prevention of their cell-surface adherence, ii) opsonization by coating the surface of a pathogen to promote phagocytosis via Fc-recognition and iii) triggering complement activation to enhance opsonization or directly lyse the pathogen.

Although B cells are efficient APCs to prime naïve T cells, their main function is to present MHC: peptides complexes on their surface to receive help from effector T cells to further initiate the humoral response. Two distinct signals are essential to generate an antibody response: antigen binding on the B cell and input signal delivered by T helper cells. First B cells are activated through sensing antigen via their BCR. Antigen that specifically binds to the B-cell receptor (BCR) is internalized to be processed to peptides, loaded on MHC molecules and presented on the B cell surface. The BCR complex is composed of a cell-surface immunoglobulin M (IgM) associated with the two invariant proteins Igα and Igβ carrying each an ITAM to form antigen-nonspecific signaling molecules (Kurosaki, 2002), as illustrated on Figure 4.
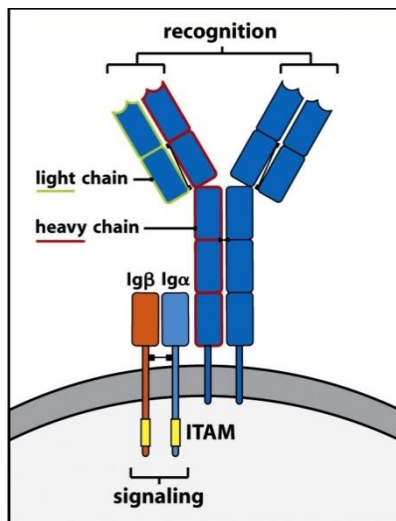
Figure 4: The B-cell receptor complex (BCR). The BCR is composed of a membrane bound IgM which recognizes and binds antigen but cannot itself generate a signal. It is associated with antigen-non specific signaling molecules, the invariant proteins Igα and Igβ, having each a single ITAM motif (yellow segments) required for signaling. Immunobiology, 7ed.(© Garland Science 2008).

Once B cells have bound antigens in the blood or lymphoid tissues, they express specific adhesion molecules and get trapped at the T-cell and B-cell zones border of peripheral lymphoid tissues. The second signal can be delivered by T helper cells in the case of a thymus-dependent (TD) antigen, mediated by the interaction of the CD40 ligand (CD40L) on T cells together with CD40 on B cells. For thymus-independent (TI) antigens, the antigen by itself can deliver the second signal, either by binding to a receptor of the innate immune system in case of TI-1 antigen (e.g. LPS), or by cross-linking BCR in case of polymeric TI-2 antigen (e.g. hapten-conjugated ficoll). B and T cells don't usually recognize the same epitope, since B cell epitopes are often conformational whereas T cell epitopes are linear. However, they respond to the same antigen thanks to linked recognition, meaning B cells can only be activated by their cognate T cells.

Once B cells have interacted with their cognate helper T cells, they start to divide and migrate to the red pulp of the spleen or to the medullary cords of lymph nodes, where they continue to proliferate and form a primary focus. A primary focus is an extrafollicular focus in which B cells do not undergo somatic hypermutation (SHM), but can still differentiate into short-lived plasma cells. Some of these B cells activated in the primary focus will migrate into a primary lymphoid follicle where they continue their clonal expansion and form a germinal center (GC) (Vinuesa et al., 2009), as depicted in Figure 5.
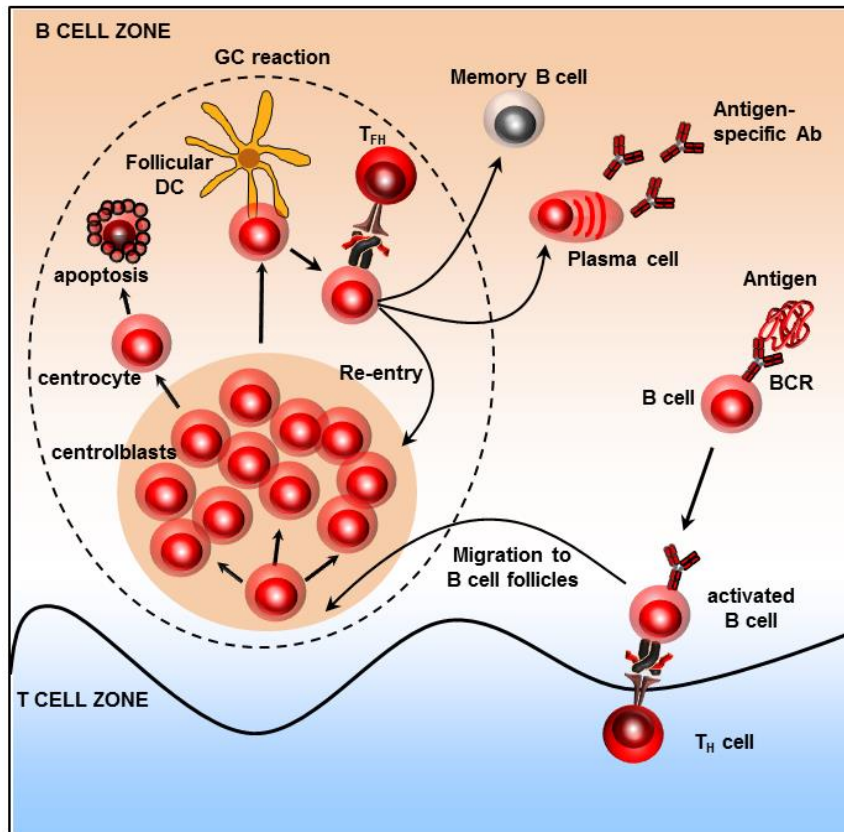
Figure 5: The germinal center reaction. See details below in the text.

A germinal center is composed of a dark zone and a light zone. The dark zone is densely packed with highly proliferative B cells called centroblasts, whose BCRs undergo somatic hypermutation in their V-regions to mature their affinities. The enzyme activation-induced cytidine deaminase (AID) is involved in this process of immunoglobulin diversification (Eisen, 2014), as well as in class-switch recombination. Indeed all naïve B cells express cell-surface IgM and IgD. Right after B cell activation the early stage of the humoral response is dominated by IgM antibodies production, whereas later on IgG is the most abundant antibody found in plasma, followed by IgA and IgE. Class-switching is also mediated by AID and the cytokine environment plays an important role in the antibody class orientation. The light zone of the germinal center is filled with less densely packed B cells named centrocytes, which show reduced proliferation but express higher levels of surface immunoglobulin. This will enable them to scan for their antigen presented as an intact molecule in the form of immune complexes on follicular DCs (FDCs) present in the light zone, as well (Heesters et al., 2014). Most of the random point mutations undergone in the dark zone during affinity maturation negatively impact the ability of a B cell to

bind antigen. These clones will die from apoptosis. Less frequently, mutations improve the affinity of a BCR for antigen, these cells will then receive survival signals from FDCs and by expressing MHC-II: peptide complexes they can further compete for binding to antigen-specific follicular helper T cells (T_{FH}) (Vinuesa et al., 2005). By this process only B cell clones with high affinity for antigen will expand. Surviving B cells that have received help from T_{FH} can then re-enter the GC for further affinity maturation, or exit the GC as a memory B cell or as a plasma cell. Plasma cells possess a high rate of Ig secretion but stop proliferating and have lost their ability to present MHC-II: peptides complexes. The majority of plasma cells will migrate in the bone-marrow to become long-lived cells and key players in the persistence of antibody responses. Memory B cells are long-lived, divide very slowly and secrete no antibody. Some plasma cells can also develop outside of the GC, whereas GC remains the dominant pathway for memory B cell formation (McHeyzer-Williams et al., 2012).

Antibodies have specialized localization and functions according to their class (Brekke and Sandlie, 2003). IgM are produced before B cells have undergone somatic hypermutation and are therefore of low affinity, but because IgM form pentamers they compensate the low affinity with increased avidity by having multiple antigen bindings sites. IgA are mainly localised on mucus surfaces lining the gut and the respiratory tract, where they actively prevent pathogens from entering or attacking the epithelium membrane. IgG predominates in plasma, and is the only class to be transported through the placenta to confer passive immunity to the fetus. Both IgG and IgM activate complement but only IgG is suitable for promoting opsonization through binding on Fc-receptors. IgE antibodies are mainly designed to fight parasite infections (e.g. helminths) and are thus present at very low levels in Western World people's blood. Still they are able to activate mast cells and play a pivotal role in response to allergens.

1.3. Lymphocytes development and self-tolerance

B cells, T cells and NK cells are all derived from a common lymphocyte progenitor located in the bone-marrow. Pro-B cells begin their Ig heavy μ chain genes rearrangement and if successful they become pre-B cells expressing intact μ heavy chain paired to "surrogate" light-chain like- proteins that form the pre-BCR. In immature B cells the Ig light chain gene rearrangement has occurred and IgM associates with Igα and Igβ to express a fully functional BCR on their surface. At this point immature B cells are tested for their reactivity against self-antigens, depending on signals delivered upon IgM interaction. Immature B cells with strong

reactivity for self-antigens undergo apoptosis (clonal deletion), anergy (state of unresponsiveness) or receptor editing by further light chain gene rearrangements to produce non-autoreactive B cells (Shlomchik, 2008). Low or non self-reactive immature B cells can leave the bone-marrow to travel to the spleen where they mature to express IgD on their surface, in addition to IgM. The development stages of a B cell are shown in Figure 6.

	Stem cell	Early pro-B cell	Late pro-B cell	Large pre-B cell	Small pre-B cell	Immature B cell	Mature B cell
H-chain genes	Germline	D–J rearranging	V–DJ rearranging	VDJ rearranged	VDJ rearranged	VDJ rearranged	VDJ rearranged
L-chain genes	Germline	Germline	Germline	Germline	V-J rearranging	VJ rearranged	VJ rearranged
Surface Ig	Absent	Absent	Absent	μ chain transiently at surface as part of pre-B-cell receptor. Mainly intracellular	Intracellular μ chain	IgM expressed on cell surface	IgD and IgM made from alternatively spliced H-chain transcripts

Figure 6: The development stages of a B-linage cell. Immunobiology, 7ed.(© Garland Science 2008).

Some of the lymphocyte progenitors leave the bone-marrow to migrate to the thymus where they proliferate and differentiate into thymocytes. These CD4 CD8 double negative thymocytes give rise to two distinct lineages of T cells, the α:β and the γ:δ CD4-CD8- T cells. α:β cells express both CD4 and CD8 co-receptors at their early stage of development. Those "double-positive" thymocytes that recognize self-peptides: MHC complexes presented on cortical thymic epithelial cells (cTEC) are positively selected (Klein et al., 2009) and they further mature into single positive CD4 T cells or into single positive CD8 T cells. These single positive mature T cells will then scan APCs (medullary thymic epithelial cells mTEC and DCs) and the ones that react too strongly with self-antigens are eliminated by apoptosis, therefore creating a pool of mature self-tolerant T cells that can migrate to the periphery (Palmer, 2003). This process is illustrated in Figure 7.
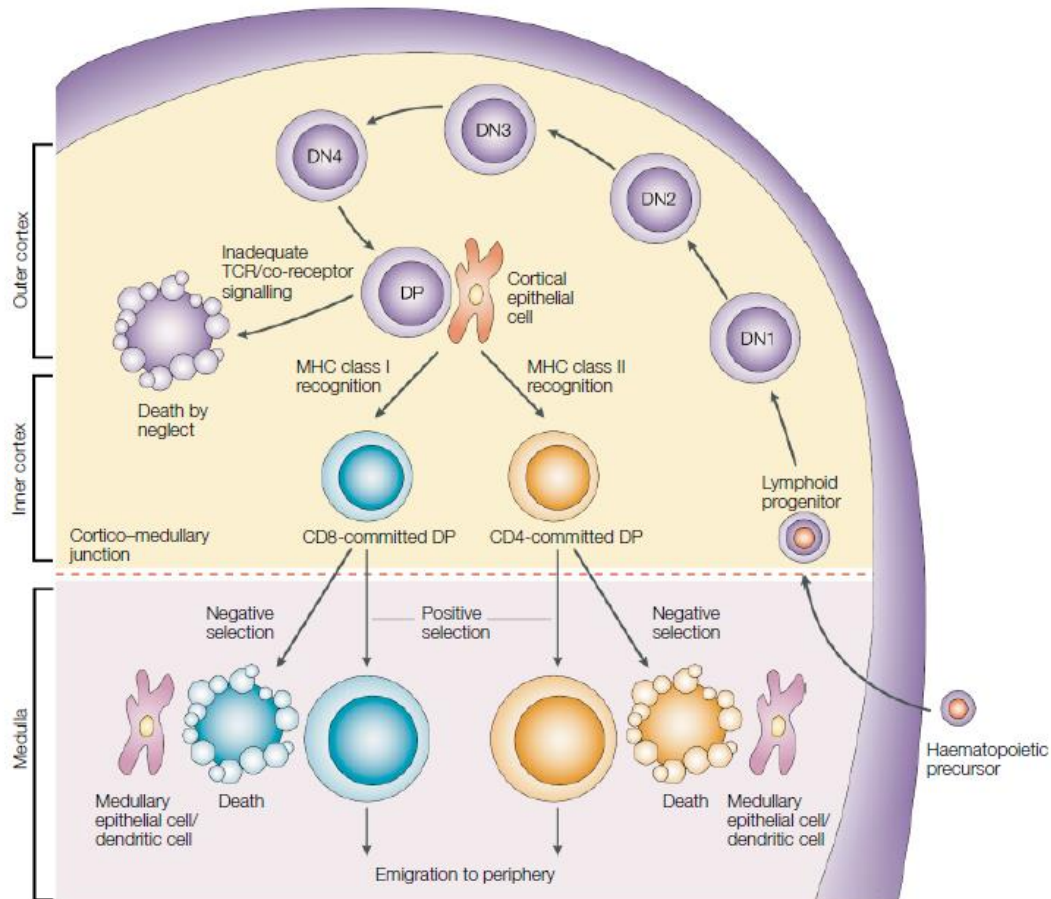
Figure 7: Overall scheme of T-cell development in the thymus. "Committed lymphoid progenitors arise in the bone marrow and migrate to the thymus. Early committed T cells lack expression of T-cell receptor (TCR), CD4 and CD8, and are termed double-negative (DN; no CD4 or CD8) thymocytes. DN thymocytes can be further subdivided into four stages of differentiation (DN1, CD44+CD25−; DN2,CD44+CD25+; DN3, CD44−CD25+; and DN4, CD44−CD25−). As cells progress through the DN2 to DN4 stages, they express the pre- TCR, which is composed of the non-rearranging pre-Tα chain and a rearranged TCR β-chain. Successful pre-TCR expression leads to substantial cell proliferation during the DN4 to double positive (DP) transition and replacement of the pre-TCR α-chain with a newly rearranged TCR α-chain, which yields a complete αβ TCR. The αβ-TCR+CD4+CD8+ (DP) thymocytes then interact with cortical epithelial cells that express a high density of MHC class I and class II molecules associated with self-peptides. The fate of the DP thymocytes depends on signalling that is mediated by interaction of the TCR with these self-peptide–MHC ligands. Too little signalling results in delayed apoptosis (death by neglect). Too much signalling can promote acute apoptosis (negative selection); this is most common in the medulla on encounter with strongly activating self-ligands on haematopoietic cells, particularly dendritic cells. The appropriate, intermediate level of TCR signalling initiates effective maturation (positive selection). Thymocytes that express TCRs that bind self-peptide– MHC-class-I complexes become CD8+ T cells, whereas those that express TCRs that bind self-peptide–MHC-class-II ligands become CD4+ T cells; these cells are then ready for export from the medulla to peripheral lymphoid sites. SP, single positive". (Germain, 2002).

The tolerance generated at this stage for both B and T cells is called the central tolerance. However, central tolerance is a "leaking" process, partly due to the fact that antigens from some tissue-specific proteins might not be found in the bone-marrow or presented on thymic cells, so cognate lymphocytes are unlikely to be deleted and might enter the periphery. Hence, it is essential to maintain peripheral tolerance, by i) anergy, ii) deletion by activation-induced cell death, iii) suppression by Tregs, or iv) linked recognition (B cells can only be activated by their cognate T cells). The MHC molecules can't travel up to the cell surface if they are not loaded with a peptide. This means that if cells are not activated by a pathogen, some self-peptides are presented on APCs surface but without co-stimulatory molecules. Naïve T cells recognizing self-peptides in the absence of second co-stimulus signal are not activated, instead they enter a state of anergy (Xing and Hogquist, 2012). This induces a long-term hyporesponsiveness in T cells, even if the antigen is later on presented on an APC together with co-stimulatory molecules. A high and constant antigen concentration, such as self-proteins that are constantly present in the body and abundant in some tissues, can provide strong and repeated stimulation to lymphocytes that are then deleted by the activation-induced cell death (AICD) mechanism (Walker and Abbas, 2002). A third way to maintain peripheral tolerance is mediated by Tregs that are believed to develop in the thymus in response to weak self-stimulation not sufficient to cause negative selection. Tregs are CD4+ cells expressing CD25 and the transcription factor Foxp3. When they are activated in the periphery, they mediate self-tolerance by inhibiting surrounding autoreactive effector T cells co-localized on the same APC, independently of their antigen specificity (bystander suppression) (Thornton and Shevach, 2000). Finally, linked recognition also helps to ensure peripheral self-tolerance. Indeed the probability is pretty low that a given B cells and the T cell that responds to the same self-antigen are present at the same time, thereby limiting the chances to initiate an autoimmune response.

We have seen above that central and peripheral tolerances are important to prevent destructive immune responses to self-tissues. The development of an autoimmune disease is a complex process that involves failures in one or several of these checkpoints, inducing a break-down of self-tolerance. Autoimmune diseases are major causes of morbidity and mortality within the world, with higher prevalence in women (Jacobson et al., 1997; Walsh and Rau, 2000). Since the exact primary causes remain unknown for most of these diseases, they can't be cured. A combination of genetic predisposition (Rioux and Abbas, 2005; Wandstrat and Wakeland, 2001), environmental factors (smoking, diet, drugs, infection) (Bach, 2005; Dooley and Hogan, 2003) as

well as stochastic events (Edwards et al., 1999) is thought to influence the development of an autoimmune disease. Among the most common autoimmune diseases are rheumatoid arthritis (joint destruction), Grave's disease (thyroid), type 1 diabetes (endocrine system), inflammatory bowel disease (gut), systemic lupus erythematosus (several internal organs), psoriasis (skin) and multiple sclerosis (nervous system). The current treatment strategies rely on immunosuppressive drugs to downregulate the overall immune response (Steinman et al., 2012) but the benefits of these drugs are counterbalanced by toxicity and serious side effects. In the last decade a wide range of therapeutic monoclonal antibodies targeting key receptors on immune cells have been developed (Rosman et al., 2013), however they do not fit for all diseases and are not effective in all patients. The unmet clinical needs are still high and antigen-specific therapies are missing.

2. What is IVIg?

2.1. Origin of IVIg

Intravenous immunoglobulin (IVIg) is a pool of IgG purified from the blood of several thousand healthy donors. In early 1950's, IVIg was introduced as a replacement therapy for patients with deficiency in immunoglobulins to render them less susceptible to microbial infections, and still remains the first-line treatment nowadays (Cunningham-Rundles, 2009). Such deficiencies in Ig can be caused either by common variable immunodeficiencies (CVID), viral infections (HIV), B cell malignancies, immunosuppressive treatments or after bone marrow transplantation. In 1980, Imbach et al. administrated IVIg as a replacement therapy in a boy affected by secondary hypogammaglobulinemia due to long-term immunosuppressive treatment of immune thrombocytopenia (ITP). Unexpectedly his platelet counts dramatically increased after IVIg infusion, and additional studies in patients with ITP but without hypogammaglobulinemia confirmed these results (Imbach et al., 1981). Since then the use of IVIg in patients with a variety of autoimmune and inflammatory disorders has considerably increased, this will be discussed in chapter 2.3.

2.2. Production and composition

Today sixteen brands of IVIg products are commercially available, with nine different manufacturing companies sharing the market (see Table 1). Products differ in their formulation and concentration. IVIg represented 46 % of the market of the worldwide plasma derivative products in 2008 (source: the Marketing Research Bureau, Inc.).

Table 1: Marketed products of IVIg.

Brand name	Manufacturer	Administration	Form	Stabilizer
Carimune NF/Sandoglobulin	CSL Behring	iv	3 to 12% lyophilized	Sucrose
Flebogamma DIF	Girfols	iv	5 or 10% liquid	Sorbitol
Gammagard	Baxter	iv	10% liquid or 5% lyophilized	Glycine or Glucose, respectively
Gammaplex	BPL	iv	5% liquid	Sorbitol, Glycine
Gammar	Aventis/Behring	iv	5% lyophilized	Sucrose
Gammastan	Talecris Biotherapeutics	im	15 to 18% liquid	Glycine
Gammunex-C	Talecris Biotherapeutics	iv or sc	10% liquid	Glycine
Hizentra	CSL Behring	sc	20% liquid	Proline
Iveegam EN	Baxter	iv	5% liquid	Glucose
Nanogam	Sanquin	iv	5% liquid	Glucose
Octagam	Octapharma	iv	5% or 10% liquid	Maltose
Panglobulin	CSL Behring	iv	3 to 12% lyophilized	Dextrose
Polygam S/D	Baxter	iv	5% and 10% lyophilized	Glycine
Privigen	CSL Behring	iv	10% liquide	Proline
Venoglobulin-S	Alpha therapeutics	iv	5% or 10% liquid	D-sorbitol
Vivaglobin	CSL Behring	sc	16% liquid	Glycine

Human normal immunoglobulin for intravenous administration should be prepared from a pool of a minimum of a 1000 donors according to the European pharmacopeia. Plasma units collected should be negative for HIV, hepatitis viruses B and C. The methods commonly used to reduce the risk of viral transmission include a combination of pasteurization, low pH treatment, treatment with solvent and detergent, methylene blue, caprylic acid and nanofiltration (Poelsler et al., 2008). Nowadays manufacturing processes of IVIg are carefully designed to preserve IgG properties and prevent its denaturation, and thus follow tight regulation. The Ig production process involves steps of fractionation and purification of plasma. Plasma fractionation is obtained by several steps of precipitation with ethanol, followed by approved different methods of purification, including a combination of cation/anion exchange chromatographies (Radosevich and Burnouf, 2010). The final product should contain more than 95 % of intact IgG, levels of

aggregates should be kept below 3 % (European pharmacopeia), and level of IgA should be minimal (mentioned on the batch label) to avoid anaphylactic shock in IgA-deficient patients (Lilic and Sewell, 2001). Its composition should reflect the one of a normal serum, with IgG isotypes present approximately in the following proportions: 60-70 % IgG1, 20-30 % IgG2, 5-7 % IgG3, and 1-3 % IgG4. Currently IVIg preparations tend to be formulated at low pH (4-5.5) since it has been proven to be well tolerated by patients, but most importantly it favors product stability. Higher protein concentration (10 %) and reducing the time of infusion is also preferred. Addition of stabilizers such as polyols (sorbitol), sugars (maltose, glucose), or amino acids (glycine, proline) have replaced the use of sucrose which has been suspected of kidney toxicity (Dantal, 2013).

IVIg formulations differ depending on the manufacturer and it's clear that its composition also varies from batch to batch since no batch is derived from the same set of donors. But these differences are kept minimal by the implementation of specific guidelines and quality controls that guarantee the consistency of IVIg batches released on the market and limit the presence of biological or chemical impurities.

2.3. Medical Indications

Today the use of IVIg in the treatment of autoimmune and systemic inflammatory diseases largely takes over its initial indication for patients with immune deficiency as we have seen in chapter 2.1. Indeed, it represents more than 75 % of IVIg administrations in USA (Gelfand, 2012). The indications approved for IVIg as anti-inflammatory therapy by the Food and Drug Administration (FDA) as in 2012 include Kawasaki syndrome, Chronic Inflammatory Demyelinating Polyneuropathy (CIDP), ITP and Multifocal Motor Neuropathy (MNN). The number of licensed indications for IVIg only account for half of the prescriptions (Looney and Huggins, 2006). This is explained by the increasing numbers of "off-labels" IVIg prescriptions (Kivity et al., 2010), notably for some of the most common autoimmune diseases where positive results have been reported in many cases, like for Grave's disease (Antonelli et al., 1992; Leibe et al., 2001), Systematic lupus erythematosus (SLE) (Toubi et al., 2005; Zandman-Goddard et al., 2005), as well as for many dermatological inflammatory diseases (Prins et al., 2007). There are only few exceptions so far for which IVIg treatment didn't prove any benefit, such as for type 1 diabetes (Colagiuri et al., 1996). Beneficial effects of IVIg also remain unclear for rheumatoid arthritis (RA) due to contradictory outcomes (Kanik et al., 1996; Tumiati et al., 1992).

Nevertheless IVIg has shown encouraging results in many other diseases in the field of rheumatology (Mulhearn and Bruce, 2015; Vaitla and McDermott, 2010). In 2008 more than 150 of off-labeled uses of IVIg have been published (Leong et al., 2008), covering a wide range of autoimmune diseases in fields of dermatology, hematology, rheumatology, neurology, and transplantation. Some of them are recognized and therefore covered by US health insurance (Looney and Huggins, 2006). However care should be taken when interpreting results, since some of the published positive cases used IVIg as last option for refractory diseases, as well as studies resulting in ineffective treatment might not be systematically published with regards to the tendency of publishing only positive outcomes. Regarding potential future licensed indications of IVIg, more and larger clinical trials have to be undertaken.

Administration of IVIg as a replacement therapy consists of a dose of 200-400 mg/kg body weight (Jolles et al., 2005), in order to achieve residual levels of IgG of at least 600 mg/dL to protect against pulmonary infections (de Gracia et al., 2004), one of the main complications in immunodeficient patients. These injections should be repeated every 3 to 4 weeks, as long as protection is necessary. However, achieving an anti-inflammatory effect during active phases of autoimmune or inflammatory diseases by using IVIg requires infusion of a much higher dose of 1–3 g/kg body weight and is therefore considered as a high-dose therapy. This dose is also required to be given repeatedly each 3 to 4 weeks, in line with the half-life of IgG in human serum (Looney and Huggins, 2006). According to pharmacokinetics studies, the increase in serum IgG after IVIg treatment varies considerably between patients, showing large standard deviations. This of course also depends on the injection time frame which varies empirically between patients and diseases, as there are no specific guidelines for off-labeled indications. A recent study (Vlam et al., 2014) conducted with 23 patients affected with multifocal motor neuropathy showed that IVIg increased the total serum IgG levels in all patients after a first IVIg cumulative dose of 2.0 g/kg in 5 days, with a peak level at day 5 of the IVIg course of 36.9 ± 7.8 g/L (mean $\pm$ SD). This represents an increase of about 3 fold compared to baseline before treatment. Three weeks after the infusions, IgG concentrations considerably dropped, but still remained higher than baseline (mean ΔIgG $5.4 \pm$ SD 4.7 g/L). 74 % patients responded well to IVIg treatment and very interestingly mean ΔIgG was higher in IVIg responders than in non-responders. This finding is in line with another study performed on patients with Guillain-Barré Syndrom and treated with 2.0 g/kg IVIg, which showed that the increase of serum IgG level significantly correlates with the disease recovery (Kuitwaard et al., 2009).

2.4. Economic challenges

Improved quality and safety of the IVIg preparations in the past years making it a well-tolerated treatment have certainly contributed to its increasing use in the clinic with a massive number of off-labeled indications. The worldwide consumption of IVIg increased by more than 6-fold in ten years to reach more than 100 tons per year in 2010 (Imbach, 2012). The consumption of IVIg is increasing at an annual rate of 5 % in Europe and 11 % in the US. Canada is the world leading country in IVIg use and just behind is the US (Pondrom, 2014), with over 4 million grams used in 2004 at a cost of $500 million (Nimmerjahn and Ravetch, 2007). The demand for IVIg therapy is ever-growing but its availability is limited, as it is a primary blood- and therefore finite- product, with number of blood donors as a major bottleneck. Another main limitation of IVIg is the high dose required for immunoregulatory properties. In general, the IgG yield is between 3.5 and 4.2 g/L plasma as 40 to 50 % of IgG are lost during the fractionation process (Buchacher and Iberer, 2006). Knowing that a blood donation is about 450 mL and that plasma accounts for 55 % (so 250 mL), it means that about 0.875-1.05 g/L IgG can be extracted from a single blood donation.

This limited availability and the increasing use of IVIg for the treatment of more and more pathological conditions worldwide have resulted in shortages in supply. The first alarming shortage happened during the late 1990's (Boulis et al., 2002) with a demand exceeding supply by about 30 % in 1998 (Bayry et al., 2007). Today, although the manufacturing processes have improved, IVIg still faces worldwide shortages so experts recommend the development of a priority system for its allocation (Pondrom, 2014). As a results of this shortage and owing the increasing demand, the cost of IVIg has increased by 17 % from 2013 to 2014, and still continues to do so (Pondrom, 2014). The economic impact of IVIg is substantial: as an example in 2015 Octagam 10 % (Octapharma) costs 77.8 CHF per gram. For an adult weighing 70 kg treated at 2 g/kg this gives a price of 10 892 CHF for one single injection. In answer to the article of Pandrom and colleagues, Van Gent et al. proposed to solve the IVIg shortage by developing cheaper IVIg "mimetics" recombinant compounds that target the IVIg receptors (van Gent and Kwekkeboom, 2015).

3. Potential mechanisms of IVIg – state of the art

Considering the increasing costs and its supply shortage, the development of a possible replacement for IVIg would have a major impact on health economy. Despite its widespread use and broad efficacy, the mechanisms that confer IVIg its immunoregulatory properties in autoimmune and inflammatory disease conditions remain poorly understood. In the interest of developing new, safer and more effective anti-inflammatory treatments, understanding IVIg mechanism of therapeutic action has drawn a big interest in research. This is shown by the 613 publications recovered in PubMed search for "IVIg" in December 2015, which is about a 2 fold increase within 10 years, as illustrated on Figure 8. There is evidence that both, the antibody Fab region and the Fc domain, might be involved in the immunomodulatory mechanisms of IVIg, and a broad range of mechanisms have been proposed so far, as illustrated on Figure 9, that we will review in the next sections.
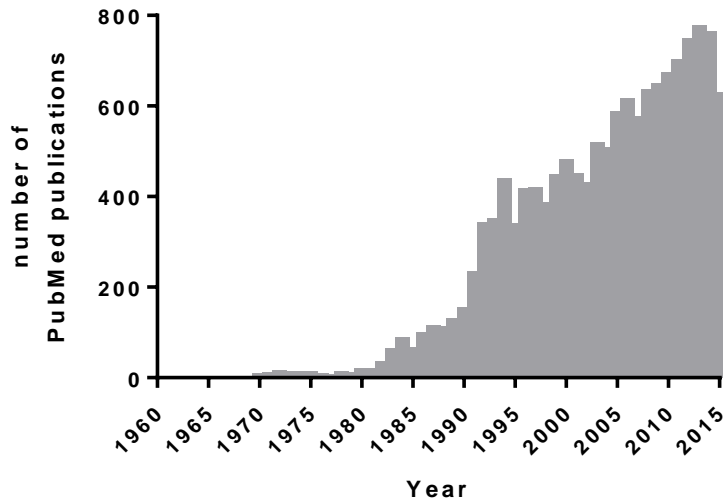
Figure 8: Number of publications in PubMed for "IVIg". As for December 2015.
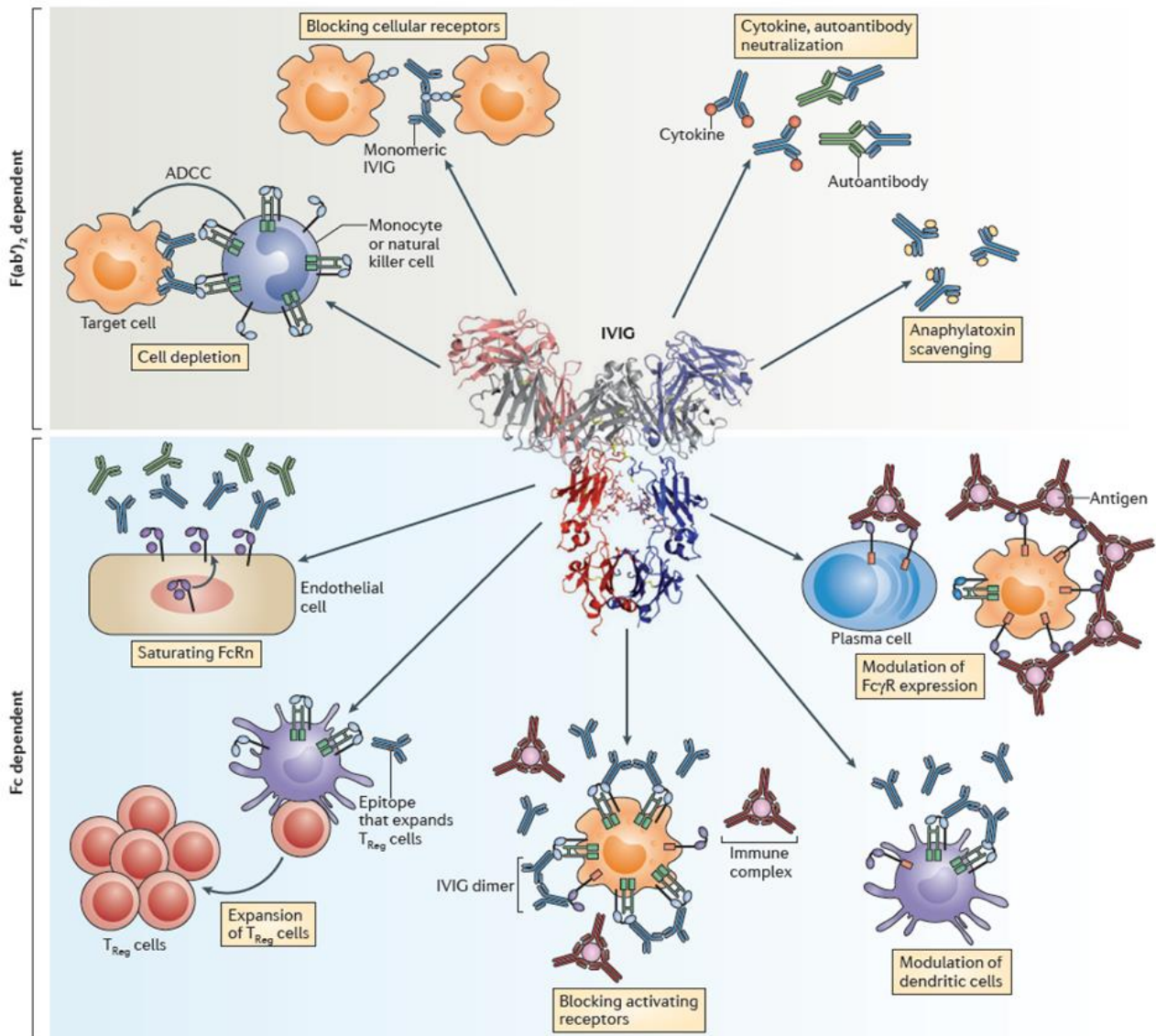
Figure 9: F(ab′)2- and Fc-dependent pathways of IVIG activity. "Shown is an overview of the different pathways that have been implicated in intravenous immunoglobulin (IVIG)-mediated immunomodulation. F(ab′)2-dependent mechanisms include: the killing of target cells by antibody-dependent cytotoxicity (ADCC); the blockade of cell–cell interactions mediated by cell-surface receptors, such as CD95 and CD95 ligand (CD95L); the neutralization of cytokines; the neutralization of autoantibodies by anti-idiotypic antibodies; and the scavenging of the anaphylatoxins C3a and C5a. Fc-dependent pathways include: the saturation of the neonatal Fc receptor (FcRn); the expansion of regulatory T (TReg) cell populations; the blockade of immune complex binding to low-affinity Fcγ receptors (FcγRs); the modulation of dendritic cell activation via FcγRIII; and the modulation of activating and inhibitory FcγR expression on innate immune effector cells and B cells". (Schwab and Nimmerjahn, 2013)

3.1. Fc-dependent mechanisms

3.1.1. Saturation of FcRn

The neonatal Fc receptor (FcRn) is a specialized receptor that binds serum IgGs and protects them from degradation. IgGs are picked up from plasma by endothelial and myeloid cells through pinocytosis and bind to FcRn present in the acidic endosomes. FcRn binds IgG at acidic pH of (<6.5) but not at neutral or higher pH. IgGs bound to FcRn are recycled to the cell surface and released into the circulation. Without this protective mechanism, IgG would pass to the lysosome and be degraded. These specialized receptors account for the long half-life of serum IgG of 2-3 weeks. Thus, one possible mechanism postulated for IVIg is that the large dose of IgGs administered saturates the FcRn receptors and accelerates the degradation of circulating pathogenic autoantibodies (Yu and Lennon, 1999), as illustrated on Figure 10.
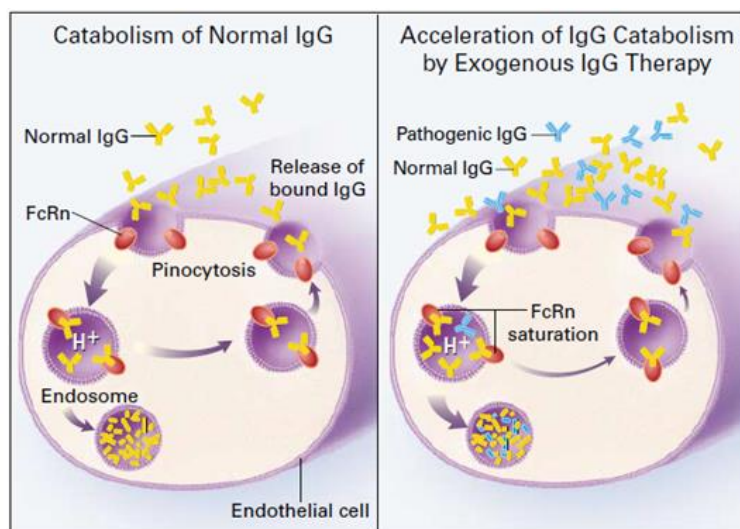
Figure 10: Regulation of the Catabolism of IgG by FcRn. "A specialized intracellular Fc receptor, FcRn, that is abundant in endothelial cells binds pinocytosed IgG only in the acidic environment of the endosome. It releases intact IgG when its transport vesicle is redirected to the neutral pH of the cell surface. Unbound IgG is transferred to lysosomes for degradation. The saturation of FcRn in states of hypergammaglobulinemia accelerates the catabolism of IgG. This IgG-depleting mechanism plausibly explains the temporary benefit of intravenous therapy with high doses of normal IgG in autoimmune diseases mediated by pathogenic IgG ". (Yu and Lennon, 1999).

In mouse models of bullous pemphigoid and arthritis, IVIg treatment prevented blistering and resulted in a reduction in pathogenic antibodies whereas no additional protective effect was observed in FcRn-deficient mice (Li et al., 2005). Nevertheless, FcRn deficient mouse models are biased since the clearance of pathologic autoantibodies is modified and it is difficult to assess their pathologic effects. It is well exemplified in this study where FcRn-deficient mice were resistant to the autoantibody-mediated induction of skin blisters. An *in vivo* study in mice postulated that a single high-dose of IVIg reduced the concentration of a continuously infused

IgG1 monoclonal antibody (mAb) by 40 % after 3 days (Bleeker et al., 2001). These findings correlate with another study (Hansen and Balthasar, 2002) where a similar dose of IVIg in a rat model of ITP has been reported to be effective and to enhance the clearance of anti-platelet antibodies by a factor of 2. When extrapolated to human, the model of Bleeker et al. predicted a decrease of autoantibody of about 25 %, 2 to 3 weeks after IVIg injection. This has been confirmed in patients with Lambert-Eaton myasthenic syndrome (Bain et al., 1996), where autoantibody levels gradually decreased by approximately 30 % 3 weeks after IVIg treatment, as well as in patients with systemic vasculitis (Jayne et al., 1993). However, in a more recent study of a murine ITP model, IVIg was still effective in increasing platelet counts in the absence of FcRn (Crow et al., 2011). Controls assessed the good binding *in vivo* of the antiplatelet antibodies to platelets in FcRn deficient mice, and they were equally well inducing ITP as in wild-type mice. Thus, the role of the FcRn receptor in conferring IVIg its protective mechanisms in autoantibody-mediated diseases is unclear.

3.1.2. Blockade of FcγRs

Antibodies effector functions are crucially dependent on their interaction with the complement system as well as with Fc receptors. Phagocytes are activated by IgG antibodies which bind to their specific Fcγ receptors (FcγRs) on their surface. To distinguish antibodies bound to a pathogen from free circulating antibodies, low affinity FcγRs bind with higher avidity to multimerized antibodies bound to antigen than to monomers and only such a cross-linking can result in cell activation. FcγRs are crucial in mediating the effector functions of antibodies. Traditionally, these receptors are divided into 2 groups, based on their activating or inhibitory properties (Figure 11). Monocytes, macrophages, and DCs express several members of the FcγRs family on their cell surface and can co-express activating FcγRs with the inhibitory FcγRIIB (Guilliams et al., 2014).
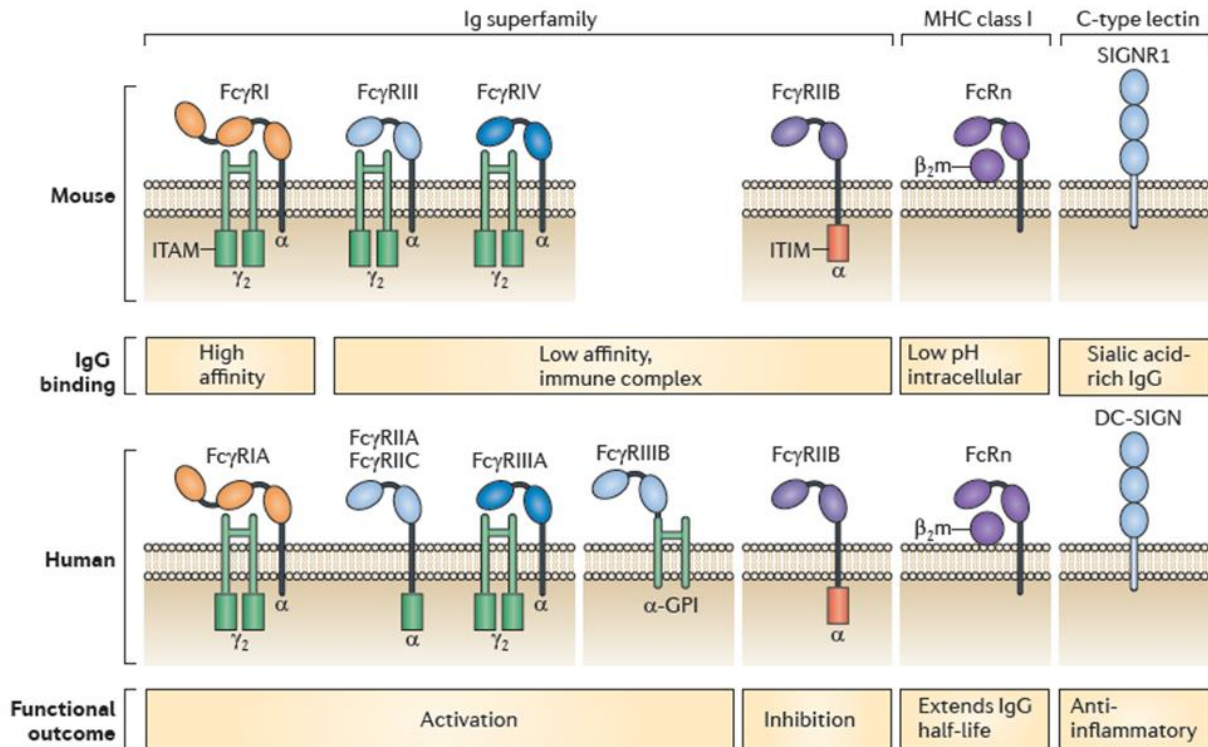
Figure 11: The family of mouse and human FcγRs. "Depicted are the families of mouse (top) and human (below) canonical Fcγ receptors (FcγRs), which both consist of several activating receptors and one inhibitory receptor. In humans but not in mice, FcγRIIIB is exclusively expressed on neutrophils. The neonatal Fc receptor (FcRn) is responsible for the long half-life of IgG and belongs to the family of MHC class I molecules. Mouse DC-SIGN-related protein 1 (SIGNR1) and its human orthologue DC-specific ICAM3-grabbing non-integrin (DC-SIGN) are also IgG-binding proteins and may be viewed as IgG glycoform-specific FcγRs. The particular requirements of these different receptors for IgG binding are indicated. Also shown are the functional outcomes of IgG binding to each receptor." (Schwab and Nimmerjahn, 2013)

FcγRs blockade was suggested as the mechanism by which platelet counts rapidly increase in patients with ITP after the administration of IVIg (Bussel, 2000; Crow and Lazarus, 2003), since platelets coated with anti-autoantibodies could not be cleared by cells whose FcγRs are saturated. Further supporting evidence for Fc receptor blockade was shown by an increase in platelet counts in patients with ITP using a monoclonal antibody directed against the FcγRIIIA receptor (Clarkson et al., 1986). Intravenous administration in children with acute ITP of Fcγ fragments prepared from plasma IgGs also resulted in a rapid increase in platelet counts (Debre et al., 1993).

The potency of IVIg in ITP patients could be explained by their capacity to inhibit phagocytosis *in vitro* in human macrophages. This inhibition most likely results from the direct blockade of FcγRs by IgG dimers that are present in IVIg preparations and have enhanced avidity for FcγRs (Nagelkerke et al., 2014; Teeling et al., 2001). However, it has also been observed that a human IgG preparation devoid of IgG dimers retained its therapeutic efficacy in a murine model of ITP (Tremblay et al., 2013), and that IVIg activity was not impaired in FcγRI and FcγRIII-deficient mice used in models of nephrotoxic nephritis and ITP (Kaneko et al., 2006a; Schwab et al., 2012a). This questions the relevance of IgG dimers in the efficacy of IVIg in ITP, as well as in other diseases. The main difficulty in investigating whether the blockade of FcγRs is relevant for IVIg immunomodulatory effects comes from the variability of FcγR expression between mouse strains, which could explain the differences observed between the different studies. The expression of FcγRs also differs between mouse and humans and FcγR polymorphisms in humans might influence the efficacy of intravenous immunoglobulin therapy for patients with certain autoimmune diseases (Binstadt et al., 2003). Despite this FcγR variability, multimeric Fc molecules have been shown to efficiently protect in several disease models. Higher-order Fc-multimers demonstrated increasingly stable associations with the FcγRs and effectively treated collagen-induced arthritis and prevent ITP in mice (Bazin et al., 2006; Jain et al., 2012). Multimeric Fc molecules have also been successfully tested to rescue a murine model of myasthenia gravis at lower dose than IVIg (Thiruppathi et al., 2014).

3.1.3. Increased expression of inhibitory FcγRIIB

The inhibitory low- affinity FcγRIIB is widely co-expressed with activating FcγRs on a variety immune cells, including macrophages and B cells. Cross-linking of FcγRIIB leads to a dominant-negative signal, resulting in cell inactivation. Combined with the triggering of activating FcγRs, both signals establish a threshold for cell activation in response to IgG immune complexes. This mechanism has been confirmed in FcγRIIB-deficient mice, which displayed elevated Ig levels after antigenic stimulation compared to wild-type, as well as a decreased threshold for mast-cell activation (Takai et al., 1996). Mice deficient in FcγRIIB have been shown to develop more severe autoimmune diseases, such as glomerulonephritis (Nakamura et al., 2000), AIA (van Lent et al., 2003), lung disease IC alveolitis (Clynes et al., 1999) and SLE (Yajima et al., 2003). In consequence, several studies addressed the hypothesis that FcγRIIB may play a role in the immune modulation of IVIg by promoting inhibitory signals within the immune

cells. This was first reported in 2001 in a study showing that FcγRIIB was up-regulated in the splenic macrophages of ITP mice after administration of IVIg and that FcγRIIB KO mice failed to respond to IVIG therapy (Samuelsson et al., 2001), which was confirmed by another study (Crow et al., 2003). Consistent with these findings, the anti-inflammatory activity of IVIg was abrogated in mice deficient in the inhibitory FcγRIIB in a variety of murine models, such as nephrotoxic nephritis (Kaneko et al., 2006a), K/BxN serum-induced arthritis (Anthony et al., 2008b; Bruhns et al., 2003), and in the T cell-mediated experimental autoimmune encephalomyelitis (EAE) (Fiebiger et al., 2015). Interestingly, it has been observed that patients with CIDP expressed lower FcγRIIB levels on naive B cells when they remained untreated, and that IVIg therapy upregulated FcγRIIB expression on monocytes and B cells (Tackenberg et al., 2009).

Thus, modulation of FcγRIIB inhibitory signaling appears to be one of the potential mechanisms of IVIg. However, this theory seems quite ambivalent since the data mentioned above could not be fully reproduced by other research groups. Indeed, it has been shown that BALB/c FcγRIIB KO mice responded well to IVIg and ameliorated ITP whereas B6 did, but only to a lesser extend (Bazin et al., 2006). The role of FcγRIIB in IVIg efficacy was also questioned in another mouse study demonstrating that FcγRIIB is dispensable to ameliorate ITP upon IVIg injections in both BALB/c and B6 KO strains (Leontyev et al., 2012a). Nevertheless B6 mice required an IVIg dose 2.5 fold higher than the one used to treat BALB/c mice, showing that both, mouse background and IVIg dosage, are critical and can lead to misinterpretation in affirming the role of FcγRIIB in IVIg efficacy. Data from an *in vitro* study on activated human B cells argue against the involvement of FcγRIIB in the suppression of human tonsillar B cell activation by IVIg (Zhuang et al., 2002). In this study pre-incubation with IVIg failed to block binding of FcγRIIB-specific antibody. In addition, anti-FcγRIIB antibodies did not reverse inhibition of B cell proliferation or antibodies production by IVIg. A more recent study revealed that FcγRIIB is dispensable as IVIg could efficiently protect B6 FcγRIIB KO mice against EAE (Othy et al., 2013). Therefore, the paradigm of FcγRIIB requirement in IVIg immunosuppressive functions remains questionable.

3.1.4.   Sialylation on the Fc-fragment

It has been well established that the Fc-mediated effects of antibodies are influenced not only by the antibody isotype, but also by Fc-linked carbohydrate structures (Arnold et al., 2007). Human IgG antibodies share a conserved N-glycosylation site within the CH2 domain of their Fc moieties, linked to the asparagine 297 (Asn297). As illustrated in Figure 12, this sugar side chain consists of a common biantennary glycan structure of four *N*-acetylglucosamine (GlcNAc) and three mannose residues, with variable additions of fucose, galactose, sialic acid, and/or bisecting GlcNAc residues. It has been shown that IgGs N-glycosylated structures, interposed between the heavy chains, are crucial for their biological activity. For instance, removal of galactose on IgGs confers an increased pro- inflammatory activity (Rademacher et al., 1994). In contrast, several studies demonstrated that the potent anti-inflammatory activity of IVIg is a direct result of Fc sialylation.
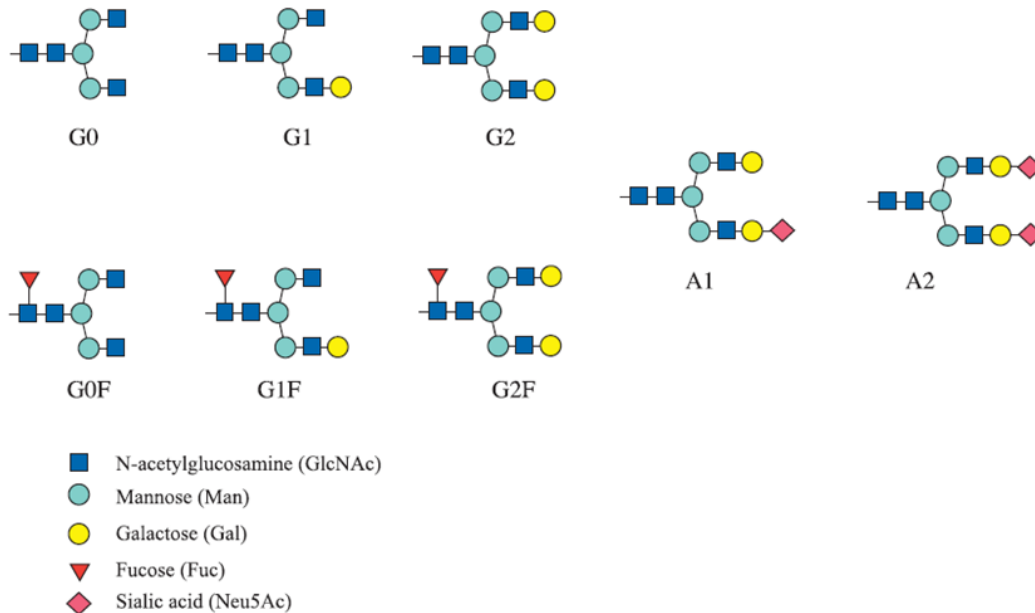
Figure 12: Schematic diagram of the IgG N-linked glycan structures. "Eight main biantennary N-glycan structures can be identified. These comprised six neutral and two acidic (sialylated) glycans. The glycans are designated as G0, G1 and G2, according to the number of terminal galactose residues, and monosialylated and or A2, according to the number of terminal sialic acid residues that decorate the core pentasaccharide (GlcNAc2, Man3). Three of the glycans are fucosylated, giving rise to G0F, G1F and G2F structures. Monosialylation and monogalactosylation may occur on either the α1,3 or a α1,6 arm of the biantennary structures".(Alavi et al., 2011).

In 2006, Kaneko and colleagues discovered that IgG antibodies with Fc domains carrying α2,6-linked sialylated N-glycans represent the anti-inflammatory portion of the IVIg (Kaneko et al., 2006b). Using a K/BxN serum-induced arthritis murine model, they showed that neuraminidase-treated IVIg, which renders them devoid of sialyic acid, were unable to inhibit the inflammatory process of arthritis. Another study demonstrated that *in vitro* α2,3-linked sialylation of IgG Fc did not result in anti-inflammatory activity (Anthony et al., 2008a). Since these specific Fc-α2,6-linked sialylated IgGs (sIgG) account for only 2-4 % of total IVIg, this would explain why such high doses are required to mediate therapeutic efficacy. When fractionating IVIg on a *Sambucus nigra* agglutinin (SNA)–lectin affinity column, the sialic-acid enriched fraction (SA-IVIg) showed protection in the K/BxN arthritis model at only 1/10th of the dosage used with intact IVIg. Similarly to IVIg that has been shown to increase the expression of the inhibitory receptor FcγRIIB on effector macrophages (Bruhns et al., 2003), the mechanism of protection of the sIgG preparation was found to be similar (Kaneko et al., 2006b). A recombinant human IgG1 Fc-sialylated has been engineered and shown to be effective at 33 mg/kg in the K/BxN arthritis model compared to native IVIg, effective at 1 g/kg (Anthony et al., 2008a). A more recent study confirmed these findings in four distinct murine models (two models of ITP using two distinct antiplatelet monoclonal antibodies, one model of inflammatory arthritis, and a model of the skin blistering disease epidermolysis bullosa acquisita pemphigus or EBA) (Schwab et al., 2014). Under both therapeutic and preventive application of IVIg, they demonstrated that the presence of both sialic acid on IVIg and the inhibitory FcγRIIB on macrophages was required for IVIg beneficial effects. The same group lately engineered a tetra-Fc–sialylated (s4-IVIg) IVIg drug candidate produced with IVIg as starting material which was enzymatically modified to maximize Fc sialylation (Washburn et al., 2015). This drug candidate revealed enhanced anti-inflammatory activity up to 10-fold higher than IVIg across the same three animal models already cited above. The importance of sialylation was confirmed in another study where administration of sialic-acid enriched IVIg (SA-IVIg), but not non-SA-IVIg, to OVA-sensitized and intranasal OVA-challenged mice attenuated airway hyperresponsiveness and inflammation comparably with IVIg (Massoud et al., 2013).

Anthony and colleagues have hypothesized that the anti-inflammatory mechanism of the sIgG fraction of IVIg is mediated through binding of the α2,6-linked sialic acid to a C-type lectin receptor, the SIGNR1, which is expressed primarily on splenic marginal zone macrophages in mice or on DCs in human (named DC-SIGN) (Anthony and Ravetch, 2010; Anthony et al.,

2008b). Indeed, the sialylation of IgG Fc leads to a conformational change that would decrease the interaction with FcγRs but trigger DC-SIGN binding (Sondermann et al., 2013). Using their K/BxN arthritis model in mice, they further established that this interaction induced the production of IL-33 from the splenic marginal zone macrophages, leading to expansion of IL-4-secreting basophils. Effector macrophages then respond by increasing expression of the inhibitory FcγRIIB, which shifts the response away from the damaging pro-inflammatory cascade (Anthony et al., 2011). In line with the dominant expression of SIGNR1 on mouse splenic marginal zone macrophages, IVIg activity was also abrogated in splenectomized mice as well as with SIGNR1-blocking Abs or in mice deficient in SIGNR1 (Anthony et al., 2008b). However, the involvement of SIGNR1 in IVIg anti-inflammatory effects may not be limited to its expression on splenic marginal zone macrophages. Indeed, a study in splenectomized mice have shown that IVIg still mediates the suppression of antibody-dependent platelet depletion (Leontyev et al., 2012a). Similarly, another study also established that IVIg activity in ITP suppression was not impaired in splenectomized mice as well as in IL-33-receptor deficient mice or in basophil-depleted mice (Schwab et al., 2012a). Despite the lack of involvement of splenic resident cells, they showed that IVIg activity was still fully dependent on terminal sialic acid residues and SIGNR1, and therefore hypothesized that SIGNR1-positive cell populations outside the spleen are crucial for IVIg activity in murine ITP. Interestingly, the same group demonstrated in a recent study that SIGNR1 was required for IVIg to ameliorate ITP in mice only in prophylactic but not therapeutic conditions (Schwab et al., 2014). Some other mechanisms have also been proposed that could explain the relevance of the sialylation fraction in IVIg. For instance increasing sialylation on monoclonal antibodies IgG1 negatively impacted their cell-surface antigen binding and subsequently lowered ADCC potency of human cells *in vitro* (Scallon et al., 2007). Another group identified that IVIg bound on DCs to the inhibitory C-type lectin DCIR (dendritic cell immune-receptor) and that inhibition of IgG internalization in DCs inhibits the effects of IVIg, but they ruled out any implication of SIGNR1 in this mechanism (Massoud et al., 2013).

In contrast to the studies previously mentioned, several studies suggested that sialylation was not relevant for the effects of IVIg in a murine ITP (Leontyev et al., 2012b) or that the protective effect of IVIg in arthritis models (K/BxN serum transfer as well as AIA) was linked to the Fc domain of IgG without the requirement of sialylation (Campbell et al., 2014). In an EAE model, it was also demonstrated that sialylation was dispensable for IVIg-mediated amelioration

of the disease (Othy et al., 2014). This could be explained by the fact that HPLC and crystallographic analyses observed no conformational changes to the Fc part upon sialylation that could account for the reported interaction with DC-SIGN (Crispin et al., 2013). It was also suggested that, rather than sialyation, it is the increased galactosylation on N-glycans which promotes the association between FcγRIIB and C-type lectin receptor dectin-1 (Karsten et al., 2012). Furthermore, one can question whether the mechanism of action for IVIg reported by Anthony and colleagues in murine studies might play a role in the human situation. Neither DC-SIGN nor sialylated IgG Fc fragments have been shown to be involved in the anti-inflammatory activity of IVIg on human DCs (Bayry et al., 2009). Phagocytosis has been studied in a human *in vitro* system and despite a remarkable inhibition by IVIg, recombinant Fc-sialylated IgG or SA-IVIg were equally active as unsialylated IgG fractions, independently of FcγRIIB expression (Nagelkerke et al., 2014). The effect of IVIg on the inhibition of stimulated human T cells proliferation was not affected after neuraminidase treatment (Issekutz et al., 2015). IVIg treatment did not alter FcγRIIB mRNA expression in circulating human monocytes from Kawasaki patients (Abe et al., 2005) nor increased FcγRIIB expression in monocytes in children with ITP (Shimomura et al., 2012).

In summary, 2-6-sialylated Fc may mediate the efficacy of IVIg in some mouse auto-immune models but may not be relevant for others. The variation in the quality of IVIg batches, as well as the various mouse strains used may explain the conflicting results obtained by the different groups. Further investigations will be therefore needed to evaluate the contribution of the sialylation of IVIg in various auto-immune models. The mechanisms by which sialylation could lead to anti-inflammatory effects, as well as its relevance for human diseases, will also need to be clarified.

3.1.5. Increase in number of regulatory T cells

Protection of EAE by IVIg in a murine model has been associated with increase of peripheral CD4+CD25+Foxp3+ Tregs numbers (Ephrem et al., 2008) and these results have been confirmed in several recent study in murine EAE as well (Othy et al., 2013; Othy et al., 2014). Tregs purified from Herpes Simplex Virus infected mice and IVIg treated mice protected mice from fatal herpes simplex encephalitis (HSE) after adoptive transfer (Ramakrishna et al., 2011). Other data show that IVIg suppressed allogeneic T-cell responses to promote skin allograft acceptance by direct activation of Tregs, indicated by increased expression of HLA-DR, CD69

and CD38 and increased ZAP70 Phosphorylation (Tha-In et al., 2010). IVIg therapy in an intranasal ovalbumin sensitized mouse model of asthma showed that it markedly attenuated lung inflammation and that the draining pulmonary lymph nodes of IVIg treated mice showed a significant increase in Tregs (Kaufman et al., 2011). In a similar model, analogous results were reproduced and interestingly IVIg-primed DCs adoptively transferred to ovalbumin sensitized mice were also able to inhibit airway hyperresponsiveness and induce Treg cells (Massoud et al., 2012).

To draw an analogy to humans, Tregs have been analyzed in 11 patients with various autoimmune rheumatic disease, before and after IVIg treatment (Bayry et al., 2012). 6 patients had a significant increase in number of Tregs, with a mean delta of +5.7 % which represents a 3-4 folds increase. Tjon and colleagues showed that high-dose, but not low-dose, IVIg treatment in patients enhanced the activation status of circulating Tregs, (increased of FoxP3 and HLA-DR expression), but interestingly the percentage of circulating Tregs remained unchanged (Tjon et al., 2013). Patients with Kawasaki disease (KD) showed lower Treg frequency (about 2-fold less, n=8) during the acute phase of disease as well as lower FoxP3 expression (Olivito et al., 2010), and both could be restored after IVIg therapy. Lack of Tregs among KD patients was also confirmed in another clinical study with a higher number of patients (n=18) and similarly Tregs were back to normal ranges after IVIg treatment (Hirabayashi et al., 2013). Importantly, this study highlighted that patients with a more severe reduction in the number of Tregs (25-fold lower compared to IVIg-sensitive patients) were associated with resistance to IVIg therapy.

Thus, the ability of IVIg to influence Treg induction has been shown both in animal models and in human diseases and several potential mechanisms have been proposed (Kaufman et al., 2015; Maddur et al., 2010). For example, Kaveri and colleagues demonstrated that the mechanism by which IVIg induces Treg cells was by the induction of cyclo-oxygenase dependent prostaglandin E2 (PGE2) from human dendritic cells (Trinath et al., 2013b). In their model system already mentioned in section 3.1.4 Massoud et al. reported that sIgGs induced Treg cells and attenuated airway hyperresponsiveness after binding to DCIR (Massoud et al., 2013). Interestingly, transfer of IVIg treated DCs from FcγRs KO mice still increased Treg cells and abrogated inflammation, suggesting that in this asthma model the effects of IVIg on Tregs were independent of FcγRs. The importance of Treg cells in the immune modulation induced by IVIg is also underlined by the studies of De Groot et al. (De Groot et al., 2008), who identified *in*

silico conserved Tregs epitopes named Tregitopes in both the IgG Fc and F(ab')$_2$ regions that bind to multiple MHC Class II determinants. When co-incubated with a specific antigen, Tregitopes suppressed immune response *in vivo* in mice and *in vitro* in human PBMCs toward this antigen, and resulted in the expansion of Tregs together with upregulation of IL-10 secretion. Although not studied directly in their model, they presumed that APCs play an important role in this pathway and by presenting Tregitopes on their surface they directly activate natural Tregs which in turn convert effector T cells in adaptive Tregs, therefore shifting the balance to immune tolerance. However, an independent study demonstrated that Tregitopes didn't prevent or reverse type 1 diabetes in NOD mice (Grant et al., 2013). Therefore, more investigation is still required to elucidate the beneficial effects of IVIg in modulation of Tregs.

3.2. Fab-dependent mechanisms

Although a lot of studies emphasize the role of the IgG Fc-portion, it has also been reported that in several murine and *in vitro* human models the $F(ab')_2$ fragment of IVIg is involved in the immune modulation of the disease process.

3.2.1.   Neutralization of autoantibodies

Considering that IVIg preparations are generated from adults who have been vaccinated and have encountered a multitude of pathogens throughout their life, it is not surprising that IVIg contains IgG molecules specific for foreign antigens that account for its beneficial effect in replacement therapy for immunodeficiencies. On the other hand, one of the first explanations for its anti-inflammatory effect in autoimmune diseases was that there are anti-idiotypic antibodies present in IVIg preparations that neutralize the pathogenic auto-antibodies. Indeed serum from healthy people contains natural antibodies of the IgG, IgM, and IgA isotypes, mostly autoantibodies generated in the absence of foreign antigens and selected by self-antigenic structures in the body. Therefore, these antibodies do not undergo affinity maturation and remain conserved throughout life in normal individuals. Natural autoantibodies are more polyreactive than immune antibodies, in the sense that they can often bind to different antigens (Coutinho et al., 1995). Thus, a considerable fraction of IVIg consists of antibodies capable of interacting with idiotypes (constituents of the variable region) of other antibodies.

Affinity purified disease-specific anti-idiotypic antibodies from IVIg showed good therapeutical effects, as highlighted in several reviews (Seite et al., 2008; Svetlicky et al., 2013; Vani et al., 2008). For instance, the beneficial effect of target-specific IVIg has been proven in animal models of SLE (anti-dsDNA anti-idiotypes) (Shoenfeld et al., 2002), EAMG (anti-acetylcholine receptor anti- idiotypes) (Fuchs et al., 2008), or Pemphigus vulgaris (anti-desmoglein 1+3 anti-idiotypes) (Mimouni et al., 2010). Others showed that pathogenic antibodies from patients' serum could be neutralized by anti-idiotypes antibodies in IVIg preparations, such as anti-factor VIII (hemophilia) (Sultan et al., 1984), anti-GM1 (Guillain-Barré syndrome) (Yuki and Miyagi, 1996), or anti-thyroglobulin (thyroiditis) (Dietrich and Kazatchkine, 1990). These studies indicate that IVIg could be effective through anti-idiotypic antibodies, and the small proportion being specific for the disease of interest might explain the requirement of high doses of IVIg.

Efficacy of anti-pathogenic autoantigen antibodies present in IVIg preparation is largely disease-specific and might vary from batch to batch. Since IVIg have demonstrated beneficial effects in the treatment of a various range of diseases, it is more likely that some additional mechanisms play a role at the same time as well.

3.2.2. Neutralization of various self-proteins

Natural autoantibodies are reactive with a variety of serum and cells self-proteins. It has been demonstrated that IVIg contains low levels of autoreactive IgG antibodies that recognize a wide array of self-antigens. Direct binding of IVIg to some pro-inflammatory proteins will neutralize them, or in some cases it can promote cell death via activation of pro-apoptosis receptors. This includes: pro-inflammatory cytokines such as BAFF and APRIL, two potent B cells activators (Le Pottier et al., 2007) or GM-CSF, IFN-α, IL-1α (Wadhwa et al., 2000); pro-apoptosis cell surface receptor such as Fas (induction of apotosis) (Prasad et al., 1998) or SIGLEC-9 and SIGLEC-8 (von Gunten et al., 2006; von Gunten et al., 2007); adhesion molecules involved in leukocyte trafficking (Vassilev et al., 1999); αβ T-cell receptor (Marchalonis et al., 1992); or against FcγRs (Bouhlal et al., 2014).

3.2.3. Scavenging of complement components

Given the potent pro-inflammatory activity of the complement components, this has been suggested in several studies as a potential pathway by which IVIg is able to block tissue inflammation. IVIg was shown to bind in an anti-idiotypic manner to several activated complement components such as C3a, C3b and C5a via its $F(ab')_2$ fragments, thereby attenuating complement-mediated tissue damage (Arumugam et al., 2007; Basta and Dalakas, 1994; Basta et al., 2003; Berger et al., 1985).

In summary, various IgG molecules reactive against self pro-inflammatory proteins are present in IVIg preparations, but more work needs to be done to elucidate their contributions to IVIg beneficial properties in patients.

3.3. Modulation of immune cells

Immune cells are involved at several stages in the pathogenesis of autoimmune diseases and inflammatory disorders, therefore many studies were aimed at investigating whether IVIg has a direct effect on cells from the innate as well as the adaptive immune system.

3.3.1. Effects of IVIg on innate cellular immunity

F(ab′)$_2$ fragments of IVIg were shown to expand Tregs via induction of cyclooxygenase (COX)-2-dependent prostaglandin E2 (PGE2) in both human DCs and murine DCs in a model of EAE (Trinath et al., 2013b). It was shown that PGE2 may have a net inhibitory effect on the functional activity of maturing DCs by decreasing their ability to attract T cells (Kalinski, 2012). Another study underlined the role of IVIg in inhibiting TLR-mediated activation in human DCs (Bayry et al., 2009). Massoud et al. showed that IVIg binds directly to DCs via DCIR to be internalized, and that DCs were directly involved in the disease recovery since DCs cultured IVIg adoptively transferred to mice before OVA challenge induced Treg cells and inhibited AHR (Massoud et al., 2013). IVIg has been shown to inhibit the maturation of human DCs in vitro by downregulating expression of co-stimulatory molecules (Bayry et al., 2003; Qian et al., 2014). However, Tjon et al. observed the contrary effect in their experiments on human DCS: IVIg did not inhibit, but instead stimulated spontaneous maturation and increased sensitivity of human DCs to T-cell stimulation in a FcγRIIa dependent manner (Tjon et al., 2014). Similarly, the clinical effects of IVIg in ameliorating ITP involved interaction of IVIg with activating FcγRs on mouse DCs, and in contrast to the prevailing theories IVIg did not interact with the inhibitory FcγRIIB (Siragam et al., 2006). Masoud et al. showed that pulmonary DCs from IVIg-treated mice express altered Notch-ligand, including increased Delta-4 and reduced Jagged-1 levels (Massoud et al., 2012). However, another study indicated that IVIg does not modulate the expression of Notch ligands on activated human DCs (Trinath et al., 2013a).

IVIg mediated neutrophils as well as eosinophil death *in vitro* by naturally occurring anti-SIGLEC-9 and anti-SIGLEC-8 autoantibodies, respectively, present in IVIg preparations (von Gunten et al., 2006; von Gunten et al., 2007). In contrast, it was shown that human neutrophils exposed to IVIg showed increased levels of bacterial cell killing, phagocytosis, and autophagy (Itoh et al., 2015).

Tha-In et al. identified a pathway in which IVIg induced maturation of DCs, which activated NK cells, which in their turn mediated apoptosis of the IVIg-DCs by ADCC (Tha-In et al., 2007). They hypothesized that this mechanism downsized the antigen-presenting pool and therefore inhibited T-cell priming. Moreover, beneficial effects of IVIg treatment in patients with Kawasaki disease have been shown to be accompanied by increased NK cell activity in peripheral blood (Finberg et al., 1992).

3.3.2. Effects of IVIg on adaptive cellular immunity

Results of *in vitro* and *in vivo* studies have shown diverse and sometimes contradictory effects of IVIg on B cells. Data obtained with purified human B cells showed that IVIg was not capable of directly inhibiting B cell proliferative responses, unlike T cell responses (Heidt et al., 2009). In line, a recent study demonstrated that inhibitory effect of IVIg on T cells activation *in vitro* was not dependent on B cells (Issekutz et al., 2015). However, some other data indicated that human B cells are resistant to immunomodulation by IVIg-treated DCs, but that IVIg directly inhibited B cell activation and proliferation (Maddur et al., 2011). A direct interaction of IVIg with B cells was shown to occur through CD22, resulting in BCR modulation and induction of apoptosis in mature human B cells in vitro (Seite et al., 2010). The apoptosis theory was also supported by a study in patients suggesting that IVIg therapy may constrain antibody responses by inducing B cell depletion through differentiation into CD21-low B cells that undergo accelerated apoptosis (Mitrevski et al., 2014). Opposing results were found when using mice deficient in B cells or CD22, showing that neither B cells nor CD22 are critical for the anti-inflammatory activity of IVIg in mouse models of rheumatoid arthritis and ITP (Schwab et al., 2012b). Another theory arose regarding IVIg effect on B cells, suggesting that it induces a silencing program similar to anergy rather than apotosis (Seite et al., 2013; Seite et al., 2011). In contrast, some other data provided evidence for stimulation of both splenic B and CD4+ T lymphocytes after i.v. administration of IVIg at high dose in BALB/c mice (Sundblad et al., 1991).

In an EAE model, both IVIg and its F(ab′)$_2$ fragments accounted equally well to the beneficial effect of the therapy, by modulating the polarization of CD4+ T cells towards Tregs and decreasing infiltration of effector T cells in the CNS by sequestering them in lymph nodes (Othy et al., 2013). Addition of IVIg to human T cells in vitro inhibited anti-CD3 and tetanus induced proliferation in a dose dependent manner and also prevented IL-2 secretion (Amran et

al., 1994). Further investigations indicated that the inhibition of IL-2 production by IVIg occurred post-transcriptionally and had no effect on the levels of IL-2 mRNA. (Modiano et al., 1997). A more recent study confirmed these findings, showing that IVIg dose-dependently inhibited T cell proliferation to anti-CD3 stimulation on human PBMCs as well as a broad range of cytokines secretion (Issekutz et al., 2015). However, in rat models of EAE and AIA, administration of IVIg lead to intact or enhanced T-cell proliferative responses to antigens specific to the disease but led to decreased production of the inflammatory cytokine TNF-α (Achiron et al., 1994). Some studies claim that IVIg exerts its anti-inflammatory effects by acting directly on T cells in the absence of accessory cells (MacMillan et al., 2009; Tawfik et al., 2012), whereas others challenged this notion suggesting that T cell modulation is the indirect consequence of a direct effect of IVIg on APCs (Padet and Bazin, 2013; Padet et al., 2011). Thus, the mode of action by which IVIg inhibits adaptive immune cell activation is, so far, not completely elucidated and probably involves multiple pathways.

3.4. Inhibition of antigen presentation

As discussed above it was shown that IVIg inhibited both the *in vivo* and *in vitro* antigen-specific T-cell responses but whether this effect is a consequence of a direct interaction or not remains unclear. Some recent evidences indicated that the suppressive effect of IVIg of T cells might be an indirect consequence of a reduction in the antigen presentation ability of APCs. Aubin and colleagues demonstrated that DO-11.10 cells (TCR transgenic T cells for OVA) incubated together with P388D1 cells (macrophage-like cell line) and OVA decreased their IL-2 secretion in the presence of IVIg (Aubin et al., 2011). Using flow cytometry, they observed that IVIg inhibited the uptake of OVA-immune complexes by P388D1 cells but not the uptake of native OVA. With the same method they showed that IVIg decreased the amount of MHC: peptide complexes presented on the APC surface. They demonstrated that the overall inhibitory effect was FcγR independent. In another study, CD40-activated B cells were co-cultured DO-11.10 cells in presence of native OVA and IVIg (Paquin Proulx et al., 2010). They showed that IVIg inhibited IL-2 secretion, and since IVIg didn't affect the level of MHC-II expression on B cells, they deduced that IVIg inhibited antigen presentation. Addition of HSA to activated B cells did not significantly decrease IL-2 secretion, and flow cytometry showed that IVIg bound to the B cell surface more efficiently than HSA. Therefore the authors suggested a positive relationship between the extent of IVIg internalization and inhibition of antigen presentation. Further studies

reported that IVIg-mediated inhibition of uptake and processing of antigens was associated with an increased accumulation of lipid in DCs, suggested to promote tolerogenic properties (Othy et al., 2012). Additional data supported the notion that such high IVIg doses suggest that only a small fraction of IgG is responsible for the anti-inflammatory effects, and underlined the role of naturally occurring cationic IgGs. Indeed they demonstrated by intracellular fluorescence staining followed by flow cytometry that highly cationic IgG molecules present in IVIg are internalized more efficiently than IVIg in mouse P388D1 cells. These highly cationic IgG also showed improved inhibition of OVA presentation by APCs as determined by the reduction in IL-2 secretion by T cells (Trepanier et al., 2012).

4. Aim of the thesis

We have seen that there is an increasing number of studies examining the potential mode of action of IVIg as an anti-inflammatory agent, but the majority of them leads to contradictory results. Such disparities could be attributed to differences in experimental approaches, animal models, IVIg source, route and timing of IVIg administration, mouse strain and other variables such as the involvement of different anti-inflammatory pathways in humans and mice. The difficulties that emerge to establish a common mechanism may also account from the fact that IVIg therapy targets a broad range of inflammatory diseases with etiologic and pathologic profiles that largely differ from one another. There have been many pathways published from the innate and adaptive immune systems to be potentially targeted by IVIg, but to date there is no convincing evidence that any of these postulated mechanisms account for all its therapeutic benefits. In light of these results, the mechanism by which IVIg mediates its anti-inflammatory activity remains an open question.

The aim of the thesis was to investigate whether IVIg has a direct impact on immune cell populations *in vivo* in mice. More specifically, we wanted to characterize the cells that are affected by IVIg treatment, to understand how this effect could explain the immunomodulatory properties of IVIg. The first part of the thesis aimed at establishing a quick but robust immunization model in mice with ovalbumin (OVA), and to see whether IVIg can efficiently downregulate the antibody response against OVA. Since this model appeared to be suitable to reproduce the inhibitory effects of IVIg on the OVA-specific response, we next determined

which cell populations were affected by IVIg injection by examining various cell surface markers. Size of the lymphoid organs and formation of germinal centers were also compared between animal groups treated with or without IVIg. Of specific interest, comparison with a human monoclonal IgG antibody, adjuvant dependency and IVIg dose dependency were investigated. Moreover, effects of IVIg in TI antigen-immunized mice were studied to clarify T cell involvement in the mediation of IVIg effects. In the second part of the thesis, we addressed the question whether mice were able to mount an efficient antibody response against IVIg and on which IgG regions this response was focused. It was also investigated whether IVIg had an effect on the total IgG present in mouse serum. Additional analyses were conducted on the bone marrow to examine the number of Ig-secreting cells (ISC), as well as to explore any changes in the different B cell populations upon IVIg administration. These studies were performed to understand if IVIg might act by inhibiting the differentiation of OVA-activated B cells into plasma cells. The last part of the thesis includes a series of key control experiments that were conducted to exclude any other parameter that could interfere with the interpretation of the results, such as the formulation of IVIg, the use of the antigen or the adjuvant. Finally, we propose a model in line with the data obtained, that describes the likely sequence of events that may be responsible for the inhibitory properties of IVIg in an antigen-specific antibody response.

Material and Methods

1. Mouse experiments

All animal experiments were performed in accordance with the Federal and Cantonal laws of Switzerland. Animal protocols were approved by the Cantonal Veterinary Office of Baselstadt, Switzerland

1.1. Mice immunization

Mice C57Bl/6NCrl were obtained from Charles River, France. All mice were used at an age of 7-11 weeks. Mice were immunized 3 times once a week s.c in the neck with 50μg OVA/mouse (Invivogen; ref. vac-efova) together with adjuvant as described on Figure 13. The following adjuvants were tested: AddaVax™ (MF59) at 1:5 v/v in 600 μL (Invivogen; ref. vac-adx-10), Aluminum Alhydrogel® 2 % at 1:5 v/v in 600 μL (Invivogen; ref. vac-alu-250), LT (R192G/L211A) at 5 μg/mouse in 500 μL, a double mutant heat-labile toxin from *Escherichia coli*, (kindly provided by Prof. J. D. Clements, Tulane University School of Medicine, USA), CpG ODN 2395 VacciGrade™ (unmethylated CpG motifs oligodeoxynucleotides) at 50 μg/mouse in 500 μL (Invivogen; ref. vac-2395-1), MPLA-SM VacciGrade™ (Monophosphoryl Lipid A from *Salmonella minnesota* R595) at 20 μg/mouse in 500 μL (Invivogen; ref. vac-mpla). Eventually the following compounds were co-injected in the same solution to be tested individually: IVIg (Octagam 10 %; Octapharma), Avastin (Bevacizumab; Roche) or Vectibix (Panitumumab; Amgen) at 50mg/mouse, and Tregitope peptides published by De Groot (De Groot et al., 2008) or peptides identified with the in-house MAPPs assay (see section 2.5) at 25 or 50 μg/mouse each as indicated. All injections volumes were completed to 500 μL or 600 μL as indicated above with DPBS (Gibco Invitrogen; ref. 14190-094). In the context of control experiments, we tested injection of BSA (50 μg/mouse; Sigma ref. A7979) or LPS (25 μg/mouse; Invivogen ref. vac-3pelps). Also as control, IVIg was centrifuged on an Amicon® Ultra centrifugal filter with a 30kDa cut-off (Merck Millipore; ref UFC903024), and flow-through was injected to mice (same volume as IVIg). Injections were performed with BD Microlance Needles 26G x 0.5"/13mm ref. 3038009 and Primo syringes (1mL, ref. 62.1002). Mice were marked and their weight was controlled twice per week. Mice were terminated 24h after the last injection.
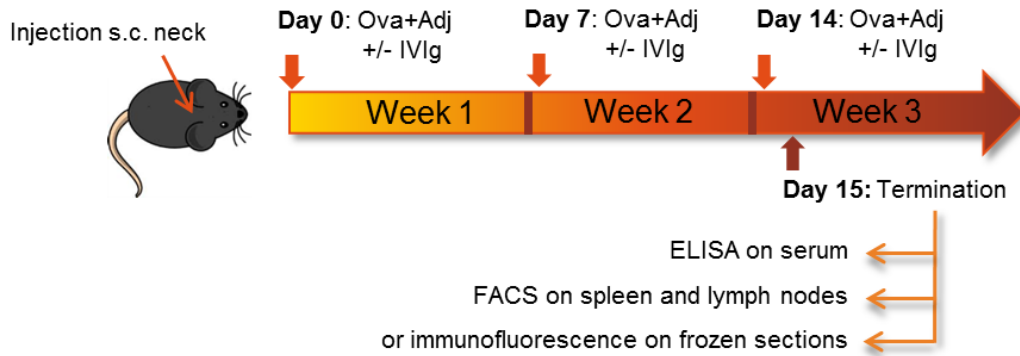
Figure 13: Mouse immunization protocol.

1.2. Necropsy

On the day of termination mice were anesthetized with Isoflurane (AbbVie; ref. B506) 4 % inhalation (supporting gas: O_2). Blood was collected via the retro-orbital path using 20 μL minicaps® disposable capillary pipettes (Hirschmann®; ref. 9000120) and placed in Micro tubes containing serum gel with clotting activator (1.1 mL Z-Gel; Sarstedt; ref. 41.1500.005). Animals were sacrificed by CO_2 inhalation. Death was confirmed by palpation of the heart and dim eyes. Spleen and lymph nodes as well as bone-marrow were dissected out and immediately placed on ice in a 12-well plate (Corning; ref. 3513) containing 2 mL of complete Iscove's media (Iscove`s Modified Dulbecco's Medium (IMDM) Invitrogen ref. 12440046; 1X Glutamax Invitrogen ref. 31980048; 10 % FCS Invitrogen ref. 161140071; 1 % penicillin/streptomycin Invitrogen ref. 15140122; 50 μM Beta-mercaptoethanol Invitrogen ref. 31350; 1x MEM non-essential amino acids Invitrogen ref. 11140; 1 mM sodium-pyruvate Invitrogen ref. 11360). Micro tubes containing blood were centrifuged at 2500 x g (model 5810R, rotor A-4-62; Eppendorf) for 15 min at 10 °C, and serum was placed into a fresh 1.5 mL Eppendorf tube (ref) to be conserved at -20 °C.

1.3. Cells isolation from mouse organs

For spleen and lymph nodes cell suspension was obtained by disrupting organs through a 40 μm nylon cell strainer (BD ref. 352340) thanks to the bottom of piston needle, and washed with 10 mL of media on top of a 50mL Falcon tube (BD ref. 352070). Bone- marrow was extracted by applying 1 mL of media inside the femur bone using a 27G needle on top of a nylon

cell strainer. Cells were then disrupted as described above for spleen and lymph nodes. All samples were centrifuged at 350 x g (Eppendorf 5810R, rotor A-4-62) for 5 min at RT (room temperature). For spleen-derived cells, 1mL of red blood cells lysing buffer (Sigma ref. R7757) was apply and lysis was performed 5 min at RT upon agitation. 20 mL of media was added on top of the spleen cells and they were centrifuged at 350 x g for 5 min. Spleen cells were resuspended in 4 mL of media and lymph nodes or bone-marrow cells in 1 mL, diluted 1:10 in media and counted with the Vi-cell[TM] XR (Beckman-Coulter).

1.4. Antibody staining and flow cytometry

2E6 cells were transferred in a 96-well V-bottom plate (Corning ref. 3894) and centrifuged 2 min at 2000 rpm at 4 °C (Eppendorf 5810R, rotor A-4-62). Cells were washed twice with 200 μL of FACS Buffer (DPBS Gibco Invitrogen ref. 14190-094; 2 % FCS Invitrogen ref. 161140071; 2 μM ETDA Gibco Invitrogen ref. 15575-038). FcγRs were blocked by resuspending cells in 25 μl of rat anti-mouse CD16/CD32 antibodies (BD clone 2.4G2 ref. 553141) diluted 1:100 in FACS Buffer and incubating 5 min at 4 °C. Surface staining was performed by adding on top 25 μl of FACS Buffer containing a combination of the following antibodies (final concentration in the well is indicated for each antibody): CD3-Brilliant violet 510 1:50 (BioLegend clone 17A2 ref. 100233), CD4-APC-Cy7 1:100 (BD Pharmingen clon GK1.5 ref. 552051), CD8α-PE-Cy7 1:100 (eBioscience clone 53-6.7 ref. 25-0081-82), CD25-PercP Cy5.5 1:100 (BioLegend clone 3C7 ref. 101912), CTLA-4-APC 1:50 (BioLegend clone C10-4B9 ref. 106310), CD69-PE 1:50 (BD Pharmingen clone H1.2F3 ref. 553237), CD11c-PercP Cy5.5 1:50 (BD Pharmingen clone HL3 ref. 560584), CD19-APC-CY7 1:100 (BD Pharmingen clone 1D3 ref. 557655), I-A/I-E-Brilliant violet 510 1:500 (BioLegend clone M5/114.15.2 ref. 107635), CD86-APC 1:100 (eBioscience clone GL1 ref. 17-0862-81), CD83-FITC 1:100 (eBioscience clone HB15 ref. 11-0832-82), CD80-PE-Cy7 1:100 (eBioscience clone 16-10A1 ref. 25-0801-82), CD45R/B220-PE-Cy7 1:100 (BioLegend clone RA3-6B2 ref. 03222), CD40-FITC 1:50 (BD Pharmingen clone Mrz 23 ref. 561845), CD43-APC 1:50 (BioLegend clone S11 ref. 143208), IgD-APC-efluor 780 1:100 (eBioscience clone 11-26c ref. 47-5993-82), CD21-PE 1:100 (BioLegend clone 7E9 ref. 123410), CD23-FITC 1:100 (BD Pharmingen clone B3B4 ref. 553138), CD19-Brilliant violet 510 1:100 (BD Pharmingen clone 1D3 ref. 562956), IgM-PercP-eFluor 710 1:100 (eBioscience clone II/41 ref. 46-5790-82), fixable viability dye-efluor 450 1:1000 (eBioscience ref. 65-0866-14). All antibodies were incubated 30 min or overnight at 4 °C.

Cells were then washed twice with 200 μL FACS Buffer, resuspended in 100 μL of Fixation/Permeabilization concentrate (eBioscience ref. 00-5123-43) at 1:4 in diluent (eBioscience ref. 00-5223-56), and incubated at 4 °C for 30 min. Cells were washed twice with 200 μL FACS Buffer and resuspended in 150 μL of FACS Buffer. For intracellular staining, after the fixation/permeabilization incubation, cells were washed twice with 200 μL of 1X permeabilization buffer (eBioscience ref. 00-8333-56), resuspended in 25 μL of 1X permeabilization buffer and incubated with 25 μL of FoxP3-FITC 1:50 final (eBioscience clone FJK-16s ref.72-5775-40) diluted in permeabilization buffer for 30 min at 4 °C. Cells were washed twice with 200 μL permeabilization buffer and resuspended in 150 μL of FACS Buffer.

Flow cytometry measurements were performed on a FACS Canto II instrument (BD) and the data were analyzed with FlowJo software (Tree Star).

1.5. Immunofluorescence

After necropsy organs were frozen in biopsy holders (Cryomold®; Medite; ref. 81-0785-00) containing OCT compound (Tissue-Tek®; Sakura; ref. 4583) by being placed directly on dry ice and later on transferred to a -80 °C deep freezer. Sections of 5 μm were cut using a cryostat (Hyrax C50; Zeiss) and applied on slides (SuperFrost® Plus; VWR ref. 631-0108). Slides were air-dried 1 h at RT before being kept at -80 °C.

Prior to staining, slides were thawed 1 h at RT to avoid water condensation on tissues. The tissue zone was delimited on the slide using the ImmEdge hydrophobic barrier pen (Vector Lab; ref. H-4000). Tissues were fixed 10 min in PFA 4 % (Sigma; ref. 16005; diluted in DBPS), rinsed 5 min under tap water, and washed in PBS-Tween 0.05 % (Calbiochem; ref. 524653; 1 tablet for 1L ddH$_2$O) twice 5 min. Blocking was performed by covering the slide with drops of Image-IT FX Signal Enhancer (Life Technologies; ref. I36933). After 30 min incubation at RT, slides were washed twice 5 min in PBS-Tween 0.05 %. Primary anti-mouse antibodies were diluted in IHC diluent (Enzo; ref. 950-244-0250) as follows: rat anti-mouse T- and B-cell activation antigen-FITC at 10 μg/mL (BD; clone GL7 ref. 562080), PNA-biotin from *Arachis hypogaea* at 10 μg/mL (Sigma; ref. L6135-1MG) polyclonal rabbit CD3ε at 10 μg/mL (Abcam; ref. ab49943), rat CD45R at 1 μg/mL (Serotec; clone RA3-6B2 ref. MCA1258GT), Armenian hamster CD11c-biotin at 10 μg/mL (BioLegend; clone N418 ref. 117304), OVA-FITC at 10 μg/mL (Molecular Probes; ref. O23020), rabbit polyclonal anti-human IgGs at 10 μg/mL (Jackson; ref. 309-005-

082), goat polyclonal anti-mouse IgGs at 10 μg/mL (LifeSpan; ref. LS-C60700-2000). 400 μl of primary antibodies mixture were applied per slide and incubated overnight at 4 °C.

Slides were washed twice for 5 min in PBS-Tween 0.05 %. Secondary antibodies were all diluted 1:200 in IHC diluent (Enzo; ref. 950-245-0100) and were the following: mouse anti-FITC-Alexa Fluor® 488 (Jackson; ref. 200-542-037), streptavidin-Alexa Fluor® 647 (Life Technologies; ref. S21374), donkey anti-rabbit-Alexa Fluor® 594 (Jackson; ref. 711-585-152), donkey anti-rat-Cy3 (Jacskon; ref. 712-165-150), streptavidin-Alexa Fluor® 594 (Life Technologies; ref. S11227), donkey anti-goat-Alexa Fluor® 647 (Jacskon; ref. 705-605-147), donkey anti-rabbit-Alexa Fluor® 488 (Jacskon; ref. 711-545-152). 400 μl of secondary antibodies mixture were applied per slide and incubated 30 min at RT. Slides were washed twice for 5 min in PBS-Tween 0.05 %.

For counterstaining DAPI (Molecular Probes; ref. D1306) was diluted to 2 ug/ml in DPBS and 400 μl were applied per slide for 15 min at RT. Slides were washed twice for 5 min in PBS-Tween 0.05 % and once for 5 min under tap water. Slides were subsequently mounted in Fluoromount™ Aqueous Mounting Medium (Sigma; ref. F4680) with coverslips (24 mm x 50 mm; VWR; ref. 631-1574), air-dried at RT and cleaned with ethanol before being kept at 4 °C in the dark.

Images were acquired with NanoZoomer 2.0 HT (Hamamatsu) and analyzed with NDP.view2 software (Hamamatsu).

1.6. ELISA

1.6.1.   Mouse anti-OVA Ig

Mouse OVA-specific IgG$_1$ antibodies were measured using the kit from Cayman; ref. 500830 and the instructions provided by the manufacturer were followed. Briefly, standard (mouse anti-OVA IgG$_1$ provided in the kit) was serially diluted 1:2 in assay buffer to get a range of 8 standard points from 1.56 ng/mL to 200 ng/mL. Mouse serum samples were thawed and diluted in assay buffer as follows: 1:10 000 for mice terminated 2 weeks after the first bolus of immunization with adjuvant LT (R192G/L211A) or Aluminum, 1:50 000 with adjuvant MF59, 1:2000 with adjuvant MPLA-SM and 1:500 with adjuvant CpG ODN 2395. 100 μL of standard and samples were applied on OVA precoated 96-well strip plate and incubated 2h at RT on an

orbital shaker (Titramax 1000; Heidolph). Plates were washed three times with the plate washer BioTek ELx 405RS and 100 μL of goat anti-mouse IgG$_1$ polyclonal antibody conjugated to HRP were added to each well for 1 h at RT with shaking. Plates were washed and 100 μL of TMB substrate solution per well were added for 15 min at RT with shaking, followed by 100 μL of HRP Stop solution. OD was acquired at a wavelength of 450 nm on a Versa max reader (Molecular Devices). Results were analyzed on the Softmax® Pro software (Molecular Devices) and data expressed as relative units compared to standard.

Mouse OVA-specific total IgG antibodies were measured using the kit from Chondrex ref. 3011, and the instructions provided by the manufacturer were followed. Briefly, plates were coated with 100 μL of OVA per well at 10 μg/mL and incubated at 4 °C overnight. Plates were washed three times with the plate washer BioTek ELx 405RS and 100 μL of blocking buffer were added to each well for 1 h at RT. Standard (mouse IgG, clone L-71 - Dr. Shin Yoshino of Kobe Pharmaceutical University) was serially diluted 1:2 in Solution C from 12.5 ng/mL to 0.098 ng/mL. Mouse serum samples were thawed and diluted 1:10 000 in Solution C. After washing, 100 μL of standards and serum samples were added to each well and incubated 2 h at RT on an orbital shaker (Titramax 1000; Heidolph). Plates were washed, 100 μL/well of detection antibody (HRP-conjugated goat Anti-Mouse IgG polyclonal antibody at 100 ng/mL) was added for 1 h at RT. After washing, 100 μL/well of TMB solution was applied for 20 min at RT, followed by 50 μL of Stop Soltion (2N sulfuric acid). OD was acquired at a wavelength of 450 nm on a Versa max reader (Molecular Devices). Results were analyzed on the Softmax® Pro software (Molecular Devices) and data expressed as relative units compared to standard.

Mouse OVA-specific IgM antibodies were detected as follows. OVA (Invivogen; ref. vac-efova) was diluted to 10 μg/mL in DPBS and plates (Greiner; medium binding, ref. 655001) were coated with 70 μL/well overnight at 4 °C. Plates were washed three times with the plate washer BioTek ELx 405RS with 300 μL/well of PBS-Tween 0.05 % (Calbiochem; ref. 524653; 1 tablet for 1 L ΔH$_2$O), and blocked for 2 h at RT with 200 μL/well of FCS 10 % in DBPS. Mouse serum samples were thawed and diluted 1:100 in blocking buffer. Standard (mouse IgM anti-OVA; Chondrex Clone 2H11A8, ref. 7097) was serially diluted 1:2 in blocking buffer from 125 ng/mL to 0.12 ng/ml. 50 μL of serum and standards samples were added into each well and incubated overnight at 4 °C. Plates were washed and 50 μL/well of detection antibody (polyclonal goat anti-mouse IgM coupled to Alcaline Phosphatase; Southern ref. 1021-04) diluted 1:500 in blocking

buffer were added for 2 h at RT under shaking (Titramax 1000; Heidolph). After washing, 100 μL/well of substrate were added (p-Nitrophenyl Phosphate from Sigma; ref. N2765; add 1 tablet of 20 mg for 20 mL of developing buffer prepared with Na_2CO_3 15 mM; $NaHCO_3$ 35 mM, NaN_3 3 mM at pH 9.6) for 15 min at RT under shaking. OD was acquired at a wavelength of 405 nm on a Versa max reader (Molecular Devices). Results were analyzed on the Softmax® Pro software (Molecular Devices) and data expressed as relative units compared to standard.

1.6.2. Mouse anti-NP IgG and IgM

Capture antigen, NP-BSA (ratio 41, Biosearch Technologies; ref. N-5050H-10) was diluted to 10 μg/mL in DPBS, and plates (Greiner; medium binding, ref. 655001) were coated with 70 μL/well overnight at 4 °C. Plates were washed three times with the plate washer BioTek ELx 405RS with 300 μL/well of PBS-Tween 0.05 % (Calbiochem; ref. 524653; 1 tablet for 1 L ΔH$_2$O), and blocked for 1 h at RT with 200 μL/well of FCS 10 % in DBPS. Mouse serum samples were thawed, diluted 1:500 in blocking buffer and added at 50 μL/well for 2 h at RT on an orbital shaker (Titramax 1000; Heidolph). After washing, 50 μL/well of detection antibody (polyclonal goat anti-mouse IgM coupled to Alcaline Phosphatase; SouthernBiotech ref. 1021-04 or polyclonal goat anti-mouse IgG coupled to Alcaline Phosphatase; SouthernBiotech ref. 1030-04) diluted 1:500 in blocking buffer were added for 1 h at RT with shaking. After washing 100 μL/well of substrate were added (p-Nitrophenyl Phosphate from Sigma; ref. N2765; add 1 tablet of 20 mg for 20 ml of developing buffer prepared with Na_2CO_3 15 mM; $NaHCO_3$ 35 mM, NaN_3 3 mM at pH 9.6) for 15 min at RT with shaking. OD was acquired at a wavelength of 405 nm on a Versa max reader (Molecular Devices).

1.6.3. Mouse total Ig

Capture antibodies were polyclonal goat anti-mouse IgM (SouthernBiotech; ref. 1021-01), anti-mouse IgG adsorbed against human sera (SouthernBiotech; ref. 1030-01) or anti-mouse IgA (SouthernBiotech; ref. 1040-01). They were diluted to 10 μg/mL in DPBS and plates (Greiner; medium binding, ref. 655001) were coated with 70 μL/well overnight at 4 °C. Plates were washed three times with the plate washer BioTek ELx 405RS with 300 μL/well of PBS-Tween 0.05 % (Calbiochem; ref. 524653; 1 tablet for 1 L ΔH$_2$O), and blocked for 1 h at RT with 200 μL/well of FCS 10 % in DBPS. Mouse serum samples were thawed and diluted in blocking buffer as follows: 1:20 for IgG$_{2a}$ detection, 1:2500 for IgG$_{2b}$, 1:800 for IgG$_3$, 1:15 000 for IgG$_1$,

1:25 000 for IgG, 1:3500 for IgM and 1:600 for IgA. Mouse Ig isotypes standards (SouthernBiotech; ref. 5300-01) were serially diluted 1:2 from 1000 ng/mL to 0.98 ng/mL in blocking buffer. Serum samples and standards were added at 50 µL/well for 2 h at RT on an orbital shaker (Titramax 1000; Heidolph). After washing, 50 µL/well of the corresponding detection antibody diluted 1:500 in blocking buffer were added: polyclonal goat anti-mouse IgM coupled to alkaline-phosphatase (SouthernBiotech; ref. 1021-04), anti-mouse IgG adsorbed against human sera (SouthernBiotech; ref. 1030-04), anti-mouse IgG_1 adsorbed against human sera (SouthernBiotech; ref. 1070-04), anti-mouse IgG_{2a} adsorbed against human sera (SouthernBiotech; ref. 1080-04), anti-mouse IgG_{2b} adsorbed against human sera (SouthernBiotech; ref. 1090-04), anti-mouse IgG_3 adsorbed against human sera (SouthernBiotech; ref. 1100-04), anti-mouse IgA (SouthernBiotech; ref. 1040-04). Plates were incubated 1 h at RT with shaking. After washing 100 µL/well of substrate were added (p-Nitrophenyl Phosphate from Sigma; ref. N2765; add 1 tablet of 20 mg for 20 mL of developing buffer prepared with Na_2CO_3 15 mM; $NaHCO_3$ 35 mM, NaN_3 3 mM at pH 9.6) for 15 min at RT with shaking. OD was acquired at a wavelength of 405 nm on a Versa max reader (Molecular Devices). Results were analyzed on the Softmax® Pro software (Molecular Devices) and data expressed as relative units compared to standard.

1.6.4.   Mouse anti-IVIg Ig and anti-Avastin Ig

IVIg (Octagam 10 %; Octapharma), Avastin (Roche), Avastin-Fc and IVIg-Fc (both internally produced, see section 5.6) were diluted to 1 µg/mL in DPBS and coated with 70 µL/well in Greiner plates medium binding (ref. 655001).   IVIg-Fab and IVIg-(Fab'$_2$) fragments were diluted to 10 µg/mL in DPBS and coated with 70 µL/well in Costar plates high binding (ref. 9018). Coating occurred overnight at 4 °C. Plates were washed three times with the plate washer BioTek ELx 405RS with 300 µL/well of PBS-Tween 0.05 % (Calbiochem; ref. 524653; 1 tablet for 1 L ΔH_2O), and blocked for 1 h at RT with 200 µL/well of FCS 10 % in DBPS. Mouse serum samples were thawed and diluted in blocking buffer as follows: 1:500 to measure mouse anti-IVIg and anti-Avastin antibodies, 1:100 for anti-IVIg-Fc and 1:50 for anti-IVIg-Fab or anti-IVIg-(Fab'$_2$). Standard (mouse polyclonal IgG anti-human IgG (H+L), Jackson Immunoresearch; ref. 209-005-082) was serially diluted 1:2 from 125 ng/mL to 0.12 ng/mL in blocking buffer. Serum samples and standards were added at 50 µL/well for 2 h at RT on an orbital shaker (Titramax 1000; Heidolph). After washing, 50 µL/well of the corresponding

detection antibody diluted 1:500 in blocking buffer were added: polyclonal goat coupled to alkaline-phosphatase anti-mouse IgM (SouthernBiotech; ref. 1021-04), anti-mouse IgG adsorbed against human sera (SouthernBiotech; ref. 1030-04), anti-mouse IgG_1 adsorbed against human sera (SouthernBiotech; ref. 1070-04), anti-mouse IgG_{2a} adsorbed against human sera (SouthernBiotech; ref. 1080-04), anti-mouse IgG_{2b} adsorbed against human sera (SouthernBiotech; ref. 1090-04), anti-mouse IgG_3 adsorbed against human sera (SouthernBiotech; ref. 1100-04), anti-mouse IgA (SouthernBiotech; ref. 1040-04). Plates were incubated 1 h at RT with shaking. After washing 100 µL/well of substrate were added (p-Nitrophenyl Phosphate from Sigma; ref. N2765; add 1 tablet of 20 mg for 20 ml of developing buffer prepared with Na_2CO_3 15 mM; $NaHCO_3$ 35 mM, NaN_3 3 mM at pH 9.6) for 15 min at RT with shaking. OD was acquired at a wavelength of 405 nm on a Versa max reader (Molecular Devices). Results were analyzed on the Softmax® Pro software (Molecular Devices) and data expressed as relative units compared to standard.

1.6.5. Competition assay

Serum from mice injected 3 times weekly with 1mg/mL of IVIg was incubated with 10, 20 or 50 mg/mL of IVIg or Avastin in a final volume of 20 uL. Samples were incubated 1 h at 37°C. IVIg-specific IgG and total mouse IgG were measured by ELISA as previously described.

1.6.6. ELISPOT

Capture antibodies (polyclonal goat anti-mouse IgG adsorbed against human sera, SoutherBiotech, ref. 1030-01; or polyclonal goat anti-mouse IgM, SoutherBiotech, ref. 1021-01) were diluted to 10 µg/mL in coating buffer (45.2 mM of $NaHCO_3$ and 18 mM of Na_2CO_3). Capture antigen (OVA, Invivogen; ref. vac-efova) was diluted to 5 µg/mL in coating buffer. Nitrocellulose membrane plates (Millipore; ref. MAHA S4510 were coated with 70 µL/well, and incubated overnight at 4 °C. Plates were washed 3 times with 1X PBS by inverting the plates and eliminating carefully the wash solution by flicking the plates firmly several times face down onto a sheet of paper tissue. For blocking, 200 µL/well of PBS + 1 % BSA were added and incubated 30 min at 37 °C. Blocking solution was eliminated carefully by flicking the plates firmly several times face down. Plates were then pre-incubated with 100 µL/well of complete B cell medium (RPMI, Invitrogen ref. 21875034; 1X MEM non-essential amino acids, Invitrogen ref. 11140; 1X Sodium Pyruvate, Invitrogen ref. 11360070; 50 µM Beta mercaptoethanol, Invitrogen ref. 1350;

1X Kanamycin, Invitrogen ref. 15160-047; 1X penicillin/streptomycin, Sigma ref. P4333; 10 % FCS Hyclone, Invitrogen ref. 10100-147), the same medium used to plate cells later. For measuring mouse total IgG and IgM secreting cells, cells obtained after mouse necropsy (see section 1.3 for cells isolation from mouse organs) were applied on the plate at 200 000, 40 000, 8000, or 1600 cells/well in 100 μL of B cell medium. To measure the specific anti-OVA IgG secreting cells, cells obtained after mouse necropsy were plated at 200 000 cells/well in 100 μL of B cell medium, and half a plate was covered for each sample to increase the chances of detection of these very specific cells. Plates were incubated overnight at 37 °C.

Plates were manually washed 4 times with PBS 0.25 % Tween 20 and 3 times with 1X PBS, before being rinsed once with distilled water (200 μL/well) for 5 minutes. Detection antibodies (polyclonal goat biotinylated anti-mouse IgG, SouthernBiotech, ref. 1030-08 or polyclonal goat biotinylated anti-mouse IgM, SouthernBiotech, ref. 1020-08) were diluted 1:2000 in PBS + 1 % BSA, added at 70 μL/well and incubated 2 h at RT. Plates were washed 4 times with PBS 0.25 % Tween 20 and 3 times with 1X PBS. Streptavidin-HRP (SouthernBiotech, ref. 7100-05) was diluted 1:400 in PBS + 1 % BSA, added at 70 μL/well and incubated 1 h at RT. Plates were washed as described above. The developing solution was prepared just before use by dissolving one tablet of AEC dye (Sigma; ref. A6926) in 1,6 mL of dimethylformamide (Sigma; ref. D4551). 200 μL of this AEC solution were then added to 9 mL of sodium acetate buffer (30 mM of glacial acetic acid + 70 mM of sodium acetate hydrate) and filtered on a 0,45 nm filter (Corning; ref. 431220) before adding 4 μL of H_2O_2 (Sigma; ref. H1009). 70 μL of the developing solution were added into each well and plates were incubated in the dark at RT until individual spots could be visualized (approximately 10 min). Finally, plates were extensively washed with tap water and air-dried at RT. Plates were read on a CTL-ImmunoSpot® Analyzer (Cellular Technology Ltd) with the ImmunoCapture[TM] Version 6.1 Software and spots were counted with ImmunoSpot® Professional Version 4.0.

1.7. AIA model

Balb/cByJ mice were purchased from Charles River (France) and used at the age of 8 weeks. Mice were sensitized on day-21 with a solution homogenate containing 2 mg/mL of methylated BSA (mBSA) (Sigma ref. A1009) in 5% glucose solution (B.Braun Medical; ref. 395147) + 1mL of Complete Freund Adjuvant (DIFCO Laboratories; ref. H37 Ra). Twice, 50 μl of this solution were injected intra-dermally in the back of the animal, once on each side respectively (*these*

injections were kindly performed by Bernhard Jost, Novartis Institute for Biomedical Research, ATI, IPH). Mice were sensitized a second time on day-14 as described above. On day 0, mice were injected intra-articularly with 10 µl of mBSA 10 mg/mL with 5 % glucose in the right knee or with 10 µl of glucose 5%. Intra-articular injections were performed with the help of a stepper (Tridak; ref. 4001.010) (*kindly done by Janet Dawson, Novartis Institute for Biomedical Research, ATI, IPH*). In the prophylactic model, IVIg (Octagam 10 %; Octapharma) was injected at 50 mg/mouse sub-cutaneously in the neck on days -21, -14 and day 0, whereas for the therapeutic model, IVIg was injected at 50 mg/mouse sub-cutaneous in the neck on day 0 only. DBPS (Gibco Invitrogen; ref. 14190-094) was injected as control. Swelling of the knee was measured every 2-3 days as indicated with a digimatic caliper (Mitutoyo; ref. CD-15CP) (*kindly done by Bernhard Jost*).

2. MAPPs assay

MAPPs stands for MHC-II associated peptides proteomics and enables isolating and identifying naturally presented MHC-II associated peptides directly from human DCs or mouse PBMCs. MAPPs assay has been described by (Rombach-Riegraf et al., 2014), as illustrated on Figure 14.
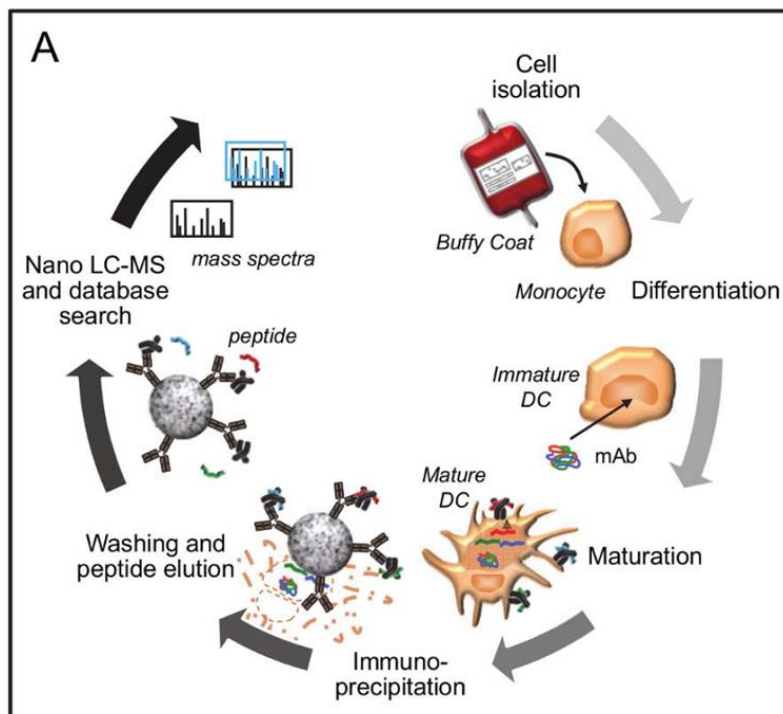
Figure 14: Illustration of MAPPs assay procedure for human DCs. "Monocytes are isolated from human buffy coats and differentiated to immature DCs in the presence of cytokines. Immature DCs are loaded with human IgGs and induced to maturation with LPS. After 24 hours, mature DCs are frozen. After lysis of mature DCs, HLA-DR:peptide complexes are isolated via immunoprecipitation using anti-HLA-DR coated beads. After several wash steps, peptides are eluted from HLA-DR complexes by pH shift and analysed by nano LC-MS with subsequent sequence identification via SEQUEST database search." (Rombach-Riegraf et al., 2014)**.**

2.1. Isolation of human monocytes

PBMCs were isolated from human buffy coats sampled from consented healthy donors (Swiss Red Cross, Bern) according to local ethical practice. Blood from one buffy coat was added to 160 mL of pre-warmed RPMI (Gibco Invitrogen ref. 31870-074) with 1000 units of Liquemine (Drossapharm) before being distributed in Leucosep® tubes (Greiner Bio One; ref. 227290) that have been pre-centrifuged quickly with 15.5 ml Ficoll Paque Plus (GE Healthcare ref. 17-1440-03). Blood was centrifuged at 1000 x g for 10 min at 18 °C (Thermo Scientific™ Sorvall Legend XTR, rotor 75003667). Supernatant above the interphase was removed by aspiration and the PBMCs layer above the filter was recovered and washed several times with warm RPMI (340 x g, 5 min). Erythrocytes were lysed by adding 50 mL of pre-warmed ammonium chloride buffer to the cell pellet previously re-suspended (144 mM of NH_4Cl + 18 mM of Tris at pH 7.2, sterile filtered). Cells were washed twice with RPMI and counted with the Vi-cell™ XR (Beckman-Coulter).

2.2. Differentiation to human DCs and loading

The isolated PBMCs were washed and resupended in 600 µL of EDTA buffer per 1 E^8 cells (0.5 % HSA Sigma; ref. A-3782-1G + 1 mM EDTA Gibco; ref.15575, in DPBS; Gibco ref. 14190094). PBMCs were labeled with 50 µL/1E^8 cells of human anti-CD14 microbeads (Milteny Biotech, MACS®, ref. 130-050-201) for 15 min at 4 °C. After filtration of labeled cells through pre-separation filters (Miltenyi Biotech, ref. 130-041-407), $CD14^+$ cells were magnetically separated with LS MACS® (Miltenyi Biotech, ref. 130-042-401) columns in a magnetic field. Cells were counted with the Vi-cell™ XR (Beckman-Coulter) and resuspended to a concentration of 3 E^5 cells/mL in DC medium (RPMI 1640, Gibco ref. 31870-025; 10 % FCS, Invitrogen ref. 161140071; 1X Glutamax, Gibco ref. 35050-038; 1X non-essential amino acids, Gibco ref. 11140-035; 1X Na-Pyruvate, Gibco ref. 11360-039; 1X Kanamycine, Gibco ref. 15160-047; 3 ng/ml IL-4, R&D ref. 204-IL-050; 33 ng/mL GM-CSF, R&D ref. 215-GM-050). Monocytes were plates in cell culture dishes (Corning; ref. 430167) at 5.4 E^6 cells/plate and differentiated to immature DCs for 5 days at 37 °C and 5 % CO_2.

Immature DCs were induced to maturation by adding LPS at 1 µg/mL (Sigma, ref. 5886). For identifying well-presented peptides derived from IVIg, DCs were simultaneously loaded with IVIg (Octagam; Octapharma) at 2.5 nmol/mL. In the context of a competition assay for peptides

presentation, DCs were simultaneously loaded with OVA at 14 nmol/mL and IVIg either at 14 nmol/mL or at 117 nmol/mL (*DCs stimulation for the competition MAPPs assay were kindly performed by Sascha Gottlieb, Novartis Pharma AG; TD NBEs; IBP).* Unloaded DCs served as negative control. After incubation for 24 hours at 37 °C and 5 % CO_2, DCs were harvested, washed in PBS, and cell pellets were frozen at -80 °C.

2.3. MHC-II peptide isolation from human DCs

Monoclonal antibodies specific for human HLA-DR molecules were generated in-house using the mouse hybridoma cell line L243. Protein A purified anti-HLA-DR antibody was immobilized on NHS-Mag Sepharose activated beads (GE Healthcare; ref. 28-9811-57) according to the manufacturer's protocol and stored at 4 °C in DPBS containing 0.02 % sodium azide. For confirmation of HLA-DR depletion efficiency of the L243-conjugated beads, cell lysates before and after immunoprecipitation with the beads were analyzed by Western Blotting using the HLA-DR-specific mAb 1B5 (Lifespan Biosciences, ref. LS-B2858-50).

For isolation of HLA-DR associated peptides, DC pellets were lysed 200 μL of hypotonic buffer containing 1 % Triton X-100 (Roche; ref. 11332481001) and protease inhibitor tablets (Roche; ref. 11836153001) for 1 hour at 4 °C on a horizontal shaker at 1100 rpm. After centrifugation, the lysate was incubated over night at 4 °C with L243-conjugated beads for immunoprecipitation. After washing with wash buffer (PBS containing 0.5 % Zwittergent) and several wash steps with distilled water, peptides were eluted from HLA-DR molecules by adding 0.1 % trifluoracetic acid (Sigma; ref. 40967) at 37 °C, lyophilized using an Eppendorf Concentrator 5301 and stored at 4 °C.

2.4. MHC-II peptides isolation from mouse lymphoid organs

Monoclonal antibodies specific for mouse I-A molecules were generated in-house using the mouse hybridoma cell line Y-3P. Protein A purified anti-I-A antibody was immobilized on NHS-Mag Sepharose activated beads (GE Healthcare; ref. 28-9811-57) according to the manufacturer's protocol and stored at 4 °C in DPBS containing 0.02 % sodium azide. For confirmation of I-Ab depletion efficiency of the Y-3P-conjugated beads, cell lysates before and after immunoprecipitation with the beads were analyzed by Western Blotting using the I-A specific mAb generated in-house using the mouse hybridoma cell line KL295.

For isolation of I-Ab associated peptides, lymphoid organs from untreated C57Bl/6NCrl mice (Charles River) mice were smashed with a polytron (Kinematica PT 1600 E) in 500 µL of hypotonic buffer containing 1 % Triton X-100 (Roche; ref. 11332481001) and protease inhibitor tablets (Roche; ref. 11836153001) and lysed for 1 hour at 4 °C on a horizontal shaker at 1100 rpm. After centrifugation, the lysate was incubated overnight at 4 °C with Y-3P-conjugated beads for immunoprecipitation. After washing with wash buffer (PBS containing 0.5 % Zwittergent) and several wash steps with distilled water, peptides were eluted from I-A molecules by adding 0.1 % trifluoracetic acid (Sigma; ref. 40967) at 37 °C, lyophilized using an Eppendorf Concentrator 5301 and stored at 4 °C.

2.5. Peptides identification and synthesis

Lyophilized peptides were resuspended in hydrophilic buffer containing 5 % acetonitrile, and 1.1 % formic acid and injected onto a self-packed fused-silica C18 reversed phase nano-HPLC column. Peptide identification was performed using liquid chromatography (nano capillary system, Dionex Corporation) on a reversed phase column connected to a mass spectrometer (LTQ Velos Orbitrap) via electrospray ionization (LC-ESI-MS/MS) (*measurements kindly performed by Stephan Koepke, Novartis Pharma AG; TD NBEs; IBP)*. A database was created by combining either the human IPI (International Protein Index) v3.70 or the mouse IPI v3.87 with the NCBI Ig sequences (NCBI IgBLAST- retrieve Ig sequences). Peptides were identified using a database search approach with the SEQUEST algorithm. Peptides with a delta mass of <10 ppm to the expected mass, cross correlation values of XCorr > 1.8 for singly charged ions, > 2.3 for doubly charged ions, >2.8 for triply charged ions and > 3.3 for quadruply charged ions and a delta cross correlation (dCn) > 0.1 were considered as true hits. Peptides were aligned against a human or a mouse antibody sequence, respectively, using an in-house sequence alignment tool. Selected peptides as well as published peptides 289 and 167 (De Groot et al., 2008) were synthesized by ProImmune with a purity >90%. Lyophilized peptides were all dissolved in DMSO at 10 mg/mL followed by sonication for 20 min, and stored at -80 °C.

3. Human T cell proliferation assays

3.1. CFSE labelling

PBMCs were isolated as described in section 2.1. PBMCs were labelled with 1 μM CFSE (Invitrogen, ref. C34554) at a concentration of 1 E^6 cells/mL in pre-warmed RPMI (Gibco Invitrogen ref. 31870-074) for 10 min at 37 °C in a 250 mL flask (Corning; ref. 734-1713) held vertically. Cells were then distributed in Falcon tubes (BD; ref. 352070) for being washed twice with 50 mL of warm RPMI (centrifugation 350 x g, 5 min, Thermo Scientific™ Sorvall Legend XTR, rotor 75003667). PBMCs were resuspended in X-Vivo 15 medium (Lonza; ref. BE04-418F) supplemented with 10 % FCS (Invitrogen; ref. 161140071) and 1X Glutamax (Invitrogen; ref. 35050038), and counted with the Vi-cell^{TM} XR (Beckman-Coulter). Cell concentration was adjusted to $5E^6$ cells/mL and 1 mL/well were distributed in a 12-well plate (Corning; ref. 3513). Unlabelled cells were also prepared and plated at the same concentration to serve as compensation control for flow-cytometry.

3.2. Cell stimulation

In order to induce T-cell proliferation, Tetanus Toxoid (TT) (Novartis Marburg; lot 317705010) was added to a final concentration of 6 μg/mL per well. Potential inhibitors of TT-induced T-cell proliferation were tested individually at the following final concentration in the well: IVIg (Octagam 10 %; Octapharma) at 6 mg/mL or 0.6 mg/mL; human Tregitopes 289 or 167 (De Groot et al., 2008) or selected in-house identified peptides (MAPPs assay as described in section 2.5) at 10 μg/mL. The allergen birch pollen Betv1a peptide (TPDGGSILKISNKYHTKGDH; ProImmune) was used as a control peptide at 10 μg/mL. Since all peptides tested were dissolved in DMSO, TT with DMSO 0.1 % v/v served as a control. PHA (Sigma; ref. L1668) was used as a positive control for T-cell proliferation and was added to a final concentration of 1 μg/mL per well. Unstimulated cells served as negative control. Cells were incubated at 37 °C and 24 h later 1 ml of fresh complete X-Vivo 15 medium was added on top of each well. Cells were harvested on day 7.

3.3. Antibody staining and flow cytometry

On day 7, plates were centrifuged at 2000 rpm for 5 min (Eppendorf 5810R, rotor A-4-62). 1 mL/well of supernatant was harvested and placed at -20 °C for ELISA measurement. Cells were resuspended by pipetting up and down and transported into a 96-deep well plate (Corning; ref. 3960), centrifuged at 2000 rpm for 5 min, washed once with 300 μL of FACS Buffer (DPBS Gibco Invitrogen ref. 14190-094; 2 % FCS Invitrogen ref. 161140071; 2μM ETDA Gibco Invitrogen ref. 15575-038), and resuspended in 200 μL of FACS Buffer. 100 μL of this cell suspension were transferred to a V-bottom 96-well plate (Corning ref. 3894) and centrifuged 2 min at 2000 rpm at 4 °C (Eppendorf 5810R, rotor A-4-62). Cells were washed twice with 200 μL of FACS Buffer (DPBS Gibco Invitrogen ref. 14190-094; 2 % FCS Invitrogen ref. 161140071; 2 μM ETDA Gibco Invitrogen ref. 15575-038). FcγRs were blocked by resuspending cells in 100 μL of 200 μg/mL of IVIg (Octagam; Octapharma) and incubating for 20 min at 4 °C. Cells were centrifuged and resuspended in 25 μL of FACS Buffer. Surface staining was performed by adding 25 μl of FACS Buffer containing a combination of the following antibodies (final concentration in the well is indicated for each antibody): CD3-Brilliant Violet 510 1:100 (BioLegend clone OKT3; ref. 317331), CD4-APC-CY7 1:100 (BD Pharmingen clone RPA-T4; ref. 557871), CD25-APC 1:100 (BD Pharmingen clone 2A3; ref. 340907), fixable viability dye-efluor 450 1:1000 (eBioscience; ref. 65-0863). All antibodies were incubated 30 min at 4 °C.

Cells were then washed twice with 200 μL FACS Buffer, resuspended in 100 μL of Fixation/Permeabilization concentrate (eBioscience ref. 00-5123-43) at 1:4 in diluent (eBioscience ref. 00-5223-56), and incubated at 4 °C for 30 min. For intracellular staining, cells were washed twice with 200 μL of 1X permeabilization buffer (eBioscience ref. 00-8333-56), resuspended in 25 μL of 1X permeabilization buffer and incubated with 25 μL of Foxp3-PE 1:50 (eBioscience clone 236A/E7; ref. 72-5774-40) diluted in permeabilization buffer for 30 min at 4 °C. Cells were washed twice with 200 μL permeabilization buffer and resuspended in 150 μL of FACS Buffer. Flow cytometry measurements were performed on a FACS Canto II instrument (BD) with and the data were analyzed with FlowJo software (Tree Star).

4. Data analyses

Graphs and statistics were generated with GraphPad Prism software.

5. IVIg versus Avastin and Vectibix analytics

The analyses described below required specific technologies and have therefore all been performed in dedicated labs by a third party. Analyses were performed on IVIg (Octagam 10 %; Octapharma), Avastin (Roche) and eventually on Vectibix (Amgen).

5.1. Endotoxin measurements

These measurements were kindly performed by Olivia Rossberg (Novartis Pharma AG; TD NBEs; IBP). Bacterial endotoxins were measured using the LAL test (Limulus Amebocyte Lysate). This assay is based on the biology of the horseshoe crab (Limulous), which produces LAL enzymes in blood cells (amoebocytes) to bind and inactivate endotoxin from invading bacteria by forming a clot. Here, a kinetic chromogenic assay was used in which a synthetic analog to coagulogen, the natural substrate, is used to measure the endotoxin mediated activation of the serine protease enzyme. The cleavage of this synthetic substrate by the activated pro-clotting enzyme results in the release of the chromophore p-nitroaniline (pNA) that can be measured photometrically at a wavelength of 385 nm - 410 nm. Samples were diluted to 1 mg/mL using endotoxin free ddH$_2$O. For each measurement 4 x 25 µL of the diluted sample were loaded on a LAL test cartridge (Charles River Laboratories; ref. PTS2005) and measured on an Endosafe Portable Test System (Charles River Laboratories) according to the manufacturer instructions.

5.2. Integrity of heavy and light chains in preparations

These measurements were kindly performed by Jasmin Widmer (Novartis Pharma AG; TD NBEs; IBP). The LabChip GXII Electrophoresis Systems (Caliper LifeSciences) uses a single sipper microfluidic chip to aspirate protein samples directly from 96-well plates. Reduced as well as non-denaturated proteins are stained with a fluorescent dye and separated by gel electrophoresis directly on a chip. The protein is detected via its fluorescent label by laser-induced fluorescence. The protein size and purity based on relative area percentage are compared to a ladder and marker calibration standard. Samples were diluted to a final concentration of 1 mg/mL and if not possible, 5 µg of samples were analysed. The measurements were performed

on the HT Protein Express LabChip (Caliper LifeSciences; ref. P/N 760499) and the chip was read on the LabChip GXII instrument (Caliper LifeSciences) following the manufacturer's procedure.

5.3. Measure of aggregates in preparations

These measurements were kindly performed by Patrick Favrod (Novartis Pharma AG; TRD; PCA. The technique used to characterize aggregates in the samples was the micro-flow imaging (MFI), that is flow microscopy applied to sub-visible particulate analysis in protein formulations. The samples have been degassed prior to measurement to avoid the presence of air bubbles. After illumination has been optimized on 0.4 mL of sample, 0.9 mL of undiluted sample has been analyzed with MFI instrument (Brightwell Technologies Inc., ref. DPA4100) following the instructions of the manufacturer. For correct size and concentration determination, NIST (National Institute of Standards and Technology) traceable particle concentration standards were used (Duke Scientific Corporation, ref. CC25-PK). The concentration of the detected beads needed to be within 10 % of the declared concentration (3000 mL^{-1}) for size ranges 4.5-5.5 μm and 9.0-11.0 μm and within 20% for size ranges 2-2.2 μm and 22.5-27.5 μm.

5.4. Fc-Glycan Profiling

These measurements were kindly performed by Christian Graf and Alicia Burr (Novartis Pharma AG; TD NBEsv; IBP). Briefly, 50 μg of protein were digested with 50 units of the Fabricator IdeS enzyme (immunoglobulin-degrading enzyme from *Streptococcus pyogenes*; Genovis), in digestion buffer (sodium phosphate pH 6.6) for 1 h at 37 °C. Fabricator is a unique enzyme that specifically digests the hinge region of IgG, producing a F(ab')$_2$ fragment and two Fc fragments. Digested fragments were then denatured and reduced by adding 5 M Guanidine hydrochloride and 40 mM TCEP and incubated for 1 h at 37 °C. Reduced antibody fragments were measured by LC-ESI-MS (H-Class UPLC, BEH C4 column, SYNAPT G2 Q-TOF) on a 70 % Isopropanol/ 20 % acetonitrile/ 9.9 % water/ 0.1 % TFA gradient. For determination of the Fc-glycan profile, the obtained mass spectrum of the Fc/2 fragment was deconvoluted using the MaxEnt1 algorithm (MassLynx 4.1 or UNIFI 1.6 software). The intensity of the different Fc-glycoform mass peaks (identity determined by exact mass) was taken for relative quantification of the main glycans.

5.5. Human protein chip

These measurements were kindly performed by Simon Mittermeier and Torsten Kuiper (Novartis Pharma AG; TD NBEs; IBP). Cross-reactivity of the tested antibodies was assessed on a ProtoArray® v5.1 (Life Technologie; ref. PAH05251020) coated with more than 9000 full-length human proteins. Each tested antibody was incubated at 5 mg/mL and detection of binding was achieved by using a DyLight649 conjugated F(ab')$_2$ -goat anti-human IgG F(ab')$_2$ fragment specific (Jackson ImmunoResearch; ref. 109-496-006) following the manufacturer's instruction. The different steps were performed on the HS 4800™ Pro Hybridization Station (Tecan) and the protein array was read on a PowerScanner™ (Tecan). Data were analysed with the GenePix® Pro 7 software (Molecular Devices).

5.6. Generation of Fc, Fab and (Fab'$_2$) fragments

These experiments were kindly performed by Tina Buch, Yasmin Widmer, Dennis Ungan, and Paulina Baczyk (Novartis Pharma AG; TD NBEs; IBP). Fc and Fab fragments were generated from IVIg and Avastin by papain digestion (Roche). Briefly, IVIg or Avastin were added to a 20 mM succinic acid /35.1 mM NaOH, pH 6.0 solution in a 50 mL Falcon tube, together with an EDTA / L-cysteine solution at a final concentration of 1 mM. The papain was added to the reaction and the falcon tubes were placed in a water bath at 37 °C with shaking. After digestion, the reaction was stopped by adding an iodacetamide solution at a final concentration of 1.2 mM. In order to separate the Fab and Fc fragments an affinity chromatography step was performed directly after the papain digest (Column: Atoll GmbH; Resin: MabSelect SuRe from GE Healthcare; System: ÄKTA Explorer from GE Healthcare). The column was equilibrated with 20 mM NaH$_2$PO$_4$/Na$_2$HPO$_4$, pH 7.0 and sample was loaded. Column was then washed with the same equilibration buffer and elution was performed with 50 mM Acetic acid. After capturing the pH of the eluate was adjusted to pH ~5.0 with 1 M Tris right after elution from the column. Flow troughs containing the Fab fragments and eluates containing the Fc parts with potential undigested IVIg or Avastin were further polished by size exclusion chromatography. About 12 mg of each flow trough/eluate were concentrated to about 0.5 mL using Amicon® Ultra Centrifugal filters (10 kDa cut-off; Merck Millipore) and loaded on a column Superdex™ 200 100/300 GL (GE Healthcare) with the ÄKTA Explorer system from GE Healthcare. Column was equilibrated with 50 mM NaH2PO4/NaOH, 150 mM NaCl, pH 7.0,

samples were loaded and elution was performed with the same equilibration buffer. 1 mL fractions were collected.

F(ab')$_2$ fragments were generated from IVIg and Avastin by FabRICATOR® digestion (Genovis). 80 µg of antibodies (at 1 mg/mL) were digested in 50 mM NaH2PO4/NaOH, 150 mM NaCl, pH 7.0 in a 50 mL Falcon tube together with 268 units of FabRICATOR®. The Falcon tubes were placed in a water bath at 37 °C for 36 h with shaking. F(ab')$_2$ fragments were collected in the flow-through after an affinity chromatography step and further polished by size exclusion chromatography as described above.

Purity of the different fragments generated was determined by the LabChip GXII Electrophoresis system (see method in section 5.2) and concentration was assessed by reversed phase chromatography. Identification of the various fragments was confirmed by mass check by LC-MS (*kindly performed by Bjoern Hueber, Coralie Etter and reviewed by Christian Graf; Novartis Pharma AG; TD NBEs; IBP*).

Results

1. IVIg effect on T and B cell populations *in vivo* in mice

1.1. IVIg inhibits anti-OVA response *in vivo* in a dose-dependent manner

Mice were injected s.c with OVA together with adjuvant MF59, and IVIg doses ranging from 1 mg to 50 mg were injected simultaneously on the same site. Mouse IgG response against OVA was measured by ELISA and results are shown in Figure 15.
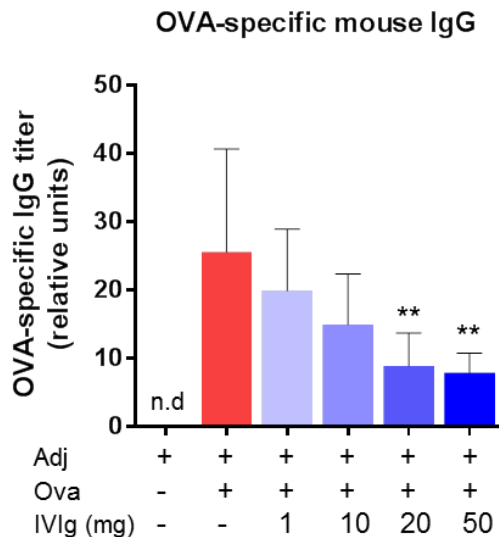

Figure 15: IVIg inhibits anti-OVA IgG response in vivo in a dose-dependent manner. C57Bl/6NCrl mice were injected 3 times weekly s.c in the neck with 50 μg OVA and Adjuvant AddaVax® MF59 (red bar) and terminated 24h after last injection (15 days after the 1st injection). IVIg doses ranging from 1 mg to 50 mg were injected simultaneously as indicated and IgG mouse response against OVA was measured by ELISA performed on mouse serum. Values are expressed as relative units to standard. Results pool data from 2 independent experiments (n=6). Bars represent mean ± SD. n.d: not detected. Statistical significance was tested using one-way ANOVA with Dunnett's correction. Each group was compared to the control group "Adj+OVA". Star maker significant difference *: $p < 0.05$; **$p < 0.01$; ***: $p < 0.001$; ****: $p < 0.0001$.

These results show that OVA immunization was efficient and an IgG response could be detected in mouse serum 15 days after the first injection (red bar in the graph). IVIg lead to decreased amount of OVA-specific mouse IgG, and importantly this reduction was proportional to the dose of IVIg that was injected. The maximum tested dose of 50 mg of IVIg lead to a a reduction of 70% of the OVA-IgG antibodies. These data hereby demonstrate that a simple immunization mouse model could mimic *in vivo* the IVIg immunomodulation properties in a dose-dependent way, as reported in the clinic with patients affected with autoimmune diseases.

1.2. IVIg increases T and B-cell numbers in secondary lymphoid organs

Despite the inhibition of the OVA-specific humoral response, treatment with 50 mg of IVIg together with adjuvant surprisingly lead to an obvious increase in the size of secondary lymphoid organs such as spleen and draining lymph nodes (Figure 16A). This observation was further confirmed by the increase of weight that have been measured (Figure 16B). Spleen weight was slightly increased upon IVIg treatment, whereas brachial, axillary and cervical lymph nodes were 2-fold larger.

To determine whether this was accompanied by an increase in the B and T-cell number, B and T cell populations were characterized by flow cytometry. Absolute cell numbers were back calculated according to the cell count established after processing the organs. The number of B cells was consistently higher in mice treated with IVIg (Figure 16B). This was reflected by an increase of 10.1 E^6 cells in the spleen, 6 E^6 cells in the axillary and brachial lymph nodes and 3.6 E^6 cells in the cervical lymph nodes, compared to the OVA-treated group. The number of T cells was not increased in the spleen of IVIg-treated animals, but in lymph nodes both, the number of CD4 and CD8 T cells were elevated upon IVIg administration (2.3 E^6 or 3.1 E^6 cells more in the cervical lymph nodes and 1.4 E^6 or 1.8 E^6 cells more in the brachial/axillary lymph nodes for CD4 and CD8 T cells, respectively). The reason for CD8 T cells mobilization with IVIg is unknown, but most likely it could be attributed to cross-presentation by certain APCs, which are able to process and present extracellular antigens on MHC class I molecules. It has been shown that limited antigen degradation correlates with efficient cross-presentation (Joffre et al., 2012). Limited proteolysis could occur in APCs due to the high dose of IVIg that might be present in the endocytic compartments, thereby favoring the presentation of IVIg-derived epitopes on MHC class I and promoting CD8 T cell activation. Taken together these data suggest a prominent activation of the immune system by IVIg, as indicated by T and B cell proliferation. Such effect was less pronounced upon OVA immunization, since a single protein will only elicit a very low number of epitope-specific immune cells, whose expansion is more difficult to detect *in vivo*.
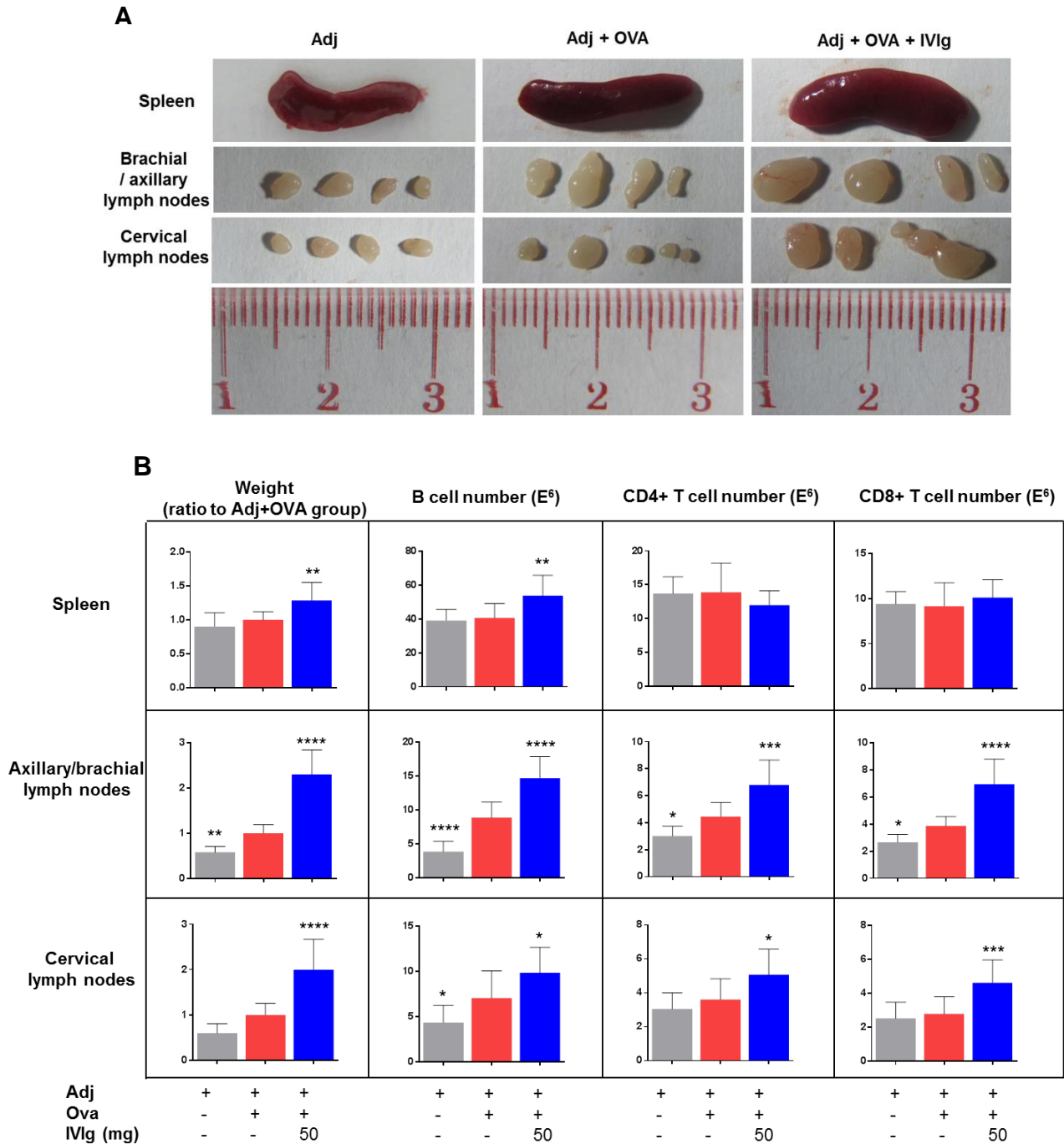
Figure 16: IVIg increases the weight of lymphoid organs as well as B and T-cell number. **(A)** Pictures of spleen and draining lymph nodes from one representative animal in each group of treatment. **(B)** Spleen and lymph nodes were collected, weighed, and flow cytometry was performed on isolated cells (Adj MF59 was used for experiments). For weight, values are expressed as ratio to the "OVA+Adj" treated group. For cell numbers, values are expressed as absolute cell numbers. Cells were gated on lymphocytes. Dead cells were excluded using a viability fluorescent dye. B cells were gated on CD19+ cells and T cells on CD4+ or CD8+ cells. Bars represent mean ± SD. Data pool 4 independent experiments (n=12). Statistical significance was tested using one-way ANOVA with Dunnett's correction. Each group was compared to the control group "Adj+OVA". Star maker significant difference *: $p < 0.05$; **$p < 0.01$; ***: $p < 0.001$; ****: $p < 0.0001$.

1.3. IVIg activates B cells in a dose-dependent manner

As data reported above revealed that the weight of the lymphoid organs was increased and the number of B cells was elevated upon IVIg administration, the effect of IVIg on various B cell markers was specifically investigated. Increasing doses of IVIg ranging from 1 mg to 50 mg were administered to mice immunized with OVA

IVIg increased the expression of co-stimulatory markers CD86 and CD83 on CD19+ B cells, as well the expression of the early activation molecule CD69, in both the spleen and draining lymph nodes (Figure 17). These effects occurred proportionally to the IVIg dose administered, with an increase of CD86, CD83 and CD69 of respectively 2.5, 1.7 and 1.6-fold, in cervical lymph nodes upon administration of 50 mg of IVIg. The weight of axillary/brachial and cervical lymph nodes was increased when mice received IVIg, and this effect was more significant with high doses of IVIg (up to 2-fold), whereas weight of the spleen only slightly varied with IVIg treatment. In the next step, expression of the MHC class II molecules (here the subclass I-A) as well as the co-stimulatory molecules CD80 and CD40 was examined on B cells. Although some statistically significant increase in expression for CD40 and I-A was observed, the effect of IVIg on these markers was considered overall as minor (Figure 18A). When gated on CD11c+ I-A+, a small percentage of DCs could be detected in the spleen, whereas the DC population was not detectable in the lymph nodes (Figure 18B). IVIg had no effect on CD86, CD83 and I-A expression on spleen DCs.

The results are in line with literature showing that peripheral blood lymphocytes have little basal expression of CD69, but their stimulation causes rapid induction of this marker on T, B and NK cells surface within a few hours (Reddy et al., 2004). Therefore analysis of CD69 expression is an approach commonly used to follow B-cell activation (Borges et al., 2007; Purtha et al., 2008). Although B cells express very low levels of co-stimulatory molecules on their surface, some studies revealed that CD86 surface expression is rapidly up-regulated following BCR or LPS induced B-cell activation both *in vitro* and *in vivo*, while CD80 remains poorly expressed after stimulation (Constant et al., 1995; Kohm et al., 2002; Lenschow et al., 1994), which is consistent with the observations presented here. Although CD83 is predominantly expressed on mature DCs, it has also been shown to be up-regulated on activated B cells *in vivo* (Breloer et al., 2007; Prazma et al., 2007). Thus, our results demonstrate that IVIg induced B cell activation in a dose-dependent manner.
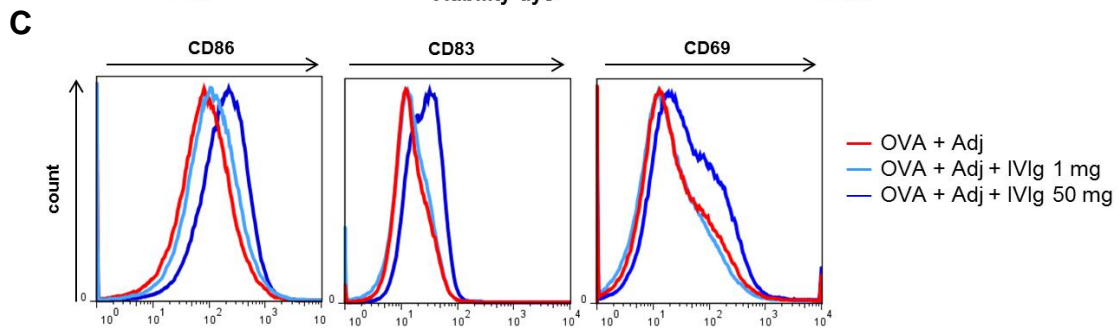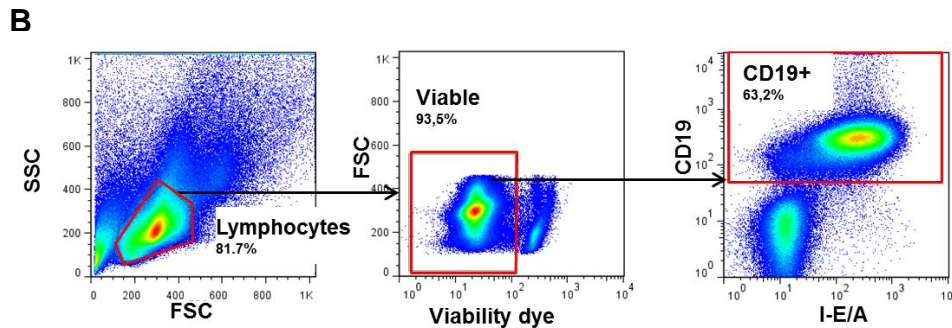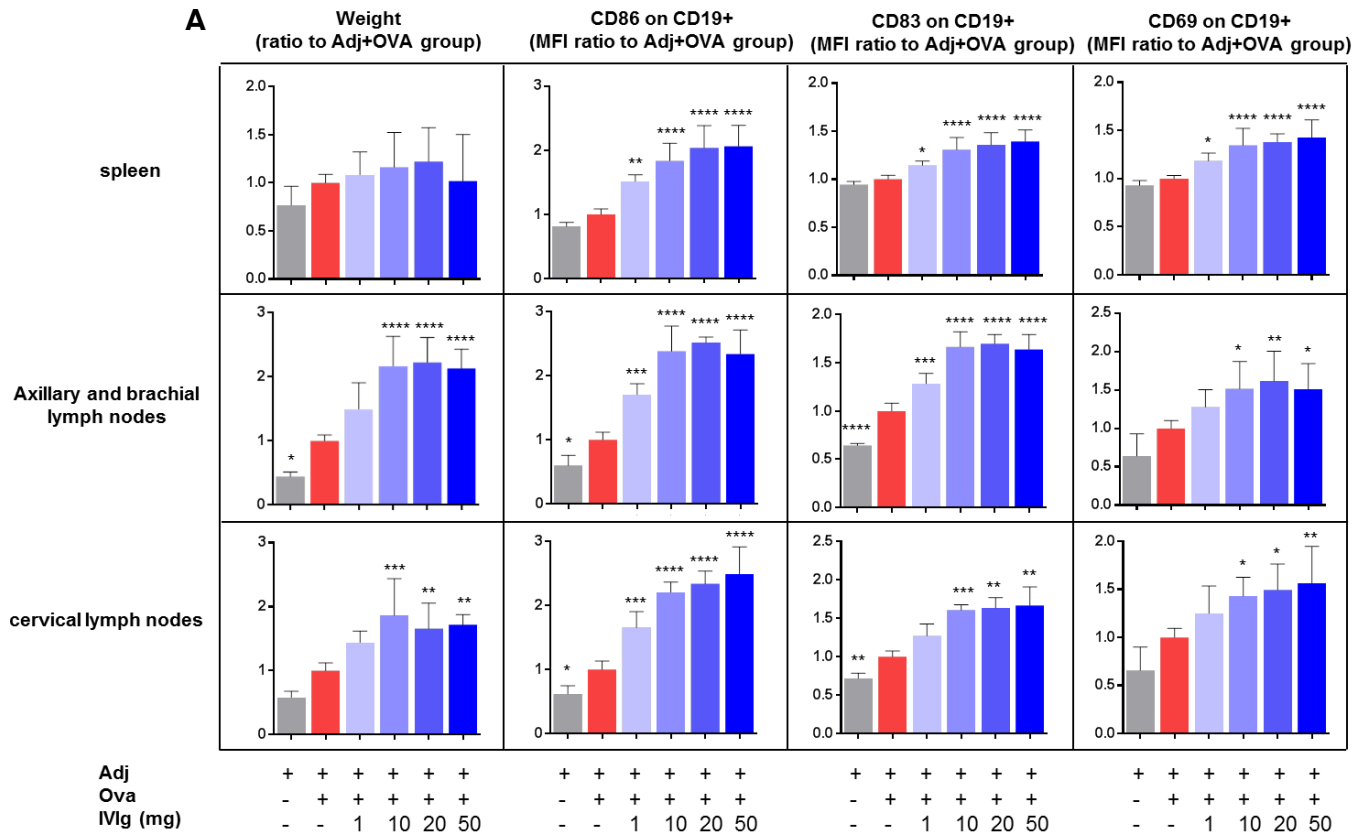
Figure 17: IVIg increased weight of the draining lymph nodes and activated B cells in a dose-dependent manner. C57Bl/6NCrl mice were injected 3 times weekly s.c in the neck with 50 µg OVA and Adjuvant AddaVax® MF59 (red bar) and terminated 24h after last injection. IVIg doses ranging from 1 mg to 50 mg were injected simultaneously. Draining lymph nodes and spleen were harvested, weighed and flow cytometry was performed on isolated cells. **(A)** Results pool data from 2 independent experiments (n=6). Values are expressed as ratio to the "Adj+OVA" group values. Bars represent mean ± SD. Median of fluorescence intensity (MFI) was measured on CD19+ B cells. Statistical significance was tested using one-way ANOVA with Dunnett's correction. Each group was compared to the control group "Adj+OVA". Star maker significance *: p < 0.05; **p<0.01; ***: p<0.001; ****: p<0.0001. **(B)** Gating strategy for B cells. **(C)** Flow cytometry histograms from one representative animal.
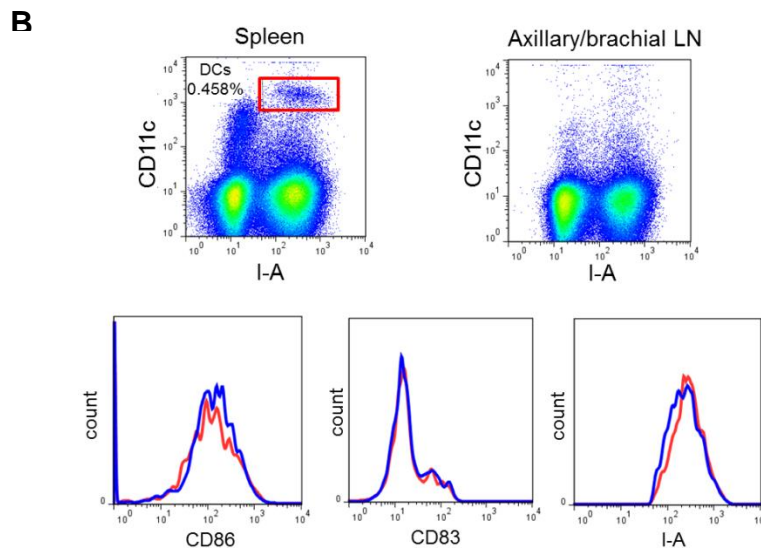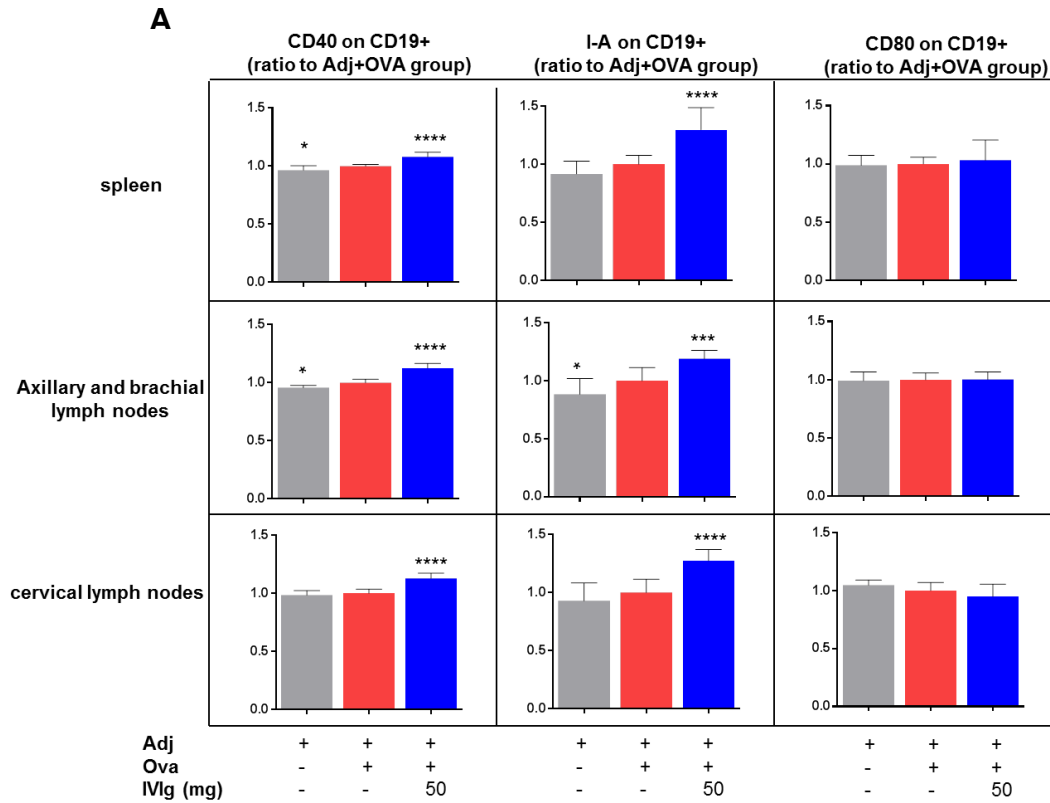
Figure 18: IVIg has a minor effect on CD40, MHC class II (subclass I-A) and CD80 expression on B cells and no effect on the expression of co-stimulatory molecules on DCs. C57Bl/6NCrl mice were injected 3 times weekly s.c in the neck with 50 µg OVA and Adjuvant AddaVax® MF59 (red bar) and terminated 24h after last injection. 50 mg of IVIg were injected simultaneously as indicated. Draining lymph nodes and spleen were harvested, and flow cytometry was performed on isolated cells. **(A)** CD40, I-A and CD80 expression on B cells. Results pool data from 4 independent experiments (n=12). Values are expressed as ratio to the "Adj+OVA" group values. Bars represent mean ± SD. Median of fluorescence intensity (MFI) was measured on CD19+ B cells. Statistical significance was tested using one-way ANOVA with Dunnett's correction. Each group was compared to the control group "Adj+OVA". Star maker significant difference *: $p < 0.05$; **$p<0.01$; ***: $p<0.001$; ****: $p<0.0001$. **(B)** Gating strategy for DCs and expression of CD86, CD83 I-A on surface of spleen DCs.

1.4. Adjuvant is required to mediate IVIg effect

To assess whether IVIg effect was depending on the presence of adjuvant or Ova, mice were treated with different combinations of IVIg, OVA and adjuvant as described below (Figure 19). Weight of lymph nodes was increased to 2 to 2.5 fold and weight of the spleen was increased to 1.5 fold in mice treated with IVIg together with adjuvant or with IVIg plus OVA and adjuvant.
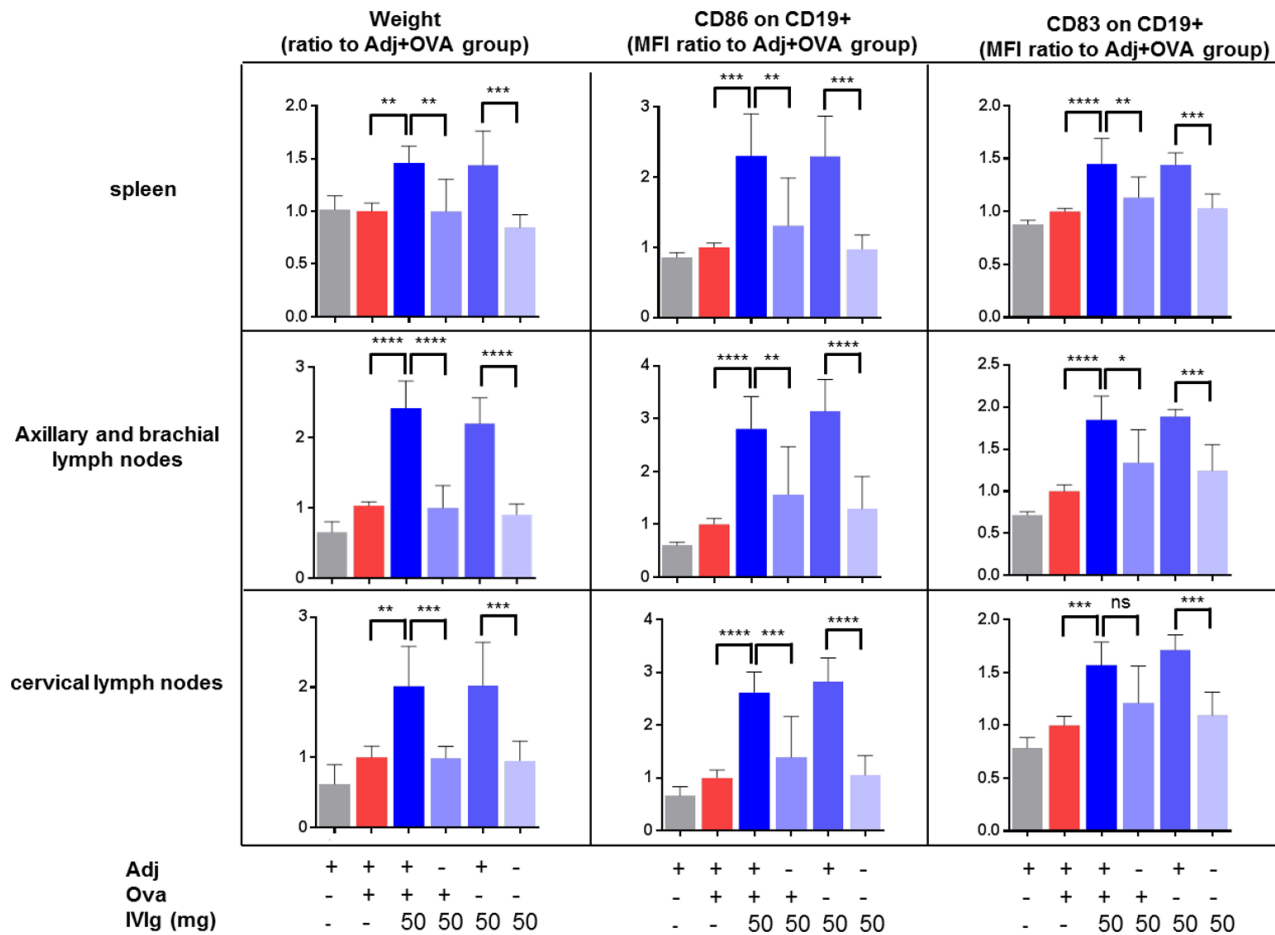

Figure 19: Presence of adjuvant is required together with IVIg to mediate increase of weight in lymphoid organs and B cells activation. C57Bl/6NCrl mice were injected 3 times weekly s.c in the neck with 50 µg OVA and Adjuvant AddaVax® MF59 (red bar) and terminated 24h after last injection. 50 mg of IVIg was injected alone or in combination to OVA and/or Adjuvant, as indicated. Draining lymph nodes and spleen were harvested, weighed and flow cytometry was performed on isolated cells. Results pool data from 2 independent experiments (n=6). Values are expressed as ratio to the "Adj+OVA" group values. Bars represent mean ± SD. Median of fluorescence intensity (MFI) was measured on CD19+ B cells. Statistical significance was tested using one-way ANOVA with Tukey's correction. Star maker significant difference *: $p < 0.05$; **$p<0.01$; ***: $p<0.001$; ****: $p<0.0001$.

When mice received IVIg in combination with adjuvant with or without OVA, the expression of CD86 and CD83 on B cells was 2 to 3 fold higher in spleen and lymph nodes compared to the group treated with OVA and adjuvant. In contrast, mice treated with IVIg alone, adjuvant alone, or IVIg in combination with OVA exhibited no such effect neither on the weight of lymphoid organs nor on the expression of co-stimulatory molecules on B cells. These data indicate that the presence of adjuvant is required to mediate B cell activation and increase the weight of lymphoid organs upon IVIg injection.

1.5. A human monoclonal antibody can't reproduce IVIg effects

Downregulation of the anti-OVA IgG response observed upon IVIg treatment as well as B cell activation may be dependent on the Fc-region of IVIg, or mediated by its high sequence diversity in the variable regions. This was addressed by testing a human monoclonal antibody, to see if it was able to inhibit the OVA-specific IgG response, as observed upon IVIg injection. For this purpose, two marketed monoclonal antibodies were carefully selected regarding their target species-specificity, to prevent cross-reactivity in mice and to exclude potential interference with the immune system that could impair the interpretation of the data. Avastin (a humanized $IgG_{1\kappa}$) has been shown to possess an extremely weak interaction with mouse VEGF-A, which fails to result in immunoneutralization (Yu et al., 2008). Similarly, Vectibix (a human $IgG_{2\kappa}$), does not cross-react with mouse EGFR (Tabrizi et al., 2006). IVIg, Avastin or Vectibix were injected together with OVA and adjuvant in mice. Anti-OVA IgG response was measured by ELISA and expression of B cell stimulation markers were assessed by flow cytometry. Avastin applied at 50 mg/mouse had no effect on the anti-OVA IgG titer when given together with MF59. Avastin given together with adjuvant LT $_{(R192G/L211A)}$ significantly increased the OVA-specific IgG response in mice. However, IVIg injected at the same dose consistently lead to a significant decrease of about 3.4-fold when adjuvant MF59 was used, and of 6.5-fold with adjuvant LT $_{(R192G/L211A)}$ (Figure 20A). Both adjuvants mediate a balanced Th1/Th2 response. Avastin administration slightly increased the weight of the spleen and the cervical lymph nodes but did not result in a significant gain in weight in axillary and brachial lymph nodes. Avastin also didn't increase expression of CD86, CD83 and CD69 on B cells as shown in Figure 20B and C. In contrast, IVIg triggered a 2- to 3-fold up-regulation of CD86 on B cells, and a 1.5-2-fold up-regulation for CD83 and CD69, in both the spleen and the corresponding draining lymph nodes.
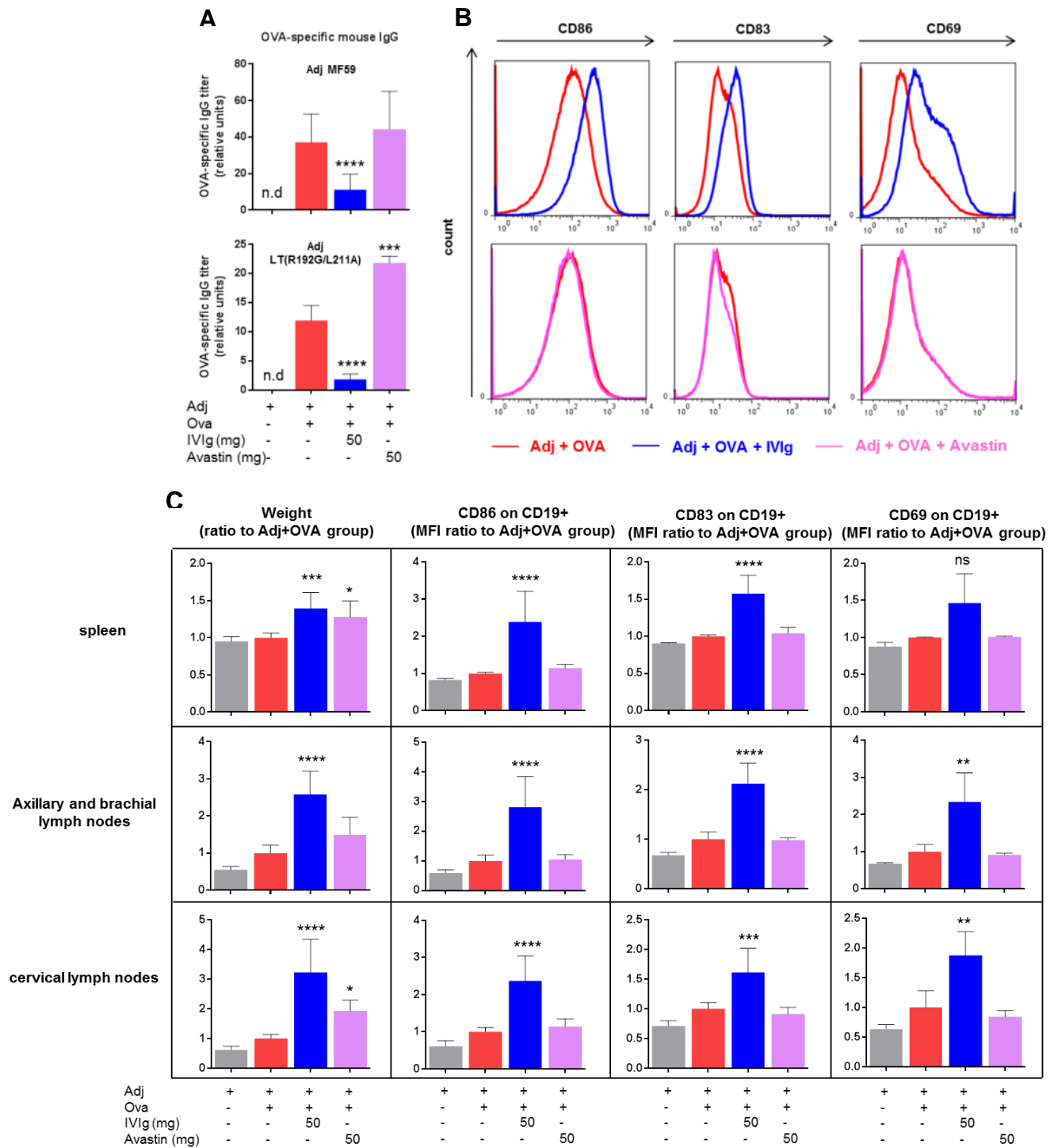
Figure 20: Avastin, a humanized monoclonal IgG$_{1\kappa}$ antibody, doesn't inhibit the anti-OVA IgG response in vivo in mice and doesn't promote B cell activation compared to IVIg. C57Bl/6NCrl mice were injected 3 times weekly s.c in the neck with 50 μg OVA and adjuvant (Adj) (red bar) and terminated 24h after last injection. IVIg or Avastin were injected simultaneously to OVA and Adj as indicated. **(A)** Anti-OVA IgGs in mouse serum were measured by ELISA. For Adj MF59, results pool data from 4 independent experiments (n=12) and for Adj LT(R192G/L211A) results are from one experiment (n=3). **(B)** Flow cytometry histograms are shown for one representative animal (Adj MF59 was used). **(C)** Draining lymph nodes and spleen were harvested, weighed and flow cytometry was performed on isolated cells (Adj MF59 was used). Results pool data from 2 independent experiments (n=6), except for CD69 for which data are derived from one experiment (n=3). Values are expressed as ratio to the "Adj+OVA" group values. Median of fluorescence intensity (MFI) was measured on CD19+ B cells. Bars represent mean ± SD. n.d: not detected. Statistical significance was tested using one-way ANOVA with Dunnett's correction. Each group was compared to the control group "Adj+OVA". Star maker significant difference *: $p < 0.05$; **$p<0.01$; ***: $p<0.001$; ****: $p<0.0001$.

75

Consistent with the observations made with Avastin, anti-OVA IgG response was not affected by the injection of Vectibix (Figure 21A and B). This was confirmed with the use of two different adjuvants, the MF59 or LT $_{(R192G/L211A)}$. Vectibix induced a minor increase in weight of the spleen and axillary/brachial lymph nodes, but did not augment CD86 expression on B cells in these organs, as observed in a substantial way with IVIg (Figure 21C).
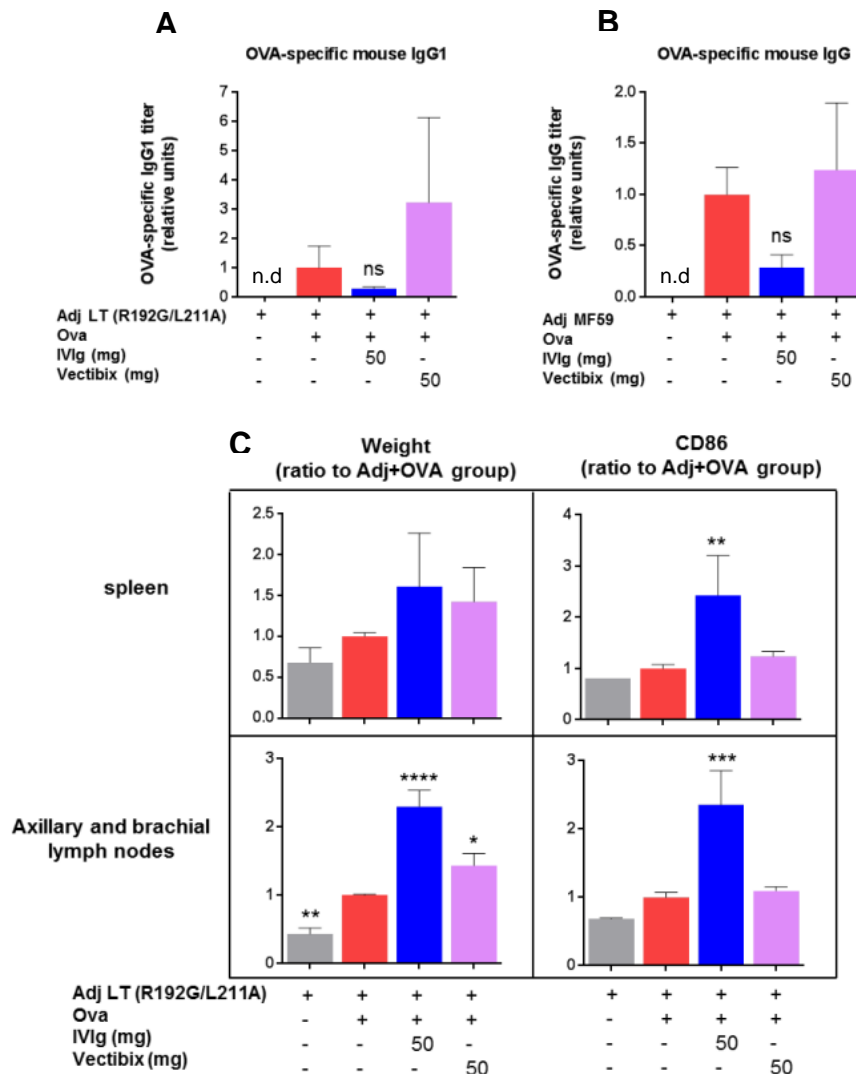

Figure 21: Vectibix, a human monoclonal IgG$_{2\kappa}$ antibody, doesn't inhibit the anti-OVA IgG response in vivo in mice and doesn't promote B cell activation compared to IVIg. C57Bl/6NCrl mice were injected 3 times weekly s.c in the neck with 50 μg OVA and adjuvant (Adj) (red bar), and terminated 24h after last injection. IVIg or Vectibix were injected simultaneously to OVA and Adj as indicated. (A) Anti-OVA IgG1 in mouse serum as measured by ELISA upon use of Adj LT (n=3). **(B)** Anti-OVA IgG in mouse serum as measured by ELISA upon use of Adj MF59 (n=3). **(C)** Draining lymph nodes and spleen were harvested, weighed and flow cytometry was performed on isolated cells (Adj LT was used). Values are expressed as ratio to the "Adj+OVA" group values. Median of fluorescence intensity (MFI) was measured on CD19+ B cells. Bars represent mean ± SD with n=3. n.d: not detected. Statistical significance was tested using one-way ANOVA with Dunnett's correction. Each group was compared to the control group "Adj+OVA". Star maker significant difference *: p < 0.05; **p<0.01; ***: p<0.001; ****: p<0.0001.

Taken together, these data indicate that a monoclonal IgG antibody injected at high dose cannot impair an antigen-specific humoral response, thus ruling out FcRn saturation as the main driver of the inhibitory effects of IVIg in this mouse modelThese results are in line with studies showing that IVIg therapeutic effects still occurred although mice were deficient for FcRn (Crow et al., 2011; Li et al., 2005).Notably, the composition of IVIg differs from a human mAb by the presence of many different IgG-variable regions. Therefore these results also point to the direction that this high sequence diversity in IVIg preparations may be relevant in decreasing the formation of antigen-specific antibodies.

1.6. IVIg doesn't induce activation of Tregs but increases the proportion of CD69+ CD4 T cells.

Having proven the effect of IVIg in up-regulating some activation markers on B-cells, we next examined by flow cytometry whether IVIg has an effect on the T-cell population. IVIg has been reported in some clinical studies to promote expansion of Tregs in patients (Bayry et al., 2012). Our data demonstrate that the percentage of CD4+CD25+Foxp3+ Tregs in lymphoid organs from IVIg-treated mice remains unchanged (Figure 22B). Since the total number of CD4+ T cells significantly increased in the draining lymph nodes (Figure 16B), the absolute number of Tregs increased as well in presence of IVIg.

To investigate whether IVIg promotes activation of Tregs, the expression of Foxp3, CD25 and CTLA-4 was assessed. Data revealed that IVIg didn't affect the level of expression of any of these markers (Figure 22D), which is in line with a pro-inflammatory context. These results are contradicting a study showing that IVIg treatment in patients enhanced the activation status of circulating Tregs while numbers remained unchanged (Tjon et al., 2013).

A

B

%CD25+ among CD4+   % CD25+Foxp3+ among CD4+   %CD69+ among CD4+

spleen

Axillary and brachial lymph nodes

Cervical lymph nodes

Adj	+	+	+	+
Ova	-	+	+	+
IVIg (mg)	-	-	50	-
Avastin (mg)	-	-	-	50

C

Gated on CD4+CD8-
Axillary/brachial lymph nodes

Adj
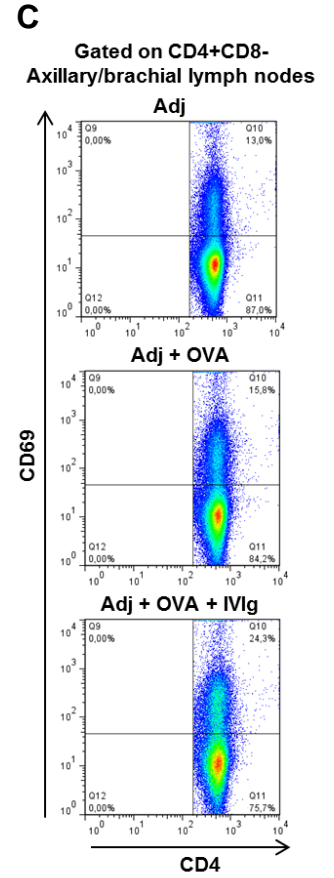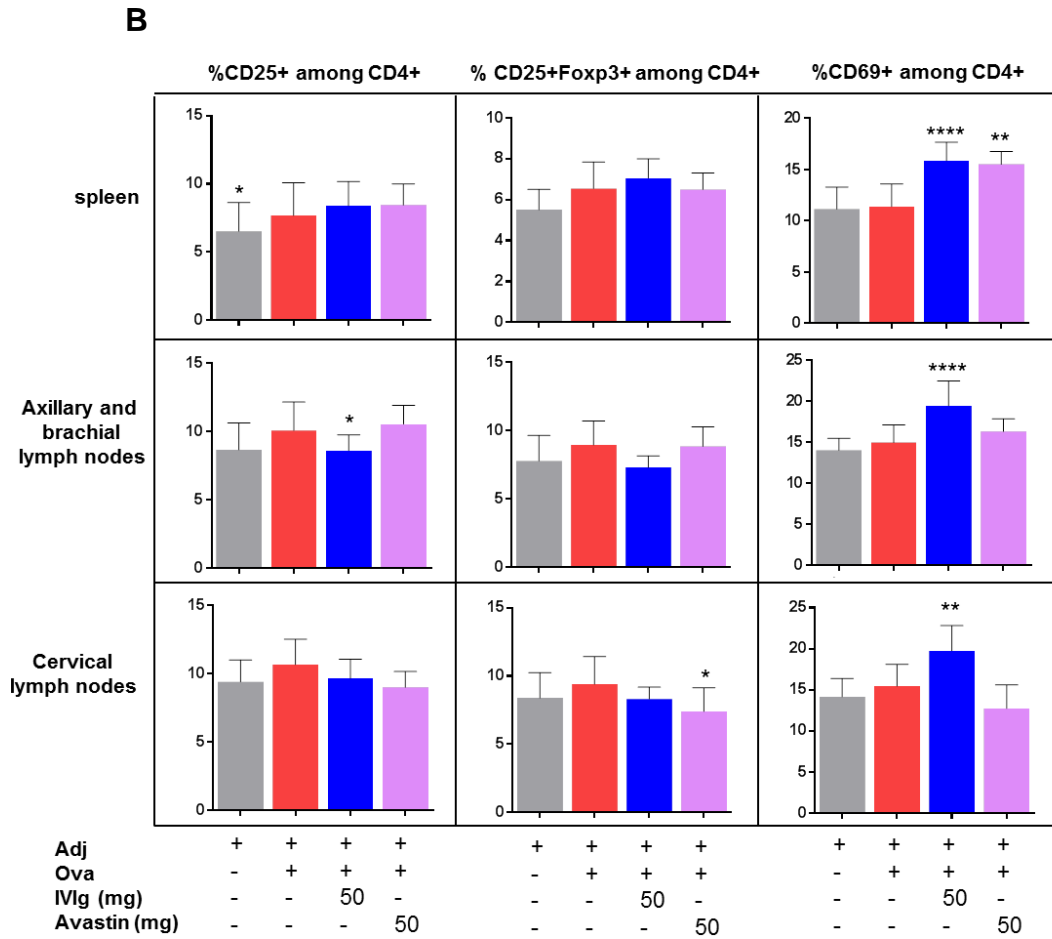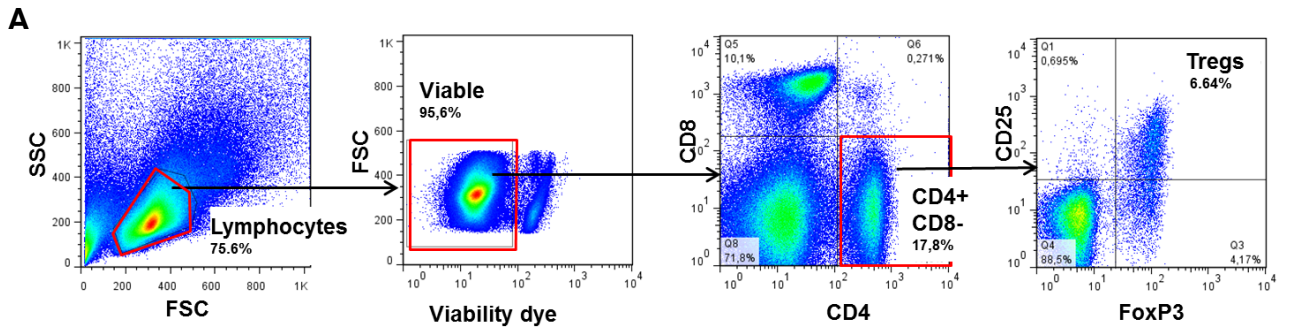
Adj + OVA

Adj + OVA + IVIg

D

MFI ratio of "Adj+OVA+IVIg" over the "Adj+OVA" group

gated on CD4+CD25+Foxp3+ cells

	Foxp3	CTLA-4	CD25
spleen	1.11	1.14	1.22
axillary/brachial LN	1.03	1.11	1.17
cervical LN	1.03	1.02	1.1

Figure 22: IVIg doesn't activate the Tregs population but triggers CD69 expression on CD4+ T cells. C57Bl/6NCrl mice were injected 3 times weekly s.c in the neck with 50 μg OVA and adjuvant (Adj MF59) (red bar), and terminated 24h after last injection. IVIg or Avastin were injected simultaneously to OVA and Adj as indicated. **(A)** Gating strategy for Tregs **(B)** Draining lymph nodes and spleen were harvested, weighed and flow cytometry was performed on isolated cells. Bars represent mean ± SD. For % CD25+ and % CD25+Foxp3+ data pool 5 independent experiments (n=15), except for Avastin group n=6 (from 2 independent experiments). For % CD69+ data pool 4 independent experiments (n=12), except for Avastin group n=3. Statistical significance was tested using one-way ANOVA with Dunnett's correction. Each group was compared to the control group "Adj+OVA". Star maker significant difference *: $p < 0.05$; **$p < 0.01$; ***: $p < 0.001$; ****: $p < 0.0001$. **(C)** Flow cytometry dot plots showing CD69+ cells among CD4+ T cells from one representative animal for each group of treatment. **(D)** MFI of Foxp3, CTLA-4 and CD25 on Tregs expressed as MFI ratio of "Adj+OVA+IVIg" over the "Adj+OVA" group (data pool 4 independent experiments; n=12).

Interestingly, the percentage of CD69+ cells among CD4+ T cells increased in IVIg-treated mice: 3.8 % more in the spleen, 4.8 % in the axillary and brachial lymph nodes and 6.2 % in the cervical lymph nodes (Figure 22C). CD69 is the earliest cell surface antigen expressed by T cells following activation and thus the increased CD69 expression indicated an inflammatory response (Caruso et al., 1997). Avastin mediated a small but significant increase of CD69+ cells within CD4+ T cells in the spleen, but had no effect in the lymph nodes, however this result was derived from only one experiment with n=3 mice, unlike the other groups of treatment which comprised 4 independent experiments with n=12 mice. Consistent with the observation that IVIg induced T cell proliferation in the lymph nodes, the data presented here demonstrates that CD4+ T cells are being activated as indicated by the expression of CD69. Overall, data suggest an inflammation rather than increased suppressive capacities of the immune system. Therefore, it is unlikely that the increased number of Tregs is the main driver of the inhibitory effect of IVIg on the anti-OVA antibody response.

1.7. IVIg induces the formation of numerous germinal centers

To further confirm the triggering the immune system by IVIg, the formation of germinal centers in the spleen and lymph nodes was evaluated by immunofluorescence. The activated B cells during the germinal center reaction can be probed with either the rat monoclonal GL7 antibody or the PNA (Peanut agglutinin). First, the specificity of the immunofluorescence staining was assessed by overlaying both stainings as illustrated in Figure 23A. GL7 antibody was used later on to specifically stain germinal centers by immunofluorescence. As expected, injection of adjuvant alone produced no germinal centers, whereas addition of OVA triggered the formation of very few and small germinal centers. Mice that have received IVIg together with OVA and adjuvant exhibited a striking number of germinal centers in their spleen and draining lymph node sections, with a markedly enlarged size in the lymph nodes (Figure 23B). This is in line with previous data presented here showing that IVIg induced B cell activation. GL7 antigen is selectively expressed on activated but not on mature B cells, and GL7^{high} B cells have been shown to have higher functional activity for producing antibodies and presenting antigens (Naito et al., 2007). In the case of a thymus-dependent antigen, formation of a germinal center involves that B cells receive an input signal from a cognate helper T cell. The data presented here thus imply that IVIg not only activated B cells but might also have mobilized many diverse T cells. Notably, mice that have been treated with Avastin together with OVA and adjuvant presented the same number and size of germinal centers compared to mice immunized with OVA and adjuvant. This supports the ELISA and FACS results showing that a monoclonal human antibody is not able to trigger the same effects as IVIg.

In line with the data reviewed previously in section 1.4, the number of germinal centers is strongly augmented in spleen as well as in lymph nodes when mice were administered with IVIg together with adjuvant, but not when mice received IVIg or adjuvant alone Figure 24. These results highlight once again the initiation of a strong immune response in mice when IVIg is injected, and – as any immune response – it can't be initiated without triggering the pattern recognition receptors on immune cells, which is mediated by the adjuvant in our model.
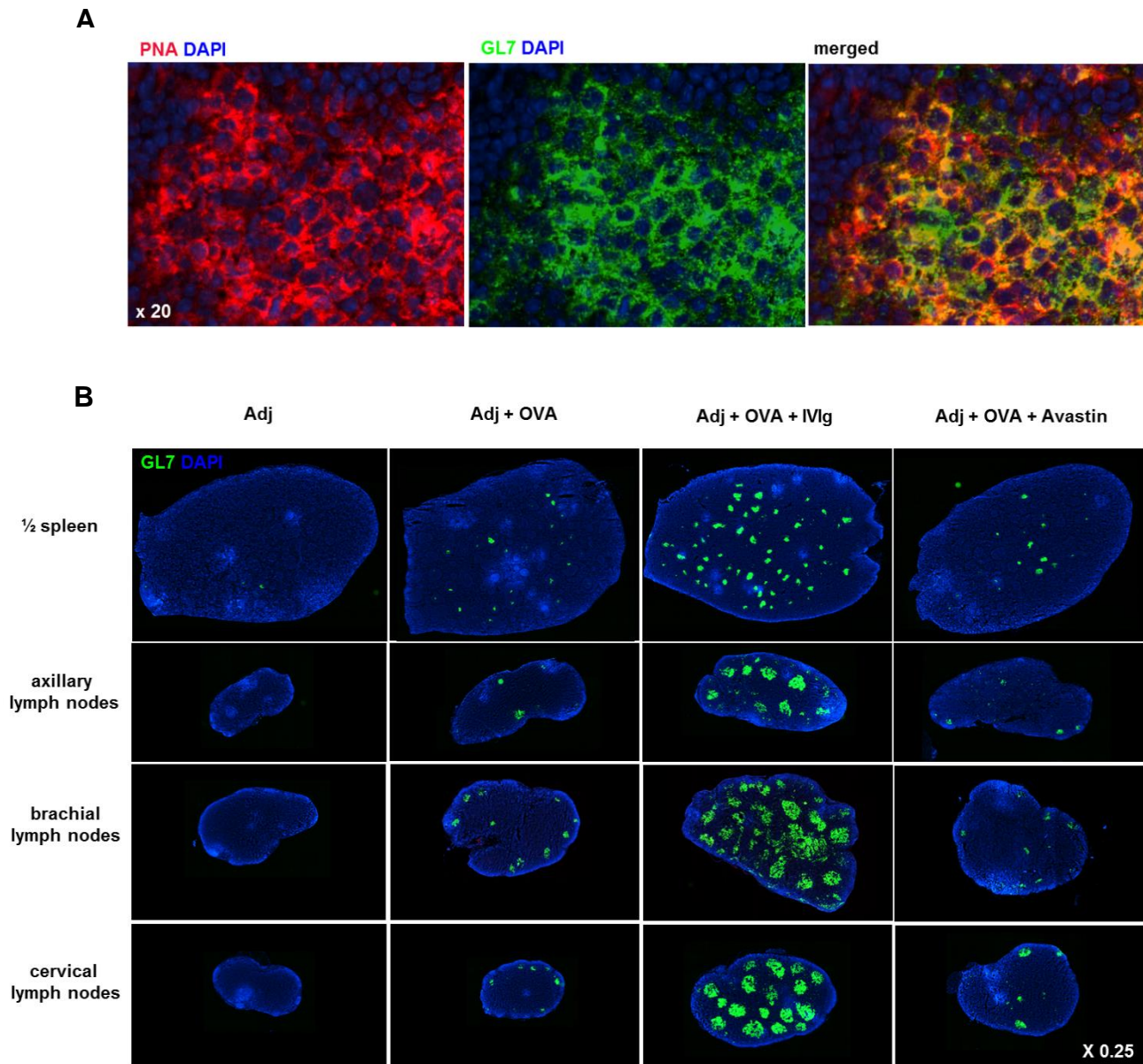
Figure 23: IVIg induces the formation of large and numerous germinal centers *in vivo* in the mouse. C57Bl/6NCrl mice were immunized 3 times weekly s.c in the neck with 50 µg OVA and adjuvant (Adj MF59), 50 mg of IVIg or Avastin were injected simultaneously to OVA and Adj as indicated, and mice were terminated 24h after last injection. **(A)** Spleen sections of mice were co-stained with PNA (red) and GL7 (green). **(B)** Spleen and draining lymph nodes were probed for germinal centers with the rat monoclonal GL7 antibody (green). Each picture is from one representative animal.
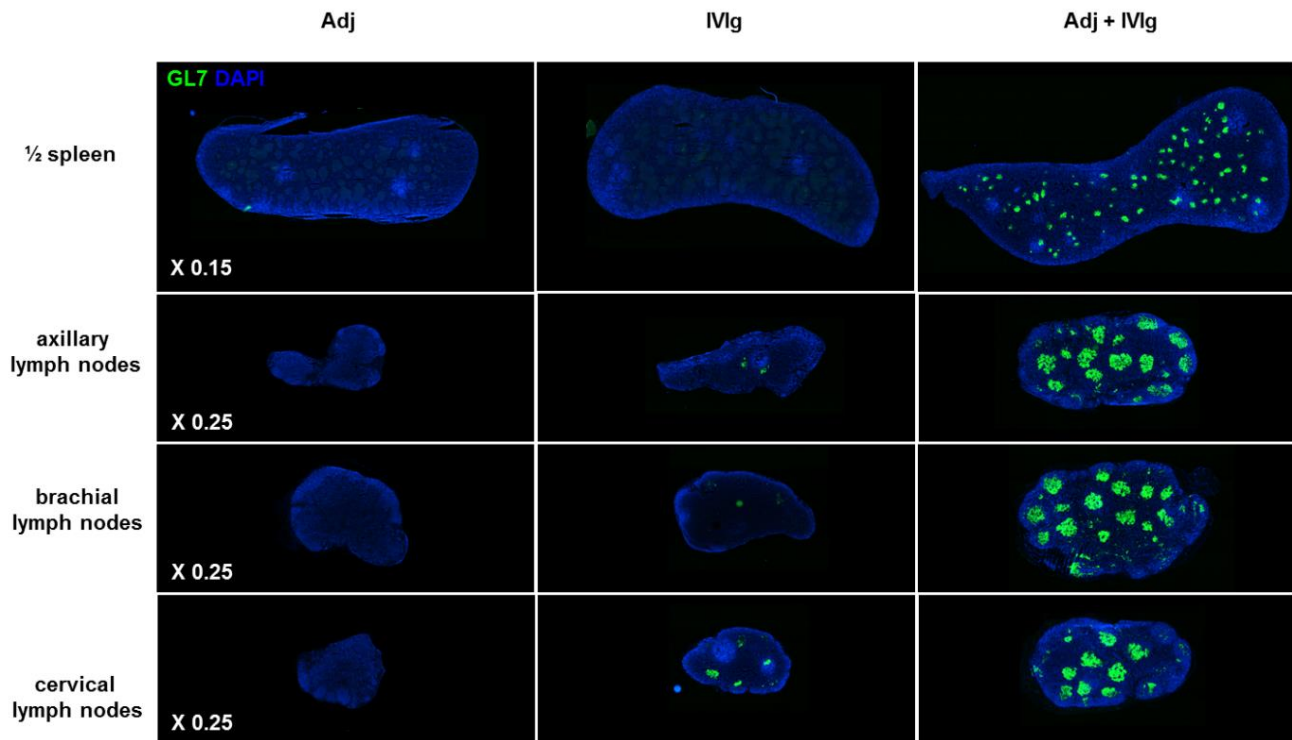
Figure 24: IVIg required the presence of adjuvant to induce the formation of numerous germinal centers *in vivo* in the mouse. C57Bl/6NCrl mice were immunized 3 times weekly s.c in the neck with 50 mg of IVIg, simultaneously or not with adjuvant (MF59). Mice were terminated 24h after last injection. Spleen and draining lymph nodes were probed for germinal centers with the rat monoclonal GL7 antibody (green). Each picture is from one representative animal.

1.8. IVIg impacts the number of re-circulating mature B cells in bone-marrow

Of specific interest, the effect of IVIg in the distribution of some specific B-cell populations in the spleen and bone marrow was investigated. Newly immature formed B cells leave the bone marrow to home in the spleen where they mature as either follicular (FO) B cells (B220+CD23^{high}CD21^{low}IgD^{high}) or marginal zone (MZ) B cells (B220+CD23^{low}CD21^{high}IgD^{low}). Mature naïve follicular B cells, that comprise more than 95 % of the B cells in peripheral lymph nodes, have the ability to freely recirculate, entering and exiting follicular niches in secondary lymphoid organs in search of antigen, and to mediate T-dependent immune responses (Pillai and Cariappa, 2009). In contrast, MZ B cells are non-recirculating cells which line the marginal sinus in the spleen and respond to blood-borne pathogens to provide T-independent immune

responsiveness. The bone marrow also constitute an alternative perisinusoidal niche for recirculating mature B cells with a follicular phenotype wherein they have immediate access to blood-borne pathogens and can be activated in a T cell-independent manner, similarly to MZ B cells. The different B cells compartments in the spleen and bone marrow were assessed by flow cytometry and the gating strategy is presented in Figure 25A. The proportion of re-circulating mature B cells in the bone-marrow was reduced in mice which were administered with IVIg together with OVA and adjuvant (Figure 25B). In fact, once they have bound antigen, B cells activate their adhesion molecules (ex: LFA-1) to get trapped at the border of the T-cell and B-cell zones of peripheral lymphoid tissues, and thus their re-circulation is prevented. This is can be observed by immunization with OVA, which reduces the proportion of mature B cells re-circulating in the bone-marrow compared to mice injected with adjuvant alone. Since IVIg amplified this effect, this may indicate that the highly diverse IVIg-epitopes increases the chance to encounter epitope-specific B cells, so that a larger number of responding mature B cells gets arrested in the peripheral lymphoid tissues and don't show-up anymore in the bone-marrow. This observation is in correlation with the increased number of B cells in these tissues upon IVIg treatment shown in section 1.2. In addition, IVIg seems also to further increase the proportion of pre-B cells in the bone-marrow significantly, compared to OVA immunization. Both effects on pre-B and recirculating mature B cells in the bone-marrow couldn't be reproduced with Avastin, which indicates that these effects are specifically linked to the high diversity of IVIg. Regarding the spleen compartments, IVIg affected neither the percentage of FO nor the MZ B cells. All results were similar when plotting number of cells instead of percentage (data not shown).
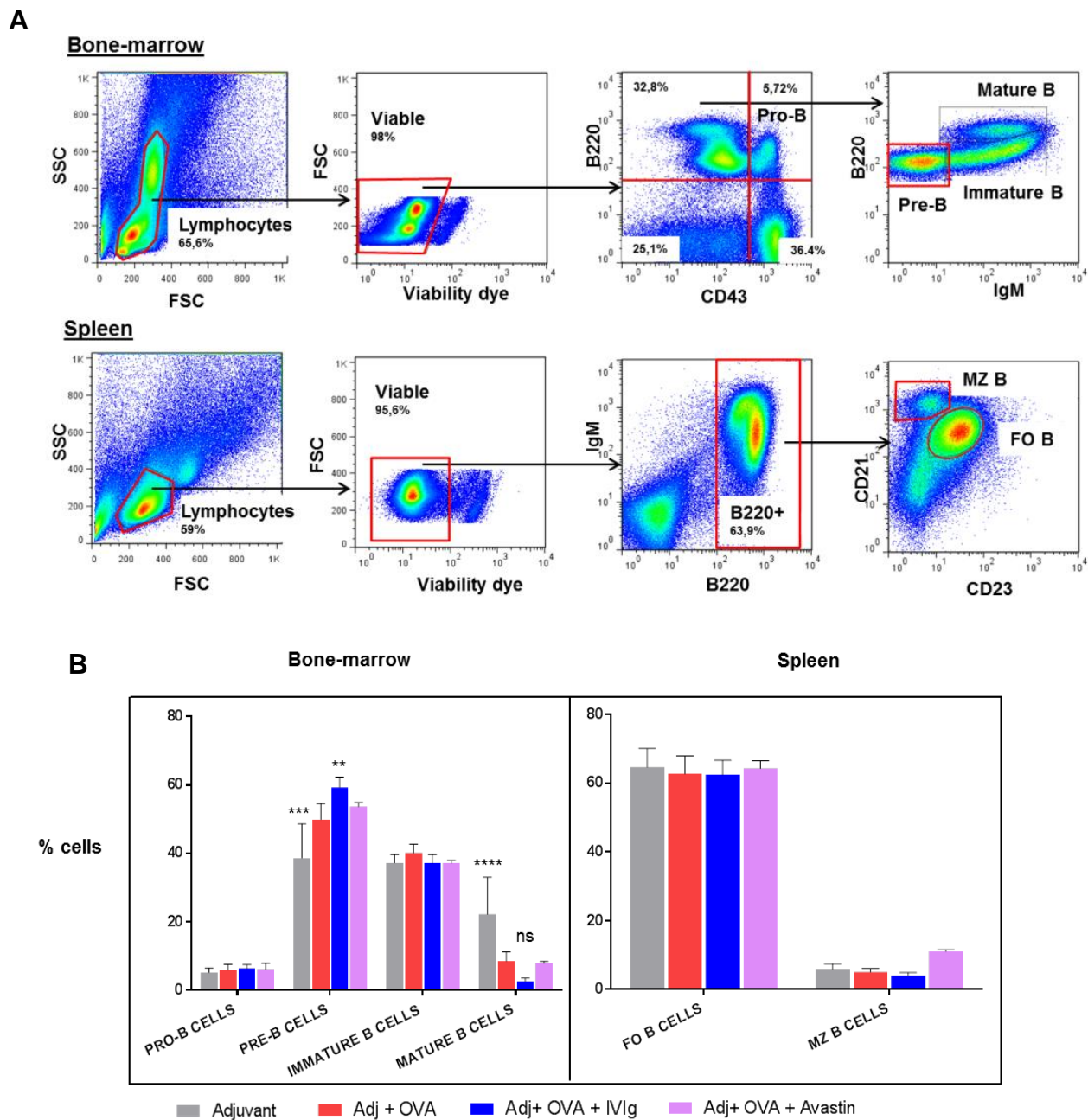
Figure 25: IVIg doesn't affect B-cell compartment in the spleen but reduces the proportion of mature re-circulating B cells in the bone-marrow and promotes pre-B cells formation. (A) Gating strategy for assessing the different B-cell compartments in the spleen and bone-marrow by flow-cytometry. **(B)** C57Bl/6NCrl mice were injected 3 times weekly s.c in the neck with 50 µg OVA and adjuvant (Adj MF59) (red bar), and terminated 24h after last injection. IVIg or Avastin were injected simultaneously to OVA and Adj as indicated. Bars represent mean ± SD (n=6; except for Avastin group n=3). Statistical significance was tested using two-way ANOVA with Dunnett's correction. Each group was compared to the control group "Adj+OVA". Star maker significant difference *: p < 0.05; **p<0.01; ***: p<0.001; ****: p<0.0001.

1.9. IVIg effects appear early

In order to understand the timing of the IVIg mediated effects, mice were injected once with IVIg and adjuvant and readouts were performed after 16h, 24h, 48h, 72h and 7 days, and compared with the OVA and adjuvant treated groups. Strikingly, some IVIg effects were already visible after only 48h (Figure 26A), such as increased weight in lymph nodes of about 1.5 to 2-fold. Similarly, CD86 expression on B cells in axillary lymph nodes was upregulated of more than 1.5-fold, and expression of CD69 of 5-fold. B and T-cell numbers were also increased of about 2-fold after 48h (Figure 26B). The peak of the effects in IVIg-treated mice appeared at day 3 in lymph nodes, with a weight increase of 2 fold in axillary lymph nodes and about 4 fold in cervical lymph nodes. On day 3 CD86 on B cells was up-regulated up to 2 fold, CD83 up-regulated to 1.5-2 fold and CD69 up-regulated to 3 fold. Increase in T and B-cell numbers, compared to the OVA immunized group, also appeared to be maximal at day 3. B-cell numbers increased up to 6 to 7-fold in lymph nodes, together with both CD4+ and CD8+ T-cell number which were 2 to 3-fold higher. These effects tend to decrease after day 3 until day 7. All together these data indicate that IVIg mediates an activation of the immune system visible as early as 2 days after injection and reaching a maximum after 3 days. Moreover, all readouts were performed after a single IVIg injection, so the effects observed here are likely to appear even earlier and/or to be more pronounced when measurements would be performed after several boosting injections.
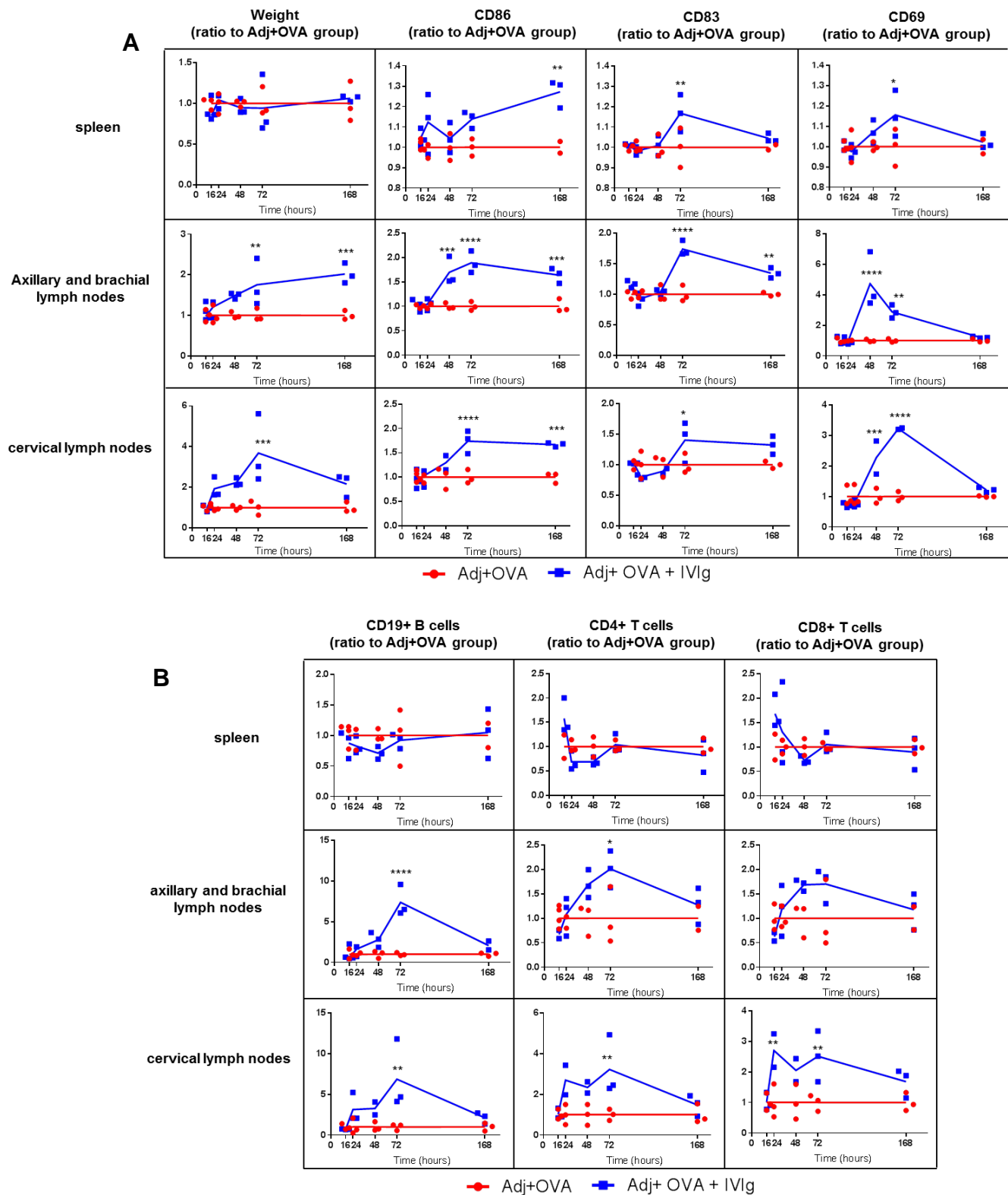
Figure 26: IVIg-mediated effects on immune cell populations appear early after injection. C57Bl/6NCrl mice were injected once s.c in the neck with 50 µg OVA and adjuvant MF59 (red lines), and with/without 50mg of IVIg in addition (blue lines). Mice were terminated 16h, 24h, 48h, 72h and 7 days after the injection. **(A)** Weight and expression of CD86, CD83 and CD69 on CD19+ B cells. **(B)** Number of B CD19+ B cells, CD4+ T cells and CD8+ T cells. Data show ratio compared to "OVA+Adj" group. Lines represent mean. Statistical significance was tested using two-way ANOVA with Sidak's correction. Star maker significant difference *: $p < 0.05$; **$p < 0.01$; ***: $p < 0.001$; ****: $p < 0.0001$.

1.10. Single shot of IVIg followed by OVA challenges doesn't promote tolerance

To investigate whether IVIg was able to promote immune tolerance against a specific antigen, a group of mice was injected once with OVA, adjuvant aluminum and IVIg. The following weeks mice were then challenged with OVA and adjuvant only. Anti-OVA IgG$_1$ titers were measured 2, 3 and 4 weeks after the first injection (Figure 27). Sustained IVIg injections together with OVA and adjuvant efficiently reduced the level of anti-OVA antibodies as measured in week 2 and week 3. However, this effect was lost in week 4 for 2 animals out of 3. This can be due to the weekly repeated OVA-adjuvant injections which might have finally overcome the inhibition mediated by IVIg. This could also be due to inter-animal variability and low number of tested animals. Interestingly, the group which received one shot of IVIg followed by weekly OVA-adjuvant challenges showed no decrease in the OVA–specific antibodies titer for all time-points. This suggests that a single dose of IVIg is not able to promote immune tolerance against a specific antigen.
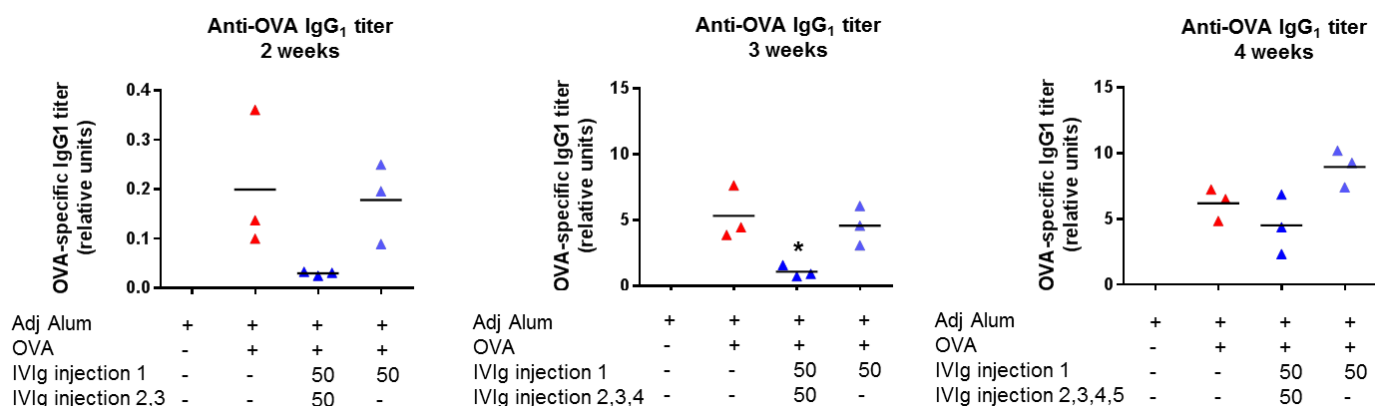
Figure 27: Single shot of IVIg followed by OVA challenges doesn't promote tolerance. ELISA measuring anti-OVA IgG$_1$ at 2, 3 and 4 weeks after first injection. C57Bl/6NCrl mice were injected once a week s.c in the neck with 50 μg OVA and adjuvant aluminum, and where indicated with 50 mg of IVIg in addition. In one group mice were administered once with OVA- alum- IVIg the first week whereas the following challenges consisted in OVA and aluminum only. Lines represent mean. Statistical significance was tested using two-way ANOVA with Dunnett's correction. Star maker significant difference *: p < 0.05; **p<0.01; ***: p<0.001; ****: p<0.0001.

2. Characterization of the humoral immune response in mice

Data presented here collectively suggest that IVIg strongly triggers the mouse immune system. To investigate whether mice mounted a substantial immune response directed against IVIg, IVIg-specific antibodies were measured in mouse serum by ELISA. In addition, the level of total mouse antibodies in serum was studied to assess whether it was affected by IVIg . For all the data presented in this section, <u>it is of importance to notice that the antibody titers can't be directly compared between the different ELISA formats</u>. Although they are expressed in relative units as compared to a standard or in OD units, antibodies used in the capture or detection steps all differ in their format, affinity and avidity between the different assays and therefore the titers obtained are not comparable on the same scale.

2.1. IVIg raises a specific antibody response in mice

2.1.1. Anti-IVIg mouse IgG

Different doses of IVIg ranging from 1 mg up to 50 mg per animal were tested to explore the effect on the formation of anti-OVA antibodies in mice. As already described in section 1.1, inhibition of the OVA-specific humoral response was proportional to the dose of IVIg injected (Figure 28A). A prominent IVIg-specific immune response was raised in mice when 1 mg of IVIg was injected (Figure 28B). Surprisingly, less IVIg-specific mouse IgG were detected in mouse serum when the dose of IVIg administered was increased, in an inversely proportional manner. FcRn saturation might not be the major factor accounting for the observed inverse correlation. FcRn saturation is a non-selective process that will accelerate the degradation of all antibodies present in mouse serum, regardless of their antigen specificity. Indeed, previous data (Figure 20A) presented here demonstrated that Avastin given at high dose didn't decrease the anti-OVA IgG in mouse serum. Titration curves measuring anti-OVA IgG nicely show that the ratio of the inhibitory effect from IVIg remains similar upon different dilutions of the samples, since the two curves are parallel in the linear range (Figure 28C). Despite a possible interference in the assay, titration of samples to measure anti-IVIg IgG is parallel to titration of the standard (Figure 28D). This means that back-calculation of the sample titer according to standard provided the same results across the different dilutions of the samples within the linear range, with a variability of ±20 %. Thus, the decrease in signal with the increase in IVIg dose can't be attributed to unspecific binding in the assay. To investigate whether this effect could be explained

by interference in the ELISA assay, a competition assay was performed by spiking IVIg into the serum of 1 mg IVIg-treated mice (Figure 29A). Indeed sera from low dose IVIg treatment still contain a high proportion of mouse anti-IVIg not complexed that could be detected by ELISA. Addition of IVIg inhibited the detection of anti-IVIg mouse IgG, with a 71 % signal inhibition at the dose of 50 mg/mL of IVIg, 49 % at 20 mg/mL and 42 % at 10 mg/mL. This demonstrates that reduction in signal observed when IVIg dose increases can most likely be explained by interference in the ELISA assay, as illustrated in Figure 29B. When mice raise an anti-IVIg IgG response, the higher the dose of IVIg present in the serum, the more IVIg-specific mouse antibodies will be complexed with IVIg. Considering their antigen-binding part being already occupied, these IVIg-specific mouse IgG are not able to bind to IVIg coated on the assay plate. In consequence of this assay interference, injection of high dose of IVIg lead to a low detection signal in the ELISA measuring IVIg-specific mouse IgG, whereas injection of low dose of IVIg lead to a high detection signal, as shown with serum from the 1 mg-treated group (Figure 28B).
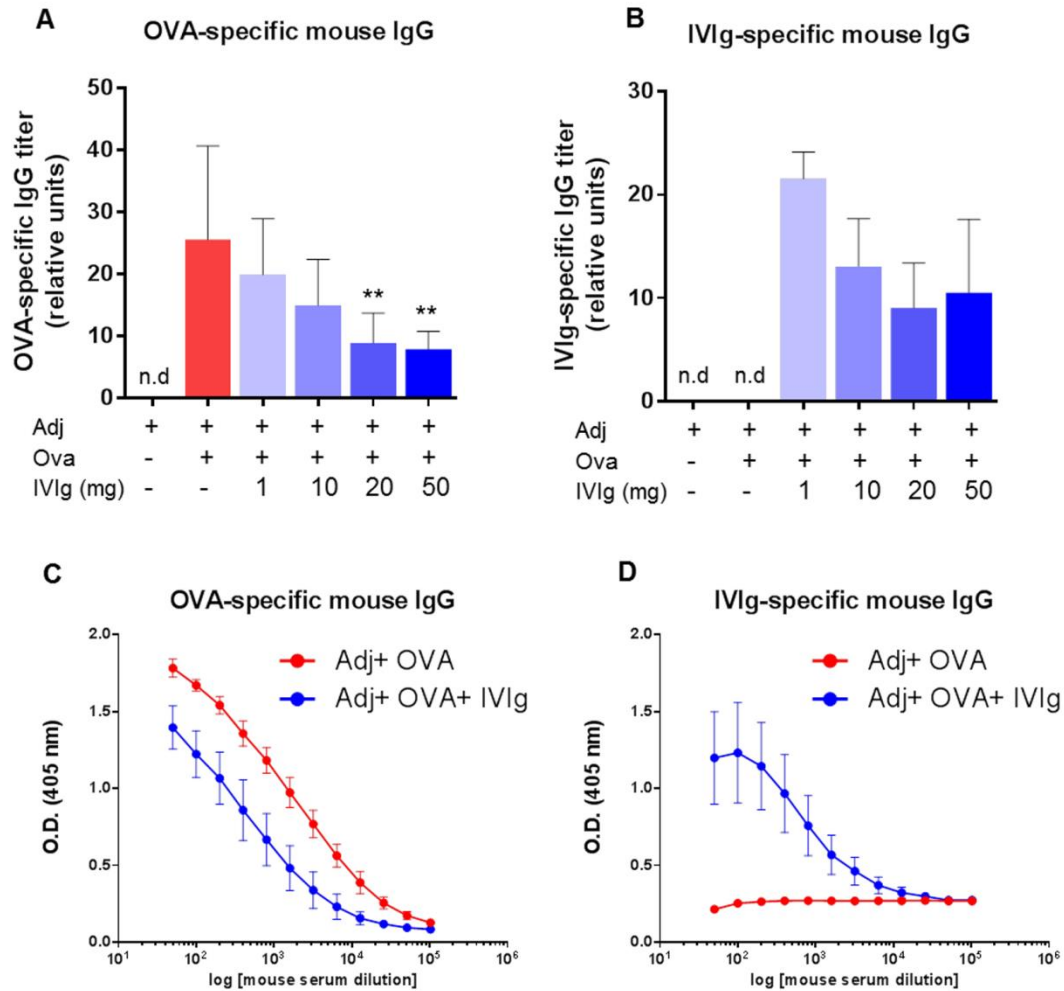
Figure 28: IVIg raises a specific antibody response in mice. C57Bl/6NCrl mice were injected 3 times weekly s.c in the neck with 50 µg OVA and adjuvant MF59 (red bar), and terminated 24h after last injection. IVIg was injected simultaneously to OVA and Adj as indicated at different doses **(A)** OVA-specific mouse IgG measured by ELISA. **(B)** IVIg-specific mouse IgG measured by ELISA. Bars represent mean ± SD. Values as expressed as relative units to standard. Data pool 2 independent experiments (n=6). **(C,D)** ELISA titration curves on serum from mice treated with OVA+Adj±IVIg at 50 mg. Dots represent mean ± SD (n=3). Statistical significance was tested using one-way ANOVA with Dunnett's correction. Each group was compared to the control group "Adj+OVA". Star maker significant difference *: $p < 0.05$; **$p<0.01$; ***: $p<0.001$; ****: $p<0.0001$.
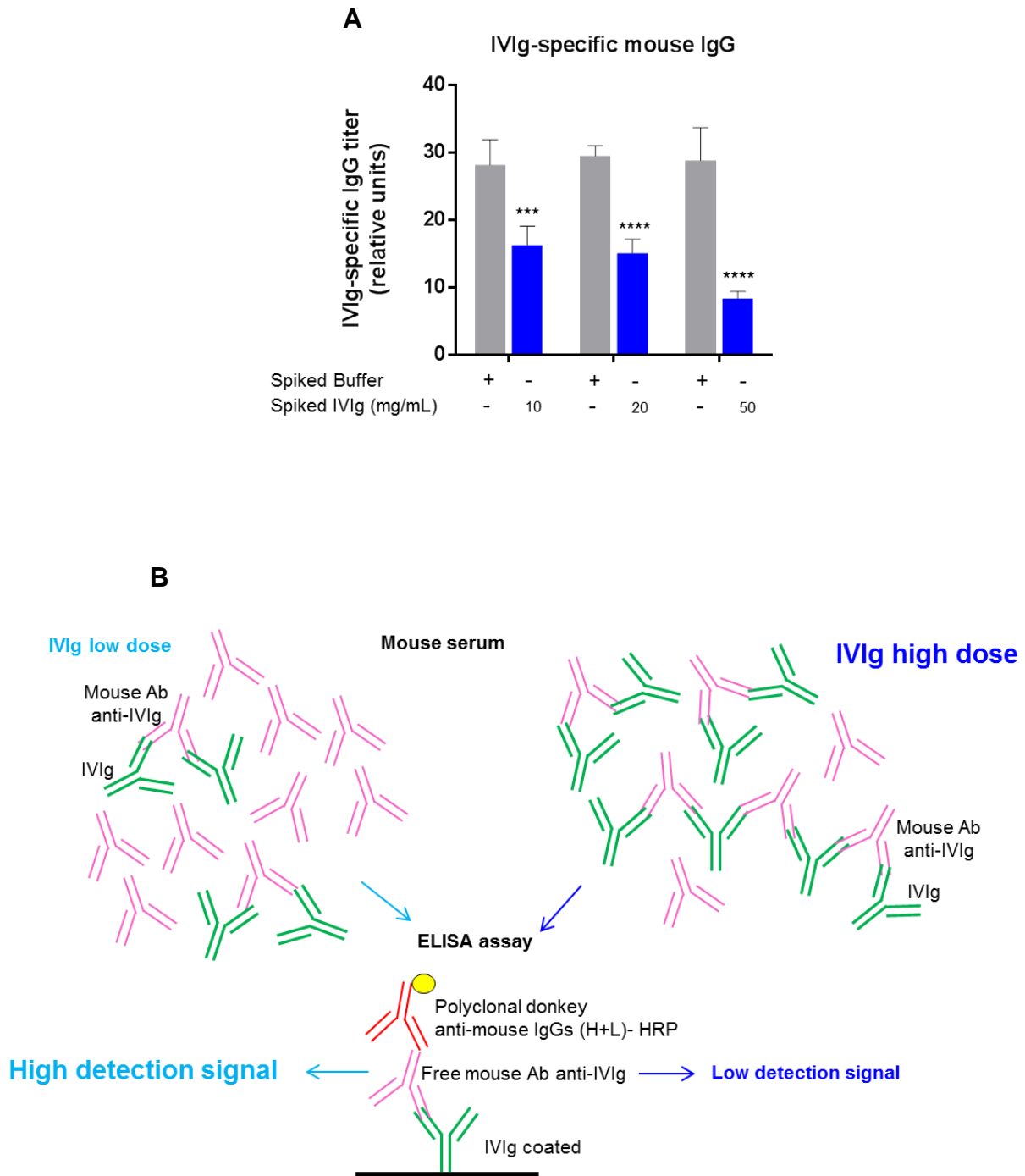
Figure 29: IVIg present in mouse serum can lead to interference in ELISA assay. (**A**) Addition of IVIg *in vitro* in mouse serum inhibits the detection of IVIg-specific mouse IgG by ELISA in a dose-dependent manner. Blocking Buffer or IVIg were added at 10, 20 or 50 mg/mL in serum from mice treated 3 times weekly with 1mg of IVIg (n=3). (**B**) Schematic representation of the ELISA assay to measure IVIg-specific mouse IgG and how IVIg can lead to interference in this assay.

2.1.2. High dose IVIg reduces total mouse IgG

Different doses of IVIg ranging from 1 mg up to 50 mg per animal were tested to explore the effect on the formation of total IgG antibodies in mice (Figure 30A). OVA immunization enhanced the total mouse IgG titer of about 0.8 relative unit compared to the adjuvant group. Injection of 1mg of IVIg led to an increase of the total mouse IgG titer of about 2 relative units compared to the OVA-immunized group. Surprisingly, less total mouse IgG were detected in mouse serum when the dose of IVIg administered was increased, in an inversely proportional manner. To investigate whether IVIg complexed with specific mouse antibodies interferes with the detection of total mouse IgG in serum, a control ELISA assay has been performed in which total mouse IgG are captured via a Fc-specific polyclonal goat anti-mouse IgG. Results obtained were identical to the results obtained with a non Fc-specific capture antibody (Figure 30C). Thus, these data rule out that steric hindrance around the CDR regions of mouse IgG could interfere with binding of the capture antibody and explain reduction in signal. In addition, these data show good reproducibility of the assay. However, steric hindrance may still occur around the Fc regions of the mouse IgG, that could potentially inhibit their capture via Fc-specific antibodies. To confirm the assumption that there is no interference in the detection of total mouse IgG due to steric hindrance, a competition ELISA was performed.

To determine if the formation of immune complexes between IVIg and mouse anti-IVIg antibodies can lead to interference in the detection of total mouse IgG antibodies, different concentrations of IVIg were spiked *in vitro* into the serum of 1mg IVIg-treated mice. Indeed sera from low dose IVIg treatment still contain a high proportion of mouse IgG not complexed that could be detected by ELISA (as shown in Figure 30A). The results depicted in Figure 30D revealed no inhibition in the detection signal of total mouse IgG following IVIg or Avastin spiking into mouse serum compared to buffer spiking, for all the three different concentrations tested. This indicates that IVIg doesn't lead to a detectable interference in this assay. The totality of mouse IgG present in mouse serum could be detected in this assay, regardless of the treatment applied.
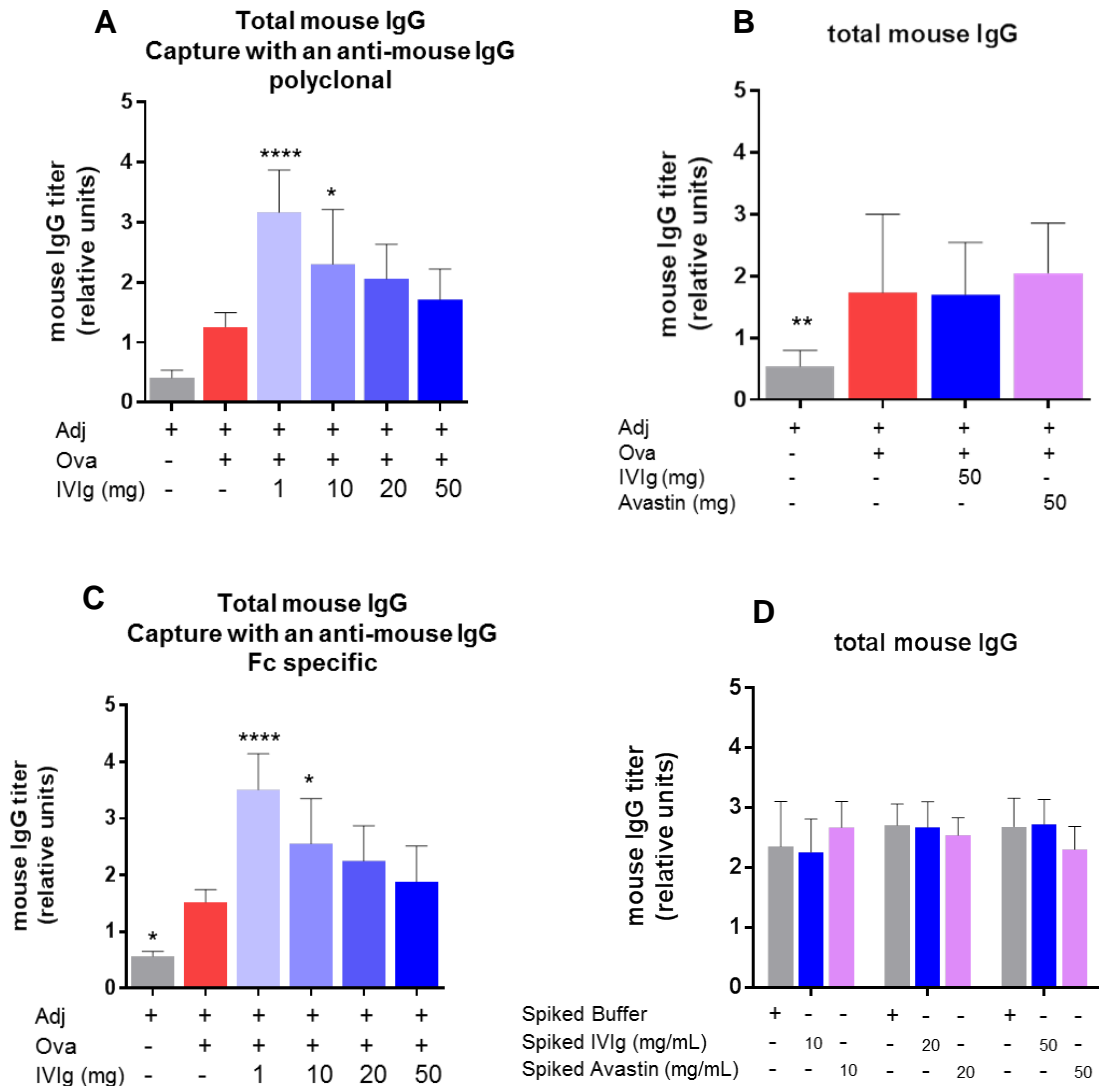
Figure 30: Detection of total mouse IgG in serum by ELISA. C57Bl/6NCrl mice were injected 3 times weekly s.c in the neck with 50 μg OVA and adjuvant MF59 (red bar), and terminated 24h after last injection. IVIg was injected simultaneously to OVA and Adj as indicated at different doses. **(A)** Total mouse IgG captured via a goat polyclonal anti-mouse IgG antibody (n=6 from 2 independent experiments). **(B)** Total mouse IgG detected in serum after IVIg or Avastin treatment. Total mouse IgG were captured via a goat polyclonal anti-mouse IgG antibody. Data pool 4 independent experiments (n=12). **(C)** Total mouse IgG captured via a goat polyclonal anti-mouse IgG Fc-specific antibody. (n=6 from 2 independent experiments). **(D)** Competition ELISA. Blocking Buffer, IVIg or Avastin were added *in vitro* at 10, 20 or 50 mg/mL in serum from mice treated 3 times weekly with 1mg of IVIg. Total mouse IgG were captured using a goat polyclonal anti-mouse IgG antibody (n=3). For (A), (B) and (C), statistical significance was tested using one-way ANOVA with Dunnett's correction. Each group was compared to the control group "Adj+OVA". For (D), statistical significance was tested using two-way ANOVA with Dunnett's correction. Each group was compared to the control group "Spiked Buffer". In all graphs bars represent mean ± SD. Values as expressed as relative units to standard. Star maker significant difference *: p < 0.05; **p<0.01; ***: p<0.001; ****: p<0.0001.

In a separated experiment we measured the titer of total mouse IgG in serum samples from mice treated with high dose of IVIg or Avastin (Figure 30B). When mice were administered with 50 mg of IVIg, the titer of total mouse IgG was comparable to the one obtained in OVA immunized mice, in line with what was already depicted in Figure 30A and C. Strikingly, treatment with the same dose of Avastin lead to the same effect.This suggests that both IVIg and Avastin induced an homeostatic effect most likely via FcRn saturation, which led to a reduction of total mouse IgG. This is in line with previous studies showing that FcRn saturation accelerates the clearance of mouse antibodies present in serum (Bleeker et al., 2001). However, data in section 1.5 demonstrated that Avastin didn't lead to a decrease of the OVA-specific IgG. This ruled out FcRn saturation as the main driver of the inhibitory effects of IVIg in the OVA-specific response in this mouse model. Schemata that illustrate the different antibodies present in mouse serum before and after clearance are depicted in Figure 31. Basically, OVA-IgG are decreased when IVIg doses are increased (Figure 31A). When IVIg doses increase, all types of IgG will decrease proportionally, due to increased clearance mechanisms (Figure 31B).
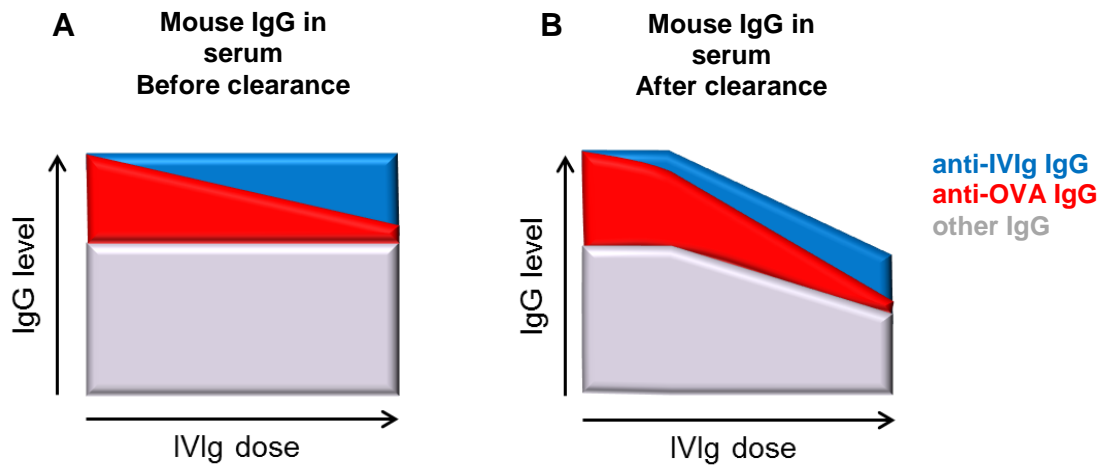
**Figure 31: Schematic of how high doses of IVIg could promote total mouse IgG clearance via FcRn saturation.**
(**A**) Increasing doses of IVIg lead to the formation of mouse anti-IVIg (in blue) antibodies and decreasing levels of anti-OVA mouse IgG (in red). (**B**) In parallel, increasing doses of IVIg augment clearance via FcRn saturation, thus leading to decreased levels of total mouse IgG.

2.1.3. Mouse antibody response against IVIg is mostly directed towards Fab

To investigate whether the mouse anti- IVIg-IgG were mostly directed towards the Fc or the Fab part of IVIg, a competition experiment was performed- IVIg or the control mAb Avastin were spiked *in vitro* into the serum of 1mg IVIg-treated mice. As already described previously, addition of IVIg inhibited the detection of anti-IVIg mouse IgG, with a 71 % signal inhibition at the dose of 50 mg/mL of IVIg (Figure 32A). Interestingly, addition of Avastin in 1 mg IVIg-treated mouse serum only lead to a significant signal interference of 30 % at the highest dose of 50 mg/mL. The most plausible explanation for such inhibition following spiking of Avastin is that a small fraction of mouse antibodies directed against IVIg recognized some common epitopes shared between IVIg and Avastin, most likely in the Fc-part of human IgG. These data thereby confirm that mice develop antibodies targeting both Fc and Fab regions of IVIg. However, since the signal inhibition following Avastin spiking was much lower as compared to IVIg spiking, we can conclude that mouse IgG are mostly directed against the variable parts of IgG which are part of the Fab region of IVIg Fab

To assess the IgG response against Avastin, serum from mice treated with 50 mg of Avastin was applied on an Avastin-coated plate and specific mouse IgG were detected. As illustrated in Figure 32B, mice elicited an IgG response against Avastin. Interestingly, serum from IVIg-treated mice contained IgG that were able to bind to Avastin and lead to a higher detection signal in the assay. ELISA with coating of Avastin-Fc further confirmed that this signal comes from antibodies directed against Avastin Fc parts. These data show that antibodies directed towards IVIg Fc parts also react with the Fc part of Avastin, which share some common epitopes since both comprise human antibodies. Very importantly, when detecting IVIg-specific mouse IgG, a part of the antibodies generated upon 50 mg of Avastin administration can bind to IVIg coated on the plate and lead to 27% of detection signal compared to mice treated with IVIg (Figure 32B). This therefore suggests that 27% of anti-IVIg IgG is directed to its Fc region.
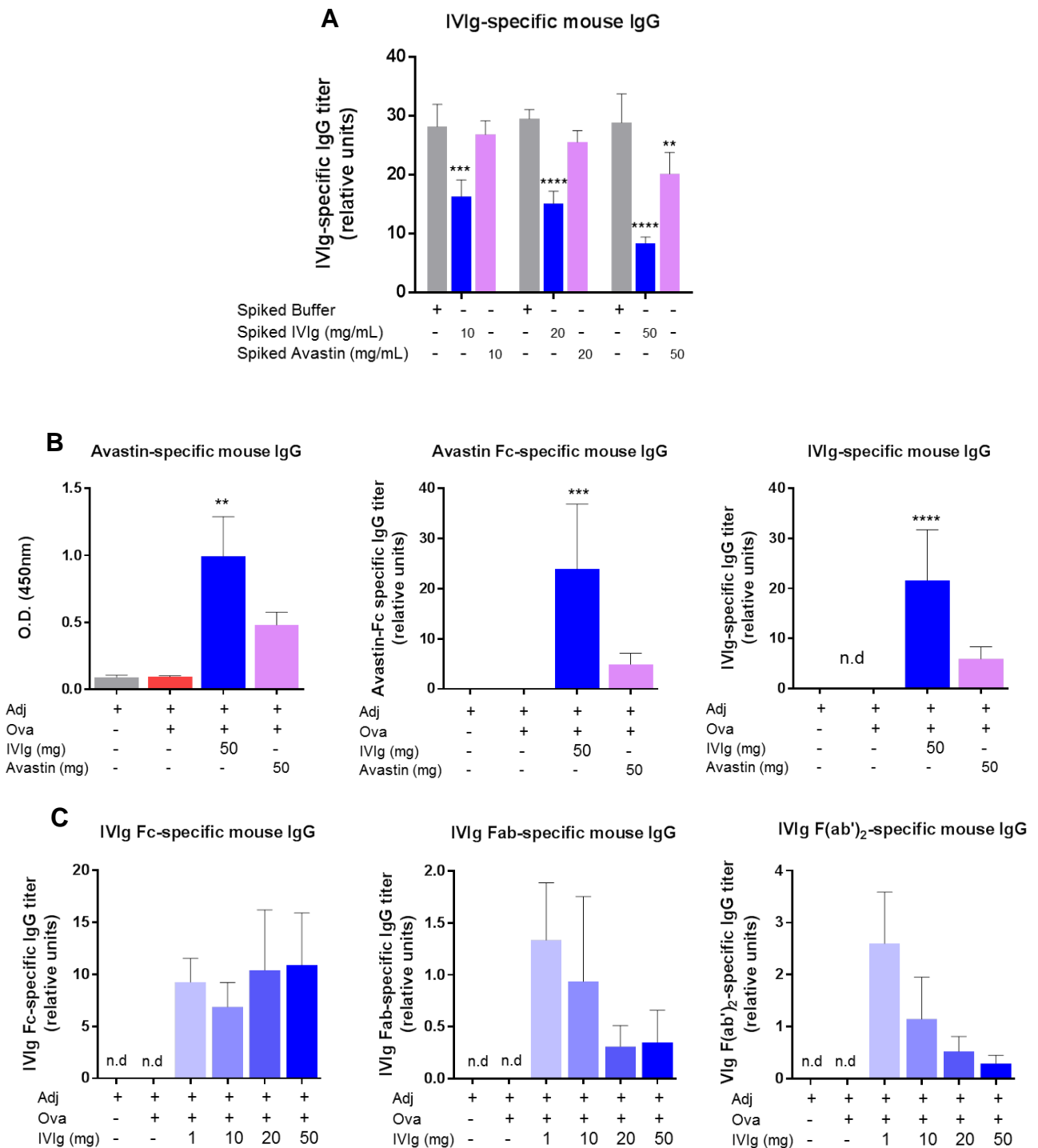
Figure 32: Mouse IgG response against IVIg is mostly directed against IVIg-Fab region. (A) Addition of IVIg *in vitro* in mouse serum inhibits the detection of IVIg-specific mouse IgG by ELISA in a dose-dependent manner. Blocking Buffer, IVIg or Avastin were added at 10, 20 or 50 mg/mL in serum from mice treated 3 times weekly with 1mg of IVIg (n=3). **(B)** Detection of mouse IgG specific for Avastin (n=6), Avastin-Fc (n=9) and IVIg (n=12) by ELISA. **(C)** ELISA measuring mouse IgG anti-IVIg-Fc, Fab or (Fab)'$_2$ fragments (n=6). In all graphs bars represent mean ± SD. Statistical significance was tested using two-way ANOVA with Dunnett's correction for (A) and with two-tailed unpaired t-test for (B). Each group was compared to the control group "Buffer". Star maker significant difference *: $p < 0.05$; **$p<0.01$; ***: $p<0.001$; ****: $p<0.0001$. n.d: not detected.

To further confirm the specificity of anti-IVIg mouse IgG, ELISA measurements were performed after coating purified IVIg-Fc, Fab or (Fab')$_2$ fragments. Titers of mouse IgG recognizing the Fab or (Fab')$_2$ fragments from IVIg were decreased while IVIg doses injected in mice were increased (Figure 32C). This inverse correlation might likely be due to the interference in the assay described in Figure 29. This suggests that mice build a humoral response mainly directed against the variable parts of IVIg. In contrast, mouse antibodies directed towards IVIg Fc-region were more or less equally well detected in ELISA, suggesting in that the signal was not inhibited in a dose-dependent manner by IVIg present in mouse serum. This could imply that the anti-Fc mouse IgG might not be the highest in affinity, and/or the highest in number in regards to the immune response generated and thus are less sensitive to IVIg high dose interference in the serum. These results suggest that anti-IVIg mouse antibodies might be mostly directly against the IVIg-Fab region (Figure 32 A and B). This is consistent with previous data showing that IVIg spiking in serum led to 71 % of signal inhibition whereas Avastin spiking to 30 % inhibition only. Ideally these data should have been confirmed by a competition ELISA assay spiking high concentrations of IVIg-Fab or Fc molecules into 1 mg IVIg-treated mouse serum. Unfortunately, with regards to the high concentrations needed for such a competition, this experiment couldn't be performed.

Taken together these results reveal that IVIg raises an antibody response in mice mainly directed towards the Fab region. This suggests that the highly diverse variable regions present in IVIg are the cause of the massive immune response we observed following IVIg injection. In line with our previous data showing that a human mAb was not able to reproduce the effect of IVIg, it seems that the highly diverse variable regions present in IVIg are responsible to some extend for the reduced anti-OVA antibody response.

2.2. Effect of adjuvant on the antibody response

ELISA data showed that the total IgG in mice treated with IVIg together with adjuvant was increased to the same level as in mice treated with adjuvant and OVA (Figure 33A). We can expect the total IgG titer to be much higher in IVIg-adj-treated mice compared to OVA-adj-treated mice, but due to the homeostatic effect via FcRn saturation (described in section 2.1.2), such difference couldn't be measured when high dose of IVIg was administered Mice treated with IVIg alone or IVIg and OVA but in the absence of adjuvant presented a titer of total IgG similar to non-immunized mice injected with adjuvant alone (Figure 33A, light blue bars). This is line with the fact that adjuvant is usually required to mount a proper antibody response. Regarding anti-OVA-specific mouse IgG, mice treated with IVIg plus OVA and adjuvant consistently showed significant lower titers (about 4.4-fold lower) compared to mice treated with OVA and adjuvant only (Figure 33B). As expected, anti-OVA antibodies could not be detected in serum from mice treated with adjuvant only or without OVA. In correlation with the data outlined in section 1.4 and 1.7 showing that presence of adjuvant was required together with IVIg to induce B cell activation and formation of numerous germinal centers, an anti-IVIg IgG response occurred only significantly when adjuvant was co-injected with IVIg (figure 33C).
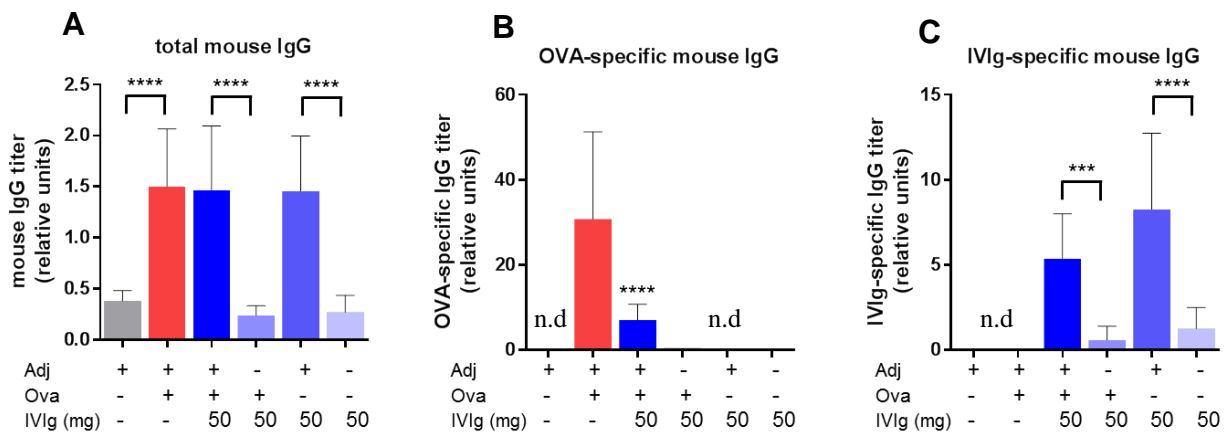
Figure 33: Co-injection of adjuvant is required to induce a mouse IgG response against IVIg. C57Bl/6NCrl mice were injected 3 times weekly s.c in the neck with 50 mg IVIg in combination with OVA and/or adjuvant MF59 as indicated. Mice were terminated 24h after last injection. ELISA to measure total mouse IgG, OVA-specific and IVIg-specific mouse IgG were performed on mouse serum. Bars represent mean ± SD. Values as expressed as relative units to standard. Data pool 3 independent experiments (n=9). Statistical significance was tested using one-way ANOVA with Tukey's correction for total IgG and anti-IVIg IgG data, and with Dunnett's correction for anti-OVA IgG data. Star maker significant difference *: $p < 0.05$; **$p<0.01$; ***: $p<0.001$; ****: $p<0.0001$. n.d: not detected.

2.3. Isotypes of the anti-IVIg response

After showing that IVIg injection together with adjuvant lead to the production of IVIg-specific IgG in mice, it was determined which isotypes of the IVIg-specific antibody response were produced. Figure 34A shows that IVIg-specific IgG_1, IgG_{2a} and IgG_{2b} titers were inversley correlated to the IVIg dose administered to mice, due to ELISA assay interference as explained in section 2.1. Importantly, titers can't be compared between the different istypes due to different assay formats. In contrast, more IgM antibodies were detected as the IVIg dose was increased. This might be due to anti-IVIg mouse IgM not being sensitive to IVIg high dose interference in the serum. Indeed, IgM antibodies are of low affinity, and might likely not be the dominant isotype produced, as for a TD antigen. IgA and IgG_3 isotypes could not be detected in serum diluted in 1/100. Consistent with ELISA data shown in Figure 33, we observed a highly significant increase in anti-IVIg IgG_1, IgG_{2a}, IgG_{2b} and IgM levels in mice treated simultaneously with IVIg and adjuvant compared to mice treated without adjuvant (Figure 34B), thus confirming the necessity of adjuvant co-administration to mount an immune response against IVIg. Here we therefore demonstrated that IgG_1, IgG_{2a} and IgG_{2b} appear to be the main isotypes of the anti-IVIg antibody response.

A
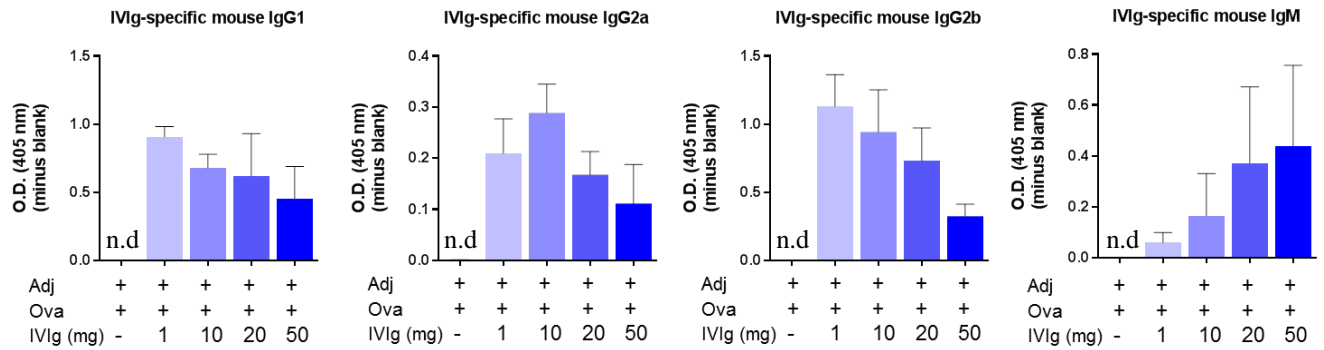
B
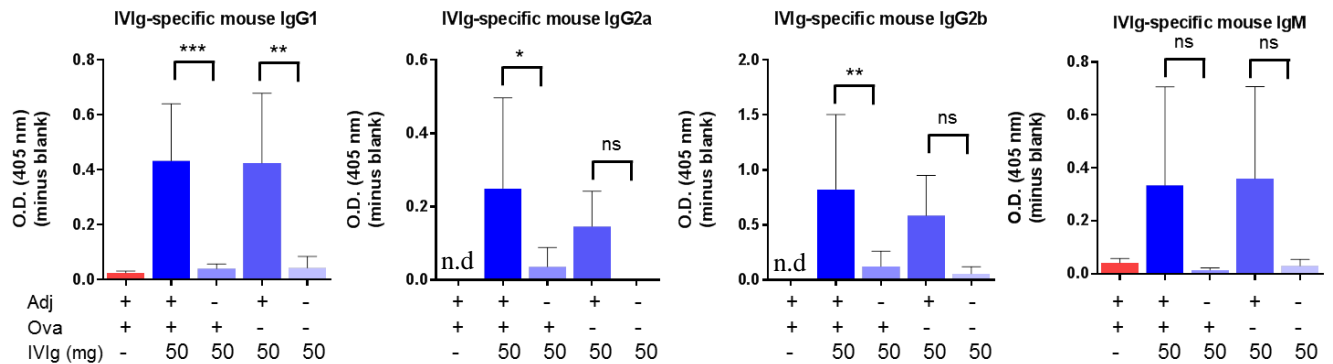
Figure 34: IgG$_1$, IgG$_{2a}$ and IgG$_{2b}$ appear to be the main isotypes of the anti-IVIg antibody response. C57Bl/6NCrl mice were injected 3 times weekly s.c in the neck with different doses IVIg in combination with OVA and/or adjuvant MF59 as indicated. Mice were terminated 24h after last injection. ELISA assays were performed on mouse serum. **(A)** IVIg-specific mouse IgG isotypes upon IVIg dosing. Data are from one experiment (n=3). **(B)** IVIg-specific mouse IgG isotypes with and without adjuvant administration. Data are from 2 independent experiments (n=6). For (A) and (B) bars represent mean ± SD. Values as expressed as O.D. measured at 405 nm.. Serum dilutions were the following: IgG$_1$ 1/1600; IgG$_{2a}$ 1/100; IgG$_{2b}$ 1/100; IgM 1/100. Statistical significance was tested using one-way ANOVA with Tukey's correction. Star maker significant difference *: $p < 0.05$; **$p<0.01$; ***: $p<0.001$; ****: $p<0.0001$. n.d: not detected. ns: not significant.

2.4. IVIg increases IgG-Immunoglobulin secreting cells as measured by ELISPOT

After it has been demonstrated that IVIg reduced the OVA-antibodies titer, it was assessed whether IVIg can inhibit the differentiation of B cells into plasma cells, or if it might impair their immunoglobulin secretion ELISPOT appeared to be the best functional assay to evaluate the frequency of immunoglobulin-secreting cells or ISC.

As illustrated in Figure 35A and B, IVIg significantly increased the number of total IgG ISC in both axillary/brachial lymph nodes and cervical lymph nodes, of about 15- and 6.5-fold respectively, compared to OVA-immunized mice. These results reveal the strong formation and activation of plasma cells in the presence of IVIg rather than exhaustion or an inhibitory effect. There was no change in the frequency of IgG-ISC in bone-marrow and spleen upon IVIg treatment. This is most likely due to the fact that these lymph nodes are the primary draining organ after IVIg injection, whereas spleen re-circulation is more systemic. These results are in line with the data reported in sections 1.3, 1.4 and 1.5 showing more prominent effects of IVIg on B cell activation in draining lymph nodes compared to the spleen. In agreement with the formation of numerous germinal centers (GC) in the spleen upon IVIg and adjuvant injection (as seen in section 1.7), it could be expected an increase in total IgG-ISC in the spleen as well. However, it is important to note that this increase in GC formation in the spleen was not systematic since it could not be observed in all experiments, whereas the effect of IVIg on GC in lymph nodes was very consistent thoughout all experiments. In addition, the ELISPOT data are derived from a single experiment with n=3. Therefore, the IgG-ISC in the spleen may have been missed in that experiment.

OVA-specific IgG antibody-secreting cells (ASC) frequency was also assessed by ELISPOT (Figure 35C). Consistent with the observation that IVIg reduced the production of OVA- specific IgG, IVIg reduced the proportion of OVA-IgG ASC relative to the total IgG ISC. These data reflect a massive recruitment of IVIg-specific B cells and their further differentiation into plasma cells, which as a consequence may reduce efficient mobilization of OVA-specific immune cells. We observed no effect of IVIg administration on total IgM-ISC (Figure 35D). Taken together these results are in line with ELISA data showing that IVIg consistently induced a strong antibody response in mice, mainly formed by IgG isotypes.
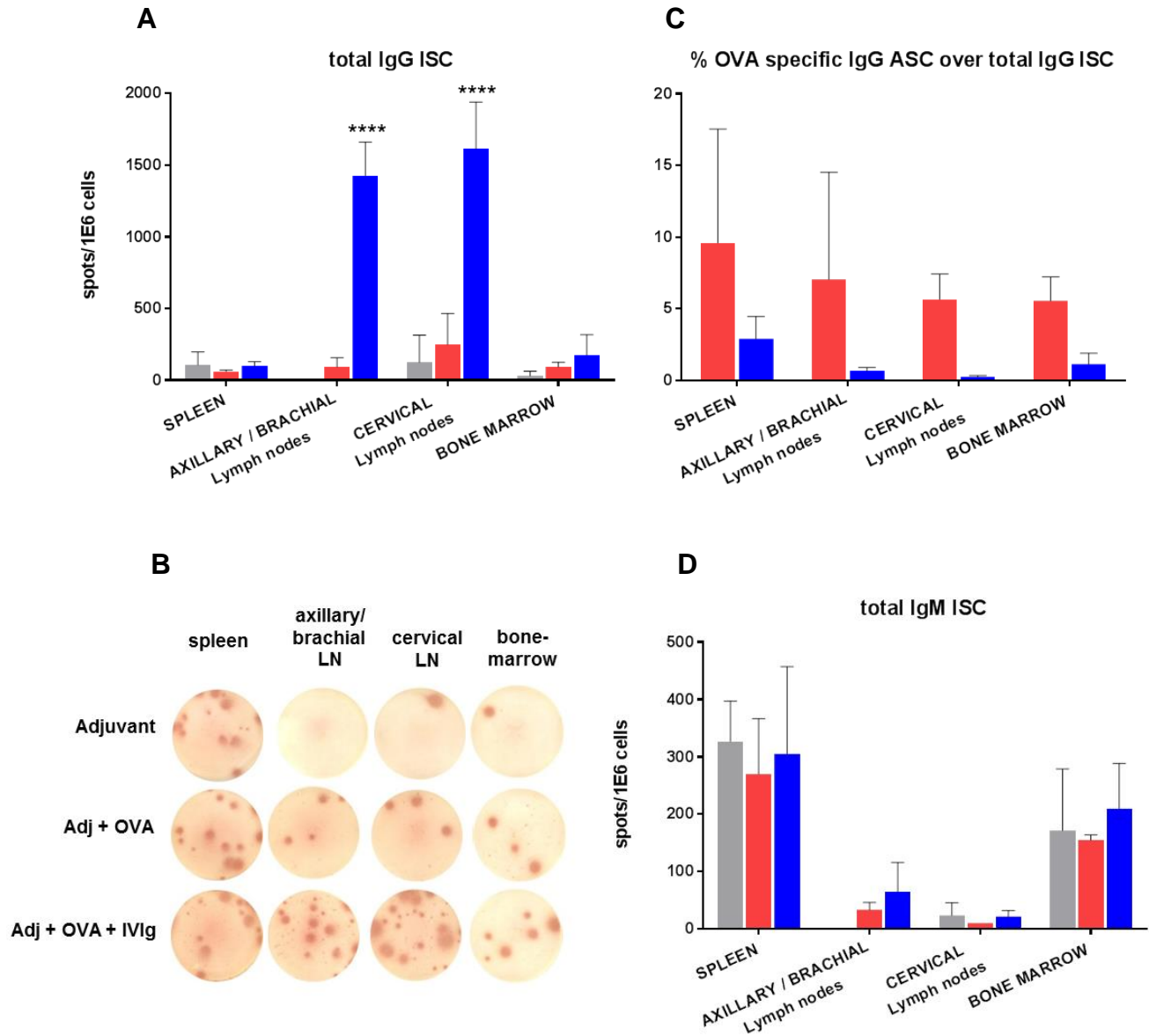
Figure 35: IVIg administration in mice increases the number of IgG-secreting cells in lymph nodes while reducing the proportion of OVA-specific IgG secreting cells. C57Bl/6NCrl mice were injected 3 times weekly s.c in the neck with 50 mg of IVIg in combination with OVA and adjuvant MF59 as indicated. Mice were terminated 24h after last injection, cells were processed from lymphoid organs and plated for ELISPOT assay. **(A)** Total IgG Immunoglobulin-secreting cells (ISC). **(B)** ELISPOT showing total IgG-ISC for one representative animal (n=3)**.** The number of spots was counted and reported in graph (A). **(C)** Proportion of OVA-specific IgG antibody secreting cells (ASC) relative to total IgG ISC. **(D)** Total IgM ISC. Bars represent mean ± SD. Data are from one experiment (n=3). Statistical significance was tested using two-way ANOVA with Dunnett's correction. Star maker significant difference *: $p < 0.05$; **$p<0.01$; ***: $p<0.001$; ****: $p<0.0001$.

2.5. IVIg can't downregulate humoral response against the thymus-independent antigen NP-Ficoll

Overall our data suggest that IVIg strongly triggers the mouse immune system, including the secretion of IVIg-specific IgG antibodies as discussed above. This points towards a massive T-cell dependent antibody response against IVIg, which might compete out the T-cell dependent antibody response against OVA. To address whether IVIg is able to downregulate the antibody response against a thymus-independent antigen (TI-Ag), the TI-Ag NP-Ficoll was co-administered together with IVIg. NP (4-Hydroxy-3-nitrophenylacetic) is a hapten, a small non-immunogenic molecule that is conjugated to Ficoll, a high molecular weight polysaccharide that is highly immunogenic. As control, a group of mice were co-injected with IVIg and NP-OVA as a thymus-dependent antigen (TD-Ag).
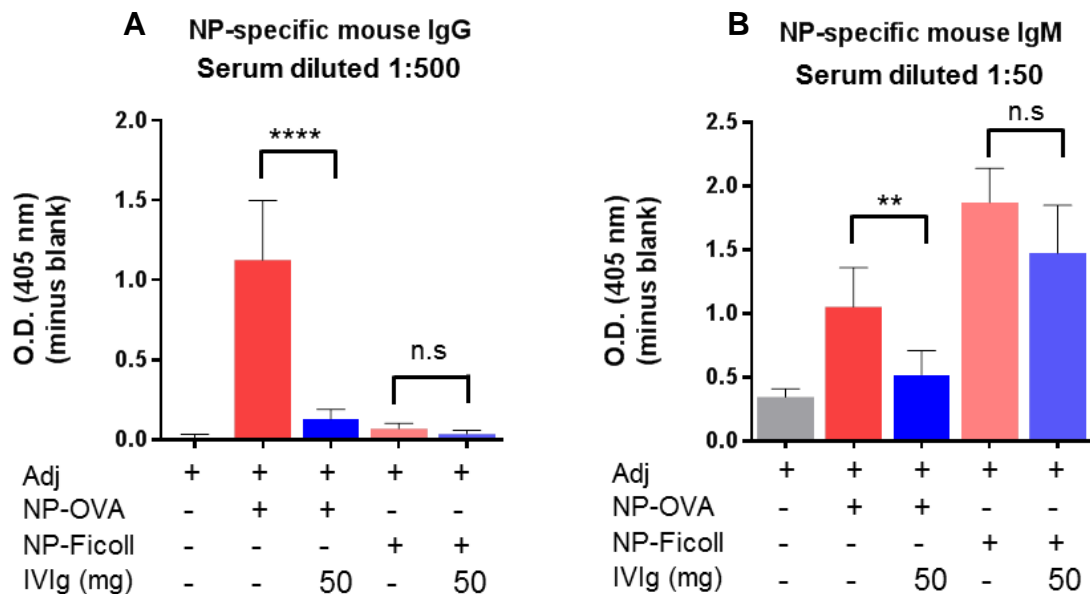
Figure 36: IVIg doesn't decrease the NP-antibody response when mice are immunized with NP-Ficoll, a TI antigen. C57Bl/6NCrl mice were injected 3 times weekly s.c in the neck with 50 µg of NP-OVA or NP-Ficoll together with adjuvant MF59, with or without IVIg as indicated. Mice were terminated 24h after last injection and serum was collected. **(A)** ELISA for NP-specific mouse IgG were on serum diluted 1:500. **(B)** ELISA for NP-specific mouse IgM on serum diluted 1:50. Bars represent mean ± SD. Data are from one experiment (n=6). Statistical significance was tested using two-tailed unpaired t-test. Star maker significant difference *: $p < 0.05$; **$p<0.01$; ***: $p<0.001$; ****: $p<0.0001$. ns: not significant.

IVIg administration efficiently decreased the production of NP-specific IgG in mice immunized with NP-OVA, with a reduction of 88% in the antibody titer (Figure 36A). This shows good reproducibility with the data obtained in OVA-immunized mice. The NP-antibody response in NP-Ficoll immunized mice was mainly of IgM isotype (Figure 36B), with almost no IgG detected (Figure 36A). This is in line with the fact that T cells are needed to mediate isotype switching from IgM to IgG. IVIg significantly reduced the NP-specific IgM titer in NP-OVA immunized mice (51% of reduction), although the inhibition was stronger in the NP-IgG titer, as expected for a TD antigen. IVIg injections didn't significantly reduce the NP-specific IgM titer in NP-Ficoll immunized mice (Figure 36B). These results demonstrate that IVIg can significantly inhibit an antibody response targeted against a TD antigen, but has no effect on the antibody response towards a TI antigen. Therefore, this suggests that T cells are essential for IVIg to exert its inhibitory effect on the antibody production.

3. Additional control experiments

3.1. Analytics on IVIg preparation versus human mAb preparations

Intrinsic factors in the IVIg product could have possibly induced a strong activation of the immune system *in vivo* in mice. Indeed, presence of endotoxins in the formulation could be responsible for such activation, as well as the presence of degraded products such as free heavy or light chains, that could potentially constitute a source of new epitopes that are normally hidden in an intact IgG molecule. In addition, aggregation of recombinant proteins has been shown to enhance activation of both innate and adaptive immunity (Joubert et al., 2012; Rombach-Riegraf et al., 2014), and to ultimately lead to the formation of anti-drug antibodies (van Beers et al., 2010).

Therefore, to rule out such possible implications in the IVIg effects observed on immune cells, endotoxin measurements, electrophoresis and sub-visible particles count were performed on the IVIg preparation which was used for the experiments reported here (Octagam; Octapharma), as well as on the human monoclonal IgG control antibody Avastin and for some analyses the second human monoclonal IgG control antibody Vectibix. Both antibodies and IVIg were free of endotoxin as the levels obtained were below the detection limit (Figure 37A). Results from capillary electrophoresis show one main peak for both, IVIg and Avastin with high purity (Figure

37B), thus excluding a significant amount of -degradation products in both, IVIg and Avastin. Sub-visible particle analyses demonstrated that the tested IVIg preparation overall contains less aggregates compared to the reference antibody Avastin (Figure 37C). This indicates that aggregates are unlikely to play a major role in IVIg-specific effects. As an additional control, Fc-glycan profile was analyzed on the human monoclonal IgG antibodies Avastin and Vectibix. Indeed, as reviewed in the introduction part (section 3.1.4), the role of Fc-sialylation in the anti-inflammatory properties of IVIg remains unclear and highly controversial. Since we observed no anti-inflammatory effects in our experiments with both Avastin and Vectibix (see results part section 1.5), presence of sialic acids on the Fc part of these two antibodies would have ruled out the role of Fc-sialylation involvement in IVIg inhibitory effect in the OVA-antibodies response. Results of glycoprofiling show that neither Avastin nor Vectibix contain sialylation on their Fc-part (indicated as S1 and S2 in Figure 37D, for glycan structures explanations please refer to figure 12 in the introduction part section 3.1.4). These data could therefore not exclude a possible role of Fc-sialylation in the anti-inflammatory properties of IVIg. Due to the complexity of IgG molecules present in IVIg, the glycan profile of IVIg couldn't be measured.

IVIg and Avastin were applied on a chip coated with more than 9000 human proteins to study potential binding interactions. Figure 38 illustrates a magnified section of each array, with each spot representing a specific coated human protein. Intense red spots seen identical on both arrays represent positive controls. IVIg bound to a lot of different human proteins as compared to Avastin, but with low signal intensity. This low signal might be explained by either a low affinity and/or unspecific polyreactive binding. Specific-antibodies present at low concentration in the IVIg preparation might also result in a low-intensity signal. These data thereby provide insights in IVIg polyspecificity for human self-proteins. This is in line with several studies showing that IVIg reacted with several human self-proteins, as reviewed in introduction section 3.2.2. Moreover, we demonstrated in a competition assay that mouse antibodies specific for IVIg are mainly directed towards its Fab region (section 2.1.3). All together this supports the notion that IVIg might likely react with B cell receptor through anti-idiotypic binding.

A Endotoxin measurements

	EU/mL	EU/mg
Avastin	< 5.00	< 0.05
Vectibix	< 5.00	< 0.05
Octagam	< 5.00	< 0.05

B Electrophoresis

Avastin — Purity intact: 94.1%

Octagam — Purity intact: 97.4%

C Sub-visible particles count by MFI

D Glycoprofilig by LC-MS

	Man5	G0-F	G0	G1	G2	S1	S2
Avastin	3%	3%	78%	16%	0%	0%	0%
Vectibix	6%	3%	37%	45%	10%	0%	0%
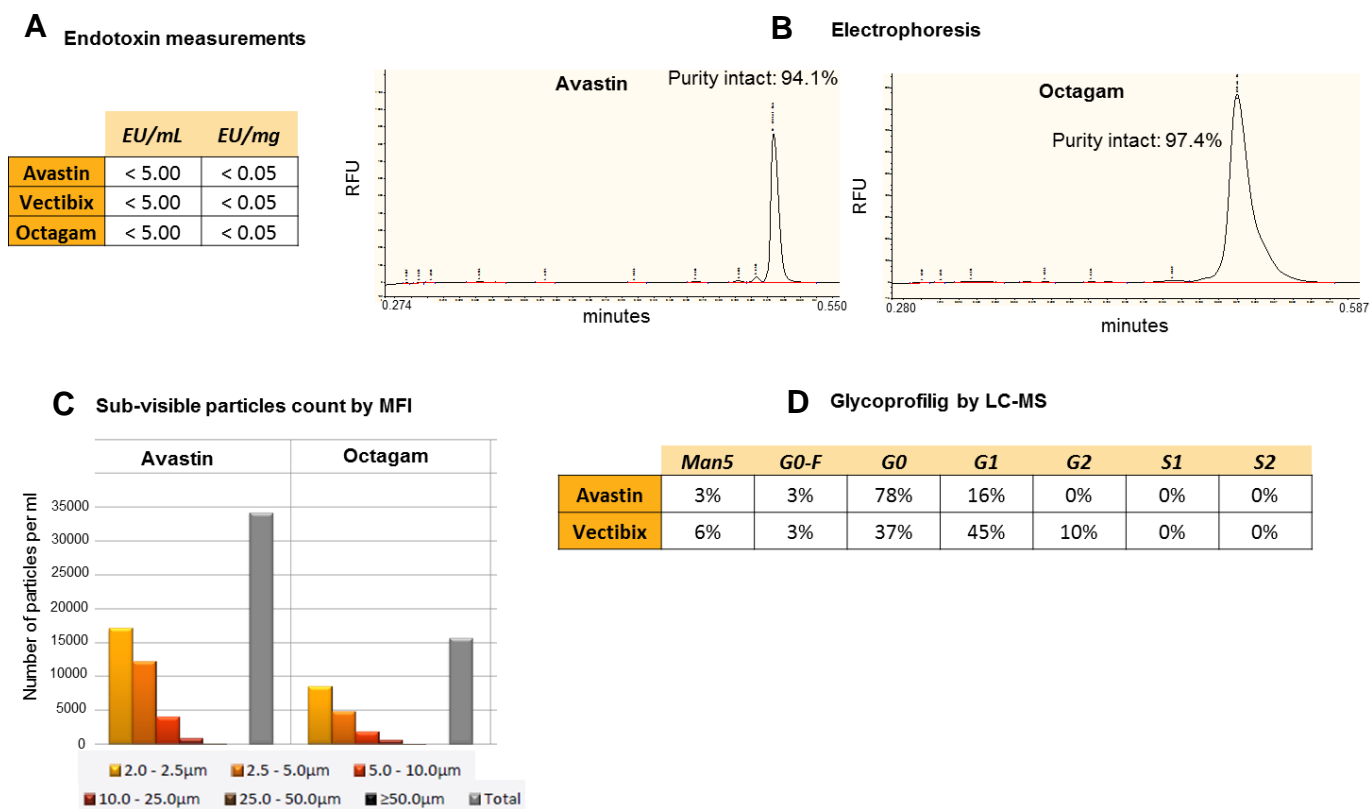
Figure 37: Various analytics performed on IVIg and Avastin preparations. (**A**) Endotoxin measurments. (**B**) Capillary electrophoresis to determine the purity and integrity of IgG molecules (Caliper LifeSciences technology). (**C**) Sub-visible particles count by MFI. (**D**) Fc-Glycan profiling by LC-MS.
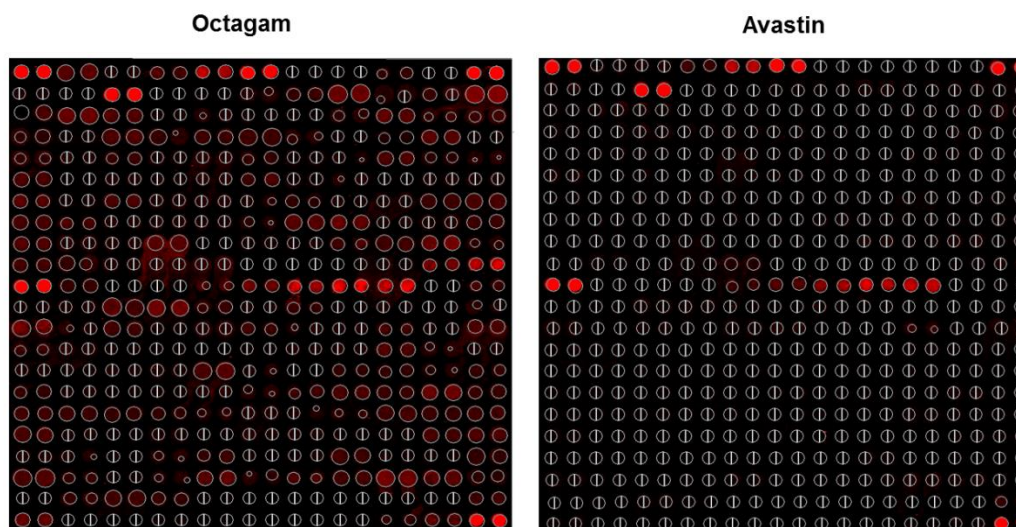
Figure 38: Evaluation of IVIg and Avastin binding to human proteins. The picture illustrates magnified section of the same region of both arrays. Antibodies were applied at 5 μg/mL each on a Invitrogen ProtoArray® 5.1 coated with a panel of human proteins. Intense red spots seen identical on both arrays represent positive controls.

3.2. Testing of various adjuvants

In order to eliminate potential bias in the experimental outcomes due to the use of a single adjuvant, various adjuvants were tested *in vivo* under the same OVA immunization procedure, and effects of IVIg were investigated. LT (R192G/L211A) and MF59 (AddaVax®) stimulate a balanced Th1/Th2 immune response, whereas CpG (ODN 2395) and MPLA-SM stimulate a Th1 response and Aluminum a Th2 response. MF59 (AddaVax®) was the adjuvant which was the most potent as it raised the highest titer of mouse IgG_1 anti-OVA (Figure 39A). Very interestingly, administration of IVIg significantly downregulated the production of IgG_1 anti-OVA in mouse serum by about 5-fold for all the five different adjuvant tested, irrespective of the potency of the adjuvant (Figure 39B). Similarly, IVIg significantly increased the weight of draining lymph nodes (2 to 3-fold). Weight of the spleen was not consistently increased upon the different adjuvants, which is in line with data showing that the IVIg effect in the spleen is not strong and consistent. The expression of CD86 and CD83 on B cells was augmented (2 to 3-fold and 1.5 to 2-fold, respectively) when co-injected with each of the five different adjuvants (Figure 39C). This data thereby demonstrate the robustness of the mouse *in vivo* model used in these studies and provide great confidence in the reproducibility of the experiments.
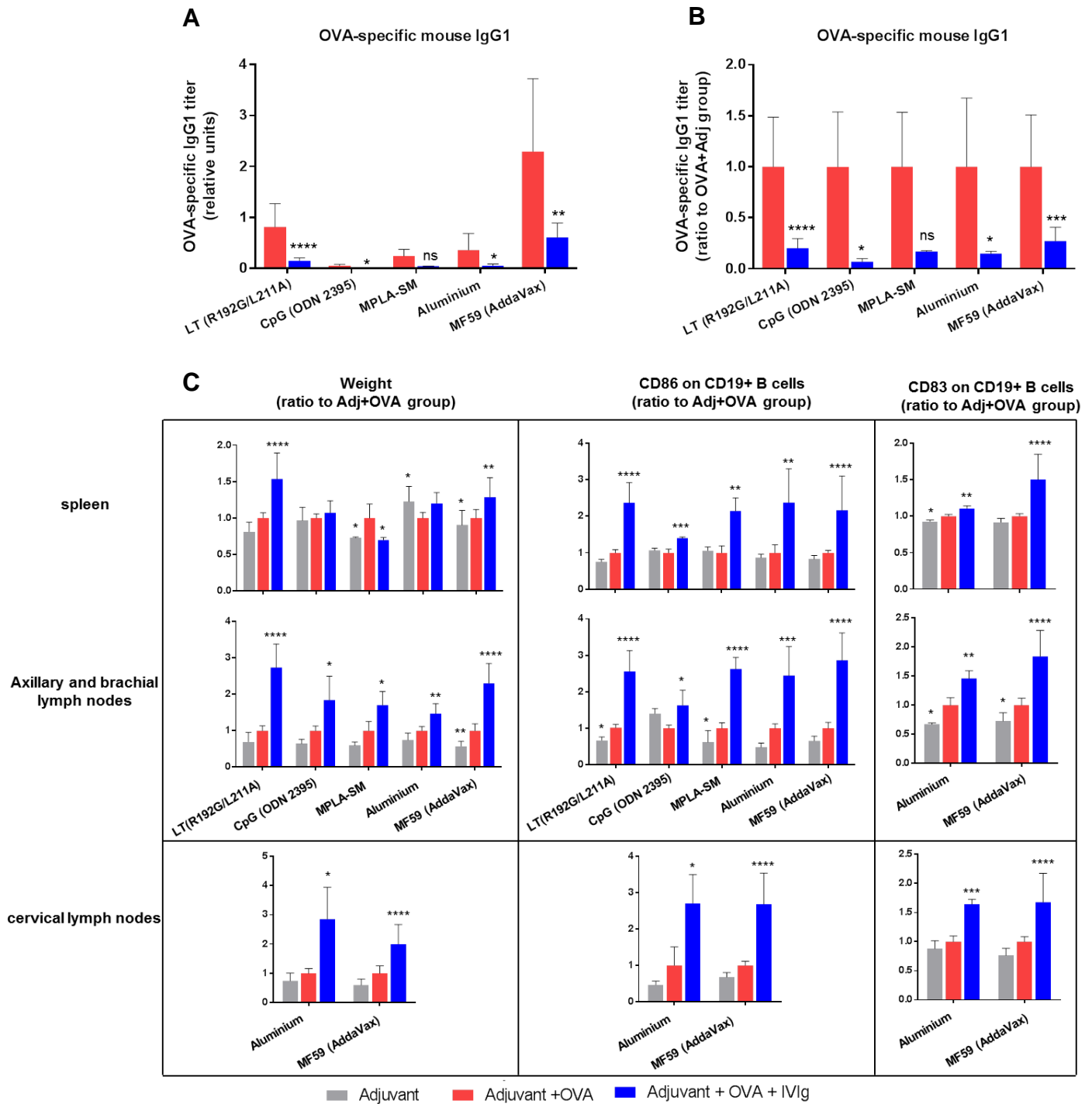
Figure 39: IVIg inhibits the formation of OVA-specific IgG1 and activates B cells when administered with different adjuvants. C57Bl/6NCrl mice were injected 3 times weekly s.c in the neck with 50 mg of IVIg in combination with OVA and different adjuvants as indicated. Mice were terminated 24h after last injection. **(A)** ELISA to measure OVA-specific mouse IgG1. **(B)** ELISA data of figure (A) presented as ratio to "OVA+Adj" group. **(C)** Results from weight measurement and flow cytometry analyses. Bars represent mean ± SD. Data are from one experiment (n=3). For figures (A) and (B) n=12 for Adjuvant LT$_{(R192G/L211A)}$ (3 independent experiments); n=3 for CpG; n=3 for MPLA-SM; n=6 for Aluminum (2 independent experiments); n=9 for MF59 (3 independent experiments). For figures (C) n=12 for Adjuvant LT$_{(R192G/L211A)}$ (3 independent experiments); n=3 for CpG; n=3 for MPLA-SM; n=6 for Aluminum (2 independent experiments) for spleen and axillary/brachial LN; n=3 for Aluminum for cervical LN; n=12 for MF59 (4 independent experiments). Statistical significance was tested using two-way ANOVA with Dunnett's correction. Star maker significant difference *: $p < 0.05$; **$p<0.01$; ***: $p<0.001$; ****: $p<0.0001$.

3.3. BSA immunization

To further evaluate the robustness of the data obtained with the OVA-immunization in an *in vivo* model, the ability of IVIg to inhibit the production of antibodies against an alternative antigen was assessed. To this purpose mice were immunized with BSA and in a separate group IVIg was co-administered, respecting the same injection scheme as in the OVA immunization model. Consistent with the observation that IVIg downregulated the humoral response against OVA, the titer of anti-BSA IgG was significantly lower upon IVIg administration (Figure 40A). Effects of IVIg on the weight of lymphoid organs as well as on CD86 and CD83 expression on B cells were even more pronounced as compared to OVA experiments (Figure 40B). For instance in the draining lymph nodes, the weight was increased of about 3-fold and CD86/CD83 expression on B cells up to 4-5-fold. These results therefore indicate that IVIg effects could be reproduced in the *in vivo* mouse model upon immunization with a different antigen, thus confirming the robustness of the results.
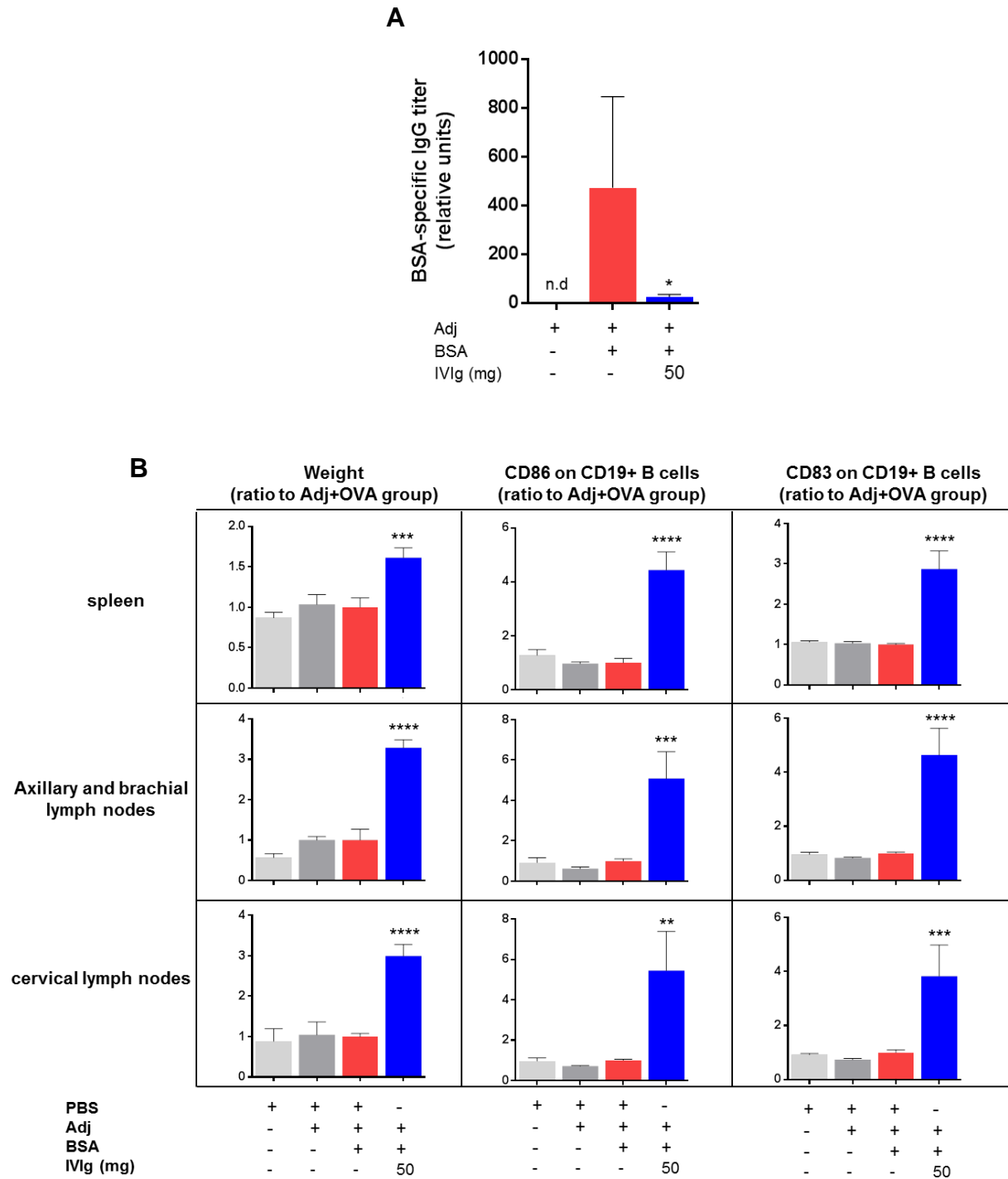
Figure 40: IVIg inhibits IgG response against BSA while activating B cells *in vivo*. C57Bl/6NCrl mice were injected 3 times weekly s.c in the neck with 50 mg of IVIg in combination with 50 μg BSA and adjuvant as indicated. Mice were terminated 24h after last injection. **(A)** ELISA to measure BSA-specific IgG antibodies. Values as expressed as relative units to standard. **(B)** Results from weight measurement and flow cytometry performed on lymphoid organs. Values as expressed as ratio to "OVA+Adj" group. Bars represent mean ± SD. Data are from one experiment (n=3). Statistical significance was tested using one-way ANOVA with Dunnett's correction. Star maker significant difference *: $p < 0.05$; **$p<0.01$; ***: $p<0.001$; ****: $p<0.0001$. n.d: not detected.

3.4. Injection of IVIg formulation buffer

In order to rule out any involvement of IVIg formulation in impairing the anti-OVA response, or in the marked activation of the mouse immune system, the buffer contained in IVIg preparation was injected in mice. After centrifugation of IVIg on a 30 kDa filter, flow-through was administered to mice at the same volume as IVIg. As expected, injection of IVIg formulation buffer was not able to diminish the titer of anti-OVA IgG produced in immunized mice, in contrast to IVIg, which reduced it 4.9-fold (Figure 41A). In a similar way, injection of IVIg formulation buffer didn't lead to an increase in the weight of draining lymph nodes or up-regulation of CD83 expression on B cells (Figure 41B), unlike IVIg which mediated these effects in a very reproducible manner.
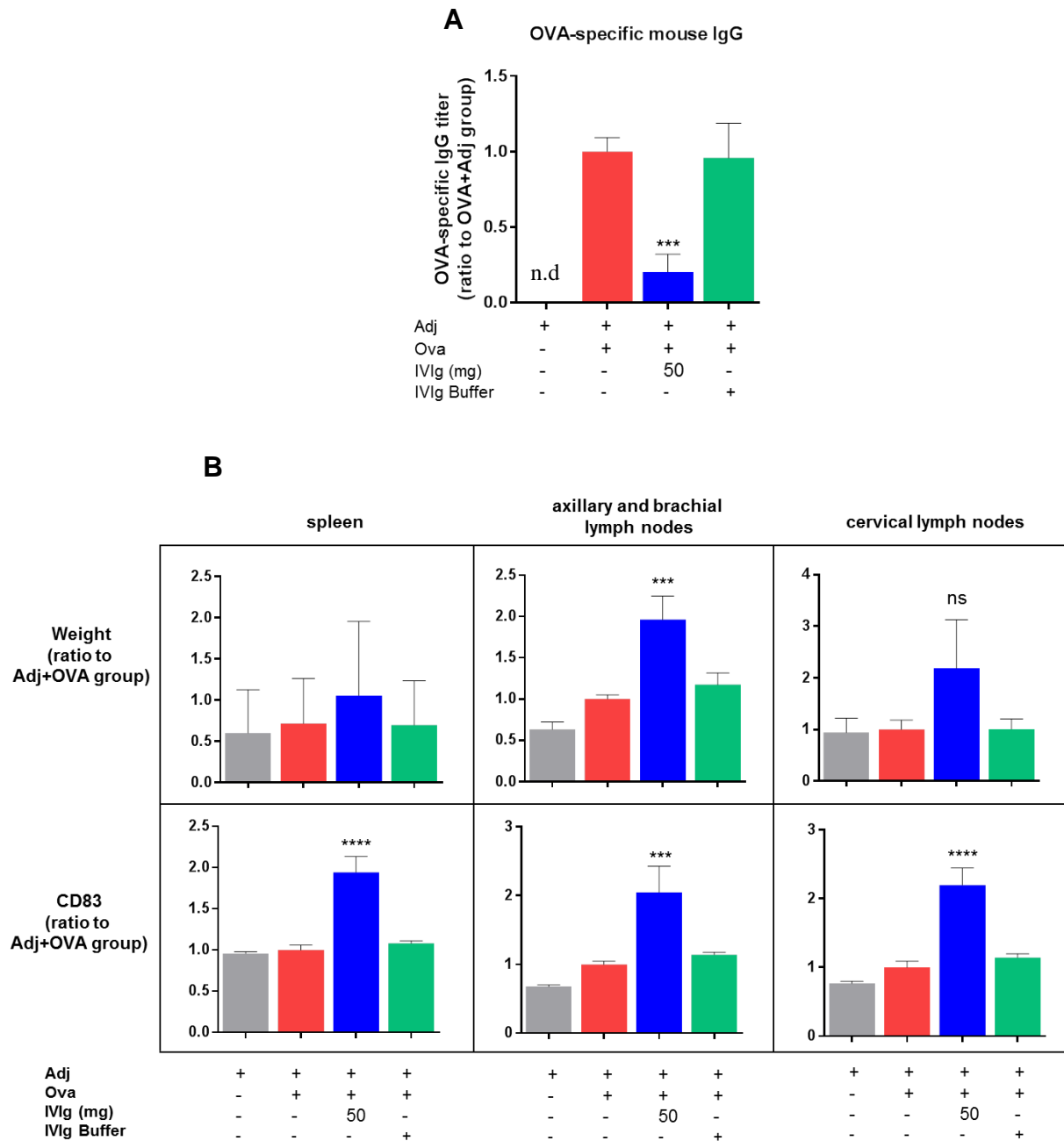
Figure 41: Formulation buffer of IVIg is not able to reproduce IVIg effects. C57Bl/6NCrl mice were injected 3 times weekly s.c in the neck with 50 µg OVA and adjuvant, and IVIg or its formulation buffer was eventually co-injected as indicated. Mice were terminated 24h after last injection. **(A)** ELISA to measure OVA-specific IgG antibodies. **(B)** Results from weight measurement and flow cytometry performed on lymphoid organs. Values as expressed as ratio to "OVA+Adj" group. Bars represent mean ± SD. Data are from one experiment (n=3). Statistical significance was tested using one-way ANOVA with Dunnett's correction. Star maker significant difference *: p < 0.05; **p<0.01; ***: p<0.001; ****: p<0.0001. n.d: not detected. ns: not significant.

3.5. Injection of LPS

As a massive and polyclonal B cells activation was associated with IVIg administration, mice were injected with LPS to test if this could mimic some or all IVIg effects. LPS is a TI antigen that is known to be a potent B-cell mitogen. Following the usual procedure, mice were immunized with OVA and adjuvant, and LPS was optionally co-injected. Administration of LPS did not result in a reduction of the anti-OVA IgG titer as it was observed in previous experiments with IVIg, but instead lead to an increased antibody response against OVA (Figure 42A). This can most likely be explained by the fact that LPS potentiated the effect of the MF59 adjuvant by acting synergistically. Despite a number of studies have reported that LPS induced up-regulation of co-stimulatory molecules on murine B cells *in vitro* (Xu et al., 2008), no such effect could be observed *in vivo* as measured by flow cytometry (Figure 42B). LPS treatment also had no influence on the weight of secondary lymphoid organs.
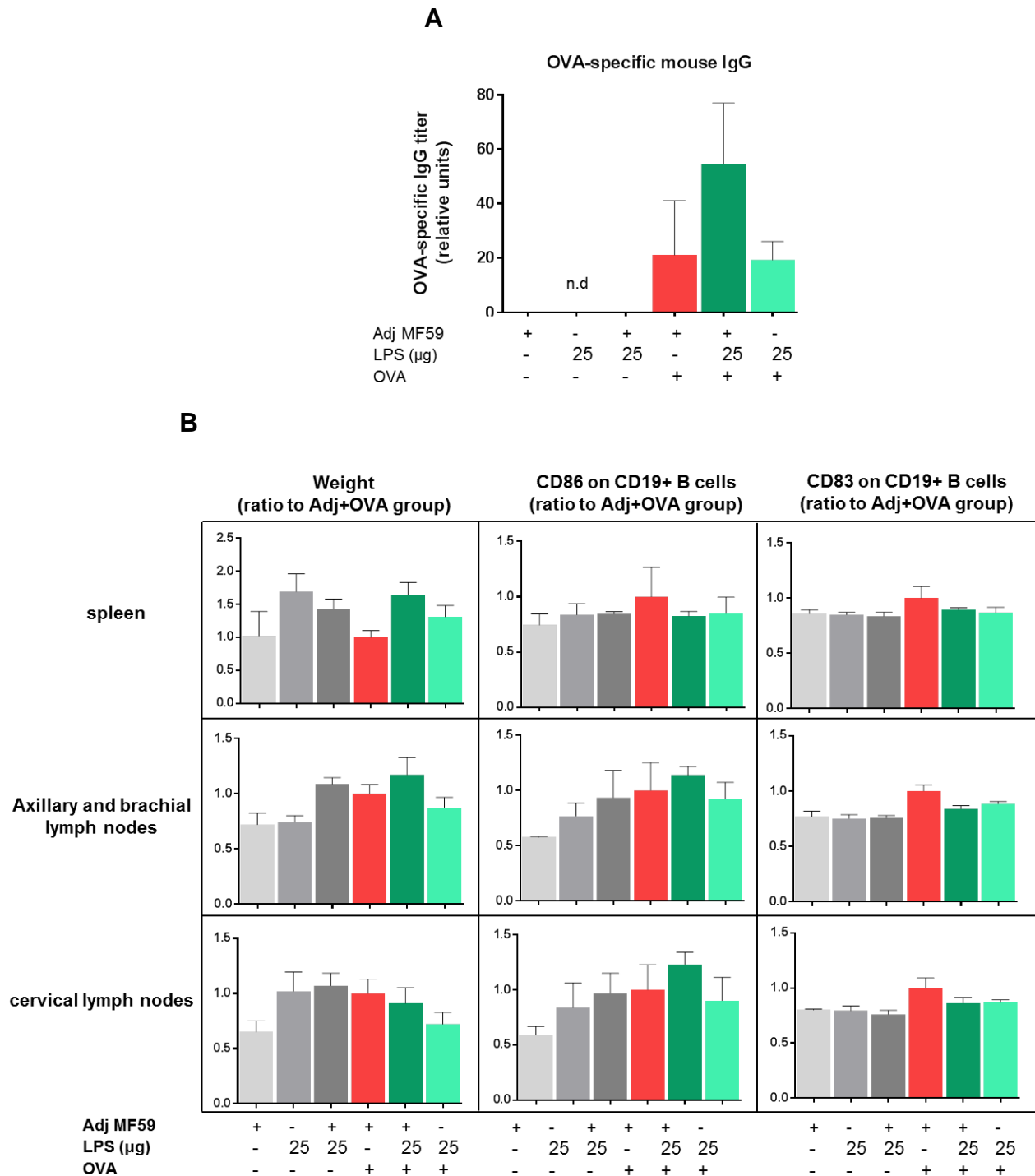
Figure 42: LPS did not mediate same effects as IVIg *in vivo*. C57Bl/6NCrl mice were injected 3 times weekly s.c in the neck with 50 μg OVA and adjuvant, and with or without LPS co-injected as indicated. Mice were terminated 24h after last injection**. (A)** ELISA to measure OVA-specific IgG antibodies. Values as expressed as relative units to standard**. (B)** Results from weight measurement and flow cytometry performed on lymphoid organs. Values as expressed as ratio to "OVA+Adj" group. Bars represent mean ± SD. Data are from one experiment (n=3). Statistical significance was tested using one-way ANOVA with Dunnett's correction. Star maker significant difference *: p< 0.05; **p<0.01; ***: p<0.001; ****: p<0.0001. n.d: not detected.

3.6. AIA mouse model

Data presented here demonstrated that IVIg reduced the OVA-specific antibody response *in vivo*, while at the same time inducing a massive activation of the immune system mostly against IVIg-Fab regions. To assess whether these effects could be reproduced in the context of an autoimmune disease mouse model, the antigen-induced arthritis model was chosen. This is a well-established model that is widely used to study the mode of action of IVIg. When administered in a prophylactic regimen (Figure 43A), IVIg efficiently reduced the severity of the induced disease as measured by the swelling of the knees in two independent experiments (Figure 43B and C), thus validating this mouse model for studying IVIg mechanisms. However, the ratio of the weight of right and left axillary/brachial and inguinal lymph nodes revealed no difference upon IVIg treatment on day 3 (data not shown). There were also no differences in the expression of B cell activation markers as measured by flow cytometry (data not shown). Because of results obtained with the OVA-immunization model, massive immune cell activation in lymph nodes and increased weight were expected to be observed on day 3 when IVIg effects have been found to be maximal (see section 1.9). The inflammatory signals generated upon BSA challenge in the knee were expected to mediate adjuvant-like effects and thus induce weight increase and B cell activation by IVIg, that might account for its effect in disease amelioration. However, these inflammatory signals were too weak, most likely because the immunization against BSA was inhibited already at the beginning of the experiment on Day -21 thanks to the co-administration of IVIg. Thus, BSA re-call in the knee didn't provoke significant inflammatory signals and couldn't allow IVIg to trigger a massive immune response. Therefore, the prophylactic regimen of IVIg was not designed for the purpose of seeing a potential B cell activation. In a follow up experiment the IVIg effect could be studied in a therapeutic setting where IVIg is injected on day 0 only. This wuld maximize the chances to observe IVIg effects on day 3. Moreover, a therapeutic regimen is closer to the clinical situation where patients are treated with IVIg after the onset of the inflammatory disease.
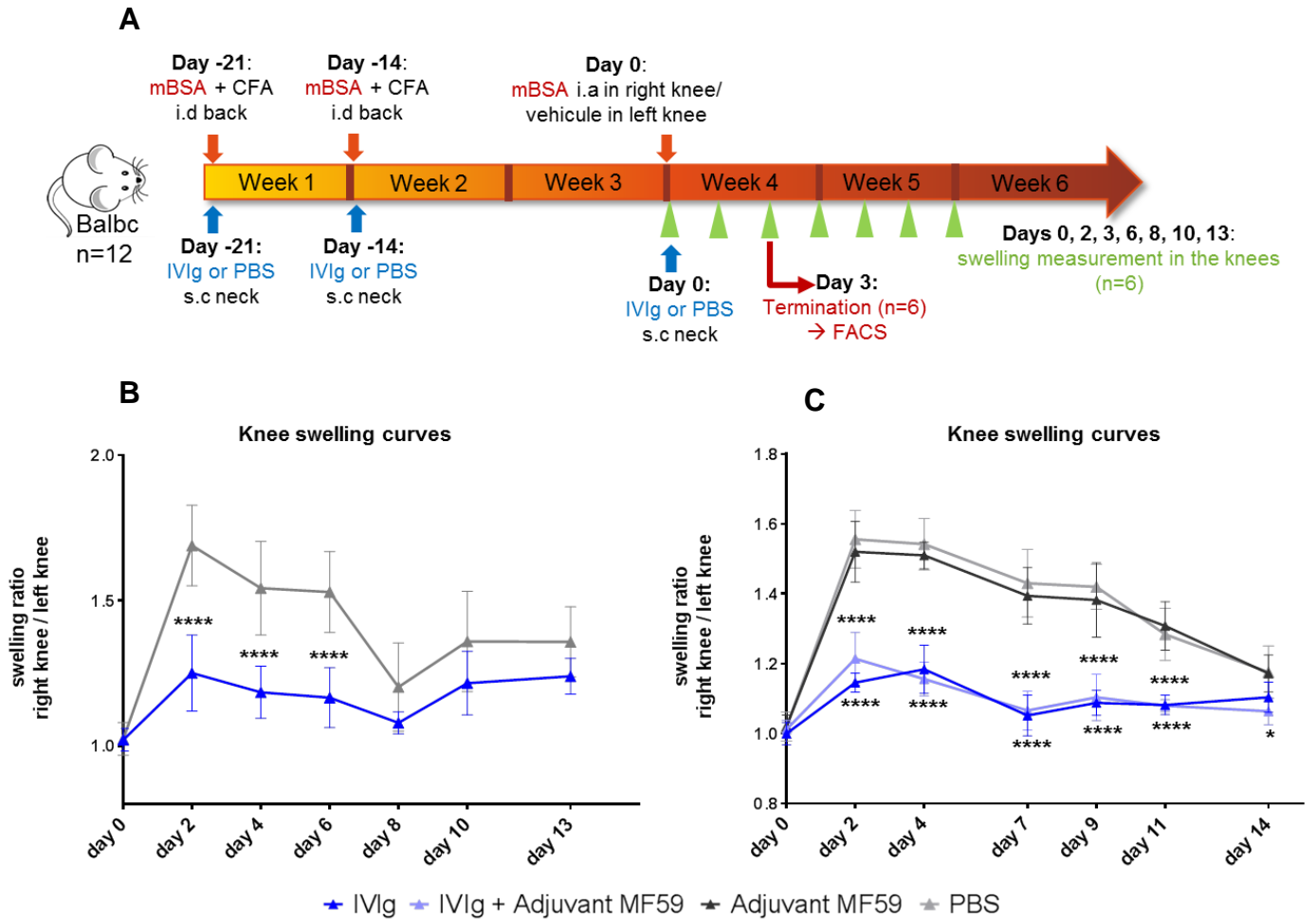
Figure 43: Prophylactic administration of IVIg ameliorates knee swelling in an AIA mouse model. (**A**) Scheme of the injections. Balb/cByJ mice were immunized intra-dermally (i.d) on day -21 and day -14 with 2x50 μL of homogenate containing 2 mg/mL of methylated BSA. On day 0 mice were challenged with 10 μL of BSA at 10mg/mL injected intra-articularly (i.a) in the right knee and with 10 μL of vehicle in the left knee. 50 mg of IVIg or PBS was given sub-cutaneously (s.c) on days -21, -14 and 0. Knee swelling was measured as indicated by green arrows. On day 3 half of the group was terminated and flow cytometry measurements were performed on cell suspension from spleen and lymph nodes. (**B**) Knee swelling curves. Triangles represent mean ± SD (n=6). (**C**) Knee swelling curves of a repetition experiment. Triangles represent mean ± SD (n=5). Statistical significance was tested using two-way ANOVA with Sidak's correction. Star maker significant difference *: $p < 0.05$; **$p < 0.01$; ***: $p < 0.001$; ****: $p < 0.0001$.

4. Tregitopes as a potential mechanism in IVIg anti-inflammatory effects?

De Groot and colleagues (De Groot et al., 2008) have identified *in silico* conserved peptides named Tregitopes in both the IgG Fc and F(ab')₂ regions that bind to multiple MHC ClassII determinants. They have published a series of experiment that demonstrate that Tregitopes, can provide immunomodulatory effects both *in vitro* and *in vivo*, and can thereby account for the therapeutic effects of IVIg. They hypothesized that these Tregitopes, once presented by APCs, activate Tregs which in turn lead to the suppression of bystander effector T cells that recognize effector epitopes. Thus, they claimed that Tregitopes lead to the suppression of antigen-specific immunogenicity by tipping the balance toward tolerance rather than effector immune response. Here we attempted to reproduce the work they published to assess if Tregitopes could indeed constitute one potential mechanism by which IVIg promotes its immunomodulatory effects. De Groot and colleagues identified two IgG Fc-derived Tregitopes, namely 167 and 289, using *in silico* screening based on their likelihood to bind to the 8 most common human HLA-DRB1 alleles.

4.1. Identification of Ig-derived MHC-II peptides in human and mouse

For evaluation of the published Tregitopes in human *in vitro* assays and mouse *in vivo* assays, suitable peptide controls had to be identified, which were well presented by HLA class II or MHC class II molecules. Some control peptides should be derived from the constant region, similar to the published Tregitopes but more importantly, peptides from non-conserved regions had to be selected which should not act as Tregitopes, based on de Groot's model. By applying MHC-II associated peptides proteomics (MAPPs) on IVIg-loaded human DCs, IVIg-derived peptides were identified, and they clustered in several regions along the sequence of the reference antibody (Figure 44A). These peptides were detected multiple times and in several different lengths, thus increasing the confidence in the peptide identification method and serving as the basis to identify sequence regions that were strongly presented by DCs. Several sequence regions showed promiscuous binding to different HLA alleles, since they occurred across several donors. In total, four strongly and commonly presented sequence regions were selected: two in the variable region and one in the constant region of the light chain as well as one in the variable region of the heavy chain. Due to the high diversity in the sequences of IgGs contained in IVIg, the presented regions showed some diversity regarding their sequence in the variable domains. This shows that several slightly different peptides are able to bind to the same HLA class II

molecule thanks to conserved binding residues. Since the number of test sequences had to be limited, we chose the corresponding sequences of well-characterized marketed mAbs, either Humira a fully human antibody or Remicade a chimeric antibody which are both immunogenic in the clinic. Moreover, additional peptides were tested that represented the consensus sequence of the different peptides identified within a sequence region. To this end, the amino acid with the highest occurrence per position was used for the consensus. Interestingly, some but not all donors tested in the MAPPs assay presented the published Tregitope 167. Notably, the published Tregitope 289 was never detected in the MAPPs assay. Finally, a total of 7 human peptides were synthesized and tested in both, *in vitro* and *in vivo* (Figure 44B).

In order to identify I-A associated IgG-derived peptides naturally presented in the mouse, we applied the MAPPs assay to cell suspensions obtained from spleen or lymph nodes collected in C57Bl/6NCrl naïve mice. In total we could identify 4 clusters, located in the constant region of the heavy chain or in the variable region of the light chain. Two additional peptides bearing the mouse equivalent sequence of human peptides HC-76 and LC-167 were also synthesized to be tested in the assays (Figure 44B).

A

Cluster 1 Cluster 2

Antibody sequence of reference for peptides alignment

CRASQGIRNYLAWYQQKPGKAPKLLIYAASTLQSGVPSRFSGSGSGTDFTLTISSLQPEDVATY

Each peptide identified by MS →

Light variable | Light constant | Heavy variable | Heavy constant

L-39 L-66   L-167   H-76   167 (De Groot et al.)
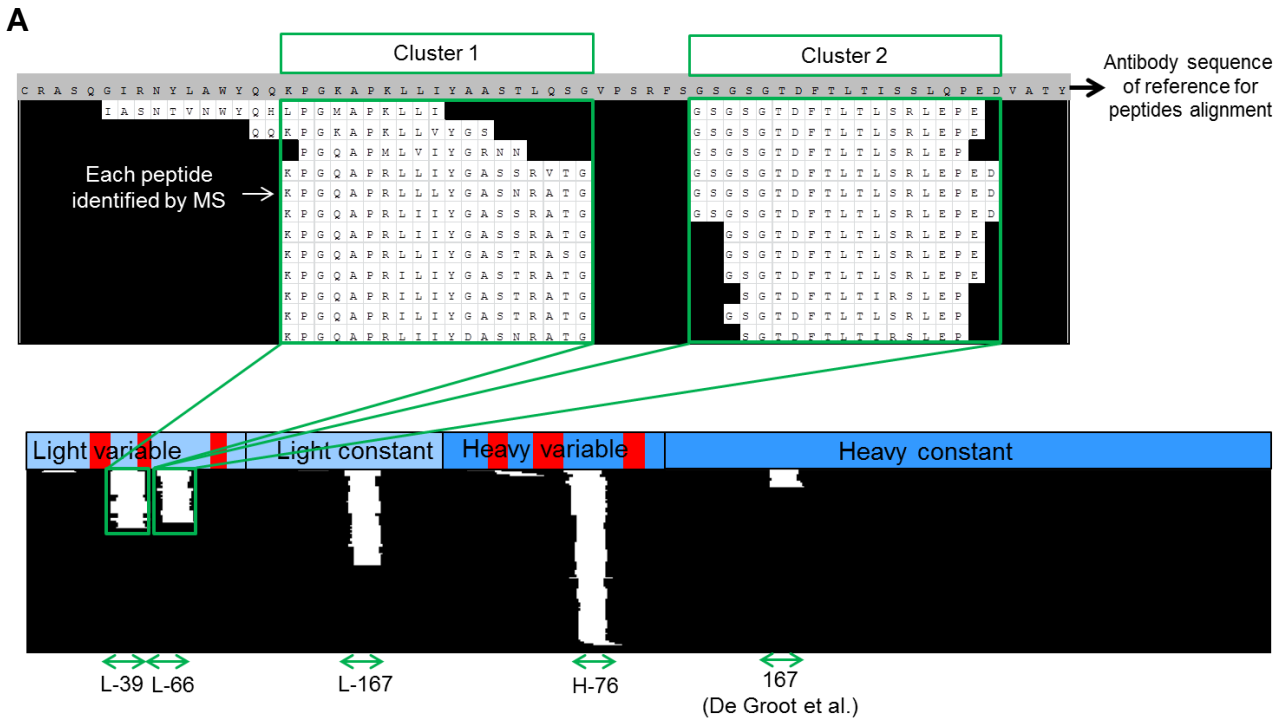
B

	name	chain	fragment	sequence	reference antibody
human peptides	289	heavy chain	constant	EEQYNSTYRVVSVLTVLHQDW	De Groot et al.
	167	heavy chain	constant	PAVLQSSGLYSLSSVVTVPSSSLGTQ	De Groot et al.
	HH-76	heavy chain	variable	KNSLYLQMNSLRAEDTA	Humira
	HR-76	heavy chain	variable	KSAVYLQMTDLRTEDTG	Remicade
	LH-39	light chain	variable	KPGKAPKLLIYAASTLQSG	Humira
	LC-39	light chain	variable	LPGTAPKLLIYSNNQRPSG	Consensus
	LH-66	light chain	variable	GSGTDFTLTISSLQPED	Humira
	LC-66	light chain	variable	GSGTDFTLTLSRLEPED	Consensus
	LH-167	light chain	constant	DSKDSTYSLSSTLTLSKA	Humira
mouse peptides	289	heavy chain	constant	EEQFNSTFRSVSELPIMHQ	De Groot et al.
	167	heavy chain	constant	PAVLQSDLYTLSSSVTVPSS	De Groot et al.
	HC-182	heavy chain	constant	VPSSTWPSQTVTCNVAHPASSTK	Consensus
	HC-395	heavy chain	constant	DTDGSYFVYSKLNVQKSNWEA	Consensus
	HC-76	heavy chain	variable	TLTADTSSSTIYMQLSSLTSEDSAIY	human-equivalent
	LC-39	light chain	variable	KPDGTVKLLIYYTSRIHSGVPS	Consensus
	LC-66	light chain	variable	GSGSGRDYSFSLSNLEPED	Consensus
	LC-167	light chain	constant	DQDSKDSTYSMSSTLTLTKD	human-equivalent

Figure 44: Identification of IgG-derived naturally presented MHC-II associated mouse and HLA-II associated human peptides by MAPPs assay. (A) Identification of main peptide-clusters from IVIg-loaded human DCs from one blood donor. The sequence of the reference antibody used for alignment is depicted in grey. Peptides were detected by LC-MS multiple times and in several different lengths, forming clusters in several regions along the sequence of the reference antibody. CDR regions are depicted in red. **(B)** List and sequences of IgG-derived human and mouse peptides identified, from IVIg-loaded human DCS or from mouse spleen and LN respectively. Peptides were numbered according their position in the sequence and named as follows: first letter H=heavy chain/ L=light chain; second letter H=Humira antibody sequence; R= Remicade antibody sequence; C= Consensus peptide (amino acid with the highest occurrence per position was used). human-equivalent means this sequence was not identified by MAPPs performed on mouse cells but still was synthesized to be further tested in the different assays.

120

4.2. *In vitro* human T cell proliferation assay

Each tested peptide was added simultaneously with tetanus toxoid (TT) to human PBMCs *in vitro,* and CD4+ T-cell proliferation was assessed by flow cytometry via CFSE staining. PHA positive control led to a high response in all donors with a proliferation rate from 50 % up to 80 %. TT stimulation led to proliferation rate between 5 and 50 % and was very donor dependent, likely due to their vaccination status. Proliferation results were calculated as stimulation index (S.I.) and normalized against the group stimulated with tetanus toxoid alone (Figure 45A). Addition of a control peptide, Betv1a (major birch pollen allergen), led to a small but not significant reduction in T-cell proliferation. This might be due to the fact that all peptides are dissolved in DMSO, with a final volume in the well of 0.1 %. DMSO is known to be toxic for cells and thus even small doses may interfere with the proliferation of T cells. Therefore, baseline for reference was not set-up at 1 (TT group) but at the mean of the Betv1a group. Unlike what has been published by De Groot et al., addition of human Tregitopes 167 and 289 had no effect on T-cell proliferation induced by TT stimulation, and neither had any of the other tested human peptides. In addition, Tregitopes 167 and 289 bearing acetylation on their N-terminus and amidation on their C-terminus were also tested, as these modifications were also used in the work published by De Groot et al. None of these modified two Tregitopes was able to reduce T-cell proliferation upon TT stimulus. Interestingly, IVIg used at 6 mg/mL led to a significant reduction of T-cell proliferation of about 50 % in average, therefore constituting a nice positive control to the experiment. When used at a dose 10 times lower, IVIg inhibition effect was lost. These data are in line with the data obtained *in vivo* with the OVA-immunization mouse model. Thus, this validates the relevance of the mouse model used here to study IVIg effects, since it nicely makes the analogy to findings in humans.
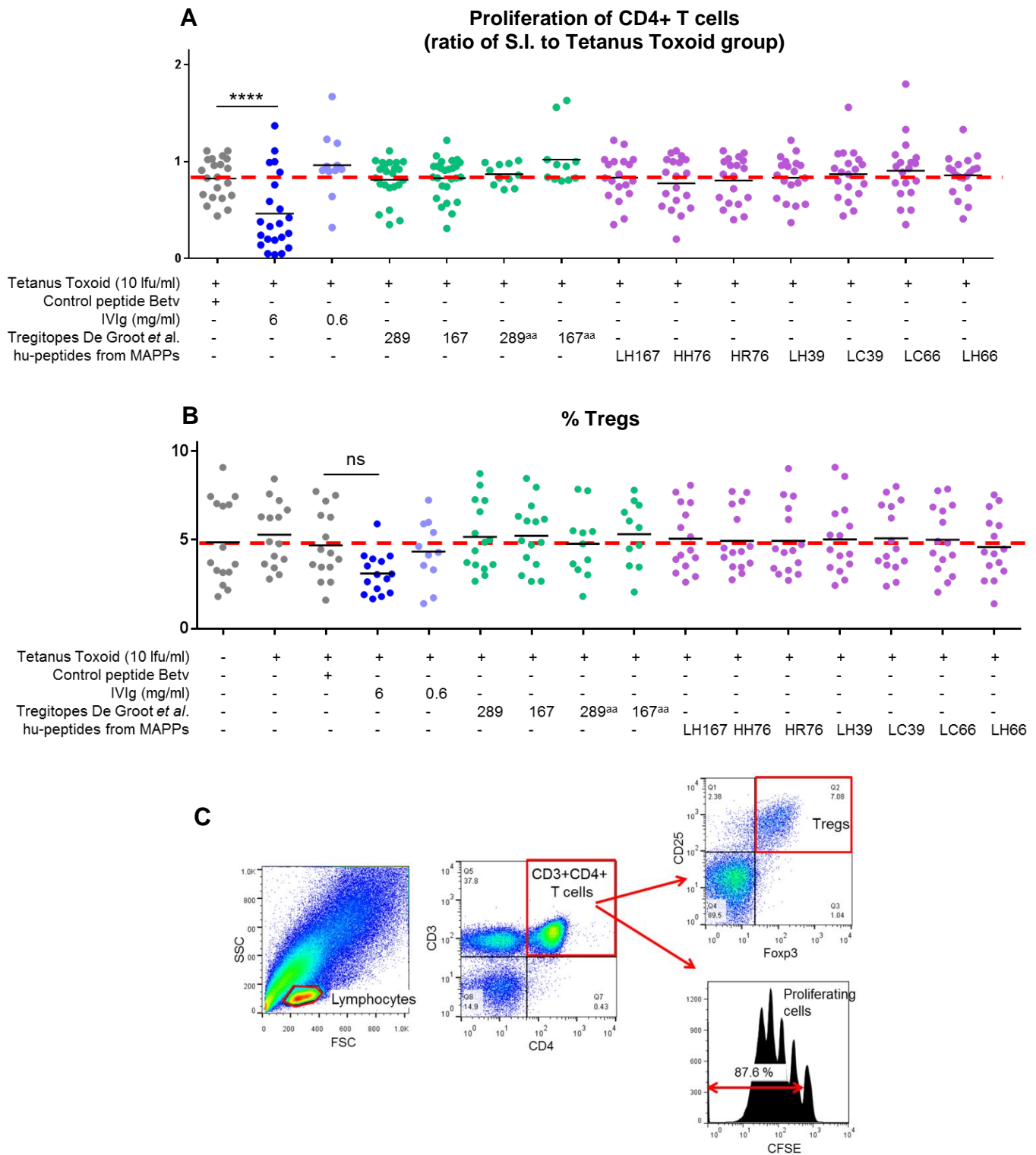
Figure 45: Published Tregitopes and peptides from diverse IgG sequence regions have no effect on human T-cell proliferation and % Tregs upon stimulation with tetanus toxoid. (A) Proliferation of CD4+ T cells. Human PBMCs were stimulated with 6 μg/mL of tetanus toxoid (TT) and peptides (10 μg/mL) were co-incubated at the same time as indicated. After 7 days proliferation of CD4+ T cells was assessed by flow cytometry via CFSE staining. Stimulation index (S.I) was calculated by dividing the % proliferation obtained by which obtained with the negative control (no stimulation, medium only). Values are expressed as S.I. ratio to the TT group. n= 11 to 26 donors. **(B)** % Tregs (CD4+CD25+Foxp3+) after 7 days. n= 15 donors. **(C)** Gating strategy for flow cytometry. For both graphs lines represent mean. Statistical significance was tested using one-way ANOVA with Dunnett's correction. Star maker significant difference *: p < 0.05; **p<0.01; ***: p<0.001; ****: p<0.0001. [aa]: acetylated and amidated peptide.

In the same set of experiments the Tregs population was investigated, which was expanding upon addition of Tregitopes *ex vivo* in the experiments published by De Groot et al... In contrast to their results, co-incubation with Tregitopes 167 and 289 (both chemically modified and non-modified) did not lead to expansion of CD4+CD25+Foxp3+ Tregs 7 days after stimulation (Figure 45B). Intriguingly, IVIg high dose led to a decrease in the percentage of Tregs, although not significant. These data are in contrast to a study published by Kessel and colleagues, showing that *in vitro* culture of IVIg with peripheral human T cells led to increase in % Foxp3 expressing cells among CD4+CD25^{high} T cells (Kessel et al., 2007). However, this decrease in Tregs upon IVIg addition is in correlation with the data obtained *in vivo* that show overall an immune activation.

4.3. *In vivo* OVA immune response

The ability of Tregitopes to suppress *in vivo* an immune response to a specific antigen was next examined, as it has been demonstrated by De Groot and colleagues in HLA-DR4 transgenic mice immunized with house dust mite lysate (De Groot et al., 2008). For this purpose the standard OVA immunization protocol was used in wild-type Bl6 mice, as described in the material and methods section 1.1. Consistent with human *in vitro* data obtained above, neither mouse Tregitopes 167 and 289 nor the other tested peptides were able to downregulate the production of OVA-specific antibodies in mouse serum (Figure 46A and B). Importantly, the same adjuvant LT $_{(R192G/L211A)}$ employed by De Groot and colleagues was used (not published, personal communication), as well as the standard adjuvant MF59 (AddaVax®) used in most of the experiments presented here, and the results obtained were similar. In addition, co-administration of OVA together with human Tregitopes 289 and 167 was tested, but similarly to their mouse counterparts they did not suppress the antibody response against OVA (Figure 46C). However, in all experiments high dose IVIg injections led to a strong and significant reduction in OVA-specific antibodies. This validates the use of this *in vivo* model for studying the potential of Tregitopes, since they are supposed to mimic the effects attributed to IVIg. Moreover, it demonstrates once again the robustness of the data obtained with IVIg.

Taken together, results from a human *in vitro* T-cell assay and a mouse *in vivo* experiment indicate that published as well other tested IgG-derived potential Tregitopes had no effect on Tregs and showed no immunosuppressive activity. This therefore challenges the concept of Tregitopes elaborated by De Groot et al.

|	A Anti-OVA IgG₁ Adj LT(R192G/L211A)					B Anti-OVA IgG₁ Adj MF59					C Anti-OVA IgG Adj MF59				
Adj	+	+	+	+	+	+	+	+	+	+	+	+	+	+
OVA	-	+	+	+	+	-	+	+	+	+	-	+	+	+
Tregitopes mo-167+289	-	-	+	-	-	-	-	+	-	-	-	-	-	-
Tregitopes mo-167+289 [ace, amid]	-	-	+	-	-	-	-	+	-	-	-	-	-	-
Peptides mo-1 to 6	-	-	-	+	-	-	-	-	+	-	-	-	-	-
Tregitopes hu-167+289	-	-	-	-	-	-	-	-	-	-	-	-	+	-
Tregitopes hu-167+289[ace, amid]	-	-	-	-	-	-	-	-	-	-	-	-	+	-
IVIg	-	-	-	-	+	-	-	-	-	+	-	-	-	+
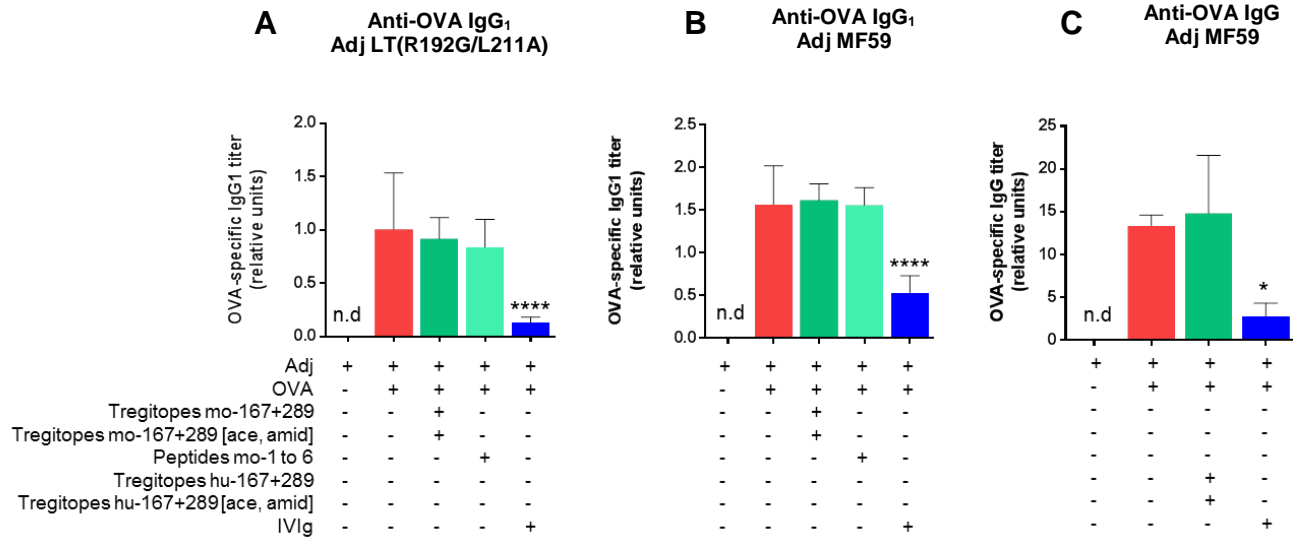
Figure 46: Published human and mouse Tregitopes as well as other test peptides were not able to reduce the titer of OVA-specific IgG in OVA immunized mice. C57Bl/6NCrl mice were injected 3 times weekly s.c in the neck with 50 μg OVA and adjuvant, with or without peptides (50 μg each) or IVIg (50 mg) co-injected as indicated. Mice were terminated 24h after last injection **(A)** ELISA anti-OVA IgG₁ upon use of Adj LT$_{(R192G/L211A)}$ (n=6). **(B)** ELISA anti-OVA IgG₁ upon use of Adj MF59 (n=6 except for tested peptides n=3). **(C)** ELISA anti-OVA IgG upon use of Adj MF59 (n=3). mo: mouse. hu: human. mo 1- to 6: mouse peptides identified *in vitro* via MAPPs assay. [ace, amid]: acetylated and amidated peptide**.** For all graphs bars represent mean ± SD. Statistical significance was tested using one-way ANOVA with Dunnett's correction. Star maker significant difference *: p<0.05; **p<0.01; ***: p<0.001; ****: p<0.0001.

5. IVIg doesn't compete with presentation of OVA-derived peptides on MHC Class-II on human DCs *in vitro*

To investigate whether IVIg could impair the presentation of OVA-derived peptides on HLA Class II molecules, human DCs were matured with LPS and simultaneously loaded with OVA and IVIg *in vitro*. IVIg and OVA-derived HLA Class II peptides were identified via the MAPPs technique. MAPPs uses liquid chromatography to separate the different peptide species in the mixture and the eluted peptides are measured by mass spectrometry. When a peptide peak is eluted from the chromatography column, the mass spectrometer will trigger multiple mass spectra. Two approaches were selected to evaluate the impact of IVIg on the presentation of OVA peptides. In the first approach, peptides were identified via database search which compares the measured spectra with theoretical spectra from a protein database. This method is only semi-quantitative since the chromatographic co-elution of several peptide species at the same time will compete with the detection in the mass spectrometer. Moreover, only high quality mass spectra are identifiable by database search. Thus, the number of peptides identified from the number of detected mass spectra is only a semi-quantitative method. For each identified peptide, the number of repeated identifications was counted (Figure 47A). The number of OVA-derived peptides presented on HLA Class II determined by this method on 5 different donors (3 low dose, 2 high dose), was similar in samples loaded with and without IVIg. Exemplarily, data for two donors are shown in Figure 47A. Similarly, IVIg didn't impair the presentation of peptides derived from two proteins, ANXA2 and MAN2B1 which are naturally presented in many donors. In the second approach, several well-presented OVA-peptides identified via the semi-quantitative approach were selected for a more robust quantification based on the integration of the area under the peptide elution peak from the extracted ion chromatograms. This allows for determination of the amount of peptide present in the DCs sample that was eluted from the LC column. The results revealed that the presentation of OVA-derived peptides on MHC Class II was not affected by IVIg. Exemplarily, data for two donors are shown in (Figure 47B).
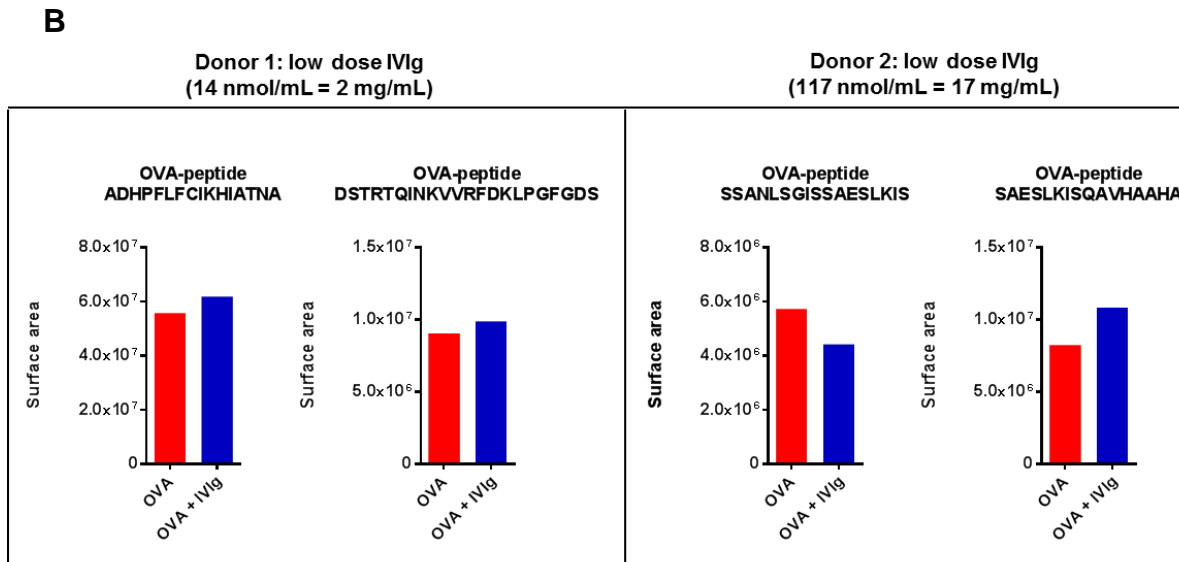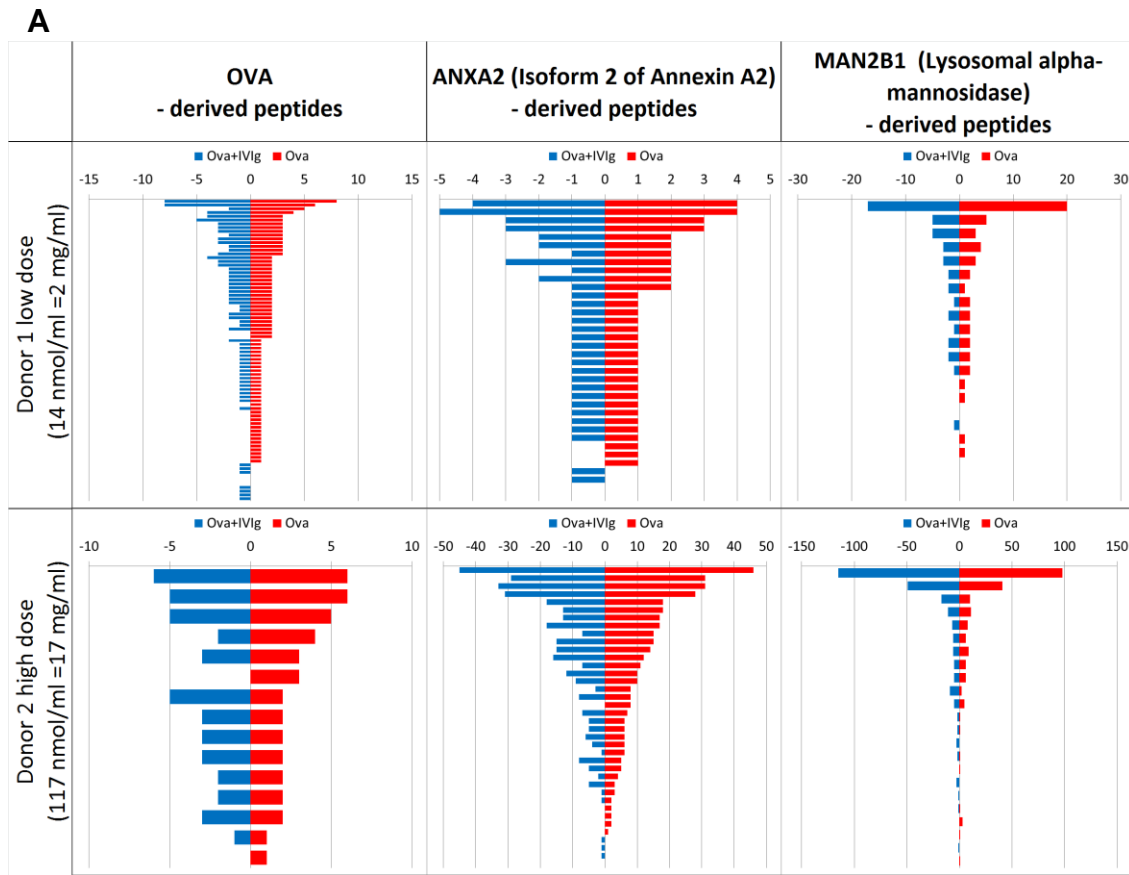
Figure 47: IVIg doesn't impair the presentation of OVA-derived peptides on MHC Class II when loaded simultaneously with OVA on human DCs in vitro. (A) Semi-quantitative number of identical peptides derived from OVA and two other well-presented proteins, ANXA2 and MAN2B1. **(B)** Quantification of the area under curve from the extracted ion chromatograms of selected OVA-peptides. Human DCs isolated from different donors were loaded *in vitro* with OVA at 14 nmol/mL, with or without IVIg either at 14 nmol/mL or at 117 nmol/mL. Exemplary data from 2 donors are shown.

Discussion and Conclusion

IVIg is a natural blood product, purified from several thousand donors and therefore constituted of a pool of highly polyclonal IgG. IVIg was initially used as a replacement therapy in patients with primary immune deficiencies to supply them with immunoglobulins. Since IVIg has been shown in 1981 to ameliorate ITP in patients, IVIg is increasingly being used in the clinic for the treatment of a wide range of autoimmune and severe inflammatory diseases, mostly as off-labeled use. Due to its elevated cost and an inevitable upcoming shortage, attention has been drawn to try to understand its therapeutic mode of action. Indeed identifying the active ingredients in IVIg would allow the development of IVIg-derived substitutes which would reduce the use of plasma-derived IVIg and thereby secure its supply for patients for which there are no alternative treatments. Despite an increasing number of studies providing new insights, they have shown a lot of discrepancies in their outcomes and thus IVIg mechanisms of action still remain poorly understood to date. The aim of this PhD project was to provide a better comprehension of the disease ameliorating mechanisms of IVIg.

First of all the OVA immunization model in Bl6 mice has been proven to be suitable to study IVIg effects. IVIg subcutaneous administration reduced immunogenicity against OVA in a dose-dependent manner and this effect was significant only for doses not lower than 1 g/kg. A high dose of IVIg led to a reduction in OVA-specific antibodies of about 70 % within 2 weeks. These results nicely reflect what has been observed in the clinical setting in pemphigus vulgaris patients, where pathogenic autoantibodies rapidly declined by an average of 59 % within 1 week after initiating IVIg treatment and by 70 % within 2 weeks (Bystryn and Jiao, 2006). Moreover, this mouse model is simple, quick, has the advantage to use wild-type mice, and provided very reproducible data throughout the different experiments. Although this model does not account for the use of intravenous Ig, subcutaneous Ig (SCIg) has been reported in several recent clinical studies as a convenient alternative to IVIg with less adverse events, most likely due to different kinetics and distribution (Danieli et al., 2014). SCIg provides ease of self-administration and a similar efficacy as IVIg (Hadden and Marreno, 2015). Even though more clinical trials are needed for all indications, the several benefits associated with SCIg make it an emerging therapeutic approach, therefore rationalizing the choice of the applied mouse model.

To summarize the findings presented here, OVA immunization consistently led to a robust OVA-specific IgG response in mice. As expected in such a context of inflammation, this leads to a small increase in the weight of the draining lymph nodes as well as in T and B cell numbers. OVA injection together with adjuvant up-regulated the expression of co-stimulatory molecules on B cells to some extent and induced the formation of a few and small germinal centers (GC), as compared to adjuvant alone. In line with this immune activation, OVA immunization decreased the number of mature re-circulating B cells in the bone-marrow. In comparison, when high dose IVIg was injected in addition to OVA and adjuvant, this led to a considerable gain in weight in the corresponding draining lymph nodes, associated with an increased number of both B and T cells. Co-stimulatory molecules CD86 and CD83 as well as the early lymphocyte activation marker CD69 were found to be strongly up-regulated on the surface of B-cells upon IVIg treatment, as compared to treatment with OVA and adjuvant. CD80 expression on B cells remained unchanged after IVIg treatment, and effect of IVIg on CD40 and MHC-II expression on B-cells was considered as negligible. These data are in line with studies showing that CD80 remains poorly expressed on B cells after stimulation (Lenschow et al., 1994), while up-regulation of CD86, CD83 and CD69 appear to be a clear signature of B-cell stimulation (Kohm et al., 2002; Prazma et al., 2007; Purtha et al., 2008). Moreover, we demonstrated that IVIg treatment triggered activation of B cells in a dose-dependent manner. In line with B cell activation, IVIg also promoted activation of T cells, as shown by the increased expression of CD69 on CD4+ T cells. Notably, B and T lymphocyte proliferation, as well as B-cell activation were visible as early as 2 days after a single shot of IVIg, reaching a maximum on day 3. Strikingly, administration of IVIg in mice provoked the formation of large and numerous GC in the draining lymph nodes and in the spleen, as compared to OVA-immunized mice. In line with a strong recruitment of immune cells ongoing after IVIg treatment, less re-circulating mature B cells were detected in the bone marrow of IVIg-treated mice compared to the OVA immunized group, suggesting that more B cells were trapped in the draining lymph nodes. Further analyses indicated that IVIg greatly increased the number of IgG-secreting cells in the draining lymph nodes while reducing the proportion of OVA-specific IgG secreting cells. This is speaking against a direct inhibition of plasma cell differentiation or antibody synthesis, while pointing towards a broad immune activation rather than an inhibition. To consolidate the findings on the involvement of IVIg in triggering the stimulation of immune cells, the antibody response in mice was further characterized. IVIg did elicit a specific IgG antibody response in mice. Additional

assays revealed that mouse antibodies raised against IVIg *in vivo* were mostly directed towards IVIg-Fab regions. All together these data suggest that IVIg raises a powerful activation of the immune system, although the final outcome is the reduction of OVA-specific antibodies. IVIg didn't impact the production of anti-NP antibodies when mice were immunized with NP-Ficoll, a TI antigen, whereas IVIg injections downregulated anti-NP antibodies in NP-OVA immunized mice, a TD antigen. These data clearly imply that IVIg inhibitory effects occur mainly in a T-cell dependent immune response.

IVIg decreased the level of total mouse IgG measured in serum in a dose-dependent manner. Injection of Avastin, an IgG_1 marketed human monoclonal antibody (mAb), had the same effect on the total mouse IgG titer. This suggests that high doses of IVIg or Avastin increased antibody clearance via FcRn blocking, as it has already been postulated (Bleeker et al., 2001). However, both Avastin and Vectibix (mAb IgG_2) didn't decrease the production of OVA-specific antibodies in mouse serum when administered at 50 mg/mouse in addition to OVA and adjuvant, whereas IVIg significantly did. These results demonstrate that FcRn saturation doesn't seem to be the main driver of IVIg inhibitory effects in the OVA-specific response. In contrast to IVIg, both Avastin and Vectibix didn't affect the weight of lymphoid organs, the number of B and T cells and their activation state, as compared to treatment with OVA and adjuvant. Unlike IVIg, Avastin treatment neither induced the extensive formation of GC, nor further reduced the number of mature re-circulating B cells in the bone-marrow, compared to treatment with OVA and adjuvant. These data demonstrate that the extensive activation of the immune system as observed upon IVIg treatment could not be achieved with monoclonal IgG molecules, although given at the same very high dose. These results collectively suggest that in the presence of adjuvant, IVIg is responsible for the powerful activation of the mouse immune system by the presence of many different variable regions from several thousand donors in IVIg preparation, comprising a huge number of very diverse foreign epitopes.

Although the number of Tregs was increased upon IVIg injection, expression of Foxp3, CTLA-4 and CD25 on their surface remained unaffected, showing there was no activation of Tregs. De Groot and colleagues (De Groot et al., 2008) described a mechanism by which Tregitopes contained in IgG tip the balance towards tolerance by activating natural Tregs, which in turn convert the surrounding effector T cells present on the same APC into adaptive Tregs. In the model they propose, teaching the immune system to tolerate a given antigen by co-delivering

it with IVIg or Tregitope peptides implies that further re-introduction of this antigen in the body would not induce any immune response, despite the absence of IVIg or Tregitopes at this time. However, *in vivo* data revealed that when IVIg injection was discontinued whereas mice were continued to be challenged with OVA, the level of OVA-specific antibodies increased over time and therefore the inhibitory effects of IVIg were lost. This correlates well with the clinical situation, where it has been shown that 87.5% of CIPD patients improved after IVIg therapy, whereas 85.7% of the responsive patients worsened only a few months after IVIg discontinuation (Nobile-Orazio et al., 2014). In addition, it is well established that IVIg does not cure but rather ameliorate most autoimmune and inflammatory diseases, since monthly injections are required over years. IVIg seems to have only a short-term effect to enable the rapid resolution of an active episode in the context of an inflammatory disease. This disagrees with the notion that IVIg is capable of promoting immune tolerance, as suggested by De Groot and colleagues. MAPPs data described here revealed that Tregitopes peptides were not well presented in both human DCs and mouse splenocytes. Moreover, addition of Tregitopes didn't induce any inhibitory effect neither on human T cell proliferation *in vitro* nor on the anti-OVA response *in vivo* in mice. These results are in line with a study performed by an independent group which investigated the potential of Tregitopes to prevent the onset of type 1 diabetes in NOD mice (Grant et al., 2013). Interestingly, there were no significant remissions observed in diabetic NOD mice treated with Tregitopes. The difficulty to reproduce De Groot and colleague's work could be explained by differences in the experimental approaches. Indeed, none of their experiment shows the use of an irrelevant peptide as a control. Knowing that peptides are dissolved in DMSO and that DMSO is a toxic agent for cells, such a negative control appears to be essential to rule out any possible non-peptide specific decrease of the immune response. In any of their experiments they used IVIg as a positive control in suppressing the immune response. Moreover, most data presented from the various suppression assays are from one single donor, which does not consider the high inter-donor variability in T cell responses. They didn't use Foxp3 as a marker to gate Tregs, which could lead to miss-interpretation of the data. Moreover, the decrease in the antigen-specific-antibody level observed *in vivo* upon Tregitopes injection was not significant. Their *in vivo* model used transgenic mice, which may behave in a different manner than wildtype mice. Finally, to our knowledge no additional paper bringing some new experimental evidence on the Tregitopes suppressive activity has been published so far, but only reviews on possible new approaches for treatment of autoimmune diseases.

Interestingly, co-injection of adjuvant was required to mediate the pro-inflammatory effects of IVIg. Indeed, IVIg injected alone or in combination with OVA didn't increase the weight of lymphoid organs and showed no effect on the number and activation state of T and B cells, unlike IVIg with adjuvant. A massive formation of GC was observed in lymphoid organs of mice treated with IVIg and adjuvant, but not in mice treated with IVIg alone. Anti-IVIg antibody response was detectable in serum only when mice were administered with IVIg and adjuvant with or without OVA, but not in mice treated without adjuvant. These data are in line with the fact that an adjuvant is usually required to stimulate the immune system and to mount a proper antibody response. Presence of adjuvant lead to up-regulation of co-stimulatory molecules on APCs, that is necessary to get T cells primed. Similarly, up-regulation of CD40 on B cells surface is required to receive an input signal from T helper cells. Thus, co-injection of adjuvant was required to initiate the immune response against IVIg in this mouse model. Furthermore, IVIg showed nice efficacy in an AIA model by significantly reducing the knee swelling when given prophylactically. Although in that case IVIg was injected without adjuvant MF59, a strong pro-inflammatory environment was set-up by the use of CFA to sensitize mice to BSA. Still, IVIg is administered in patients without adjuvant. To parallel our mouse model to the clinical situation, we suggest that inflammation that occurs during an active episode of an autoimmune disease in patients would provide danger signals in an "adjuvant-like" manner. This would likely be sufficient to activate immune cells against IVIg and reduce the recruitment of other immune cells that are antigen-disease specific.

IVIg has been shown to target the cellular immune compartment at multiple levels, including innate and adaptive immune cells. All together our data highlight a massive activation of the adaptive immune response upon IVIg administration in mice, resulting in the production of IVIg-specific IgG. Although IVIg is generally considered as a safe therapy, some adverse effects still frequently occur in patients. These side effects mostly cause discomfort but are often mild and not serious. They commonly include headache, nausea, diarrhea, back pain, blood pressure changes or urticaria. To be highlighted, some of the frequent side effects also include fever, chills, fatigue, flushing, arthralgia (joint pain) or even myalgia (muscle pain) (Hamrock, 2006; Katz et al., 2007). Intriguingly, these latter are common symptoms of infection, and are the consequence of the recruitment of effector immune cells to sites of infection. A recent study collected adverse events in patients given IVIg infusions over 10 years, mostly indicated for Kawasaki disease (Palabrica et al., 2013). 32 % experienced adverse reactions, and symptoms

occurred within a few hours after infusion. Notably, fever was the most common side effect (30.6 %), followed by rash (22.2 %) and chills (19.4 %). Another clinical study following patients treated with high dose IVIg for pemphigus and pemphigoid over 10 years reported for the first time hoarseness of voice and swelling of cervical lymph nodes as side effects (Gurcan and Ahmed, 2007). These are typical symptoms of an inflammation as well and correlate with our finding that IVIg increased the weight of cervical lymph nodes when administered in mice. Acute renal failure, a rare but serious adverse event, has also been reported to occur upon IVIg infusions. Products containing sucrose as a stabilizer are thought to be responsible for such kidney nephrosis (Dantal, 2013). Another clinical study performed over 119 IVIg-treated patients for a variety of indications revealed that 6.7 % of patients developed impairment of renal function (Levy and Pusey, 2000). However, they showed that this was not associated with the amount of sucrose in the IVIg preparation. Interestingly, production of large amounts of IgG and IgM subsequently to an inflammatory response can lead to the deposition of immune complexes in the kidney. This is a major cause of glomerulonephritis, a commonly associated condition as a result of type III hypersensitivity response (Rajan, 2003). Renal failure, although it occurs less frequently, could possibly indicate the overproduction of IgG following IVIg infusion and the accumulation of immune complexes in the kidney. Strikingly, all the adverse effects listed above that commonly occur after IVIg administration are "flu-like" symptoms and might possibly reflect a strong immune activation in patients, as we demonstrated in mice.

Based on the *in vivo* studies performed here and on the literature about IVIg-treated patients, we propose a model that may likely explain IVIg immunomodulatory properties, in which T-cell competition is the key inhibitory event, as illustrated in Figure 48. This model is based on antigenic competition.
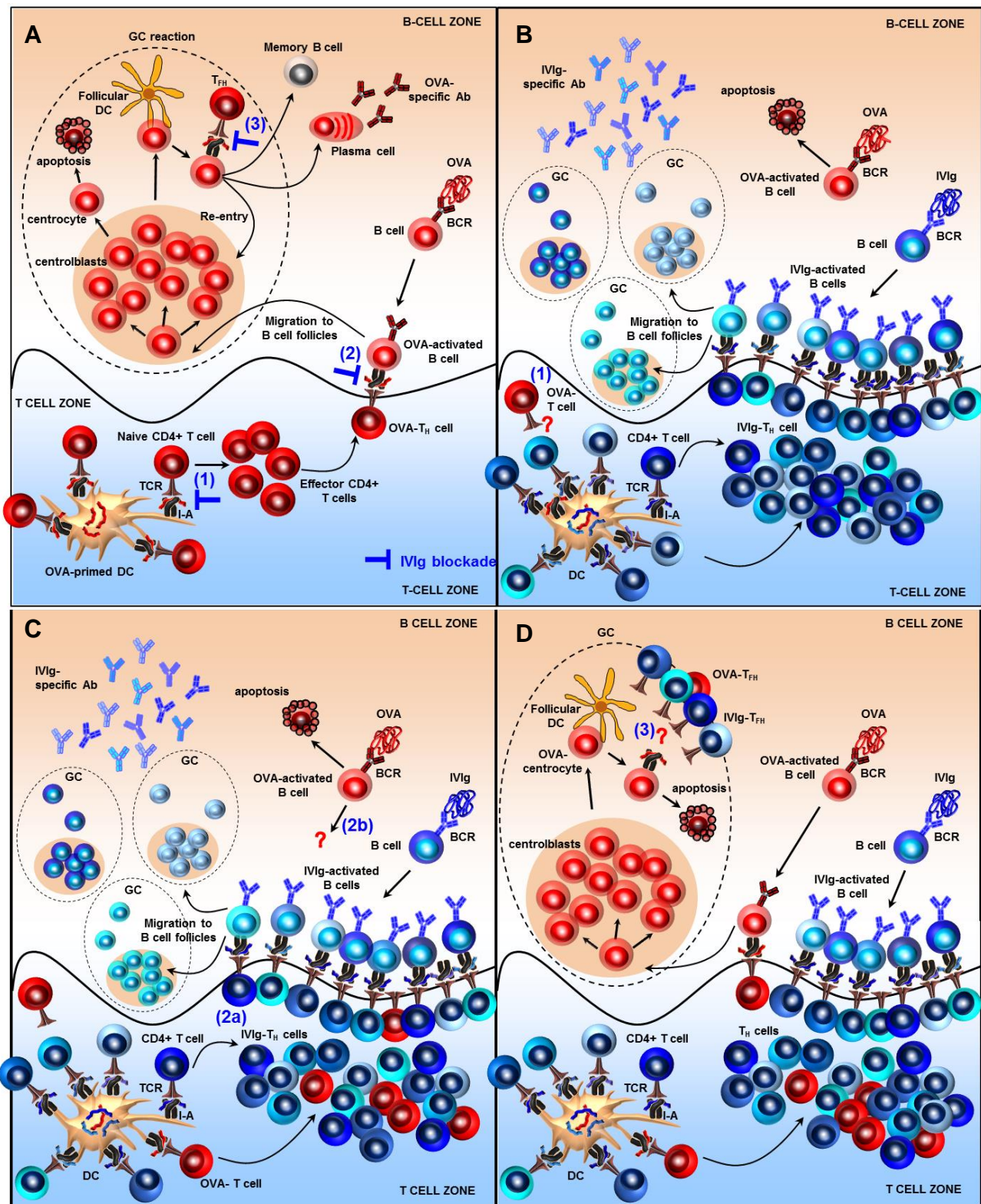
Figure 48: A proposed mechanism of action of IVIg based on T-cell competition effects occurring at several stages of the adaptive immune response. (A) Classical immune response and germinal center formation after OVA immunization. T cells primed by OVA-derived epitopes presented on APCs differentiate into effector T helper cells (T_H) and migrate at the T cell–B cell border of the lymph node. OVA-activated B cells take up and present antigenic peptides to T_H. After receiving co-stimulatory signals they initiate the formation of a germinal center (GC). After a cycle of proliferation and somatic hypermutations in the dark zone, B cells moves to the light zone to meet with their antigen exposed on follicular dendritic cells (FDCs). If the affinity of the mutated B cell receptor (BCR) is very low, the B cell will not receive survival signals and will undergo apoptosis. The surviving B cells need to compete for help from T follicular helper cells (T_{FH}), thus favoring the high affinity B cells. B cells can then either re-enter the dark zone to further mature its BCR affinity, or exit the GC as plasma cells or memory B cells. **(B)** IVIg blockade mechanism 1): T-cell competition for DCs access. In addition to OVA-peptides, DCs present a lot of IVIg-derived diverse epitopes. This favors the attraction of many different IVIg-specific T cell clones that will compete out OVA-T cell clones to receive priming from DCs. **(C)** IVIg blockade mechanism 2): competition for accessing T cell-B cell zones border. When a few OVA-T cells clones managed to get primed by DCs, they will be outnumbered by the numerous IVIg- T_H clones to access the T cell-B cell zones border (2a), so the chances they can engage with their cognate OVA-B cells are pretty low. Likewise OVA-activated B cells will be competed out to access their cognate OVA-T_H by the number of IVIg-B cells at the border (2b). This results in apoptosis of OVA-activated B cells. **(D)** IVIg blockade mechanism 3): T_{FH} competition for centrocytes priming in GC. When a few OVA-T cells clones managed to get primed by DCs and to deliver helper signals to their cognate OVA-activated B cells, these latter will start forming a GC. However, the help delivered by T_{FH} to centrocytes in GC is very limited. It is therefore more likely that OVA-centrocytes will die from apoptosis, the numerous IVIg-T_{FH} competing out the few OVA- T_{FH} for centrocytes access.

Figure 48A illustrates the classical course of an immune reaction that occurs after OVA immunization and results in the production of OVA-specific antibodies. In this OVA-specific immune reaction, IVIg might potentially interfere at three different stages, as indicated in the figure with blue markings. First, T-cell competition can arise for access to DCs (Figure 48B). When IVIg is administered together with OVA, DCs will process both OVA and the polyclonal human IgG to peptides. The variable regions from billions of different IgG sequences will produce a lot of different peptides. When adjuvant is co-injected, highly diverse IVIg-derived potential T cell epitopes are presented on the surface of DCs in the presence of co-stimulatory molecules. Due to allelic restriction, normally only a few specific peptides from an antigen can stably bind to MHC-II. However, due to the sequence diversity and also to the high dose of IVIg injected, it is likely that many more MHC-II: IVIg peptide complexes can be presented by DCs, as compared to a conventional antigen. Even if efficiently presented, OVA-derived epitopes might be outnumbered by the many different IVIg-derived epitopes on the surface of DCs. Their presentation in presence of adjuvant will induce a massive recruitment of T cells with different specificities. Consequently, the presence of multiple T cell clones specific for IVIg-peptides scanning for their cognate peptides on DCs may compete with OVA-specific T cells regarding spatial access to the DCs. Indeed, several studies have already shown that a competition between

T cells occurs for antigenic complexes on the surface of APC, inhibiting activation of other potentially reactive T cells. This competition has been demonstrated for both CD4+ T cells (Hayball et al., 2004; Weaver et al., 2009) and CD8+ T cells (Willis et al., 2006). Heyball and colleagues have shown both *in vitro* and *in vivo* that T cells with the highest affinity compete more efficiently with T cells that are specific for a different antigen but of lower affinity, whereas the reverse is not true. Thus, T-cell competition for DCs access was shown to be independent of antigen specificity, meaning it can occur for the same antigen as well as for different antigens. Such competition resulted in fewer T cells recruited for the immune response, but the activation state of the cells that responded was not affected (Willis et al., 2006). Several studies demonstrated *in vivo* and *in vitro* that interference between T cell responses doesn't result from diminished presentation of peptides on MHC-II (Weaver et al., 2009; Wolpert et al., 1998). Moreover our data from MAPPs peptide competition experiments indicate that OVA-derived peptides were still presented at the same levels even when competed with high doses of IVIg of 17 mg/ml. Interestingly, it has been collectively reported that competition is detectable only if target peptides were presented on the same DC (Weaver et al., 2009; Willis et al., 2006; Wolpert et al., 1998). In line with these findings, Weaver and colleagues determined *in vivo* that T-cell competition doesn't occur systematically but is rather a local event that requires the competitor peptides to be in the same draining lymph node (Weaver et al., 2009). Two-photon microscopy imaging enabled to show that DCs can interact with up to 5000 T cells per hour in a process of stochastic T cell repertoire scanning (Miller et al., 2004a). Very importantly, the same group revealed that after T cells recognized their cognate antigen, they form dynamic but dense clusters on DCs, thereby supporting a possible competition for DCs access (Miller et al., 2004b). Strikingly, this clustering behavior on DCs was observed only under experimental conditions of abundant antigen and large numbers of cognate T cells, thus reinforcing the T-cell competition aspect upon high doses of IVIg. Through a series of experiments, Heyball and colleagues demonstrated that the most likely mechanism by which T-cell competition occurs is via steric hindrance on the cell surface of the APC. This finding is completely in line with the model we propose here for IVIg blockade mechanism (1) detailed in Figure 48B, where IVIg-T cells physically occupy the surface of DC, and as consequence limit the access of other potential OVA-reactive T cells.

Another possible mechanism for IVIg inhibition, referred to as (2), is depicted in Figure 48C and implies a competition for accessing the T cell-B cell zone border. Despite the competition that occurs between T cells to access DCs, a few OVA-specific T cell clones may still get primed by DCs, as demonstrated by the residual OVA response in our studies. They will then proliferate and differentiate into T_H cells. However, their access to the T cell-B cell zone border might be restricted once again by steric hindrance caused by the many IVIg specific T_H clones interacting with their cognate B cells (2a). Therefore, a competition between the multiple T_H cells might occur to prime their cognate B cells T cell-B cell zone border, since space is lacking for scanning peptide complexes on the surface of B cell. The reverse might also be true, meaning a competition might occur between the multiple activated B cells to get primed by their cognate T_H. Indeed, the OVA-activated B cells might also be physically hindered by the many B cells activated by IVIg that have migrated to the T cell-B cell border (2b). Indeed, our data demonstrate a marked activation of B cells upon IVIg. Importantly, about 20% of B lymphocytes present in the peripheral blood of normal individuals produce polyreactive antibodies (Notkins, 2004). They generally bind to a wide variety of self and non-self-antigens (Avrameas et al., 2007). Therefore, owing to its polyreactive nature, IVIg may bind to a large number of BCRs and consequently lead to the extensive activation of B cells we observed. Our data correlate with a number of studies where they specifically demonstrated that IVIg stimulated B cells. Intravenous administration of high dose IVIg in Balb/c mice has been shown to increase B cell and CD4+ T cell numbers in the spleen, as well as to elevate the number of splenic IgG-secreting cells (Sundblad et al., 1991). IVIg treatment of CD40-activated B cells isolated from SLE patients accelerated their differentiation, characterized by increased secretion of IgG and IgM (Neron et al., 2009). In line with this study, de Grandmont and colleagues showed that addition of IVIg *in vitro* to CD40-activated B cells promoted their differentiation into IgG-secreting cells (de Grandmont et al., 2003). They revealed that these de novo synthesized IgG were reactive with self-antigens such as nucleoprotamine, dsDNA, or myoglobin. As expected, these IgG strongly reacted with tetanus toxin, because of the vaccination status of the respective donors. Notably, whereas no reactivity was observed for human IgG Fc fragments, IVIg-induced IgG were highly reactive against human IgG F(ab')$_2$ fragments, which supports our data. Another study brought the evidence that IVIg induced BCR signaling, as demonstrated by an increased phosphorylation of intracellular transduction pathways such as ERK1/2, Gab1 and Akt in human B cells, when treated with IVIg *in vitro* (Dussault et al., 2008). Leucht and colleagues analyzed Fab fragments

derived from one Kawasaki patient that specifically bound to IVIg by phage display, before and after IVIg treatment (Leucht et al., 2001). Sequencing revealed that the favored V_H germline gene segments of the isolated IVIg-bound Fabs were 3-23 or 3-30/3-30.5, the most frequently rearranged V_H genes among human B cells. Of particular interest, they showed that the majority of Fab-phages selected from the patient after IVIg treatment displayed a significantly stronger reactivity with IVIg than those from the library before therapy. In addition, the expression of the above V_H gene segments increased after the IVIg treatment. They concluded that IVIg can act as a superantigen *in vivo* and reshaped the B cell repertoire of this patient by activating and expanding B cells that presented BCRs derived from these two germline genes, with the highest affinity for IVIg. Overall the different studies published support the notion of a direct anti-idiotypic interaction of IVIg with the BCR, followed by B cell activation, which is line with the data presented here. To summarize, we suggest the existence of a competition between T_H for scanning peptides complexes on B cells surface, as well as an additional competition between the numerous activated B cells and T cells to access the T cell-B cell zone border. Both phenomena will inevitably result in less OVA-specific B cell priming. An antigen-activated B cell that fails to interact with its cognate T_H cell will die by apoptosis within 24h. Therefore, we suggest that inhibition of priming of OVA-activated B cells by T_H cells might account for the effect of IVIg in lowering anti-OVA antibodies in mouse serum.

The third and last mechanism for IVIg blockade we propose in this model, depicted as (3) in Figure 48A, occurs via T_{FH} competition for priming of centrocytes in the GC (Figure 48D). Similarly to T cells that have been demonstrated to compete for access to DCs, the numerous T_{FH} activated by IVIg might compete out the few OVA-specific T_{FH} for peptide scanning on centrocytes. Supporting this idea, it has been demonstrated that T_{FH} cells are present in a limiting amount in the GC (Pratama and Vinuesa, 2014). This is essential to ensure competition amongst the different B cells clones generated by somatic hypermutation and to ensure optimal affinity maturation within the GC. Thus, in the eventuality that a few OVA-specific B cell clones can initiate the formation of a GC, they will rapidly die by apoptosis without receiving any input signal from their cognate OVA-T_{FH}.

In presence of IVIg, cross-talk phenomena might also occur between T cells to provide help to B cells. The pool of IgG contained in IVIg shares some common epitopes since they are all from human origin. T cells that are triggered by the same T cell epitope on DCs (e.g. Fc peptide) can interact with several B cell showing this T cell epitope, although the BCR specificity of these B cells may be different. Therefore, an individual IgG can trigger the antibody response against a different IgG molecule via shared T cell epitopes. This is facilitated by the fact that the many T-cell epitopes presented from IVIg trigger a high number of T cells and the many B cell epitopes in IVIg can be recognized by many different B cells. Thus, the diversity of the IgG molecules contained in IVIg might lead to an amplification of the immune response against IVIg, favoring the competition described in the model here.

The model described above is based on adaptive immune cells fighting to physically access their cognate partner, and relies on antigenic competition. Antigenic competition is the diminution of the antibody response to an antigen by the simultaneous or sequential injection of an unrelated antigen. It has already been described several decades ago, by Brody and colleagues who performed a series of immunization experiments in the rabbit (Brody and Siskind, 1969). Very interestingly, they found that competition was enhanced when larger doses of antigen were used. This may explain the IVIg dose-dependency observed in our *in vivo* model, as well as the requirement of high doses of IVIg in the clinic to treat autoimmune diseases. Importantly, they demonstrated that antigenic competition occurred only if the two antigens were injected so that they drained into the same lymph nodes, which is well in line with the findings reported here. In another study, intraperitoneal injections of ferritin and human serum albumin in mice in various doses and ratios showed that the degree of suppression of both primary and secondary antibody responses to HSA was dependent on the dose of ferritin injected simultaneously, and vice versa (Rhodes and Larsen, 1972). Another example where such competition occurs is a vaccine against ovine footrot that incorporates nine serogroups of pili from *Dichelobacter nodosus*. Such a multivalent vaccine elicited lower levels of pili serogroup-specific antibodies than the corresponding monovalent vaccine (Schwartzkoff et al., 1993). A murine model that parallels this phenomenon has been established, showing that competition was more pronounced in the presence of high doses of the heterologous antigens (Hunt et al., 1995). Hunt and colleagues demonstrated that there was an upper limit of the number of T cells that can be induced following vaccination with pili. They showed this limit in T cell responsiveness was not due to impaired antigen presentation on APC. This is in line with our MAPPs data showing that IVIg didn't

compete with OVA for peptide presentation on MHC-II in human DCs *in vitro*. They concluded that under limited T cell stimulation within a lymph node, T cell help has to be shared between B cells specific for each serogroup of pili, which may explain the decrease of serogroup specific antibodies. All together these studies support the notion that antigenic competition may occur upon IVIg treatment.

In this model based on antigenic competition, requirement for high doses of IVIg might likely be explained by the need to overcome immunodominance. Immunodominance is the phenomenon that the T cell response is mainly focused on few epitopes derived from the antigen, although the antigen may possess a multitude of potential epitopes that T cells are capable to recognize. Immunodominance likely ensures that the resources of the immune system are mobilized economically against foreign invaders (Yewdell and Bennink, 1999). Thus, we suggest that at low doses of IVIg, only the dominant epitopes will trigger a few T cells and raise a classical immune response, likely not enough to induce competition with OVA-specific T cells. Whereas upon high doses of IVIg, more epitopes are presented on DCs at a meaningful concentration, thereby increasing the chances of weak epitopes to activate their cognate T cell clones. The unusually large number of T cells recruited following IVIg high dose injection might consequently re-direct the immune system, increasing competition against OVA-specific T cells. This idea is supported by our data showing that the antibody response against IVIg is mostly directed towards its variable regions. With regards to the huge diversity of the variable regions contained in IVIg, high doses are likely required to concentrate weak epitopes on the surface of APCs, so that they are able to further induce T cell activation and ultimately competition.

To consolidate our findings involving antigenic competition as one possible IVIg inhibitory mechanism, several areas might be worth to look into in this context. For instance, some studies demonstrated that it was possible to tolerize mice against specific antigens when injecting them right after birth (Madoiwa et al., 2004). Such induction of immune tolerance against IVIg may provide a good basis for studying if IVIg inhibitory effects still occur in those adult mice. Antigen labeling might represent a nice tool to follow antigen-specific GC formation with and without IVIg. Since growing attention has been focused on sialylation of the IVIg-Fc part, testing de-sialylated IVIg in our mouse model would be of interest too. Finally, analyzing the anti-IVIg antibody response and the IVIg-specific B cell precursor frequency directly in samples from IVIg-treated patients would bring some more insights about a possible antigenic competition.

IVIg has been proven over the past decades as a safe and effective therapy in the context of autoimmune and severe inflammatory diseases. Still, the physiological means by which IVIg modulates the immune system had remained a mystery. Owing to the composition of IVIg comprising a broad spectrum of antibodies, it is likely that multifactorial and non-mutually exclusive mechanisms are involved in its immunomodulatory effect. Through the work presented here, it has been demonstrated for the first time *in vivo* that IVIg triggers a massive activation and recruitment of immune cells that lead to the formation of anti-IVIg antibodies. We suggest that this overwhelming of the immune system might consequently diminish its ability to respond to a specific antigen, most likely via a phenomenon of antigenic competition. We have provided evidence that IgG variable regions may mostly account for these effects. Therefore we propose that there might be no anti-inflammatory magic content in IVIg, but it rather comprises a multitude of potentially immunogenic epitopes through the unique high diversity it contains. Although research over the past decade has emphasized the role of IVIg in promoting anti-inflammatory effects, the data presented here point to a paradigm shift and reveal that IVIg establish a pro-inflammatory environment that interferes with efficient immune response against a specific antigen.

References

Abe, J., T. Jibiki, S. Noma, T. Nakajima, H. Saito, and M. Terai. 2005. Gene expression profiling of the effect of high-dose intravenous Ig in patients with Kawasaki disease. *Journal of immunology* 174:5837-5845.

Achiron, A., R. Margalit, R. Hershkoviz, D. Markovits, T. Reshef, E. Melamed, I.R. Cohen, and O. Lider. 1994. Intravenous immunoglobulin treatment of experimental T cell-mediated autoimmune disease. Upregulation of T cell proliferation and downregulation of tumor necrosis factor alpha secretion. *The Journal of clinical investigation* 93:600-605.

Alavi, A., O. Fraser, E. Tarelli, M. Bland, and J. Axford. 2011. An open-label dosing study to evaluate the safety and effects of a dietary plant-derived polysaccharide supplement on the N-glycosylation status of serum glycoproteins in healthy subjects. *European journal of clinical nutrition* 65:648-656.

Amran, D., H. Renz, G. Lack, K. Bradley, and E.W. Gelfand. 1994. Suppression of cytokine-dependent human T-cell proliferation by intravenous immunoglobulin. *Clinical immunology and immunopathology* 73:180-186.

Anthony, R.M., T. Kobayashi, F. Wermeling, and J.V. Ravetch. 2011. Intravenous gammaglobulin suppresses inflammation through a novel T(H)2 pathway. *Nature* 475:110-113.

Anthony, R.M., F. Nimmerjahn, D.J. Ashline, V.N. Reinhold, J.C. Paulson, and J.V. Ravetch. 2008a. Recapitulation of IVIG anti-inflammatory activity with a recombinant IgG Fc. *Science* 320:373-376.

Anthony, R.M., and J.V. Ravetch. 2010. A novel role for the IgG Fc glycan: the anti-inflammatory activity of sialylated IgG Fcs. *Journal of clinical immunology* 30 Suppl 1:S9-14.

Anthony, R.M., F. Wermeling, M.C. Karlsson, and J.V. Ravetch. 2008b. Identification of a receptor required for the anti-inflammatory activity of IVIG. *Proceedings of the National Academy of Sciences of the United States of America* 105:19571-19578.

Antonelli, A., A. Saracino, B. Alberti, R. Canapicchi, F. Cartei, A. Lepri, M. Laddaga, and L. Baschieri. 1992. High-dose intravenous immunoglobulin treatment in Graves' ophthalmopathy. *Acta endocrinologica* 126:13-23.

Arnold, J.N., M.R. Wormald, R.B. Sim, P.M. Rudd, and R.A. Dwek. 2007. The impact of glycosylation on the biological function and structure of human immunoglobulins. *Annual review of immunology* 25:21-50.

Arumugam, T.V., S.C. Tang, J.D. Lathia, A. Cheng, M.R. Mughal, S. Chigurupati, T. Magnus, S.L. Chan, D.G. Jo, X. Ouyang, D.P. Fairlie, D.N. Granger, A. Vortmeyer, M. Basta, and M.P. Mattson. 2007. Intravenous immunoglobulin (IVIG) protects the brain against experimental stroke by preventing complement-mediated neuronal cell death. *Proceedings of the National Academy of Sciences of the United States of America* 104:14104-14109.

Aubin, E., D.P. Proulx, P. Trepanier, R. Lemieux, and R. Bazin. 2011. Prevention of T cell activation by interference of internalized intravenous immunoglobulin (IVIg) with MHC II-dependent native antigen presentation. *Clinical immunology* 141:273-283.

Avrameas, S., T. Ternynck, I.A. Tsonis, and P. Lymberi. 2007. Naturally occurring B-cell autoreactivity: a critical overview. *Journal of autoimmunity* 29:213-218.

Bach, J.F. 2005. Infections and autoimmune diseases. *Journal of autoimmunity* 25 Suppl:74-80.

Bain, P.G., M. Motomura, J. Newsom-Davis, S.A. Misbah, H.M. Chapel, M.L. Lee, A. Vincent, and B. Lang. 1996. Effects of intravenous immunoglobulin on muscle weakness and calcium-channel autoantibodies in the Lambert-Eaton myasthenic syndrome. *Neurology* 47:678-683.

Basta, M., and M.C. Dalakas. 1994. High-dose intravenous immunoglobulin exerts its beneficial effect in patients with dermatomyositis by blocking endomysial deposition of activated complement fragments. *The Journal of clinical investigation* 94:1729-1735.

Basta, M., F. Van Goor, S. Luccioli, E.M. Billings, A.O. Vortmeyer, L. Baranyi, J. Szebeni, C.R. Alving, M.C. Carroll, I. Berkower, S.S. Stojilkovic, and D.D. Metcalfe. 2003. F(ab)'2-mediated neutralization of C3a and C5a anaphylatoxins: a novel effector function of immunoglobulins. *Nature medicine* 9:431-438.

Bayry, J., K. Bansal, M.D. Kazatchkine, and S.V. Kaveri. 2009. DC-SIGN and alpha2,6-sialylated IgG Fc interaction is dispensable for the anti-inflammatory activity of IVIg on human dendritic cells. *Proceedings of the National Academy of Sciences of the United States of America* 106:E24; author reply E25.

Bayry, J., M.D. Kazatchkine, and S.V. Kaveri. 2007. Shortage of human intravenous immunoglobulin--reasons and possible solutions. *Nature clinical practice. Neurology* 3:120-121.

Bayry, J., S. Lacroix-Desmazes, C. Carbonneil, N. Misra, V. Donkova, A. Pashov, A. Chevailler, L. Mouthon, B. Weill, P. Bruneval, M.D. Kazatchkine, and S.V. Kaveri. 2003. Inhibition of maturation and function of dendritic cells by intravenous immunoglobulin. *Blood* 101:758-765.

Bayry, J., L. Mouthon, and S.V. Kaveri. 2012. Intravenous immunoglobulin expands regulatory T cells in autoimmune rheumatic disease. *The Journal of rheumatology* 39:450-451.

Bazin, R., R. Lemieux, and T. Tremblay. 2006. Reversal of immune thrombocytopenia in mice by cross-linking human immunoglobulin G with a high-affinity monoclonal antibody. *British journal of haematology* 135:97-100.

Berger, M., P. Rosenkranz, and C.Y. Brown. 1985. Intravenous and standard immune serum globulin preparations interfere with uptake of 125I-C3 onto sensitized erythrocytes and inhibit hemolytic complement activity. *Clinical immunology and immunopathology* 34:227-236.

Binstadt, B.A., R.S. Geha, and F.A. Bonilla. 2003. IgG Fc receptor polymorphisms in human disease: implications for intravenous immunoglobulin therapy. *The Journal of allergy and clinical immunology* 111:697-703.

Bleeker, W.K., J.L. Teeling, and C.E. Hack. 2001. Accelerated autoantibody clearance by intravenous immunoglobulin therapy: studies in experimental models to determine the magnitude and time course of the effect. *Blood* 98:3136-3142.

Borges, O., G. Borchard, A. de Sousa, H.E. Junginger, and A. Cordeiro-da-Silva. 2007. Induction of lymphocytes activated marker CD69 following exposure to chitosan and alginate biopolymers. *International journal of pharmaceutics* 337:254-264.

Bouhlal, H., D. Martinvalet, J.L. Teillaud, C. Fridman, M.D. Kazatchkine, J. Bayry, S. Lacroix-Desmazes, and S.V. Kaveri. 2014. Natural Autoantibodies to Fcgamma Receptors in Intravenous Immunoglobulins. *Journal of clinical immunology*

Boulis, A., S. Goold, and P.A. Ubel. 2002. Responding to the immunoglobulin shortage: a case study. *Journal of health politics, policy and law* 27:977-999.

Brekke, O.H., and I. Sandlie. 2003. Therapeutic antibodies for human diseases at the dawn of the twenty-first century. *Nature reviews. Drug discovery* 2:52-62.

Breloer, M., B. Kretschmer, K. Luthje, S. Ehrlich, U. Ritter, T. Bickert, C. Steeg, S. Fillatreau, K. Hoehlig, V. Lampropoulou, and B. Fleischer. 2007. CD83 is a regulator of murine B cell function in vivo. *European journal of immunology* 37:634-648.

Brody, N.I., and G.W. Siskind. 1969. Studies on antigenic competition. *The Journal of experimental medicine* 130:821-832.

Bruhns, P., A. Samuelsson, J.W. Pollard, and J.V. Ravetch. 2003. Colony-stimulating factor-1-dependent macrophages are responsible for IVIG protection in antibody-induced autoimmune disease. *Immunity* 18:573-581.

Buchacher, A., and G. Iberer. 2006. Purification of intravenous immunoglobulin G from human plasma--aspects of yield and virus safety. *Biotechnology journal* 1:148-163.

Bussel, J.B. 2000. Fc receptor blockade and immune thrombocytopenic purpura. *Seminars in hematology* 37:261-266.

Bystryn, J.C., and D. Jiao. 2006. IVIg selectively and rapidly decreases circulating pathogenic autoantibodies in pemphigus vulgaris. *Autoimmunity* 39:601-607.

Campbell, I.K., S. Miescher, D.R. Branch, P.J. Mott, A.H. Lazarus, D. Han, E. Maraskovsky, A.W. Zuercher, A. Neschadim, D. Leontyev, B.S. McKenzie, and F. Kasermann. 2014. Therapeutic Effect of IVIG on Inflammatory Arthritis in Mice Is Dependent on the Fc Portion and Independent of Sialylation or Basophils. *Journal of immunology*

Caruso, A., S. Licenziati, M. Corulli, A.D. Canaris, M.A. De Francesco, S. Fiorentini, L. Peroni, F. Fallacara, F. Dima, A. Balsari, and A. Turano. 1997. Flow cytometric analysis of activation markers on stimulated T cells and their correlation with cell proliferation. *Cytometry* 27:71-76.

Clarkson, S.B., J.B. Bussel, R.P. Kimberly, J.E. Valinsky, R.L. Nachman, and J.C. Unkeless. 1986. Treatment of refractory immune thrombocytopenic purpura with an anti-Fc gamma-receptor antibody. *The New England journal of medicine* 314:1236-1239.

Clynes, R., J.S. Maizes, R. Guinamard, M. Ono, T. Takai, and J.V. Ravetch. 1999. Modulation of immune complex-induced inflammation in vivo by the coordinate expression of activation and inhibitory Fc receptors. *The Journal of experimental medicine* 189:179-185.

Colagiuri, S., G.M. Leong, Z. Thayer, G. Antony, J.M. Dwyer, W. Kidson, and D. Wakefield. 1996. Intravenous immunoglobulin therapy for autoimmune diabetes mellitus. *Clinical and experimental rheumatology* 14 Suppl 15:S93-97.

Constant, S., N. Schweitzer, J. West, P. Ranney, and K. Bottomly. 1995. B lymphocytes can be competent antigen-presenting cells for priming CD4+ T cells to protein antigens in vivo. *Journal of immunology* 155:3734-3741.

Coutinho, A., M.D. Kazatchkine, and S. Avrameas. 1995. Natural autoantibodies. *Current opinion in immunology* 7:812-818.

Crispin, M., X. Yu, and T.A. Bowden. 2013. Crystal structure of sialylated IgG Fc: implications for the mechanism of intravenous immunoglobulin therapy. *Proceedings of the National Academy of Sciences of the United States of America* 110:E3544-3546.

Crow, A.R., and A.H. Lazarus. 2003. Role of Fcgamma receptors in the pathogenesis and treatment of idiopathic thrombocytopenic purpura. *Journal of pediatric hematology/oncology* 25 Suppl 1:S14-18.

Crow, A.R., S. Song, J. Freedman, C.D. Helgason, R.K. Humphries, K.A. Siminovitch, and A.H. Lazarus. 2003. IVIg-mediated amelioration of murine ITP via FcgammaRIIB is independent of SHIP1, SHP-1, and Btk activity. *Blood* 102:558-560.

Crow, A.R., S.J. Suppa, X. Chen, P.J. Mott, and A.H. Lazarus. 2011. The neonatal Fc receptor (FcRn) is not required for IVIg or anti-CD44 monoclonal antibody-mediated amelioration of murine immune thrombocytopenia. *Blood* 118:6403-6406.

Cunningham-Rundles, C. 2009. Lung disease, antibodies and other unresolved issues in immune globulin therapy for antibody deficiency. *Clinical and experimental immunology* 157 Suppl 1:12-16.

Danieli, M.G., C. Gelardi, V. Pedini, R. Moretti, A. Gabrielli, and F. Logullo. 2014. Subcutaneous IgG in immune-mediate diseases: proposed mechanisms of action and literature review. *Autoimmunity reviews* 13:1182-1188.

Dantal, J. 2013. Intravenous immunoglobulins: in-depth review of excipients and acute kidney injury risk. *American journal of nephrology* 38:275-284.

de Gracia, J., M. Vendrell, A. Alvarez, E. Pallisa, M.J. Rodrigo, D. de la Rosa, F. Mata, J. Andreu, and F. Morell. 2004. Immunoglobulin therapy to control lung damage in patients with common variable immunodeficiency. *International immunopharmacology* 4:745-753.

de Grandmont, M.J., C. Racine, A. Roy, R. Lemieux, and S. Neron. 2003. Intravenous immunoglobulins induce the in vitro differentiation of human B lymphocytes and the secretion of IgG. *Blood* 101:3065-3073.

De Groot, A.S., L. Moise, J.A. McMurry, E. Wambre, L. Van Overtvelt, P. Moingeon, D.W. Scott, and W. Martin. 2008. Activation of natural regulatory T cells by IgG Fc-derived peptide "Tregitopes". *Blood* 112:3303-3311.

Debre, M., M.C. Bonnet, W.H. Fridman, E. Carosella, N. Philippe, P. Reinert, E. Vilmer, C. Kaplan, J.L. Teillaud, and C. Griscelli. 1993. Infusion of Fc gamma fragments for treatment of children with acute immune thrombocytopenic purpura. *Lancet* 342:945-949.

Dietrich, G., and M.D. Kazatchkine. 1990. Normal immunoglobulin G (IgG) for therapeutic use (intravenous Ig) contain antiidiotypic specificities against an immunodominant, disease-associated, cross-reactive idiotype of human anti-thyroglobulin autoantibodies. *The Journal of clinical investigation* 85:620-625.

Dooley, M.A., and S.L. Hogan. 2003. Environmental epidemiology and risk factors for autoimmune disease. *Current opinion in rheumatology* 15:99-103.

Dunlop, M.B., P.C. Doherty, R.M. Zinkernagel, and R.V. Blanden. 1977. Cytotoxic T cell response to lymphocytic choriomeningitis virus. Properties of precursors of effector T cells, primary effector T cells and memory T cells in vitro and in vivo. *Immunology* 33:361-368.

Dussault, N., E. Ducas, C. Racine, A. Jacques, I. Pare, S. Cote, and S. Neron. 2008. Immunomodulation of human B cells following treatment with intravenous immunoglobulins involves increased phosphorylation of extracellular signal-regulated kinases 1 and 2. *International immunology* 20:1369-1379.

Edwards, J.C., G. Cambridge, and V.M. Abrahams. 1999. Do self-perpetuating B lymphocytes drive human autoimmune disease? *Immunology* 97:188-196.

Eisen, H.N. 2014. Affinity enhancement of antibodies: how low-affinity antibodies produced early in immune responses are followed by high-affinity antibodies later and in memory B-cell responses. *Cancer immunology research* 2:381-392.

Ephrem, A., S. Chamat, C. Miquel, S. Fisson, L. Mouthon, G. Caligiuri, S. Delignat, S. Elluru, J. Bayry, S. Lacroix-Desmazes, J.L. Cohen, B.L. Salomon, M.D. Kazatchkine, S.V. Kaveri, and N. Misra. 2008. Expansion of CD4+CD25+ regulatory T cells by intravenous immunoglobulin: a critical factor in controlling experimental autoimmune encephalomyelitis. *Blood* 111:715-722.

Fiebiger, B.M., J. Maamary, A. Pincetic, and J.V. Ravetch. 2015. Protection in antibody- and T cell-mediated autoimmune diseases by antiinflammatory IgG Fcs requires type II FcRs. *Proceedings of the National Academy of Sciences of the United States of America*

Finberg, R.W., J.W. Newburger, M.A. Mikati, A.H. Heller, and J.C. Burns. 1992. Effect of high doses of intravenously administered immune globulin on natural killer cell activity in peripheral blood. *The Journal of pediatrics* 120:376-380.

Fuchs, S., T. Feferman, R. Meidler, R. Margalit, C. Sicsic, N. Wang, K.Y. Zhu, T. Brenner, O. Laub, and M.C. Souroujon. 2008. A disease-specific fraction isolated from IVIG is essential for the immunosuppressive effect of IVIG in experimental autoimmune myasthenia gravis. *Journal of neuroimmunology* 194:89-96.

Gallucci, S., and P. Matzinger. 2001. Danger signals: SOS to the immune system. *Current opinion in immunology* 13:114-119.

Gelfand, E.W. 2012. Intravenous immune globulin in autoimmune and inflammatory diseases. *The New England journal of medicine* 367:2015-2025.

Germain, R.N. 2002. T-cell development and the CD4-CD8 lineage decision. *Nature reviews. Immunology* 2:309-322.

Grant, C.W., C.M. Moran-Paul, S.K. Duclos, D.L. Guberski, G. Arreaza-Rubin, and L.M. Spain. 2013. Testing agents for prevention or reversal of type 1 diabetes in rodents. *PloS one* 8:e72989.

Guilliams, M., P. Bruhns, Y. Saeys, H. Hammad, and B.N. Lambrecht. 2014. The function of Fcgamma receptors in dendritic cells and macrophages. *Nature reviews. Immunology* 14:94-108.

Gurcan, H.M., and A.R. Ahmed. 2007. Frequency of adverse events associated with intravenous immunoglobulin therapy in patients with pemphigus or pemphigoid. *The Annals of pharmacotherapy* 41:1604-1610.

Hadden, R.D., and F. Marreno. 2015. Switch from intravenous to subcutaneous immunoglobulin in CIDP and MMN: improved tolerability and patient satisfaction. *Therapeutic advances in neurological disorders* 8:14-19.

Hamrock, D.J. 2006. Adverse events associated with intravenous immunoglobulin therapy. *International immunopharmacology* 6:535-542.

Hansen, R.J., and J.P. Balthasar. 2002. Effects of intravenous immunoglobulin on platelet count and antiplatelet antibody disposition in a rat model of immune thrombocytopenia. *Blood* 100:2087-2093.

Hayball, J.D., B.W. Robinson, and R.A. Lake. 2004. CD4+ T cells cross-compete for MHC class II-restricted peptide antigen complexes on the surface of antigen presenting cells. *Immunology and cell biology* 82:103-111.

Heesters, B.A., R.C. Myers, and M.C. Carroll. 2014. Follicular dendritic cells: dynamic antigen libraries. *Nature reviews. Immunology* 14:495-504.

Heidt, S., D.L. Roelen, C. Eijsink, M. Eikmans, F.H. Claas, and A. Mulder. 2009. Intravenous immunoglobulin preparations have no direct effect on B cell proliferation and immunoglobulin production. *Clinical and experimental immunology* 158:99-105.

Hirabayashi, Y., Y. Takahashi, Y. Xu, K. Akane, I.B. Villalobos, Y. Okuno, S. Hasegawa, H. Muramatsu, A. Hama, T. Kato, and S. Kojima. 2013. Lack of CD4(+)CD25(+)FOXP3(+) regulatory T cells is associated with resistance to intravenous immunoglobulin therapy in patients with Kawasaki disease. *European journal of pediatrics* 172:833-837.

Hunt, J.D., D.C. Jackson, P.R. Wood, D.J. Stewart, and L.E. Brown. 1995. Immunological parameters associated with antigenic competition in a multivalent footrot vaccine. *Vaccine* 13:1649-1657.

Imbach, P. 2012. Treatment of immune thrombocytopenia with intravenous immunoglobulin and insights for other diseases. A historical review. *Swiss medical weekly* 142:w13593.

Imbach, P., S. Barandun, V. d'Apuzzo, C. Baumgartner, A. Hirt, A. Morell, E. Rossi, M. Schoni, M. Vest, and H.P. Wagner. 1981. High-dose intravenous gammaglobulin for idiopathic thrombocytopenic purpura in childhood. *Lancet* 1:1228-1231.

Issekutz, A.C., D. Rowter, S. Miescher, and F. Kasermann. 2015. Intravenous IgG (IVIG) and subcutaneous IgG (SCIG) preparations have comparable inhibitory effect on T cell activation, which is not dependent on IgG sialylation, monocytes or B cells. *Clinical immunology* 160:123-132.

Itoh, H., H. Matsuo, N. Kitamura, S. Yamamoto, T. Higuchi, H. Takematsu, Y. Kamikubo, T. Kondo, K. Yamashita, M. Sasada, A. Takaori-Kondo, and S. Adachi. 2015. Enhancement of neutrophil autophagy by an IVIG preparation against multidrug-resistant bacteria as well as drug-sensitive strains. *Journal of leukocyte biology* 98:107-117.

Jacobson, D.L., S.J. Gange, N.R. Rose, and N.M. Graham. 1997. Epidemiology and estimated population burden of selected autoimmune diseases in the United States. *Clinical immunology and immunopathology* 84:223-243.

Jain, A., H.S. Olsen, R. Vyzasatya, E. Burch, Y. Sakoda, E.Y. Merigeon, L. Cai, C. Lu, M. Tan, K. Tamada, D. Schulze, D.S. Block, and S.E. Strome. 2012. Fully recombinant IgG2a Fc multimers (stradomers) effectively treat collagen-induced arthritis and prevent idiopathic thrombocytopenic purpura in mice. *Arthritis research & therapy* 14:R192.

Jayne, D.R., V.L. Esnault, and C.M. Lockwood. 1993. ANCA anti-idiotype antibodies and the treatment of systemic vasculitis with intravenous immunoglobulin. *Journal of autoimmunity* 6:207-219.

Joffre, O.P., E. Segura, A. Savina, and S. Amigorena. 2012. Cross-presentation by dendritic cells. *Nature reviews. Immunology* 12:557-569.

Jolles, S., W.A. Sewell, and S.A. Misbah. 2005. Clinical uses of intravenous immunoglobulin. *Clinical and experimental immunology* 142:1-11.

Joubert, M.K., M. Hokom, C. Eakin, L. Zhou, M. Deshpande, M.P. Baker, T.J. Goletz, B.A. Kerwin, N. Chirmule, L.O. Narhi, and V. Jawa. 2012. Highly aggregated antibody therapeutics can enhance the in vitro innate and late-stage T-cell immune responses. *The Journal of biological chemistry* 287:25266-25279.

Kalinski, P. 2012. Regulation of immune responses by prostaglandin E2. *Journal of immunology* 188:21-28.

Kaneko, Y., F. Nimmerjahn, M.P. Madaio, and J.V. Ravetch. 2006a. Pathology and protection in nephrotoxic nephritis is determined by selective engagement of specific Fc receptors. *The Journal of experimental medicine* 203:789-797.

Kaneko, Y., F. Nimmerjahn, and J.V. Ravetch. 2006b. Anti-inflammatory activity of immunoglobulin G resulting from Fc sialylation. *Science* 313:670-673.

Kanik, K.S., C.H. Yarboro, Y. Naparstek, P.H. Plotz, and R.L. Wilder. 1996. Failure of low-dose intravenous immunoglobulin therapy to suppress disease activity in patients with treatment-refractory rheumatoid arthritis. *Arthritis and rheumatism* 39:1027-1029.

Karsten, C.M., M.K. Pandey, J. Figge, R. Kilchenstein, P.R. Taylor, M. Rosas, J.U. McDonald, S.J. Orr, M. Berger, D. Petzold, V. Blanchard, A. Winkler, C. Hess, D.M. Reid, I.V. Majoul, R.T. Strait, N.L. Harris, G. Kohl, E. Wex, R. Ludwig, D. Zillikens, F. Nimmerjahn, F.D. Finkelman, G.D. Brown, M. Ehlers, and J. Kohl. 2012. Anti-inflammatory activity of IgG1 mediated by Fc galactosylation and association of FcgammaRIIB and dectin-1. *Nature medicine* 18:1401-1406.

Katz, U., A. Achiron, Y. Sherer, and Y. Shoenfeld. 2007. Safety of intravenous immunoglobulin (IVIG) therapy. *Autoimmunity reviews* 6:257-259.

Kaufman, G.N., A.H. Massoud, S. Audusseau, A.A. Banville-Langelier, Y. Wang, J. Guay, J.A. Garellek, W. Mourad, C.A. Piccirillo, C. McCusker, and B.D. Mazer. 2011. Intravenous

immunoglobulin attenuates airway hyperresponsiveness in a murine model of allergic asthma. *Clinical and experimental allergy : journal of the British Society for Allergy and Clinical Immunology* 41:718-728.

Kaufman, G.N., A.H. Massoud, M. Dembele, M. Yona, C.A. Piccirillo, and B.D. Mazer. 2015. Induction of Regulatory T Cells by Intravenous Immunoglobulin: A Bridge between Adaptive and Innate Immunity. *Frontiers in immunology* 6:469.

Kessel, A., H. Ammuri, R. Peri, E.R. Pavlotzky, M. Blank, Y. Shoenfeld, and E. Toubi. 2007. Intravenous immunoglobulin therapy affects T regulatory cells by increasing their suppressive function. *Journal of immunology* 179:5571-5575.

Kivity, S., U. Katz, N. Daniel, U. Nussinovitch, N. Papageorgiou, and Y. Shoenfeld. 2010. Evidence for the use of intravenous immunoglobulins--a review of the literature. *Clinical reviews in allergy & immunology* 38:201-269.

Klein, L., M. Hinterberger, G. Wirnsberger, and B. Kyewski. 2009. Antigen presentation in the thymus for positive selection and central tolerance induction. *Nature reviews. Immunology* 9:833-844.

Kohm, A.P., A. Mozaffarian, and V.M. Sanders. 2002. B cell receptor- and beta 2-adrenergic receptor-induced regulation of B7-2 (CD86) expression in B cells. *Journal of immunology* 168:6314-6322.

Kuitwaard, K., J. de Gelder, A.P. Tio-Gillen, W.C. Hop, T. van Gelder, A.W. van Toorenenbergen, P.A. van Doorn, and B.C. Jacobs. 2009. Pharmacokinetics of intravenous immunoglobulin and outcome in Guillain-Barre syndrome. *Annals of neurology* 66:597-603.

Kurosaki, T. 2002. Regulation of B-cell signal transduction by adaptor proteins. *Nature reviews. Immunology* 2:354-363.

Le Pottier, L., T. Sapir, B. Bendaoud, P. Youinou, Y. Shoenfeld, and J.O. Pers. 2007. Intravenous immunoglobulin and cytokines: focus on tumor necrosis factor family members BAFF and APRIL. *Annals of the New York Academy of Sciences* 1110:426-432.

Leibe, A., Y. Levy, and Y. Shoenfeld. 2001. [Intravenous immunoglobulins treatment of patients with Graves' ophthalmopathy]. *Harefuah* 140:392-394, 455, 454.

Lenschow, D.J., A.I. Sperling, M.P. Cooke, G. Freeman, L. Rhee, D.C. Decker, G. Gray, L.M. Nadler, C.C. Goodnow, and J.A. Bluestone. 1994. Differential up-regulation of the B7-1 and B7-2 costimulatory molecules after Ig receptor engagement by antigen. *Journal of immunology* 153:1990-1997.

Leong, H., J. Stachnik, M.E. Bonk, and K.A. Matuszewski. 2008. Unlabeled uses of intravenous immune globulin. *American journal of health-system pharmacy : AJHP : official journal of the American Society of Health-System Pharmacists* 65:1815-1824.

Leontyev, D., Y. Katsman, and D.R. Branch. 2012a. Mouse background and IVIG dosage are critical in establishing the role of inhibitory Fcgamma receptor for the amelioration of experimental ITP. *Blood* 119:5261-5264.

Leontyev, D., Y. Katsman, X.Z. Ma, S. Miescher, F. Kasermann, and D.R. Branch. 2012b. Sialylation-independent mechanism involved in the amelioration of murine immune thrombocytopenia using intravenous gammaglobulin. *Transfusion* 52:1799-1805.

Leucht, S., M.M. Uttenreuther-Fischer, G. Gaedicke, and P. Fischer. 2001. The B cell superantigen-like interaction of intravenous immunoglobin (IVIG) with Fab fragments of V(H) 3-23 and 3-30/3-30.5 germline gene origin cloned from a patient with Kawasaki disease is enhanced after IVIG therapy. *Clinical immunology* 99:18-29.

Levy, J.B., and C.D. Pusey. 2000. Nephrotoxicity of intravenous immunoglobulin. *QJM : monthly journal of the Association of Physicians* 93:751-755.

Li, N., M. Zhao, J. Hilario-Vargas, P. Prisayanh, S. Warren, L.A. Diaz, D.C. Roopenian, and Z. Liu. 2005. Complete FcRn dependence for intravenous Ig therapy in autoimmune skin blistering diseases. *The Journal of clinical investigation* 115:3440-3450.

Lilic, D., and W.A. Sewell. 2001. IgA deficiency: what we should-or should not-be doing. *Journal of clinical pathology* 54:337-338.

Looney, R.J., and J. Huggins. 2006. Use of intravenous immunoglobulin G (IVIG). *Best practice & research. Clinical haematology* 19:3-25.

MacMillan, H.F., T. Lee, and A.C. Issekutz. 2009. Intravenous immunoglobulin G-mediated inhibition of T-cell proliferation reflects an endogenous mechanism by which IgG modulates T-cell activation. *Clinical immunology* 132:222-233.

Maddur, M.S., P. Hegde, M. Sharma, S.V. Kaveri, and J. Bayry. 2011. B cells are resistant to immunomodulation by 'IVIg-educated' dendritic cells. *Autoimmunity reviews* 11:154-156.

Maddur, M.S., S. Othy, P. Hegde, J. Vani, S. Lacroix-Desmazes, J. Bayry, and S.V. Kaveri. 2010. Immunomodulation by intravenous immunoglobulin: role of regulatory T cells. *Journal of clinical immunology* 30 Suppl 1:S4-8.

Madoiwa, S., T. Yamauchi, Y. Hakamata, E. Kobayashi, M. Arai, T. Sugo, J. Mimuro, and Y. Sakata. 2004. Induction of immune tolerance by neonatal intravenous injection of human factor VIII in murine hemophilia A. *Journal of thrombosis and haemostasis : JTH* 2:754-762.

Marchalonis, J.J., H. Kaymaz, F. Dedeoglu, S.F. Schluter, D.E. Yocum, and A.B. Edmundson. 1992. Human autoantibodies reactive with synthetic autoantigens from T-cell receptor beta chain. *Proceedings of the National Academy of Sciences of the United States of America* 89:3325-3329.

Massoud, A.H., J. Guay, K.H. Shalaby, E. Bjur, A. Ablona, D. Chan, Y. Nouhi, C.T. McCusker, M.W. Mourad, C.A. Piccirillo, and B.D. Mazer. 2012. Intravenous immunoglobulin attenuates airway inflammation through induction of forkhead box protein 3-positive regulatory T cells. *The Journal of allergy and clinical immunology* 129:1656-1665 e1653.

Massoud, A.H., M. Yona, D. Xue, F. Chouiali, H. Alturaihi, A. Ablona, W. Mourad, C.A. Piccirillo, and B.D. Mazer. 2013. Dendritic cell immunoreceptor: A novel receptor for intravenous immunoglobulin mediates induction of regulatory T cells. *The Journal of allergy and clinical immunology*

McHeyzer-Williams, M., S. Okitsu, N. Wang, and L. McHeyzer-Williams. 2012. Molecular programming of B cell memory. *Nature reviews. Immunology* 12:24-34.

Miller, M.J., A.S. Hejazi, S.H. Wei, M.D. Cahalan, and I. Parker. 2004a. T cell repertoire scanning is promoted by dynamic dendritic cell behavior and random T cell motility in

the lymph node. *Proceedings of the National Academy of Sciences of the United States of America* 101:998-1003.

Miller, M.J., O. Safrina, I. Parker, and M.D. Cahalan. 2004b. Imaging the single cell dynamics of CD4+ T cell activation by dendritic cells in lymph nodes. *The Journal of experimental medicine* 200:847-856.

Mimouni, D., M. Blank, A.S. Payne, G.J. Anhalt, C. Avivi, I. Barshack, M. David, and Y. Shoenfeld. 2010. Efficacy of intravenous immunoglobulin (IVIG) affinity-purified anti-desmoglein anti-idiotypic antibodies in the treatment of an experimental model of pemphigus vulgaris. *Clinical and experimental immunology* 162:543-549.

Mitrevski, M., R. Marrapodi, A. Camponeschi, C. Lazzeri, L. Todi, I. Quinti, M. Fiorilli, and M. Visentini. 2014. Intravenous immunoglobulin replacement therapy in common variable immunodeficiency induces B cell depletion through differentiation into apoptosis-prone CD21 B cells. *Immunologic research*

Modiano, J.F., D. Amran, G. Lack, K. Bradley, C. Ball, J. Domenico, and E.W. Gelfand. 1997. Posttranscriptional regulation of T-cell IL-2 production by human pooled immunoglobin. *Clinical immunology and immunopathology* 83:77-85.

Mulhearn, B., and I.N. Bruce. 2015. Indications for IVIG in rheumatic diseases. *Rheumatology* 54:383-391.

Nagelkerke, S.Q., G. Dekkers, I. Kustiawan, F.S. van de Bovenkamp, J. Geissler, R. Plomp, M. Wuhrer, G. Vidarsson, T. Rispens, T.K. van den Berg, and T.W. Kuijpers. 2014. Inhibition of FcgammaR-mediated phagocytosis by IVIg is independent of IgG-Fc sialylation and FcgammaRIIb in human macrophages. *Blood* 124:3709-3718.

Naito, Y., H. Takematsu, S. Koyama, S. Miyake, H. Yamamoto, R. Fujinawa, M. Sugai, Y. Okuno, G. Tsujimoto, T. Yamaji, Y. Hashimoto, S. Itohara, T. Kawasaki, A. Suzuki, and Y. Kozutsumi. 2007. Germinal center marker GL7 probes activation-dependent repression of N-glycolylneuraminic acid, a sialic acid species involved in the negative modulation of B-cell activation. *Molecular and cellular biology* 27:3008-3022.

Nakamura, A., T. Yuasa, A. Ujike, M. Ono, T. Nukiwa, J.V. Ravetch, and T. Takai. 2000. Fcgamma receptor IIB-deficient mice develop Goodpasture's syndrome upon immunization with type IV collagen: a novel murine model for autoimmune glomerular basement membrane disease. *The Journal of experimental medicine* 191:899-906.

Neron, S., G. Boire, N. Dussault, C. Racine, A.J. de Brum-Fernandes, S. Cote, and A. Jacques. 2009. CD40-activated B cells from patients with systemic lupus erythematosus can be modulated by therapeutic immunoglobulins in vitro. *Archivum immunologiae et therapiae experimentalis* 57:447-458.

Nobile-Orazio, E., D. Cocito, S. Jann, A. Uncini, P. Messina, G. Antonini, R. Fazio, F. Gallia, A. Schenone, A. Francia, D. Pareyson, L. Santoro, S. Tamburin, G. Cavaletti, F. Giannini, M. Sabatelli, E. Beghi, and I.M.C.T.G. for the. 2014. Frequency and time to relapse after discontinuing 6-month therapy with IVIg or pulsed methylprednisolone in CIDP. *Journal of neurology, neurosurgery, and psychiatry*

Notkins, A.L. 2004. Polyreactivity of antibody molecules. *Trends in immunology* 25:174-179.

Olivito, B., A. Taddio, G. Simonini, C. Massai, S. Ciullini, E. Gambineri, M. de Martino, C. Azzari, and R. Cimaz. 2010. Defective FOXP3 expression in patients with acute

Kawasaki disease and restoration by intravenous immunoglobulin therapy. *Clinical and experimental rheumatology* 28:93-97.

Othy, S., P. Bruneval, S. Topcu, I. Dugail, F. Delers, S. Lacroix-Desmazes, J. Bayry, and S.V. Kaveri. 2012. Effect of IVIg on human dendritic cell-mediated antigen uptake and presentation: role of lipid accumulation. *Journal of autoimmunity* 39:168-172.

Othy, S., P. Hegde, S. Topcu, M. Sharma, M.S. Maddur, S. Lacroix-Desmazes, J. Bayry, and S.V. Kaveri. 2013. Intravenous gammaglobulin inhibits encephalitogenic potential of pathogenic T cells and interferes with their trafficking to the central nervous system, implicating sphingosine-1 phosphate receptor 1-mammalian target of rapamycin axis. *Journal of immunology* 190:4535-4541.

Othy, S., S. Topcu, C. Saha, P. Kothapalli, S. Lacroix-Desmazes, F. Kasermann, S. Miescher, J. Bayry, and S.V. Kaveri. 2014. Sialylation may be dispensable for reciprocal modulation of helper T cells by intravenous immunoglobulin. *European journal of immunology* 44:2059-2063.

Padet, L., and R. Bazin. 2013. IVIg prevents the in vitro activation of T cells by neutralizing the T cell activators. *Immunology letters* 150:54-60.

Padet, L., I. St-Amour, E. Aubin, and R. Bazin. 2011. Neutralization of mitogenic lectins by intravenous immunoglobulin (IVIg) prevents T cell activation: does IVIg really have a direct effect on T cells? *Clinical and experimental immunology* 166:352-360.

Palabrica, F.R., S.L. Kwong, and F.R. Padua. 2013. Adverse events of intravenous immunoglobulin infusions: a ten-year retrospective study. *Asia Pacific allergy* 3:249-256.

Palmer, E. 2003. Negative selection--clearing out the bad apples from the T-cell repertoire. *Nature reviews. Immunology* 3:383-391.

Paquin Proulx, D., E. Aubin, R. Lemieux, and R. Bazin. 2010. Inhibition of B cell-mediated antigen presentation by intravenous immunoglobulins (IVIg). *Clinical immunology* 135:422-429.

Pillai, S., and A. Cariappa. 2009. The follicular versus marginal zone B lymphocyte cell fate decision. *Nature reviews. Immunology* 9:767-777.

Pitcher, L.A., and N.S. van Oers. 2003. T-cell receptor signal transmission: who gives an ITAM? *Trends in immunology* 24:554-560.

Poelsler, G., A. Berting, J. Kindermann, M. Spruth, T. Hammerle, W. Teschner, H.P. Schwarz, and T.R. Kreil. 2008. A new liquid intravenous immunoglobulin with three dedicated virus reduction steps: virus and prion reduction capacity. *Vox sanguinis* 94:184-192.

Pondrom, S. 2014. The IVIg dilemma. *American journal of transplantation : official journal of the American Society of Transplantation and the American Society of Transplant Surgeons* 14:2195-2196.

Prasad, N.K., G. Papoff, A. Zeuner, E. Bonnin, M.D. Kazatchkine, G. Ruberti, and S.V. Kaveri. 1998. Therapeutic preparations of normal polyspecific IgG (IVIg) induce apoptosis in human lymphocytes and monocytes: a novel mechanism of action of IVIg involving the Fas apoptotic pathway. *Journal of immunology* 161:3781-3790.

Pratama, A., and C.G. Vinuesa. 2014. Control of TFH cell numbers: why and how? *Immunology and cell biology* 92:40-48.

Prazma, C.M., N. Yazawa, Y. Fujimoto, M. Fujimoto, and T.F. Tedder. 2007. CD83 expression is a sensitive marker of activation required for B cell and CD4+ T cell longevity in vivo. *Journal of immunology* 179:4550-4562.

Prins, C., E.W. Gelfand, and L.E. French. 2007. Intravenous immunoglobulin: properties, mode of action and practical use in dermatology. *Acta dermato-venereologica* 87:206-218.

Purtha, W.E., K.A. Chachu, H.W.t. Virgin, and M.S. Diamond. 2008. Early B-cell activation after West Nile virus infection requires alpha/beta interferon but not antigen receptor signaling. *Journal of virology* 82:10964-10974.

Qian, J., L. Wang, X. Yuan, L. Wang, and T. Chen. 2014. Dose-related regulatory effect of intravenous immunoglobulin on dendritic cells-mediated immune response. *Immunopharmacology and immunotoxicology* 36:33-42.

Rademacher, T.W., P. Williams, and R.A. Dwek. 1994. Agalactosyl glycoforms of IgG autoantibodies are pathogenic. *Proceedings of the National Academy of Sciences of the United States of America* 91:6123-6127.

Radosevich, M., and T. Burnouf. 2010. Intravenous immunoglobulin G: trends in production methods, quality control and quality assurance. *Vox sanguinis* 98:12-28.

Rajan, T.V. 2003. The Gell-Coombs classification of hypersensitivity reactions: a re-interpretation. *Trends in immunology* 24:376-379.

Ramakrishna, C., A.N. Newo, Y.W. Shen, and E. Cantin. 2011. Passively administered pooled human immunoglobulins exert IL-10 dependent anti-inflammatory effects that protect against fatal HSV encephalitis. *PLoS pathogens* 7:e1002071.

Reddy, M., E. Eirikis, C. Davis, H.M. Davis, and U. Prabhakar. 2004. Comparative analysis of lymphocyte activation marker expression and cytokine secretion profile in stimulated human peripheral blood mononuclear cell cultures: an in vitro model to monitor cellular immune function. *Journal of immunological methods* 293:127-142.

Rhodes, J.M., and S.O. Larsen. 1972. Studies on antigenic competition. Effect of antigen dose on the immune response of mice injected simultaneously with human serum albumin and ferritin. *Immunology* 23:817-827.

Rioux, J.D., and A.K. Abbas. 2005. Paths to understanding the genetic basis of autoimmune disease. *Nature* 435:584-589.

Rombach-Riegraf, V., A.C. Karle, B. Wolf, L. Sorde, S. Koepke, S. Gottlieb, J. Krieg, M.C. Djidja, A. Baban, S. Spindeldreher, A.V. Koulov, and A. Kiessling. 2014. Aggregation of human recombinant monoclonal antibodies influences the capacity of dendritic cells to stimulate adaptive T-cell responses in vitro. *PloS one* 9:e86322.

Rosman, Z., Y. Shoenfeld, and G. Zandman-Goddard. 2013. Biologic therapy for autoimmune diseases: an update. *BMC medicine* 11:88.

Samuelsson, A., T.L. Towers, and J.V. Ravetch. 2001. Anti-inflammatory activity of IVIG mediated through the inhibitory Fc receptor. *Science* 291:484-486.

Scallon, B.J., S.H. Tam, S.G. McCarthy, A.N. Cai, and T.S. Raju. 2007. Higher levels of sialylated Fc glycans in immunoglobulin G molecules can adversely impact functionality. *Molecular immunology* 44:1524-1534.

Schwab, I., M. Biburger, G. Kronke, G. Schett, and F. Nimmerjahn. 2012a. IVIg-mediated amelioration of ITP in mice is dependent on sialic acid and SIGNR1. *European journal of immunology* 42:826-830.

Schwab, I., S. Mihai, M. Seeling, M. Kasperkiewicz, R.J. Ludwig, and F. Nimmerjahn. 2014. Broad requirement for terminal sialic acid residues and FcgammaRIIB for the preventive and therapeutic activity of intravenous immunoglobulins in vivo. *European journal of immunology*

Schwab, I., and F. Nimmerjahn. 2013. Intravenous immunoglobulin therapy: how does IgG modulate the immune system? *Nature reviews. Immunology* 13:176-189.

Schwab, I., M. Seeling, M. Biburger, S. Aschermann, L. Nitschke, and F. Nimmerjahn. 2012b. B cells and CD22 are dispensable for the immediate antiinflammatory activity of intravenous immunoglobulins in vivo. *European journal of immunology* 42:3302-3309.

Schwartzkoff, C.L., J.R. Egerton, D.J. Stewart, P.R. Lehrbach, T.C. Elleman, and P.A. Hoyne. 1993. The effects of antigenic competition on the efficacy of multivalent footrot vaccines. *Australian veterinary journal* 70:123-126.

Seite, J.F., D. Cornec, Y. Renaudineau, P. Youinou, R.A. Mageed, and S. Hillion. 2010. IVIg modulates BCR signaling through CD22 and promotes apoptosis in mature human B lymphocytes. *Blood* 116:1698-1704.

Seite, J.F., C. Goutsmedt, P. Youinou, J.O. Pers, and S. Hillion. 2013. Intravenous immunoglobulin induces a functional silencing program similar to anergy in human B cells. *The Journal of allergy and clinical immunology*

Seite, J.F., J.O. Pers, P. Youinou, and S. Hillion. 2011. Intravenous immunoglobulin induces anergy statelike of auto-reactive B lymphocytes in Sjogren's syndrome. *Bulletin du Groupement international pour la recherche scientifique en stomatologie & odontologie* 50:16-17.

Seite, J.F., Y. Shoenfeld, P. Youinou, and S. Hillion. 2008. What is the contents of the magic draft IVIg? *Autoimmunity reviews* 7:435-439.

Shimomura, M., S. Hasegawa, Y. Seki, R. Fukano, N. Hotta, and T. Ichiyama. 2012. Intravenous immunoglobulin does not increase FcgammaRIIB expression levels on monocytes in children with immune thrombocytopenia. *Clinical and experimental immunology* 169:33-37.

Shlomchik, M.J. 2008. Sites and stages of autoreactive B cell activation and regulation. *Immunity* 28:18-28.

Shoenfeld, Y., L. Rauova, B. Gilburd, F. Kvapil, I. Goldberg, J. Kopolovic, J. Rovensky, and M. Blank. 2002. Efficacy of IVIG affinity-purified anti-double-stranded DNA anti-idiotypic antibodies in the treatment of an experimental murine model of systemic lupus erythematosus. *International immunology* 14:1303-1311.

Siragam, V., A.R. Crow, D. Brinc, S. Song, J. Freedman, and A.H. Lazarus. 2006. Intravenous immunoglobulin ameliorates ITP via activating Fc gamma receptors on dendritic cells. *Nature medicine* 12:688-692.

Sondermann, P., A. Pincetic, J. Maamary, K. Lammens, and J.V. Ravetch. 2013. General mechanism for modulating immunoglobulin effector function. *Proceedings of the National Academy of Sciences of the United States of America* 110:9868-9872.

Steinman, L., J.T. Merrill, I.B. McInnes, and M. Peakman. 2012. Optimization of current and future therapy for autoimmune diseases. *Nature medicine* 18:59-65.

Sultan, Y., M.D. Kazatchkine, P. Maisonneuve, and U.E. Nydegger. 1984. Anti-idiotypic suppression of autoantibodies to factor VIII (antihaemophilic factor) by high-dose intravenous gammaglobulin. *Lancet* 2:765-768.

Sundblad, A., F. Huetz, D. Portnoi, and A. Coutinho. 1991. Stimulation of B and T cells by in vivo high dose immunoglobulin administration in normal mice. *Journal of autoimmunity* 4:325-339.

Svetlicky, N., O.D. Ortega-Hernandez, L. Mouthon, L. Guillevin, H.J. Thiesen, A. Altman, M.S. Kravitz, M. Blank, and Y. Shoenfeld. 2013. The advantage of specific intravenous immunoglobulin (sIVIG) on regular IVIG: experience of the last decade. *Journal of clinical immunology* 33 Suppl 1:S27-32.

Tabrizi, M.A., C.M. Tseng, and L.K. Roskos. 2006. Elimination mechanisms of therapeutic monoclonal antibodies. *Drug discovery today* 11:81-88.

Tackenberg, B., I. Jelcic, A. Baerenwaldt, W.H. Oertel, N. Sommer, F. Nimmerjahn, and J.D. Lunemann. 2009. Impaired inhibitory Fcgamma receptor IIB expression on B cells in chronic inflammatory demyelinating polyneuropathy. *Proceedings of the National Academy of Sciences of the United States of America* 106:4788-4792.

Takai, T., M. Ono, M. Hikida, H. Ohmori, and J.V. Ravetch. 1996. Augmented humoral and anaphylactic responses in Fc gamma RII-deficient mice. *Nature* 379:346-349.

Tawfik, D.S., K.R. Cowan, A.M. Walsh, W.S. Hamilton, and F.D. Goldman. 2012. Exogenous immunoglobulin downregulates T-cell receptor signaling and cytokine production. *Pediatric allergy and immunology : official publication of the European Society of Pediatric Allergy and Immunology* 23:88-95.

Teeling, J.L., T. Jansen-Hendriks, T.W. Kuijpers, M. de Haas, J.G. van de Winkel, C.E. Hack, and W.K. Bleeker. 2001. Therapeutic efficacy of intravenous immunoglobulin preparations depends on the immunoglobulin G dimers: studies in experimental immune thrombocytopenia. *Blood* 98:1095-1099.

Tha-In, T., H.J. Metselaar, A.R. Bushell, J. Kwekkeboom, and K.J. Wood. 2010. Intravenous immunoglobulins promote skin allograft acceptance by triggering functional activation of CD4+Foxp3+ T cells. *Transplantation* 89:1446-1455.

Tha-In, T., H.J. Metselaar, H.W. Tilanus, Z.M. Groothuismink, E.J. Kuipers, R.A. de Man, and J. Kwekkeboom. 2007. Intravenous immunoglobulins suppress T-cell priming by modulating the bidirectional interaction between dendritic cells and natural killer cells. *Blood* 110:3253-3262.

Thiruppathi, M., J.R. Sheng, L. Li, B.S. Prabhakar, and M.N. Meriggioli. 2014. Recombinant IgG2a Fc (M045) multimers effectively suppress experimental autoimmune myasthenia gravis. *Journal of autoimmunity*

Thornton, A.M., and E.M. Shevach. 2000. Suppressor effector function of CD4+CD25+ immunoregulatory T cells is antigen nonspecific. *Journal of immunology* 164:183-190.

Tjon, A.S., H. Jaadar, R. van Gent, P.J. van Kooten, N. Achatbi, H.J. Metselaar, and J. Kwekkeboom. 2014. Prevention of immunoglobulin G immobilization eliminates artifactual stimulation of dendritic cell maturation by intravenous immunoglobulin in vitro. *Translational research : the journal of laboratory and clinical medicine*

Tjon, A.S., T. Tha-In, H.J. Metselaar, R. van Gent, L.J. van der Laan, Z.M. Groothuismink, P.A. te Boekhorst, P.M. van Hagen, and J. Kwekkeboom. 2013. Patients treated with high-dose intravenous immunoglobulin show selective activation of regulatory T cells. *Clinical and experimental immunology* 173:259-267.

Toubi, E., A. Kessel, and Y. Shoenfeld. 2005. High-dose intravenous immunoglobulins: an option in the treatment of systemic lupus erythematosus. *Human immunology* 66:395-402.

Tremblay, T., I. Pare, and R. Bazin. 2013. Immunoglobulin G dimers and immune complexes are dispensable for the therapeutic efficacy of intravenous immune globulin in murine immune thrombocytopenia. *Transfusion* 53:261-269.

Trepanier, P., E. Aubin, and R. Bazin. 2012. IVIg-mediated inhibition of antigen presentation: predominant role of naturally occurring cationic IgG. *Clinical immunology* 142:383-389.

Trinath, J., P. Hegde, K.N. Balaji, S.V. Kaveri, and J. Bayry. 2013a. Intravenous immunoglobulin-mediated regulation of Notch ligands on human dendritic cells. *The Journal of allergy and clinical immunology* 131:1255-1257, 1257 e1251.

Trinath, J., P. Hegde, M. Sharma, M.S. Maddur, M. Rabin, J.M. Vallat, L. Magy, K.N. Balaji, S.V. Kaveri, and J. Bayry. 2013b. Intravenous immunoglobulin expands regulatory T cells via induction of cyclooxygenase-2-dependent prostaglandin E2 in human dendritic cells. *Blood* 122:1419-1427.

Tumiati, B., P. Casoli, M. Veneziani, and G. Rinaldi. 1992. High-dose immunoglobulin therapy as an immunomodulatory treatment of rheumatoid arthritis. *Arthritis and rheumatism* 35:1126-1133.

Vaitla, P.M., and E.M. McDermott. 2010. The role of high-dose intravenous immunoglobulin in rheumatology. *Rheumatology* 49:1040-1048.

van Beers, M.M., M. Sauerborn, F. Gilli, V. Brinks, H. Schellekens, and W. Jiskoot. 2010. Aggregated recombinant human interferon Beta induces antibodies but no memory in immune-tolerant transgenic mice. *Pharmaceutical research* 27:1812-1824.

van Gent, R., and J. Kwekkeboom. 2015. The IVIg dilemma: a way out? *American journal of transplantation : official journal of the American Society of Transplantation and the American Society of Transplant Surgeons* 15:1725-1726.

van Lent, P., K.C. Nabbe, P. Boross, A.B. Blom, J. Roth, A. Holthuysen, A. Sloetjes, S. Verbeek, and W. van den Berg. 2003. The inhibitory receptor FcgammaRII reduces joint inflammation and destruction in experimental immune complex-mediated arthritides not only by inhibition of FcgammaRI/III but also by efficient clearance and endocytosis of immune complexes. *The American journal of pathology* 163:1839-1848.

Vani, J., S. Elluru, V.S. Negi, S. Lacroix-Desmazes, M.D. Kazatchkine, J. Bayry, and S.V. Kaveri. 2008. Role of natural antibodies in immune homeostasis: IVIg perspective. *Autoimmunity reviews* 7:440-444.

Vassilev, T.L., M.D. Kazatchkine, J.P. Duong Van Huyen, M. Mekrache, E. Bonnin, J.C. Mani, C. Lecroubier, D. Korinth, D. Baruch, F. Schriever, and S.V. Kaveri. 1999. Inhibition of cell adhesion by antibodies to Arg-Gly-Asp (RGD) in normal immunoglobulin for therapeutic use (intravenous immunoglobulin, IVIg). *Blood* 93:3624-3631.

Vinuesa, C.G., I. Sanz, and M.C. Cook. 2009. Dysregulation of germinal centres in autoimmune disease. *Nature reviews. Immunology* 9:845-857.

Vinuesa, C.G., S.G. Tangye, B. Moser, and C.R. Mackay. 2005. Follicular B helper T cells in antibody responses and autoimmunity. *Nature reviews. Immunology* 5:853-865.

Vlam, L., E.A. Cats, E. Willemse, H. Franssen, J. Medic, S. Piepers, J.H. Veldink, L.H. van den Berg, and W.L. van der Pol. 2014. Pharmacokinetics of intravenous immunoglobulin in multifocal motor neuropathy. *Journal of neurology, neurosurgery, and psychiatry* 85:1145-1148.

von Gunten, S., A. Schaub, M. Vogel, B.M. Stadler, S. Miescher, and H.U. Simon. 2006. Immunologic and functional evidence for anti-Siglec-9 autoantibodies in intravenous immunoglobulin preparations. *Blood* 108:4255-4259.

von Gunten, S., M. Vogel, A. Schaub, B.M. Stadler, S. Miescher, P.R. Crocker, and H.U. Simon. 2007. Intravenous immunoglobulin preparations contain anti-Siglec-8 autoantibodies. *The Journal of allergy and clinical immunology* 119:1005-1011.

Wadhwa, M., A. Meager, P. Dilger, C. Bird, C. Dolman, R.G. Das, and R. Thorpe. 2000. Neutralizing antibodies to granulocyte-macrophage colony-stimulating factor, interleukin-1alpha and interferon-alpha but not other cytokines in human immunoglobulin preparations. *Immunology* 99:113-123.

Walker, L.S., and A.K. Abbas. 2002. The enemy within: keeping self-reactive T cells at bay in the periphery. *Nature reviews. Immunology* 2:11-19.

Walsh, S.J., and L.M. Rau. 2000. Autoimmune diseases: a leading cause of death among young and middle-aged women in the United States. *American journal of public health* 90:1463-1466.

Wandstrat, A., and E. Wakeland. 2001. The genetics of complex autoimmune diseases: non-MHC susceptibility genes. *Nature immunology* 2:802-809.

Washburn, N., I. Schwab, D. Ortiz, N. Bhatnagar, J.C. Lansing, A. Medeiros, S. Tyler, D. Mekala, E. Cochran, H. Sarvaiya, K. Garofalo, R. Meccariello, J.W. Meador, 3rd, L. Rutitzky, B.C. Schultes, L. Ling, W. Avery, F. Nimmerjahn, A.M. Manning, G.V. Kaundinya, and C.J. Bosques. 2015. Controlled tetra-Fc sialylation of IVIg results in a drug candidate with consistent enhanced anti-inflammatory activity. *Proceedings of the National Academy of Sciences of the United States of America*

Weaver, J.M., F.A. Chaves, and A.J. Sant. 2009. Abortive activation of CD4 T cell responses during competitive priming in vivo. *Proceedings of the National Academy of Sciences of the United States of America* 106:8647-8652.

Willis, R.A., J.W. Kappler, and P.C. Marrack. 2006. CD8 T cell competition for dendritic cells in vivo is an early event in activation. *Proceedings of the National Academy of Sciences of the United States of America* 103:12063-12068.

Wolpert, E.Z., P. Grufman, J.K. Sandberg, A. Tegnesjo, and K. Karre. 1998. Immunodominance in the CTL response against minor histocompatibility antigens: interference between responding T cells, rather than with presentation of epitopes. *Journal of immunology* 161:4499-4505.

Xing, Y., and K.A. Hogquist. 2012. T-cell tolerance: central and peripheral. *Cold Spring Harbor perspectives in biology* 4:

Xu, H., L.N. Liew, I.C. Kuo, C.H. Huang, D.L. Goh, and K.Y. Chua. 2008. The modulatory effects of lipopolysaccharide-stimulated B cells on differential T-cell polarization. *Immunology* 125:218-228.

Yajima, K., A. Nakamura, A. Sugahara, and T. Takai. 2003. FcgammaRIIB deficiency with Fas mutation is sufficient for the development of systemic autoimmune disease. *European journal of immunology* 33:1020-1029.

Yewdell, J.W., and J.R. Bennink. 1999. Immunodominance in major histocompatibility complex class I-restricted T lymphocyte responses. *Annual review of immunology* 17:51-88.

Yu, L., X. Wu, Z. Cheng, C.V. Lee, J. LeCouter, C. Campa, G. Fuh, H. Lowman, and N. Ferrara. 2008. Interaction between bevacizumab and murine VEGF-A: a reassessment. *Investigative ophthalmology & visual science* 49:522-527.

Yu, Z., and V.A. Lennon. 1999. Mechanism of intravenous immune globulin therapy in antibody-mediated autoimmune diseases. *The New England journal of medicine* 340:227-228.

Yuki, N., and F. Miyagi. 1996. Possible mechanism of intravenous immunoglobulin treatment on anti-GM1 antibody-mediated neuropathies. *Journal of the neurological sciences* 139:160-162.

Zandman-Goddard, G., Y. Levy, and Y. Shoenfeld. 2005. Intravenous immunoglobulin therapy and systemic lupus erythematosus. *Clinical reviews in allergy & immunology* 29:219-228.

Zhuang, Q., S. Bisotto, E.D. Fixman, and B. Mazer. 2002. Suppression of IL-4- and CD40-induced B-lymphocyte activation by intravenous immunoglobulin is not mediated through the inhibitory IgG receptor FcgammaRIIb. *The Journal of allergy and clinical immunology* 110:480-483.

Acknowledgments

First of all I would like to express my deepest gratitude to my supervisor Anette Karle, for her full support, guidance and encouragement during my research study. I would also like to thank Sebastian Spindeldreher for the co-supervision of my work and especially acknowledge his capacity to quickly delve into my data despite his countless other responsibilities. It was a real pleasure to perform my PhD studies under Anette's and Sebastian's supervision, and a chance to share their excellent scientific knowledge. I greatly appreciated their kindness, the nice motivating words they had towards me, and very importantly the broad freedom they gave me to perform my studies which made me incredibly grow scientifically.

I would like to say a big thank you to Ed Palmer, my Doctor Father. His scientific input was very meaningful for the orientation of my project, and his door was always open for discussion. I valued his warm attitude with all of us.

I would also like to thank Antonius Rolink for being a member of my thesis committee and for the helpful directions he gave for my experiments.

I very much thank Jocelyne Fiaux and Steffen Hartmann for giving me the opportunity to carry out my PhD thesis within the IBP group.

I would like extend my thanks to all members from IBP, PCS, ATI, NBC and DMPK for the nice interactions we had together.

I would like to address a very special thank you to Tina Rubic, Elisabetta Traggiai, and Isabelle Isnardi for the time they took to discuss my data, as well as their valuable comments and suggestions in my experimental approaches.